63-4-2

AFSWC-TR-59-47

408 467

SWC
TR
59-47
B Series

CATALOGED BY DDC
AS AD No. 408467

GROUND SHOCK ISOLATION OF BURIED STRUCTURES

TECHNICAL REPORT NO. AFSWC-TR-59-47
August 1959

PERMANENT RETENTION
DO NOT RETURN DOCUMENT
TO F/F W.L (WLL 3)

Research Directorate
AIR FORCE SPECIAL WEAPONS CENTER
Air Force Systems Command
Kirtland Air Force Base
New Mexico

Project No. 1080, Task No. 10801

(Prepared under Contract No. AF 29(601)-1134
by Eugene Sevin, Armour Research Foundation
of Illinois Institute of Technology, Technology
Center, Chicago 16, Illinois)

HEADQUARTERS
AIR FORCE SPECIAL WEAPONS CENTER
Air Force Systems Command
Kirtland Air Force Base
New Mexico

When Government drawings, specifications, or other data are used for any purpose other than in connection with a definitely related Government procurement operation, the United States Government thereby incurs no responsibility nor any obligation whatsoever; and the fact that the Government may have formulated, furnished, or in any way supplied the said drawings, specifications, or other data, is not to be regarded by implication or otherwise as in any manner licensing the holder or any other person or corporation, or conveying any rights or permission to manufacture, use, or sell any patented invention that may in any way be related thereto.

This report is made available for study upon the understanding that the Government's proprietary interests in and relating thereto shall not be impaired. In case of apparent conflict between the Government's proprietary interests and those of others, notify the Staff Judge Advocate, Air Force Systems Command, Andrews AF Base, Washington 25, DC.

This report is published for the exchange and stimulation of ideas; it does not necessarily express the intent or policy of any higher headquarters.

Qualified requesters may obtain copies of this report from ASTIA. Orders will be expedited if placed through the librarian or other staff member designated to request and receive documents from ASTIA.

AFSWC-TR-59-47

GROUND SHOCK ISOLATION OF BURIED STRUCTURES (U)

by

Eugene Sevin

Armour Research Foundation
of
Illinois Institute of Technology
Technology Center
Chicago 16, Illinois

August 1959

Research Directorate
AIR FORCE SPECIAL WEAPONS CENTER
Air Research and Development Command
Kirtland Air Force Base
New Mexico

Classification canceled (or changed to Unclas.)
by authority of SWC Ltr 14 Dec 1960
by G. B. Morrison 4 Jan 61
Name & Grade of Officer making change
Date

Approved:

Eric Wang
ERIC H. WANG
Chief, Structures Division

Leonard A. Eddy
LEONARD A. EDDY
Colonel USAF
Director, Research Directorate

Project Number 1080
Task Number 10801
Contract AF 29(601)-1134

ABSTRACT

This report deals with the problem of alleviating the damaging effects of blast-induced ground shock on underground structures of the type presently contemplated for hardened missile sites. This first year's effort has been directed primarily toward the design and implementation of an experimental program utilizing small cylinders and several types of shock-isolation devices.

The test items (rigid aluminum cylinders, 2 inches in diameter and 8 inches long) were emplaced vertically in a bed of Ottawa sand with one end at the surface. The ground disturbance was created by means of a small (0.02-lb) HE charge. Acceleration measurements were obtained at three points within the models. The isolation devices consisted of (1) a wrapping of a low-density (2 lb/cu ft) flexible polyurethane foam, (2) a simulated pile foundation for the model with an air void between the model and the sand, and (3) a simulated pile foundation for the model with pre-expanded polystyrene beads between the model and the sand. (As used in this report, the term "model" does not imply that scaling of structures was intended.)

The experimental technique was developed to the point where a satisfactory level of shot-to-shot reproducibility of effects was attained. Of the isolation devices tested, the polyurethane foam material proved to be the most effective, reducing peak accelerations (relative to the unisolated model) by a factor of from 5 to 10. The stress level in the sand is estimated to be on the order of 1 psi. Various theoretical considerations relating to both the unisolated and isolated models are discussed.

PUBLICATION REVIEW

This report has been reviewed and is approved.

CAREY L. O'BRYAN, JR.
Colonel USAF
Deputy Commander

CONTENTS

Page

CHAPTER 1 INTRODUCTION 1

1.1 Program Objectives 1

1.2 Program Scope 1

CHAPTER 2 PRELIMINARY CONSIDERATIONS 5

2.1 Review of the Literature 5

2.2 A Basis for Small-Scale Experimentation 8

2.3 Isolation of Prototype Structures 11

CHAPTER 3 THE EXPERIMENTAL PROGRAM 13

3.1 Basis for Experiment Design 13
3.1.1 Test Medium 13
3.1.2 Model Geometry 14
3.1.3 Shock Generation 14
3.1.4 Instrumentation 14

3.2 Description of Experimental Setup 15
3.2.1 Test Chamber 15
3.2.2 Models 15
3.2.3 HE Charge 16
3.2.4 Instrumentation 16

3.3 Preliminary Experiments 18

3.4 Experimental Procedure 19
3.4.1 General Procedure 19
3.4.2 Specific Procedures 20

3.5 Reproducibility Tests 21

3.6 Isolation Tests 24

CHAPTER 4 THEORETICAL INVESTIGATIONS 49

4.1 Free-Field Theory 49
4.1.1 General Requirements 49
4.1.2 Rayleigh Surface Waves 51

4.2 Control Model Response 57
4.2.1 One-Dimensional Theory 57
4.2.2 Modified One-Dimensional Theory 60
4.2.3 Variation-of-Parameter Study 63

4.3 Two- and Three-Dimensional Effects 64

CONTENTS (continued)

	Page
4.4 Isolation Model Response	65
4.4.1 Elastic Isolation Systems	65
4.4.2 Energy-Dissipative Isolation Systems	66
4.4.2.1 Introduction	66
4.4.2.2 Totally Locking Material	67
4.4.2.3 Response of Isolation Model	69
CHAPTER 5 DISCUSSION OF RESULTS	84
5.1 The Experimental Procedure	84
5.2 The Experimental Results	85
CHAPTER 6 CONCLUSIONS AND RECOMMENDATIONS	88
6.1 Conclusions	88
6.2 Recommendations	88
BIBLIOGRAPHY	90
APPENDIX A EXPERIMENTAL DATA	A-1
APPENDIX B DESCRIPTION OF SAND	B-1
APPENDIX C SUMMARY OF SOLUTIONS TO CONTROL-MODEL EQUATIONS	C-1

FIGURES

3.1	Test cell	30
3.2	Interior view of test cell	31
3.3	Test model	32
3.4	Polyurethane foam isolation models	33
3.5	Pile isolation model	33
3.6	Tetryl charge and detonator	34
3.7	Diagram of the instrumentation and control system of the recording equipment	35
3.8	View of crater	36
3.9	Test 3 Accelerometer records	37

3.10	Test 16 Accelerometer records	38
3.11	Test 16 Accelerometer records	39
3.12	Model numbers and locations for tests 7 through 19 . .	40
3.13	Typical forms of acceleration traces	41
3.14	Model positions for tests 7 through 19	42
3.15	Comparison of tests 13, 15 and 16 at position 1	43
3.16	Comparison of tests 13, 15 and 16 at position 2	43
3.17	Comparison of tests 13 and 17 at position 1	44
3.18	Comparison of tests 7, 8 and 13 at position 2	44
3.19	Comparison of positions 1, 2 and 3 in test 13	45
3.20	Comparison of positions 1, 2 and 3 in test 15	45
3.21	Test 19 Accelerometer records	46
3.22	Polyurethane foam isolation models in place	47
3.23	Pile isolation model in place.	48
4.1	Rayleigh-surface-wave radial acceleration	74
4.2	One-dimensional sand-model configuration	75
4.3	Modified one-dimensional sand-model configuration . . .	75
4.4	Triangular stress pulse and response, Short rise time, $\beta = 2$	76
4.5	Triangular stress pulse and response, Short decay time, $\beta = 2$	77
4.6	Triangular stress pulse and response, Equal rise and decay time, $\beta = 2$	78
4.7	Triangular stress pulse and response, Displacement, velocity, acceleration, $\beta = 2$	79
4.8	Triangular stress pulse and response; 1, 2 - equal rise and decay time, $\beta = 1$ 3 - short decay time, $\beta = 1$	80
4.9	Triangular stress pulse and response Equal rise and decay time, $\beta = 1$	81
4.10	Stress-strain curve of flexible polyurethane foam ($1/2$ lb/ft^3)	82
4.11	One-dimensional length of totally locking element . . .	83
4.12	One-dimensional sand-isolation-model configuration . .	83
A-1 through A-31	Graphs of test data redrawn from films	A-1

B-1 Grain-size analysis B-3
B-2 In-place density apparatus B-4

TABLES

3.1 Summary of Experiments 26
3.2 Comparison of Results 27

Chapter 1

INTRODUCTION

1.1 PROGRAM OBJECTIVES

This study, entitled "Ground Shock Isolation of Buried Structures", has as its primary objective the establishment of techniques for alleviating the damaging effects of blast-induced ground shock on underground structures of the type presently contemplated for hardened military facilities.[1/] The eventual accomplishment of this goal, it is believed, should properly involve tests of prototype structures under field conditions. Aside from the practical aspects of such an effort at this time, however, it seemed appropriate to first consider the behavior of small-scale structures in soil or soil-like media. ARF suggested in its Research Proposal to this contract that a laboratory test program employing miniature models would bring into focus those parameters which principally influence the shock isolation properties of selected systems, and that subsequent tests based on these results and employing larger, but still small-scale, models would determine the actual techniques and/or mechanisms that show the most promise for prototype application. From the results of these latter tests it is to be hoped that realistic full-scale designs could be prepared (preferably in conjunction with field tests).

1.2 PROGRAM SCOPE

This first year's effort has been directed primarily toward the design and implementation of an experimental program utilizing miniature models of silo-like structures and several so-called shock-isolation devices.

1/ This report represents the final report on ARF Project No. 8147 and covers work performed during the period May 1958 to June 1959. ARF personnel who contributed materially to the project include F. K. Halwax, T. M. Kroll, R. W. Sauer, E. Sevin (Project Engineer), E. H. Scharres, S. Shenkman, E. Vey, and R. E. Welch. Data are recorded in ARF Logbooks No. C8847 and C8980.

In any miniature-scale-model experimentation, one is clearly concerned with the applicability of results to the full-scale situation. In the present instance, it is impossible to guarantee such application because of the practical impossibility of constructing true models of either the structure or the isolation system. Prototype installations involving shock-isolation schemes are only in a conceptual stage at this time, and there is also a general lack of similitude relationships for the generation and the interaction of shock in soil media. The utility of the results obtained must rest, therefore, on the following two hypotheses:

1. Isolation techniques feasible for prototype application may be characterized by a few essential parameters, which, in turn, may be effectively modeled on a miniature scale.

2. Although there exists a certain dissimilarity in free-field phenomena between the full- and miniature-scale situations, the latter may still serve to rate the relative effectiveness of different approaches to isolation.

The second hypothesis is critical and most open to question. Imagine a spring base designed to cushion the fall of a man from a jump of a certain height. This same base would be totally inadequate if a several-ton weight were dropped on it from the same height. Here, then, is an obvious example wherein the effectiveness of the isolation in an absolute sense is totally dependent on the scale of the input. We are concerned, however, with establishing only relative effectiveness of system types. That is, to continue the analogy, we would assume that the relative effectiveness of various isolation designs intended to arrest the motion of the heavier weight, could be established by observing the relative effectiveness of model devices in cushioning the impact of a man. A design suitable for the larger weight would then have to be prepared in accordance with the "model" test results.

Although the validity of these hypotheses cannot be demonstrated at this time (and, of course, they may be generally invalid), it is our view that they are sufficiently plausible to justify the present experimental approach.

The following specific method of approach was formulated in accordance with the views indicated above:

1. Review of existing information, both experimental and theoretical, relating to ground-shock free-field phenomena, response of underground structures, and attempts at shock isolation.

2. Consideration of possible approaches to isolation of prototype silo-like structures with attempts to establish the essential parameters of each.

3. Design of a miniature-scale laboratory test program for simulating blast-induced ground shock in soil-like media, and construction of several models of isolation systems in accordance with the results of item 2 above.

4. Attempt at formulation of a mathematical model of the soil-isolation interaction, so as to yield analytical results for interpreting and guiding the experimentation.

5. On the basis of the experimental and analytical results obtained, development of an experimental program utilizing small-scale models of a size sufficient to reflect more faithfully proposed isolation schemes for prototype structures.

On the basis of the literature review, together with certain practical considerations, it was decided to use an Ottawa sand and a high-explosive-induced (HE) ground shock for the minature-scale tests (see Chapter 3). Great emphasis was placed on attaining reproducibility of effects at a constant radius in the sand bed for a single shot (symmetry of field), and at the same point in the bed on a shot-to-shot basis; for without a reasonable degree of reproducibility, there would be little justification indeed for any generalization of results. As discussed in Chapter 3, only a very few experiments could be performed with shock-isolation models.

The study of past attempts at shock isolation was limited to the Plumbbob 3.5 experiment, recent theories of packaging and dynamic cushioning, and, briefly, conventional applications of vibration absorbers in mechanical systems. On the basis of this material, it seemed appropriate to classify shock-isolation devices as to whether they were primarily of an energy-dissipative type (e.g., a crushable material, the Plumbbob 3.5 "gin bottles") or of a non-energy-dissipative type (e.g., an elastic spring mount). Further, it appeared desirable to seek a model isolation material that might exhibit either property depending on the nature of the shock input.

On the basis of the results obtained, the flexible polyurethane foam of low density selected for this purpose acted as an efficient isolator of the nondissipative type (see Chapter 6).

A theoretical study of the sand-model-interaction problem was conducted on the basis of an elastic one-dimensional soil, modified so as to incorporate certain aspects of the two-dimensional situation (see Chapter 4). The results obtained are largely qualitative in nature but do not discredit the assumption of elastic action. An idealized model of an energy-dissipative type of isolation material was then incorporated into the analysis in order to treat the sand-isolation-model-interaction problem. The results of this work indicate that the dissipative action could not be achieved at the low stress levels (approximately 1 psi) present in our experimental setup. The test results seem to bear this out and indicate a need for experimentation at higher stress levels.

In view of the limited results obtained with the isolation material tested, it is considered desirable to continue the laboratory experimentation prior to the design of a larger, but still small-scale, tests. Thus, no detailed design of such tests is proposed--other than a continuation of the present type of experiments on a slightly larger scale in another type of soil (using the same type of instrumentation).

Chapter 2

PRELIMINARY CONSIDERATIONS

2.1 REVIEW OF THE LITERATURE

We present in this section the results of a limited literature survey undertaken as one of the initial activities on the program. The survey deals with selected areas of interest to the general problem at hand and is meant to be current but by no means exhaustive in scope. The reference material studied is listed in the Bibliography to this report and is indicated throughout the text by a number enclosed in parentheses.

Inasmuch as most theoretical considerations of ground-shock propagation are based on the classical theory of linear elasticity, standard texts on that subject and also related, more specialized works, such as those by Ewing, Jardestsky, and Press (14) and by Kolsky (19), serve as invaluable introductory material and general reference volumes. More detailed studies by numerous Japanese investigators concern behavior close-in to a disturbance and the effects on surface motion of factors such as surface curvature, sub-surface elastic and water layers (34), and variations in disturbance sources (32). Of more recent date are the series of studies by the Rand Corporation regarding the earth stresses and motions produced by a surface blast. These include, for example, the effects of an impulsive surface load (20) and a theoretical solution for the air-induced ground shocks (27).

As indicated in a summary on soil stress waves published by the Stanford Research Institute (37), a major problem is that of representing the true nature of dynamic soil behavior. There is much literature available presenting the attempts of many investigators to develop a satisfactory non-elastic model of soil behavior. These attempts encompass many different approaches. A brief summary follows for each of the more plausible ideas.

Anisotrophy: The most direct approach would seem to be the modification of the soil behavior on a large scale to include the more obvious soil characteristics. The work of J. L. Synge (38), then, is an attempt to characterize the soil as a linear elastic medium but with different soil properties in the vertical direction. The development of elastic waves in a half-space, however, is still faced with the known, non-linear, inelastic soil properties.

Visco-Elasticity and Plastic-Elasticity: References (6) and (30), which respectively incorporate a velocity-dependent energy loss and permanent set of the medium, attempt to modify the mathematical model of the soil. Wave equations developed on these bases characterize some soils sufficiently, namely, those having high moisture content or some degree of internal cohesion but do not adequately represent more granular materials.

Granular Materials: Other investigators concentrated their efforts primarily on granular materials. Mindlin and others (23, 16) basing their work on the Hertzian elasticity solution for spheres in contact, studied the mechanics of wave propagation in various bodies composed of packed spheres. Salvadori and Weidlinger (25), in investigating a similar medium, dealt with a material that compresses suddenly at a certain stress level and afterward remains locked in that position, which action gives rise to the propagation of a pseudo-shock-front in the soil.

Others: Two other approaches are also of some importance. The first of these, the "hydrodynamic" theory (12), postulates that under impact a solid will assume a state similar to that of a fluid and that the initial phase of the shock wave will, therefore, be similar to the shock wave in a fluid. This method seems applicable only to extremely high stress levels such as are found in the immediate vicinity of a blast. The second approach, not yet fully elaborated, depends on the development of general stress-strain relations for "mesoscopic" (finite-dimensioned) elements of soil and the subsequent derivation of wave equations. As explained by Pinney (42), this method would make use of the known average properties of a soil to good advantage.

Coincident with development of the above theories of wave propagation, a number of basic studies, such as that by Bernhard and Finelli (5), were undertaken from the viewpoint of pure soil mechanics. The actual dynamic behavior of a given soil particle, however, seems most complicated, and, as yet, such studies have not been fruitful.

Field observations of ground motion, employed since the beginning of seismology, have evolved to the current, precise techniques used in earthquake measurement, and similar techniques have also been used for the more relevant problem of vibrations due to blasting operations. Investigations by Morris (24), Leet (21), and others (9) consist of empirical studies of the effect on surface-motion amplitude of such factors as charge weight, distance from charge, and location of maximum amplitude. Morris and Leet, in particular, present interesting qualitative discussions of the mechanics of blasts, describing the development of zones of rupture, slight cracking, and elastic action.

More recent work in a similar vein has been undertaken by various organizations (13, 18, 35) in connection with full-scale weapons effects programs. Empirical analyses have been made of wave form, attenuation with distance, and variation of peak stress and acceleration magnitudes with size of weapon and depth in soil.

Aside from such large-scale testing operations, some work has been done in developing and employing laboratory facilities for smaller scale testing. Two such programs are described in recent reports by Massachusetts Institute of Technology (44) and Armour Research Foundation (2) dealing with the use of rapid-loading devices in studying wave propagation in soils and the use of soil-simulating photo-elastic materials to investigate stress wave action and as a check on various acceleration gages. Related work has also been done by Scopek (26) in measuring sand density in place by means of gamma radiation and by Goodier, Jahsman, and Ripperger (17) in estimating the time variation of a given impulse on a steel block by graphical integration of an observed surface wave. (This latter work was instrumental in the consideration of the Rayleigh wave development given in Chapter 4.) Also of interest, chiefly by way of encouragement, is the early work of Terada and Tsuboi (39) in investigating the response of an agar-agar bed to a steady-state vibration.

We are immediately concerned with the response of a structure in a soil to an incident stress pulse. While primary interest lies in the behavior of a shock isolating material or device, a thorough understanding of this demands a corresponding understanding of the response of the unisolated structure. Unfortunately, the available store of literature is weakest in these two areas.

Some problems involving wave scattering have been solved in such fields as fluid mechanics (4), but the physical differences between fluid and soil-like media make these solutions inapplicable here. Of a more promising nature are the early efforts of Sezawa (33) in his work on the scattering and diffraction of elastic waves by such rigid inclusions as screens and cylinders of various cross sections. His treatment covers the effect on elastic waves of both movable and immovable obstacles and predicts both resultant field motions and, where applicable, the motion of the inclusion. Similar work

was also done by White (43), but his main interest was in such inclusions as empty and fluid-filled cylinders.

Turning now to the isolation device itself, one finds little applicable information. To be sure, much information is available concerning the engineering treatment of vibration-isolation problems such as are commonly encountered in designing machinery, machine foundations and structural components. In such cases, standard materials (cork, rubber, felt, springs, etc.) usually prove satisfactory. Experimental research (29) with such materials has been concerned only with their over-all effects on vibrating systems and has not considered the actual mechanics of their behavior. Only two references touch on the isolation of large-scale motions such as considered in this report; and these, only in a brief or empirical way. Creskoff (11) makes brief mention of the use of a vertical layer of large-size gravel about the below-ground walls of buildings as a means of reducing earthquake damage. Although this is apparently a common practice, no further mention of it is made in the available literature. The other source of information is Project 3.5 of Operation Plumbbob, (36), in which a silo-like structure was surrounded by a layer of "gin bottles" and shear barriers as isolating devices. Quantitative results indicated a considerable reduction of observed accelerations, but some control data were lost and no analysis is presented.

2.2 A BASIS FOR SMALL-SCALE EXPERIMENTATION

The design of a small-scale ground-shock-isolation experiment depends to a large extent on what one means by shock isolation as applied to an entire structure. In Section 1.1 shock isolation was indicated to be the alleviation of the damaging effects of ground shock on the structure. If this is accepted as a meaningful, if rather vague definition, one must then designate the "effects" of interest. Possibly, this is best approached in terms of the purpose of isolation systems.

Underground structures of the type being considered are built to house and protect functioning components of a weapons system. As such, the structure is adequate only if the performance of the components is unimpaired as a result of the design inputs being applied to the structure.

The designer is properly concerned not only with assuring the integrity of the primary structure, but also with assuring tolerable inputs to the functioning elements of the system housed within. Shock isolation of the primary structure may be viewed, therefore, either as a means of reducing soil-transmitted forces on the structure (so as to permit a more efficient structural design), or as a means of alleviating the motions of the structure (so as to mitigate the requirements on the design of interior equipment and mountings). In the latter case, isolation of the structure is to be considered part of the overall approach to shock mounting of interior equipment, since structural integrity is presumably assured without recourse to any means of external isolation. [1/] As argued in the following paragraphs, it is preferable to think of shock isolation for the purposes of this study in the sense of alleviating structural motions rather than in reducing soil-transmitted forces. While this may be a somewhat arbitrary distinction that does not constitute an essential limitation of the results obtained, it does provide more of a rationale for the test plan.

An experiment designed to establish the effectiveness of an isolation system for reducing soil-transmitted forces would seem to require some measurement of these forces, either by direct or indirect means. Both approaches present formidable difficulties. In view of the dependence of soil-transmitted stress on the local response of the structure and of the impracticality of true structural modeling on a small scale, direct measurement of stress could have only limited meaning--irrespective of the serious uncertainties in instrumentation technique. The interpretation of an indirect measurement, such as the acceleration or velocity of a point on the structure, depends for its validity on the adequacy of the theory governing the soil-structure-interaction problem, concerning which too little is known. It is, of course, this very dependence of the loading on the structural response that distinguishes the underground-structural-effects problem from the superficially similar air-blast-effects problem, and explains in part the great analytical difficulty encountered in the former.

[1/] Of course, there inevitably must be a trade-off between the extent to which one shock mounts the entire structure relative to the surrounding soil medium and the equipment relative to the structure.

The influence of structural parameters on the forces transmitted by the soil to the structure can be illustrated most simply with reference to a one-dimensional, elastic soil model. If in this case an incident stress pulse impinges on a structure (i.e., on the soil-structure interface) that is effectively rigid relative to the soil, the pulse is reflected in kind, and the force on the interface becomes twice that of the incident pulse. When the stiffness of the interface is considerably less than that of the soil, the structure acts much as a void, and little or no force is transmitted. (Energy input to the structure is then in the form of kinetic energy of the void-like material.) For intermediate structural stiffnesses, the transmitted stress pulse depends on the relative velocity of the interface.

A small-scale experimental study appears more promising when viewed as an attempt to alleviate the motions of the primary structure. For one thing, it is the acceleration of the primary structure which acts as a driving force on interior components, rather than the direct forces acting on the primary structure. This is most easily seen if the interior component is visualized as single-degree-of-freedom system of effective mass m, whose equation of motion is given by

$$m\ddot{x} + R(x - y, \dot{x} - \dot{y}, t) = 0 . \qquad (2.1)$$

In Eq 2.1, x is the coordinate defining the motion of the component, y is the coordinate defining the motion of the primary structure, and R is the resistance to motion of the component which is taken to be a function of the relative displacements $x - y$, relative velocity $\dot{x} - \dot{y}$, and the time t Letting $z = x - y$ denote the relative displacement, Eq 2.1 may be written as

$$m\ddot{z} + R(z, \dot{z}, t) = -m\ddot{y} \qquad (2.2)$$

The acceleration of the primary structure, $\ddot{y}$, thus is seen to represent the disturbing force on the component, as was stated above.

Viewed in this manner, the acceleration of the model becomes a measurement of direct interest, which is practical to obtain on miniature-scale models. Moreover, since acceleration is a primary measurement, it is a simpler matter to rate the effectiveness of the various isolation schemes tested than if direct force measurements were attempted.

The use of effectively rigid models, desirable in view of the inability to model structurally as well as the practical aspects of mounting accelerometers, appears somewhat more reasonable when the gross motion of the structure is of primary interest.

It is true that if an isolation device is effective in reducing the motions executed by the primary structure, it is also effective in attenuating the forces transmitted by the soil to the structure. For this reason, it may not be too important to conceive the present experimentation as being directed necessarily toward the former rather than the latter application. Nonetheless, the experiments are in no way intended to represent structural models, they do not consider the possibility of structural "failure", and soil-transmitted forces are neither a direct nor an intended indirect measurement.

2.3 ISOLATION OF PROTOTYPE STRUCTURES

We offer some brief comment in this section as to the manner in which one might isolate prototype structures. This discussion is quite incomplete, since detailed considerations of this nature are clearly outside the scope of this effort. It is our purpose to indicate that isolation can be achieved in various ways and also to suggest an approach to model testing.

Since the present state of knowledge does not permit a precise statement of the input function against which the structure is to be isolated, it is convenient to suppose that the disturbance is primarily a sudden displacement of the medium in which the structure is embedded. This appears to be a rough approximation to the truth, although the magnitude of the displacement in a given situation is not well defined from available test data. Isolation, then, is a means of preventing the structure from partaking of the sudden motion of the medium in which it is embedded.

Clearly, an absolute method of isolation would be to create, and maintain, a complete void between the structure and its surrounding medium. This idealized situation of course can never be realized, since the weight of the structure must be supported, the earth held back around the structure, and the alignment of the structure maintained within the cavity. To some extent, then, the motion of the free field will be imparted to the structure through its vertical and horizontal support system. To be at all effective

these supports must approximate the action of the void, so that they will be substantially less stiff than the surrounding earth. Two general types of isolation seem possible: (1) an energy-dissipative device, such as a frangible or crushable material whose ultimate compressive strength is well below that of the adjacent soil, and (2) a non-energy-dissipative material, such as a soft elastic spring mount.

Various types of frangible materials could be employed. Against the more severe vertical forces, suitable plastic-flow energy absorbers could be designed. Thus, a silo could be supported on blocks of material capable of sustaining large plastic deformations, such as soft aluminum, copper, lead, or similar materials. The blocks could be proportioned so that their yield stress would be only moderately greater than the static stress necessary to support the structure. Isolation against lateral forces could be provided by a frangible backfill of lesser unit strength. A soft elastic suspension for the structure, assuming any of a number of guises, should also provide good isolation. The structure could be surrounded with materials such as flexible polyurethane foams, pneumatic springs, or, for that matter, even a mechanical spring system could be devised. It might even be practical to achieve a soft spring mount by essentially floating the structure in water. Suspensions of both types could be incorporated in the structure-within-a-structure concept, i.e., in which the function of the outer structure is simply to maintain its integrity under shock loading.

It is the intent of this study to determine the particular properties of an isolation material that make it most effective. There does not seem to be much question that various approaches will prove effective to some extent, and, therefore, an actual design might be strongly influenced by the necessities of construction practice. For example, this might be the basis for selecting the frangible material over the spring suspension, despite the energy-absorbing characteristics of the former. With regard to the tremendous energy input associated with free-field motions, it may be, unrealistic to base the effectiveness of an isolation device solely on the energy-dissipative character of the material.

Chapter 3

THE EXPERIMENTAL PROGRAM

3.1 BASIS FOR EXPERIMENT DESIGN

The design of the experimental program involved four major phases. These were (1) selection of the test medium, (2) selection of model geometry, (3) selection of shock-generating technique, and (4) selection of instrumentation. Various considerations entering into the decisions made are discussed in the following paragraphs.

3.1.1 Test Medium. The choice of a test medium was based on three main considerations: namely, (1) the requirement that the shock-transmission properties of the medium approximate as much as possible those of real soils, (2) the desire to achieve the highest degree of reproducibility of results, and (3) the practical aspects of achieving a sufficiently large expanse of the medium.

In view of the wide range of actual soil types that are presumed to be of eventual interest in practical applications, the first requirement does not provide any firm guides. However, it does suggest the use of prototype soils rather than unproven synthetic materials. The requirement for reproducibility of effects implies the practical ease in achieving uniformity and reproducibility in the physical description of the medium, e.g., water content, relative density. Synthetics are generally more desirable in this respect. The overall size of the medium governs the time of observation during which the response of the test models is unaffected by reflections from the sides of the soil-containing structure. To maximize this observation time and also to enable the use of models of a desirable size, the largest possible extent of the test medium is required. Factors which tend to limit the size of the medium are (1) cost and (2) practical means and facilities for generating shock strengths of interest.

On the basis of these considerations, the choice of a test medium was reduced to that of urethane rubber or a dry non-cohesive sand. In favor of the former was the fact that considerable experience with it had already been gained in connection with another AFSWC-sponsored program at ARF. Also, it appeared possible to share the use of the medium with that program.

To construct another block of urethane rubber for the exclusive use of the present program was ruled out as being of prohibitive cost. However, when it appeared that scheduling and conflicting interests would minimize the joint use of the medium, it was decided to utilize dry sand. All experiments thus were conducted in a dry Ottawa sand, a precise description of which is given in Appendix B.

3.1.2 Model Geometry. At the outset of the program it was decided with the sponsor to concentrate our efforts on a silo-like geometry representative of missile containment structures. Thus, the model structures selected were right circular cylinders positioned with their axes normal to the surface of the medium and one end flush with the surface. In view of the impossibility of achieving true structural models, it was decided to make the models essentially rigid. The size of the models was held to a minimum compatible with available instrumentation. A detailed description of all models is given in Section 3.2.2.

3.1.3 Shock Generation. Three shock generation techniques were considered: (1) small high-explosive (HE) charges, (2) the 6-ft-diameter shock tube, and (3) mechanical devices. The decision was made in favor of HE charges for the following reasons:

1. Desirable facilities for conducting the experiment were immediately available.

2. ARF possesses wide experience in designing and in preparing charges for specialized purposes.

3. Use of the shock tube at the time would have involved serious problems of scheduling.

4. Mechanical devices, while undoubtedly practical, appeared to require considerable design and fabrication effort.

3.1.4 Instrumentation. The matter of instrumentation had mostly to do with the determination of the type of measurements to be obtained. It was decided at the outset that no special effort would be devoted toward obtaining free-field data of any type because of the particular application of results intended. As discussed in Section 2.2, measurements of model acceleration appeared most meaningful, especially for a rigid model.

Therefore, it was decided to make acceleration the primary measurement. Other measurements obtained in some of the tests consisted of (1) free-field air pressures, (2) free-field sand pressures, (3) time of detonation, and (4) crater formation by means of a high-speed motion picture camera. A complete description of the instrumentation and associated electronics is given in Section 3.2.4.

3.2 DESCRIPTION OF EXPERIMENTAL SETUP

3.2.1 Test Chamber. The experimental program was conducted in the ARF Test Cell, which has facilities for the firing of small caliber weapons and explosives and was easily adapted to our purposes. In addition to the explosive chamber that housed the sand bed, the cell had complete provisions for firing, data recording, photographic development, and shop space.

A partial sketch of the test cell is shown in Fig. 3.1. The explosive chamber measures approximately 16-ft by 5-ft by 6-ft in height. It is of reinforced-concrete construction, and the one-foot-thick walls are clad with 1/2-in. steel plating. It accommodates a sand bed 7-ft-7-in. by 4-ft-10-in. by 3-ft-9-in. high (Fig. 3.1). Figure 3.2 is a photograph of the sand bed taken from within the chamber.

3.2.2 Models. The test models consisted of 2-in. diameter, thick-wall (1/4-in.), aluminum tubing, 8-1/8 in. in length. Both ends of the tube were capped. A sketch of a typical model is shown in Fig. 3.3, which also indicates the positions of the accelerometer gages. The accelerometer leads were brought out through the top cap. The weight of a model, including caps and accelerometers, was determined to be 667 grams.

The basic model, when placed in direct contact with the sand, is referred to as a control model. The isolation models consisted of this same model wrapped with a sheet of flexible polyurethane foam. Two thicknesses (1/4 and 1/2 in.) of a 2-lb/cu-ft foam were used. Figure 3.4 shows a control model and the two isolation models. Figure 3.22 shows the models in place in the bed. The only other type of model tested consisted of a control model with a 1-1/2-ft length of 1/2-in.-diameter steel rod affixed to its base (Fig. 3.5). This model was an attempt to simulate a structure founded on

a deep pile. It was tested once with an air void created between it and the surrounding sand (Fig. 3.23a) and twice with the void filled with pre-expanded polystyrene beads (see Fig. 3.23b).

3.2.3 HE Charge. The ground disturbance for the tests was created by detonating a charge made up of four 1/2-in.-diameter by 1/2-in.-long pressed Tetryl pellets[1/]. Each pellet weighed 0.00558 lb and was specially prepared by ARF personnel. It is estimated that the variation in pellet size did not exceed 0.001 in. in any dimension or 1 percent-by-weight.

The pellets were taped together with a 1-in. length of 1/2-in.-OD steel tubing at one end to form a cylinder, 1/2 in. in diameter and 3 in. long. The detonator was a No. 6 DuPont electric blasting cap inserted inside the steel tube and taped securely. A photograph of the charge and detonator is shown in Fig. 3.6.

3.2.4 Instrumentation. Instrumentation consisted of (1) accelerometers, (2) air pressure gage, (3) sand pressure gage, (4) detonation sensor, and (5) Fastax high-speed camera, together with the necessary recording equipment. The acceleration data were the sole measurements obtained from the models. The air pressure gage was used initially to monitor the air shock in the chamber and later to indicate the presence of air shock under the test bed cover. (see Section 3.3). The sand pressure gage was used to measure free-field conditions, and the detonation sensor was used to establish a zero time for the initiation of the disturbance.

The accelerometers were Columbia Research Model 302 compression-piezoelectric-type gages. The gage sensitivity with the cable lengths and input circuity used was approximately 1 mv per g of acceleration. The dynamic acceleration range of the gages was 0.02 to 40,000 g; their natural frequency was 75 kcps. The accelerometers weighed 23 grams and were attached to the models with a single #10-32 stud. A maximum of three gages was used in each model, positioned as shown in Fig. 3.3.

1/ Various size charges were tested until finally this size was decided upon; see Section 3.3.

Air pressure measurements were obtained with a Glennite Model P-401 piezoelectric blast gage. It consists of a circular-disk sensing element attached to a tubular support and is commonly referred to as a "lollipop" gage.

Sand pressure was measured with a miniature crystal gage developed by ARF. It consisted of a 1/2-in.-diameter by 1/8-in.-long crystal of barium titanate mounted on a phenolic base.

The detonation sensor consisted simply of a loop of fine wire placed around the charge. Fracture of the wire, which occurred when the blast broke the surface of the bed, caused a momentary interruption of the trace on the recorder.

A photographic record of the sand bed during detonation was obtained for several tests using a Fastax camera operating at about 4000 fps. In this connection, a rectangular grid work of colored sand was placed on the surface of the bed covering the models. Figure 3.2 shows a view of the sand bed just prior to a test with the camera in position. Still photography was utilized liberally both before and after a test.

Dynamic recording was accomplished on three, 4-channel-recording, cathode-ray oscillographs using 35-mm photographic film. Provision was made for recording an accurately known charge on the gage circuits for calibration just prior to each test. In addition, one-millisecond timing dots were recorded on one edge of the film. Response of the sensors and recording equipment used was flat dc to 70 kcps $\pm$ 5%.

Detonation of the HE charge was accomplished by a source of voltage controlled by sequencing circuits. When manually triggered, the sequence timer started the recording cameras, recorded the gage calibration signals, applied the firing voltage to the blasting cap, recorded the time of break of the detonation sensor, and then recorded the analog response data of the models. Finally, the end of each of the three film strips was imprinted with a serial number for later correlation by the engineer with his notes and logged observations. A schematic diagram of the circuitry is shown in Fig. 3.7.

3.3 PRELIMINARY EXPERIMENTS

The first tests were directed toward establishing the proper range of charge size and relative position of the models. Up to three control models were utilized, each with a single accelerometer.[2] An initial 8-in.-long cylinder of Tetryl was successively reduced in size until the 2-in.-long charge described in Section 3.2.3 was decided upon. After various positions of the charge in the bed had been considered, it was finally decided to place the charge against the back wall with the closest model 36 in. away. The charge, which was buried with its axis normal to the surface and one end flush with the surface, uniformly produced a semicircular crater measuring 22 in. in diameter and 5 in. deep (Fig. 3.8); there was no visually observable permanent motion of the sand and model at the closest model position. An observation time of approximately 10 msec during which the model was uninfluenced by reflections from the bottom and downstream walls of the sand container could be obtained at the central 36-in. position. Reflections from the back wall occur instantaneously and act to effectively increase the charge weight. The presence of this wall, therefore, strongly influences the free-field disturburance, but not the observation time at the model locations.

Also of interest during these first tests was the nature of the accelerometer records obtained, both as to their individual significance and shot-to-shot reproducibility. The results were disappointing in both respects. The records all exhibited considerable amounts of high-frequency hash, and, generally, the same gages did not indicate any obvious similarity of salient features from shot-to-shot. A typical set of records is shown in Fig. 3.9.

During these tests the surface of the sand bed was exposed to the blast, therefore the motion of models resulted from some combination of direct and air-induced ground shock. The models themselves were covered with 8-in.-diameter, metal pie plates resting on the sand. It was at first thought that the poor records were principally due to an inadequate technique

---

[2] The CRL gages were not available at this time and a Gulton accelerometer similar in size but of considerably less sensitivity was used.

for conditioning the bed and emplacing the models and charge. This technique was refined to a substantial degree with but little improvement; the ringing of the gages was still predominant.[3/] It was then decided to shield the surface of the bed from the direct air shock by constructing a suitable baffle and cover. This shielding noticeably improved the results, as can be seen in Fig. 3.10 and 3.11, which show typical records obtained in a later series of tests. Since there appeared to be no other way in which clean records consistently could be obtained, it was decided to conduct all future tests with the bed covered. It was recognized, of course, that prototype isolation scheme must be effective against both direct and air-induced ground shock, and that with the bed covered the latter phenomenon would not be reproduced in the laboratory tests. As discussed in Section 1.2, however, the validity of the experimental approach rests on the hypothesis that the relative effectiveness of isolation schemes can be determined despite such dissimilarities in shock input.

3.4 EXPERIMENTAL PROCEDURE

Before proceeding to a discussion of the primary experiments and results obtained, it will be well to describe the experimental procedure in some detail, as this procedure is in itself a major result of the year's effort. The present technique is the product of all experimentation to date, and it is to be expected that refinements will continually be made as the work progresses. There are basically three phases to the procedure, having to do with (1) conditioning of the sand bed, (2) emplacing the models, and (3) emplacing the charge. A description of the general procedure and then a step-by-step outline follows.

3.4.1 General Procedure. The sand bed is conditioned by leveling it and vibrating it at length in a set pattern using a standard rotating concrete vibrator unit both before and after emplacing the models. In some instances the models are left in position from the previous test and then only the refilled crater area is vibrated. A paper sleeve, 1-1/4 in. in diameter and 3-1/2 in. long, is inserted into the sand at the charge position, and the sand is removed. The charge is set into the sleeve just prior to firing. The

---

[3/] Electrical filtering was attempted and, while superficially effective, was considered undesirable.

models are emplaced with the aid of a length of 5-in.-diameter stove pipe set into a template which, in turn, is affixed to rails on the walls of the chamber so as to insure accurate positioning. The sand is removed from the stove pipe, the model set in place, and the sand carefully replaced and compacted; the stove pipe is then removed, and the area surrounding the model is vibrated without causing the model to shift position. Boards spanning the side rails serve as a working platform so that the surface of the bed is not disturbed. The bed is covered after all models are in place, and the charge is then set. After complete checkout of all electronic equipment, the charge is detonated.

3.4.2 Specific Procedures.

Procedure for Conditioning the Bed and Emplacing Models and Charge:

1. Roughly level sand bed with screed.
2. Vibrate bed a quarter area at a time, proceeding away from charge area and filling in holes left by vibration.
3. Level bed.
4. Hand finish back-wall area.
5. Insert sleeve for charge and remove sand from sleeve.
6. Set front baffle of cover in place and adjust to sand level, filling in all spaces.
7. Set template in place against appropriate stops on side rails.
8. Insert stovepipe through appropriate hole in template to a depth 1/2 in. below bottom level of model.
9. Excavate sand from stovepipe to depth of model.
10. Place model in position, center, and orient, using guide marks to insure that horizontal accelerometers lie along a radial line from the charge position.
11. Fill in void area and tamp each 3-in. layer 50 times.
12. Remove stovepipe and template and hand finish around model.
13. Vibrate on two sides of model not closer than 18 in. to model. Take care that depression left by vibration is not in line with a model to be subsequently placed.

14. Repeat steps 7 through 13 for remaining models; the model furthest from the charge is emplaced last.

15. Place auxiliary instrumentation, e.g., sand gage, air gage, Fastax camera.

16. Cover the entire sand bed from the baffle to the far end with 2-by-10-in. boards spanning the side rails, and place board in front of baffle.

17. Place detonation sensor around charge sleeve.

18. Place charge into sleeve, taking care that it is centered and vertical, and connect to firing line (authorized personnel only).

19. Check out all electronic equipment.

20. Fire.

With four models, this procedure involves several-days effort.

Procedure for Reconditioning Bed and Emplacing Charge with Models Already in Place:

1. Refill crater area and remove any debris from previous shot. Do not remove cover boards.

2. Vibrate crater area, taking care not to leave vibrator impressions in line with any of the models.

3. Proceed as in steps 4, 5, and 17 through 20, above.

Several tests of this nature can be run in a single day.

3.5 REPRODUCIBILITY TESTS

From the outset, it was felt that the relative success of the experimental procedure should properly be measured in terms of shot-to-shot reproducibility at selected positions within the bed. Also, for a particular shot, one desires substantial symmetry of field at various radial locations. With this in mind, a prolonged series of tests were conducted using only control models in various positions throughout the bed. While the primary aim was to establish a satisfactory level of reproducibility, these tests were also the means whereby the experimental technique described previously was evolved.

Sixteen tests were performed in this series. The first six of these were performed without the bed being covered and are not reported in

detail.[4/] Tests 7 through 16 are summarized in Table 3.1, and the records are presented in Appendix A. The location of the models is indicated in Figs. 3.12 and 3.14.[5/] In Table 3.1, the column labeled "Shot No. on Bed" refers to the number of tests for which the models were left in position, thus the bed was completely conditioned only for "Shot No. 1".

In tests 9 and 10, the crater was refilled by hand but not vibrated. The results of these tests were found to be markedly dissimilar from the previous (and subsequent) tests and the records obtained are not repeated. Subsequently, the crater area was vibrated for all shots. In test 14, no crater was formed, and the records obtained were again dissimilar. It is surmised that the charge was inadvertantly pulled from the sleeve prior to firing and that a direct air blast occurred.

Inspection of Table 3.1 and of the records themselves indicates that the performance of the gages and recording system was quite satisfactory. The only exception to this was the performance of the sand pressure gage, from which no meaningful records were obtained. The gages produced a large signal at shot time and apparently had not recovered at actual arrival time. This behavior is attributed to electromagnetic effects and was probably due to inadequate shielding of the gage and the connecting cables.

The degree of reproducibility attained is observed by close inspection of the records during the first 5 msec or so after shock arrival. It is found that the records from all gages are two typical forms, a and b, as indicated in Fig. 3.13. Table 3.2 lists the coordinates of the typical

---

4/ Tests 5 and 6 were for the purpose of obtaining a photographic record of crater formation and sand motion and did not contain any other instrumentation.

5/ Each of the models is identified by a number (1 through 5) as shown in Fig. 3.12. This number was retained throughout the program, whether or not the model was of the control or isolation type in any one test. In addition to the model numbers, each position in the bed was identified by a number (1 through 8) as shown in Fig. 3.14. This scheme was intended to facilitate comparison of gage records for the various models which occupied the same location in the bed on different shots. However, care must be taken, not to confuse the model and position numbers. For example, Fig. 3.12 and 3.14 together indicate that Model No. 2 occupied Position No. 6 on test 7 through 12, Position No. 2 on tests 13 through 16, and Position No. 5 on tests 17 through 19. Also, it is seen that Models No. 1, 2, and 3 each occupied Position No. 2 during certain of the tests.

record forms for direct comparison of reproducibility at the same position.[6, 7] The positions, identified in Fig. 3.14, apply to all tests. Care should be taken not to confuse references to the position numbers of Fig. 3.14 with the model numbers of Fig. 3.12 (see footnote No. 5 on p. 22).

It is seen that the upper horizontal acceleration records are primarily of Form a, the initial peak being absent only in six out of twenty-two instances. Similarly, the vertical acceleration records show the initial peak of Form a in only two out of twenty instances. The lower horizontal acceleration records are only of Form b.

Careful study of Table 3.2 indicates the following tentative conclusions based upon the data obtained:

1. Records from the first shot on a bed at a given position may be significantly different from those of succeeding shots at the same position. The differences are primarily in arrival time, although the shape of the pulse may also differ markedly.

2. It is possible to obtain good reproducibility of effects for successive shots after the first shot on the bed.

3. It is possible to obtain good reproducibility of effects for each first shot on the bed.

4. It is possible to obtain reasonably good radial symmetry on both the first and later shots on the bed, although arrival times may differ in any shot.

5. The greatest differences in peak accelerations on a shot-to-shot basis occur in the vertical accelerations.

6. The difference in arrival time between the upper and lower accelerometer would correspond to a wave front having a curvature about twice as great as that associated with a spherical wave centered about the charge.

7. The average wave velocity in the sandbed based on relative time of arrival measurements at different model locations is approximately 800 fps, with variations of several hundred fps about this value.

6/ One control model was used in the isolation experiments, Tests 17, 18 and 19, and the data for this model also are listed in Table 3.2.

7/ Positive g-values refer to downstream acceleration.

Reference is made to Fig. 3.15 through 3.20 in support of these tentative conclusions. Figures 3.15 and 3.16 show the initial signals recorded at Positions 1 and 2 for the first, second, and third shots on the same bed. (The records are aligned on the basis of zero time as indicated by the detonation sensor.) The differences between the records from the first and the later shots are clearly evident, as is the marked similarity between the results for Shots 2 and 3. Figures 3.17 and 3.18 compare the results obtained at the same position for successive first shots on the bed. The similarity in most instances is truly striking, except for the extreme differences in vertical acceleration. Figures 3.19 and 3.20 illustrate the extent of radial symmetry obtained in the first and third shots on a bed.

3.6 ISOLATION TESTS

Tests 17, 18, and 19 involved isolation models. The records obtained are summarized in Table 3.1 and are presented in Fig. 3.21 and Appendix A, Fig. A-24 through A-31. The position of the models in the bed is shown in Fig. 3.14 and the models themselves are described in Section 3.2.2. Figures 3.22 and 3.23 show the models in place in the bed.

Inspection of records indicates that the foam isolation material is definitely effective in attenuating peak acceleration. The peak upper horizontal acceleration from Model 1 in Test 19 is about 1.9 g whereas the corresponding acceleration for the control model is 10 g; the effective period of the pulse has increased from about 1 msec for the control model to almost 9 msec for the isolation model. While there are some quantitative differences in results from the three tests, the essential reproducibility of effects is clearly evident. The 1/2-in. thickness of foam (Model 1) appears slightly more effective than the 1/4-in. thickness (Model 2), in the sense that the acceleration amplitude is somewhat smaller for the former. Direct comparison is difficult since the two models were not at the same radial location in the bed (see Fig. 3.14). This result would be expected, of course, at the same location, since the thicker material is effectively a softer spring.

Model 3 in Test 17 consisted of a control model mounted on a steel rod (see Section 3.2.2), which was embedded in the sand. An air void was created between the model and the sand by using a 5-in.-diameter section

of stove pipe as a retaining wall (Fig. 3.23a). This setup was an attempt to simulate a structure founded on deep "piles" and otherwise completely isolated from its surroundings.[8] The acceleration records shown in Fig. A-24 through A-26 indicate that this scheme was not particularly effective. The horizontal accelerations suggest that the model was vibrating as a rigid mass atop a column. An effective column length of 6 in. was computed on the basis of the measured period. The explanation that the top 6 in. of the 18-in. "pile" might be effectively unsupported by the sand seems plausible.

In Tests 18 and 19, the air void was filled with pre-expanded polystyrene beads, approximately 0.05 in. in diameter, which were intended to act as a damping agent (Fig. 3.23b). That this proved effective to only a slight degree can be seen in the records of Fig. A-27 through A-31.

---

[8] The bore of this model was probably in contact with loose sand.

Table 3.1

SUMMARY OF EXPERIMENTS

Test No.	Shot No. on Bed	Crater Area Vibrated	Recorder	Records Obtained
7	1	-	A	No records
			B	1 l.h., 2 l.h., 4 l.h.[c], air pressure
			C	1 v., 2 v.[c], 4 u.h.[c], free field
8	1	-	A	1 u.h., 2 u.h.[a], 3 u.h., 4 v.[a]
			B	1 l.h., 2 l.h., 4 l.h.[c], air pressure
			C	1 v., 2 v.[a], 4 u.h.[c], free field
9	2	no	-	-
10	3	no	-	-
11	4	yes	A	1 u.h., 2 u.h.[a], 3 u.h.[a], 4 v.[c]
			B	1 l.h.[b], 2 l.h., 4 l.h., air pressure
			C	1 v., 2 v., 4 u.h.[c], free field
12	5	yes	A	1 u.h., 2 u.h.[a], 3 u.h.[a], 3 u.h.[a], 4 v.[c]
			B	1 l.h.[b], 2 l.h., 4 l.h., air pressure
			C	1 v., 2 v., 4 u.h.[c], free field
13	1	-	A	1 u.h., 2 u.h., 3 l.h., 4 v.[b]
			B	1 l.h., 2 l.h., 3 l.h., 4 l.h.
			C	1 v., 2 v., 4 u.h., free field
14	2	yes	air blast	
15	3	yes	A	1 u.h., 2 u.h., 3 l.h., 4 v.
			B	1 l.h., 2 l.h., 3 l.h., 4 l.h.
			C	1 v., 2 v., 4 u.h., free field
16	4	yes	A	1 u.h., 2 u.h., 3 l.h., 4 v.
			B	1 l.h., 2 l.h., 3 l.h., 4 l.h.
			C	1 v., 2 v., 4 u.h., free field
17	1	-	A	1 u.h.[c], 2 u.h.[c], 4 v., 3 u.h.
			B	1 l.h., 2 l.h., 4 l.h.[b], 3 l.h.
			C	1 v.[c], v.[c], 4 u.h., 3 v.
18	2	yes	A	1 u.h.[c], 2 u.h.[c], 4 v., 3 u.h.
			B	No record
			C	1 v., 2 v., 4 u.h., 3 v.
19	3	yes	A	1 u.h., 2 u.h., 4 v., 3 u.h.
			B	1 l.h., 2 l.h., 4 l.h., 3 l.h.
			C	1 v., 2 v.[c], 4 u.h.[a], 3 v.

* Numbers refer to models whose position is shown in Fig. 3.12 and 3.14. Abbreviations indicate by which accelerometer the record was obtained: u.h., upper horizontal; l.h., lower horizontal; v., vertical. Superscript letters indicate: a , nonrepresentative trace; b, off scope; c, gain too low.

Table 3.2

COMPARISON OF RESULTS

Position No.*	Test No.	Model and Gage **	Arrival Time, msec	Shot No. on Bed	Crater Area Vibrated	Coordinates of Typical Record Forms							
						a		b		c		d	
						msec	g	msec	g	msec	g	msec	g
1	13	1 u.h.	3.13	1	-	3.28	5.92	3.34	0	3.50	15.76	3.99	0
	15	1 u.h.	3.64	3	yes	3.94	4.27	3.97	0	4.26	8.55	4.70	0
	16	1 u.h.	3.90	4	yes	4.00	6.06	4.10	0	4.32	10.26	5.04	0
	13	1 l.h.	3.45	1	-	-	-	-	-	3.80	9.03	4.25	0
	15	1 l.h.	4.18	3	yes	-	-	-	-	4.50	13.92	5.41	0
	16	1 l.h.	4.17	4	yes	-	-	-	-	4.50	16.03	5.43	0
	13	1 v.	3.36	1	-	-	-	-	-	3.67	42.40	4.15	0
	15	1 v.	4.04	3	yes	-	-	-	-	4.33	37.40	5.57	0
	16	1 v.	4.07	4	yes	-	-	-	-	4.35	40.80	5.60	0
	17	4 u.h.	3.15	1	-	3.39	7.45	3.43	0	3.62	18.65	4.06	0
	18	4 u.h.	4.13	2	yes	4.27	4.18	4.36	0	4.50	15.85	4.85	0
	19	4 u.h.	4.06	3	yes	-	-	-	-	4.62	10.00	5.16	0
	17	4 l.h.	3.32	1	-	-	-	-	-	-	-	-	-
	19	4 l.h.	4.20	3	yes	-	-	-	-	4.45	18.30	4.79	0
	17	4 v.	2.79	1	-	-	-	-	-	3.10	7.43	3.56	0
	18	4 v.	3.76	2	yes	-	-	-	-	4.05	17.50	4.46	0
	19	4 v.	3.94	3	yes	-	-	-	-	4.19	10.45	4.60	0
	8	1 u.h.	3.08	1	-	3.40	3.05	3.52	0	3.71	11.88	4.19	0
	9	1 u.h.	2.85	2	no	3.13	1.84	3.40	0	3.88	4.43	-	-
	11	1 u.h.	3.12	4	yes	3.32	9.81	3.42	0	3.70	13.78	4.07	0
	12	1 u.h.	3.21	5	yes	3.38	5.03	3.43	0	3.67	16.31	4.06	0
	13	2 u.h.	3.08	1	-	3.30	4.35	3.34	0	3.46	17.08	4.03	0
	15	2 u.h.	3.66	3	yes	3.94	2.66	4.16	0	4.57	5.49	4.95	0
	16	2 u.h.	3.79	4	yes	3.99	3.73	4.17	0	4.57	5.95	4.93	0

* See Fig. 3.14 for position numbers

** Numbers refer to models whose position is given in the column "Position No." above. Abbreviations indicate by which accelerometer the record was obtained (see Fig. 3.3): u.h., upper horizontal; l.h., lower horizontal; v., vertical.

Table 3.2 (continued)

COMPARISON OF RESULTS

Position No.*	Test No.	Model and Gage **	Arrival Time, msec	Shot No. on Bed	Crater Area Vibrated	Coordinates of Typical Record Forms							
						a		b		c		d	
						msec	g	msec	g	msec	g	msec	g
2	7	1 l.h.	3.46	1	-	-	-	-	-	3.73	10.04	4.19	0
	8	1 l.h.	3.46	1	-	-	-	-	-	3.96	10.78	4.75	0
	9	1 l.h.	3.04	2	no	-	-	-	-	3.96	5.65	5.34	0
	11	1 l.h.	3.47	4	yes	-	-	-	-	-	-	4.56	0
	12	1 l.h.	3.37	5	yes	-	-	-	-	-	-	4.78	0
	13	2 l.h.	3.37	1	-	-	-	-	-	3.85	7.42	4.45	0
	15	2 l.h.	4.22	3	yes	-	-	-	-	4.51	8.92	5.43	0
	16	2 l.h.	4.15	4	yes	-	-	-	-	4.48	11.22	5.32	0
	7	1 v.	3.87	1	-	-	-	-	-	4.21	24.28	5.00	0
	8	1 v.	3.32	1	-	-	-	-	-	3.64	14.72	4.55	0
	9	1 v.	3.13	2	no	-	-	-	-	3.61	13.10	4.38	0
	11	1 v.	3.51	4	yes	-	-	-	-	3.75	40.4	4.93	0
	12	1 v.	3.25	5	yes	-	-	-	-	3.71	40.98	6.57	0
	13	2 v.	3.27	1	-	-	-	-	-	3.50	13.70	3.81	0
	15	2 v.	3.81	3	yes	3.97	5.18	4.07	0	4.24	18.70	4.57	0
	16	2 v.	4.05	4	yes	-	-	-	-	4.31	21.65	4.54	0
3	13	4 v.	2.83***	1	-	-	-	-	-	-	-	-	-
	15	4 v.	3.60	3	yes	-	-	-	-	3.76	15.98	4.22	0
	16	4 v.	3.60	4	yes	-	-	-	-	3.80	13.05	4.25	0
	13	4 l.h.	3.39	1	-	-	-	-	-	3.50	9.06	4.30	0
	15	4 l.h.	4.22	3	yes	-	-	-	-	4.58	15.24	4.79	0
	16	4 l.h.	4.07	4	yes	-	-	-	-	4.31	14.58	4.62	0
	13	4 u.h.	3.41	1	-	3.62	7.20	3.73	0	3.92	17.30	4.18	0
	15	4 u.h.	4.03	3	yes	4.32	6.23	4.42	0	4.66	8.30	5.14	0
	16	4 u.h.	3.94	4	yes	4.14	2.92	4.23	0	4.49	8.01	4.95	0

*** Arrival time is uncertain.

Table 3.2 (continued)

COMPARISON OF RESULTS

Position No.*	Test No.	Model and Gage**	Arrival Time, msec	Shot No. on Bed	Crater Area Vibrated	Coordinates of Typical Record Forms							
						a		b		c		d	
						msec	g	msec	g	msec	g	msec	g
4	13	3 l.h.	4.28	1	-	-	-	-	-	4.67	3.28	5.28	0
	15	3 l.h.	4.91	3	yes	-	-	-	-	5.49	2.26	5.64	0
	16	3 l.h.	4.90	4	yes	-	-	-	-	5.52	2.21	6.02	0
5	13	5 l.h.	4.73	1	-	-	-	-	-	5.15	7.47	5.51	0
	15	5 l.h.	5.64	3	yes	-	-	-	-	5.97	4.25	6.63	0
	16	5 l.h.	5.47	4	yes	-	-	-	-	5.79	4.49	6.38	0
6	8	2 u.h.	4.91	1	-	-	-	-	-	5.98	1.80	6.67	0
	11	2 u.h.	5.80	4	yes	-	-	-	-	6.23	2.83	6.77	0
	12	2 u.h.	5.47	5	yes	-	-	-	-	5.89	2.13	6.50	0
	7	2 l.h.	5.42	1	-	-	-	-	-	5.90	2.58	6.37	0
	8	2 l.h.	5.35	1	-	-	-	-	-	6.42	2.08	6.74	0
	9	2 l.h.	4.75	2	no	-	-	-	-	5.67	2.08	6.24	0
	11	2 l.h.	5.43	4	yes	-	-	-	-	5.99	3.43	6.71	0
	12	2 l.h.	5.15	5	yes	-	-	-	-	5.79	4.25	6.50	0
	8	2 v.	5.03	1	-	5.43	0.95	5.74	0	6.32	2.56	6.75	0
	9	2 v.	4.93	2	no	-	-	-	-	5.44	1.99	6.08	0
	11	2 v.	5.49	4	yes	-	-	-	-	6.09	3.45	6.67	0
7	8	3 u.h.	4.07***	1	-	4.47	0.51	4.69	0	4.94	1.26	5.11	0
	11	3 u.h.	5.66	4	yes	-	-	-	-	6.17	3.07	6.71	0
	12	3 u.h.	5.13	5	yes	-	-	-	-	5.86	3.38	6.23	0
8	11	4 l.h.	6.07	4	yes	-	-	-	-	6.45	0.44	6.76	0
	12	4 l.h.	6.16	5	yes	-	-	-	-	6.54	1.10	6.88	0

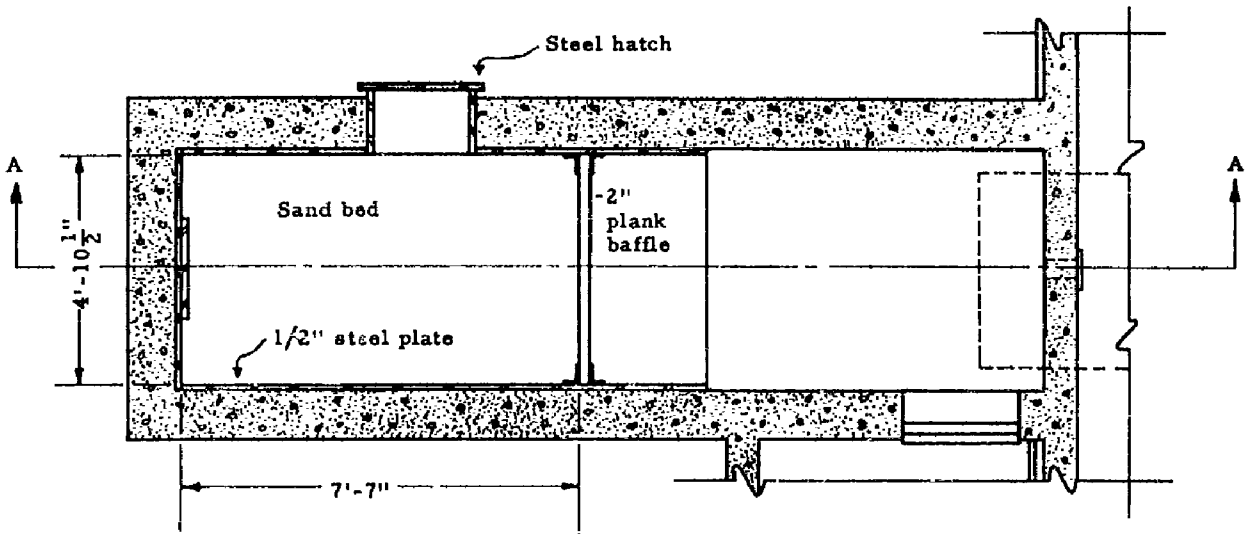

a. Partial plan.

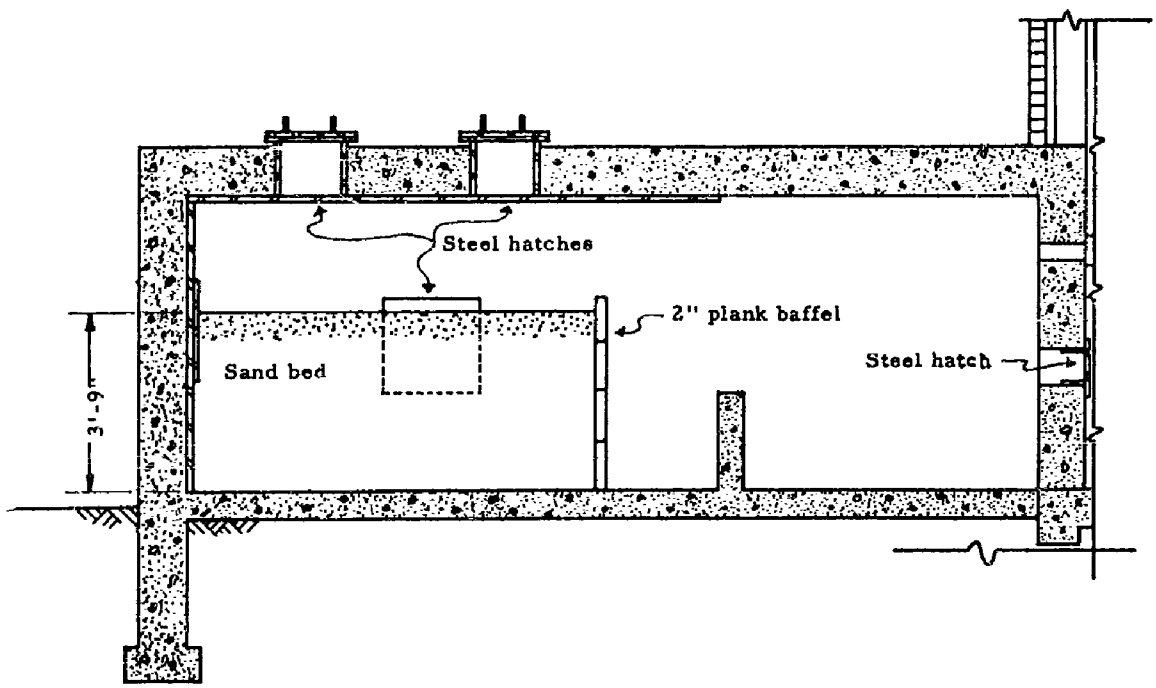

b. Section A-A.

Figure 3.1 Test cell.

Figure 3.2 Interior view of test cell.

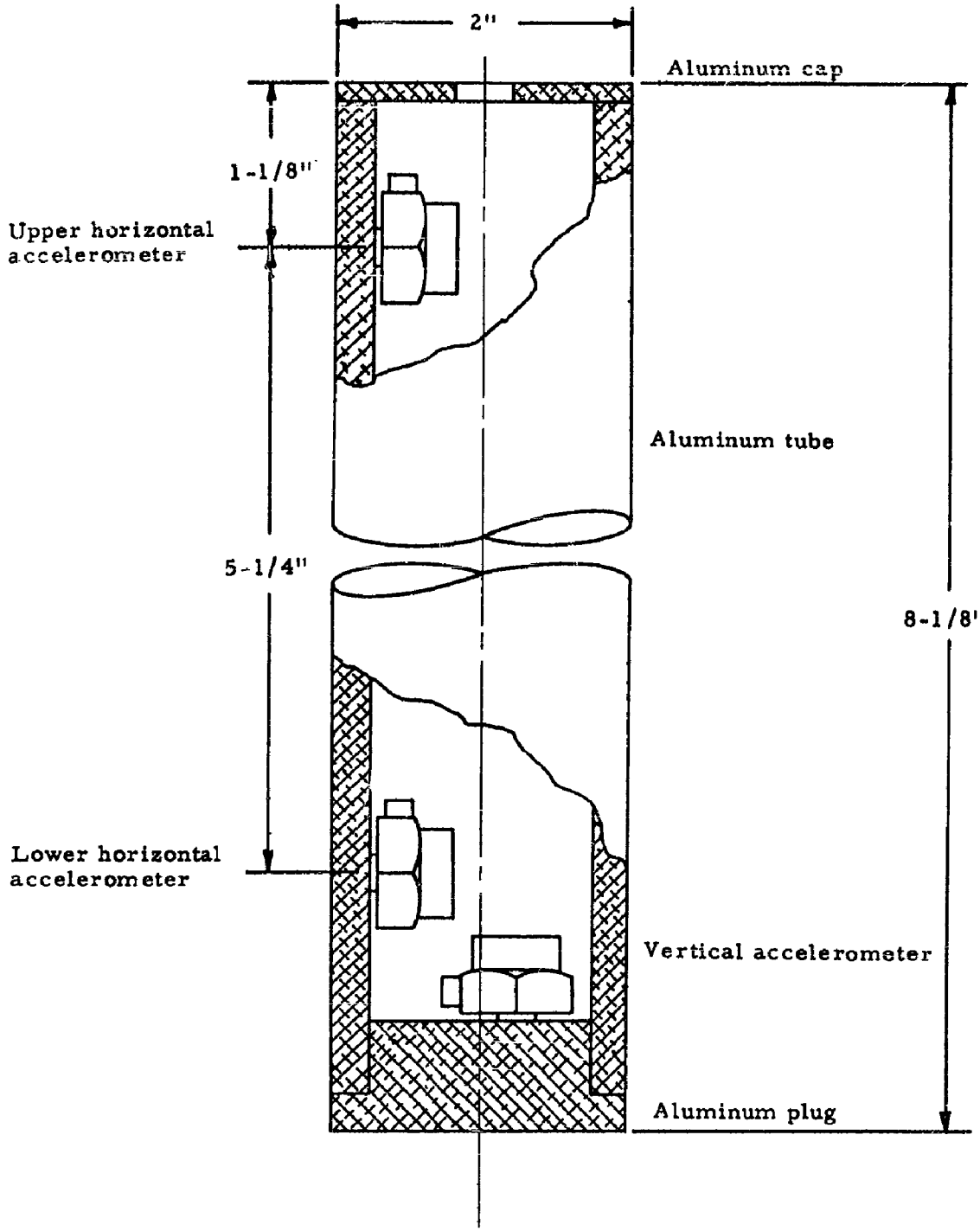

Figure 3.3 Test model.

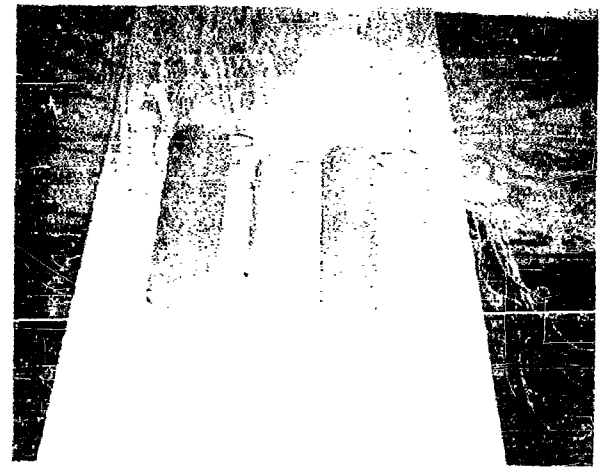

Figure 3.4 Polyurethane foam isolation models:
No. 1 - 1/2-in. thickness,
No. 2 - 1/4-in. thickness,
No. 4 - control model.

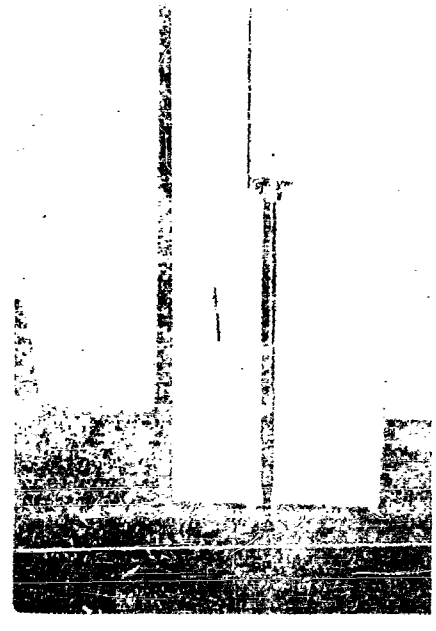

Figure 3.5 Pile isolation model.

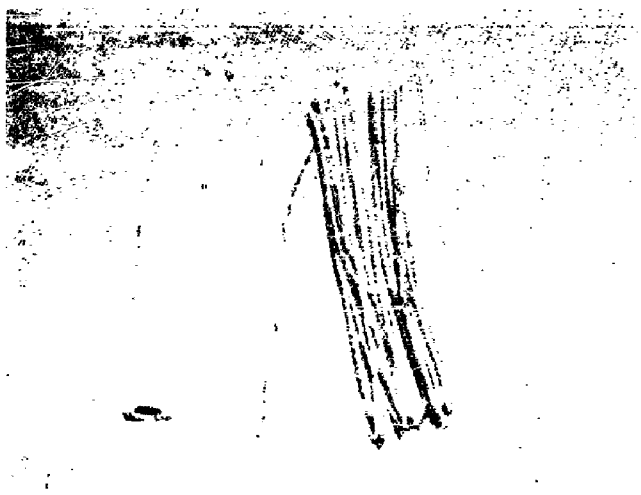

Figure 3.6 Tetryl charge and detonator.

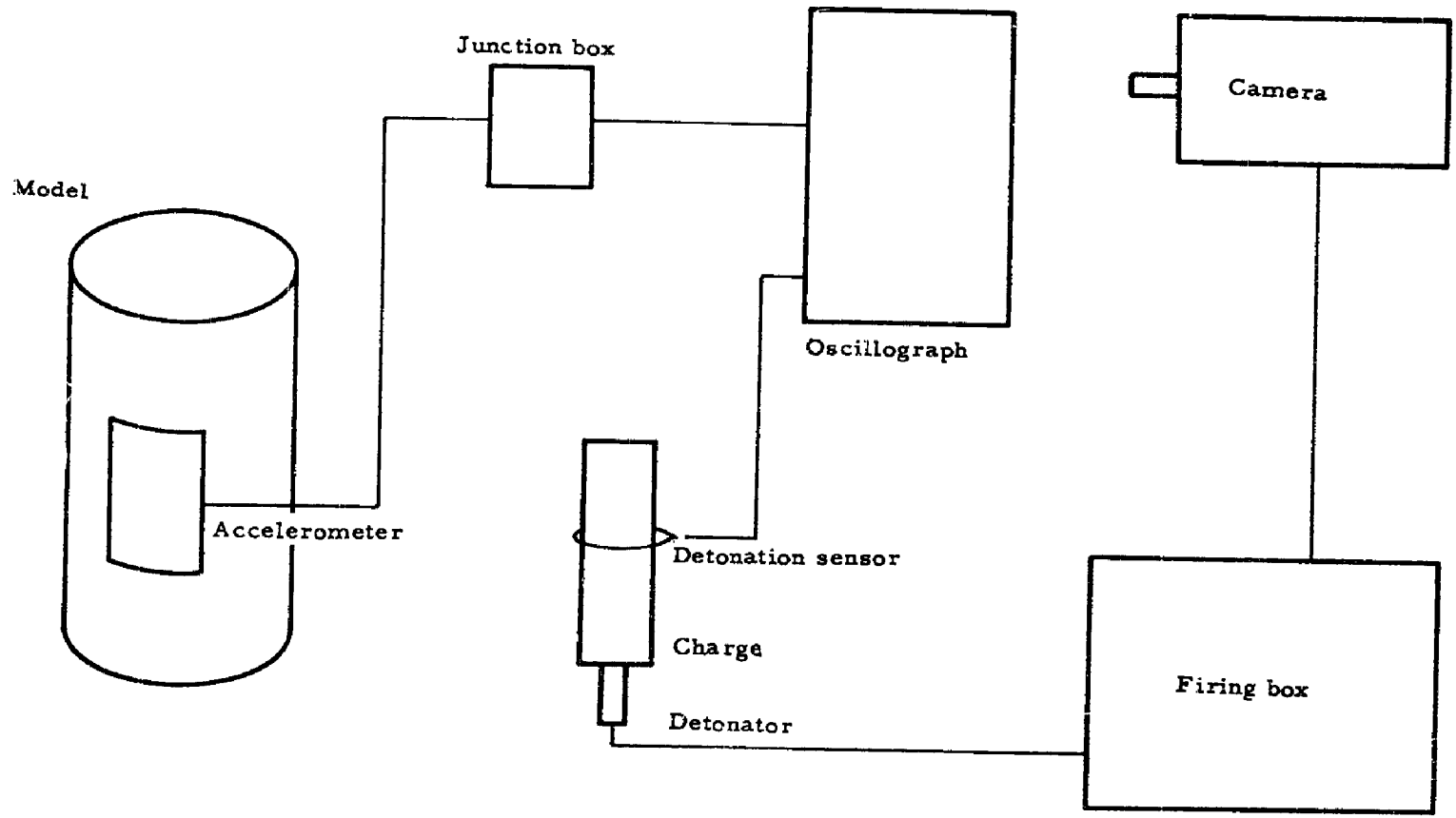

Figure 3.7 Diagram of the instrumentation and control system of the recording equipment.

Figure 3.8 View of crater.

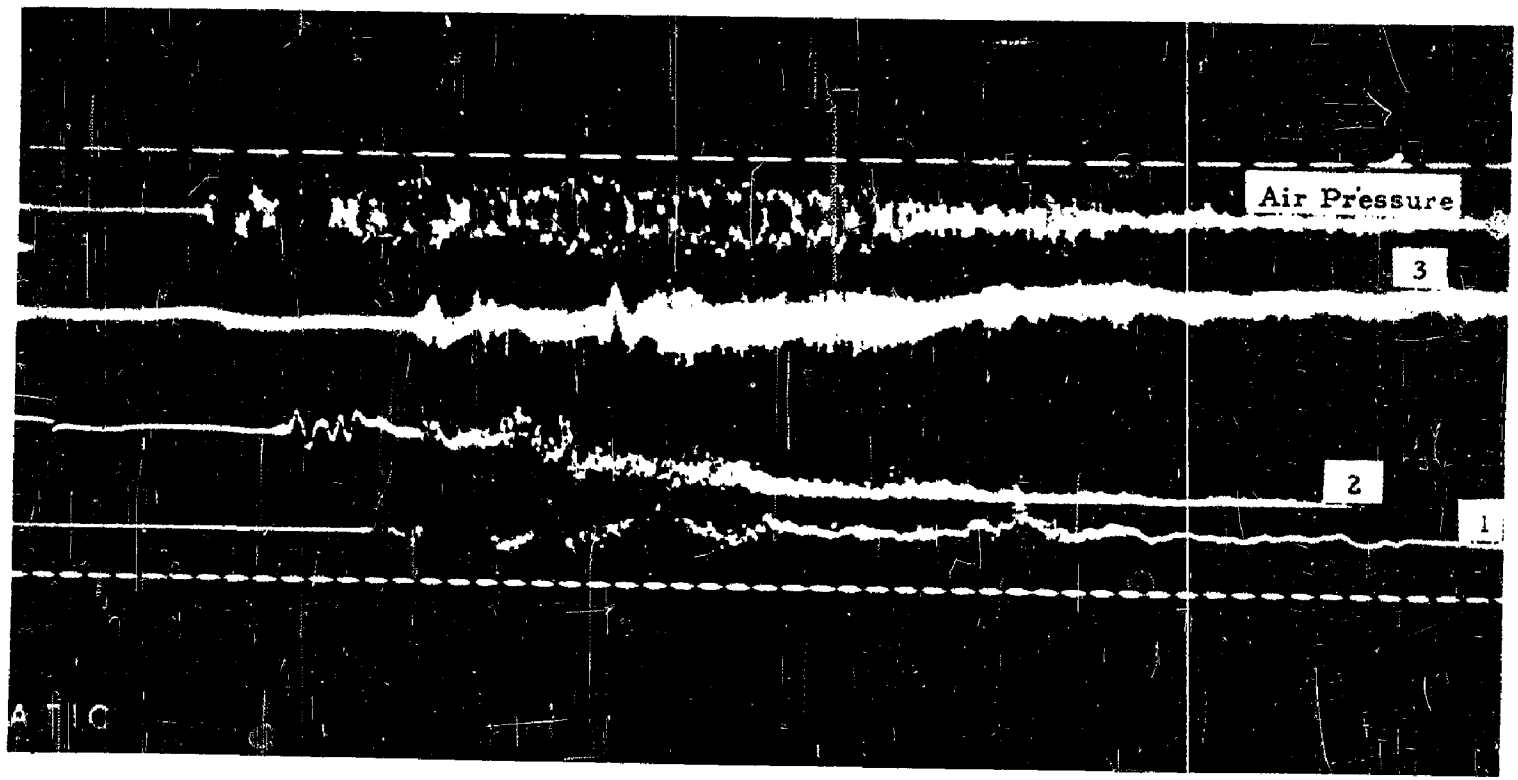

Figure 3.9 Test 3 accelerometer records. Accelerometers in models 1, 2 and 3, and air pressure readings above model 3 .

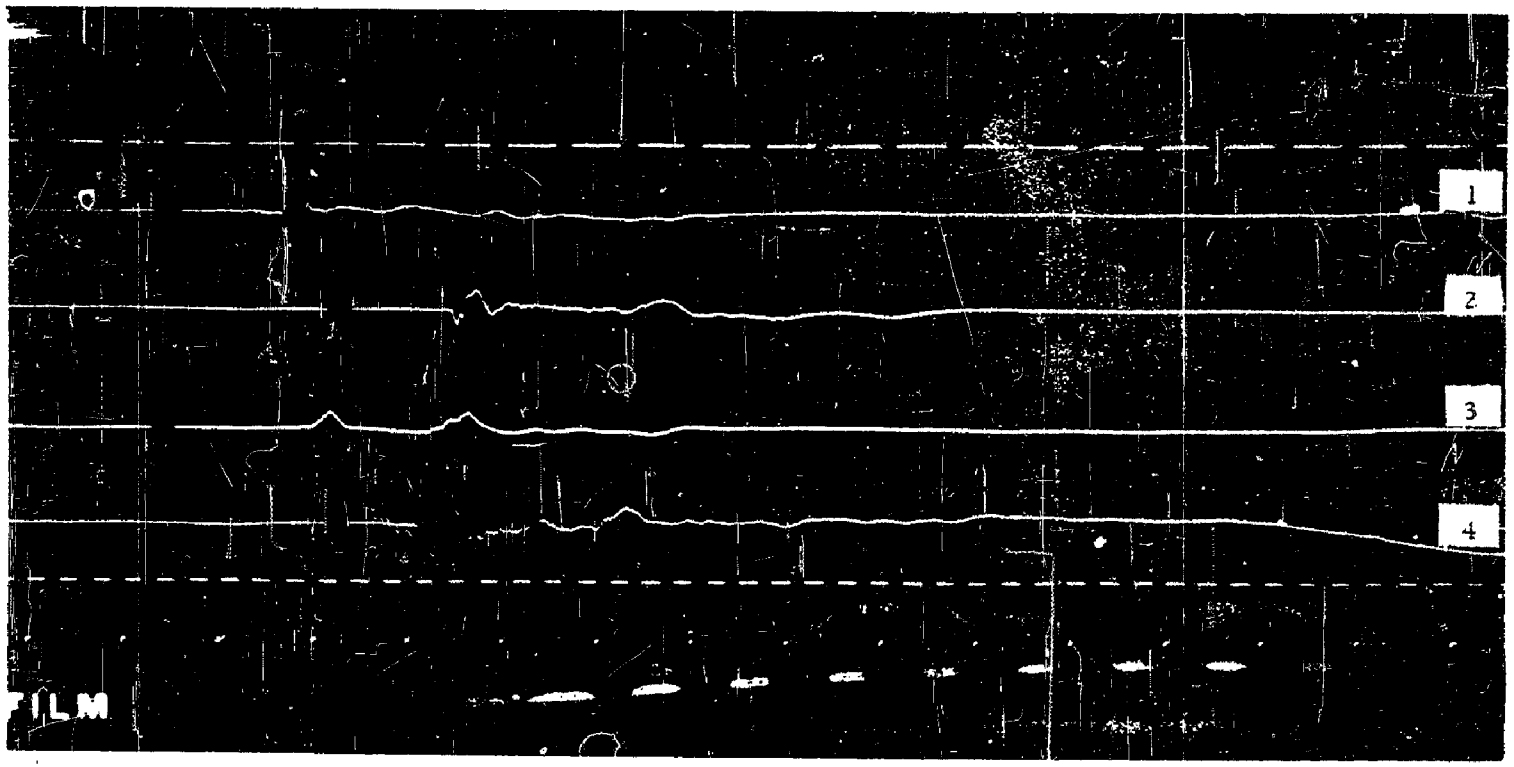

Figure 3.10 Test 16 accelerometer records. Upper horizontal accelerometer in models 1 and 2, lower horizontal accelerometer in model 3, and vertical accelerometer in model 4.

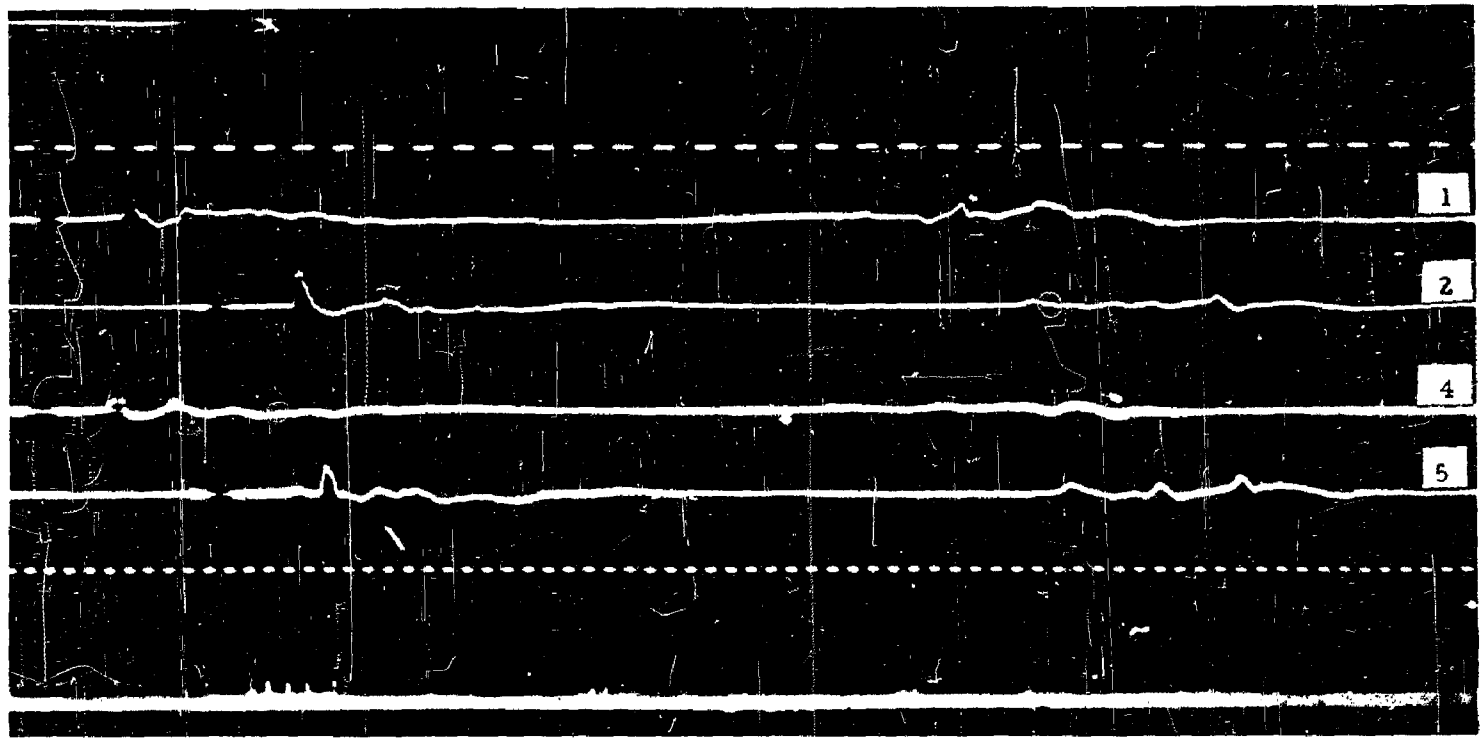

Figure 3.11 Test 16 accelerometer records. Lower horizontal accelerometer in models 1, 2, 4 and 5

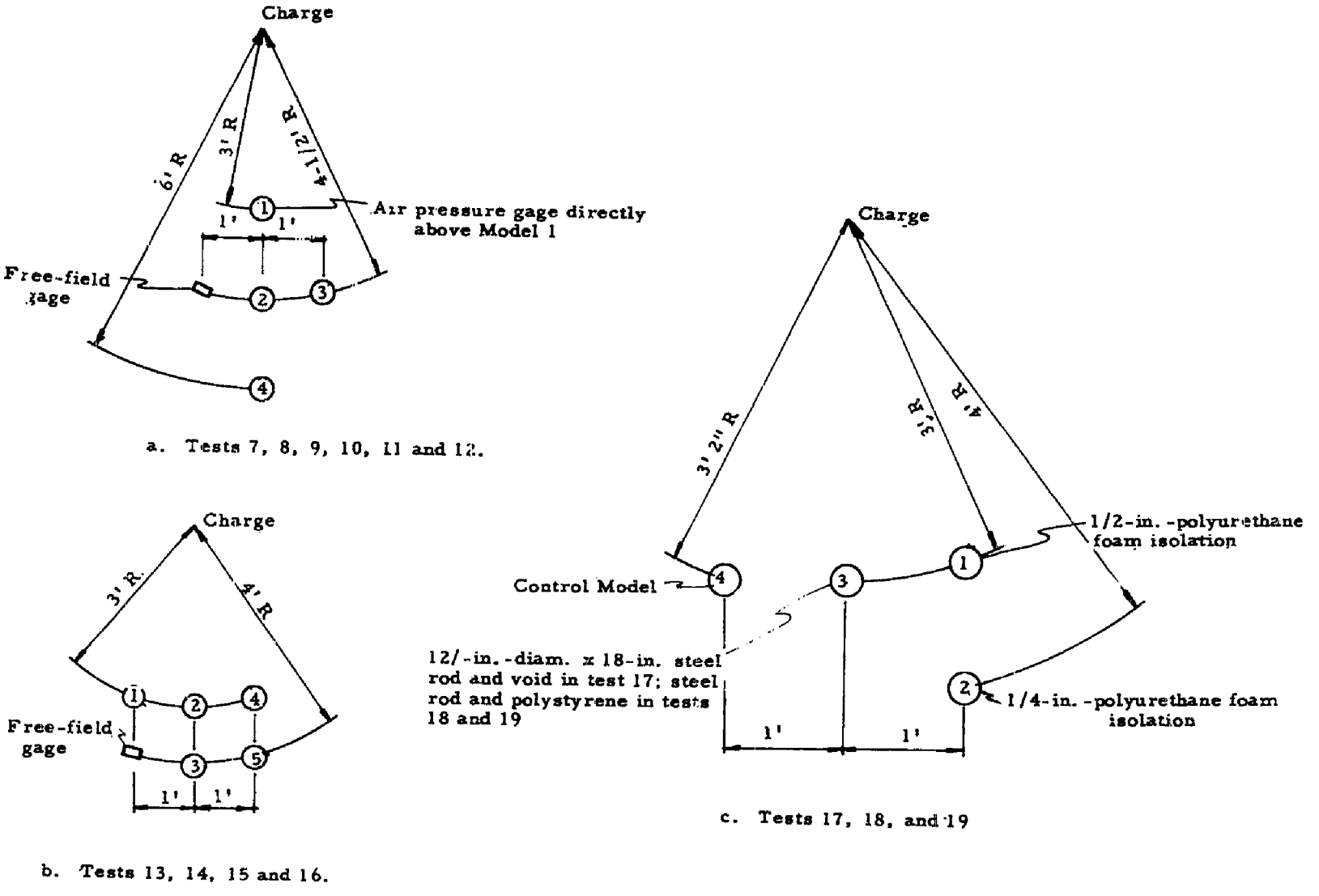

Figure 3.12 Model numbers and locations for tests 7 through 19.

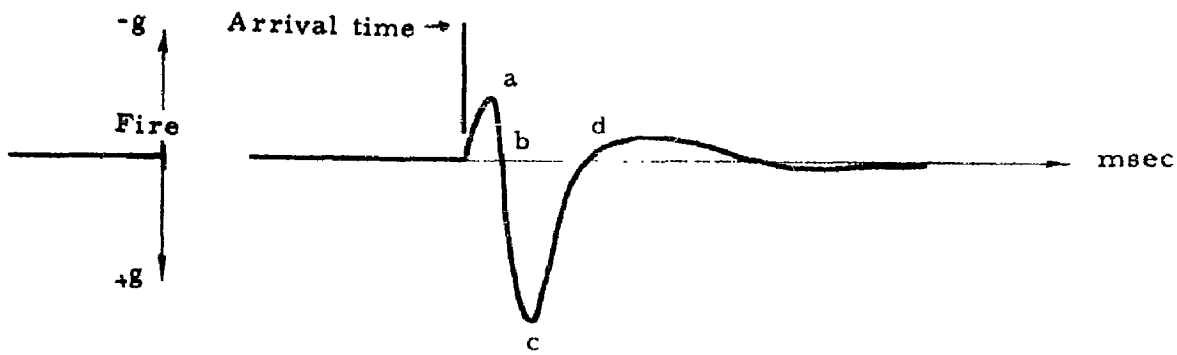

a. Upper horizontal and vertical acceleration traces.

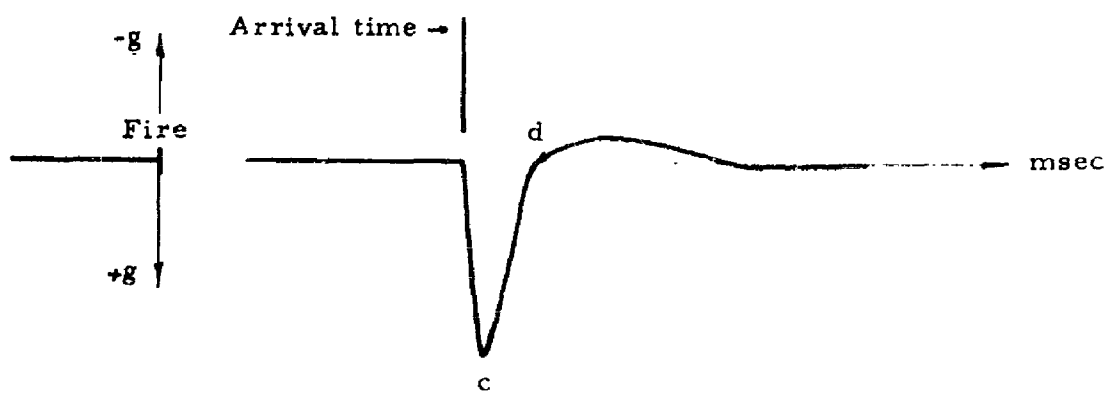

b. Upper horizontal, lower horizontal, and vertical acceleration traces.

Note: Positive horizontal acceleration vector points downstream; positive vertical acceleration vector points downward.

Figure 3.13 Typical forms of acceleration traces.

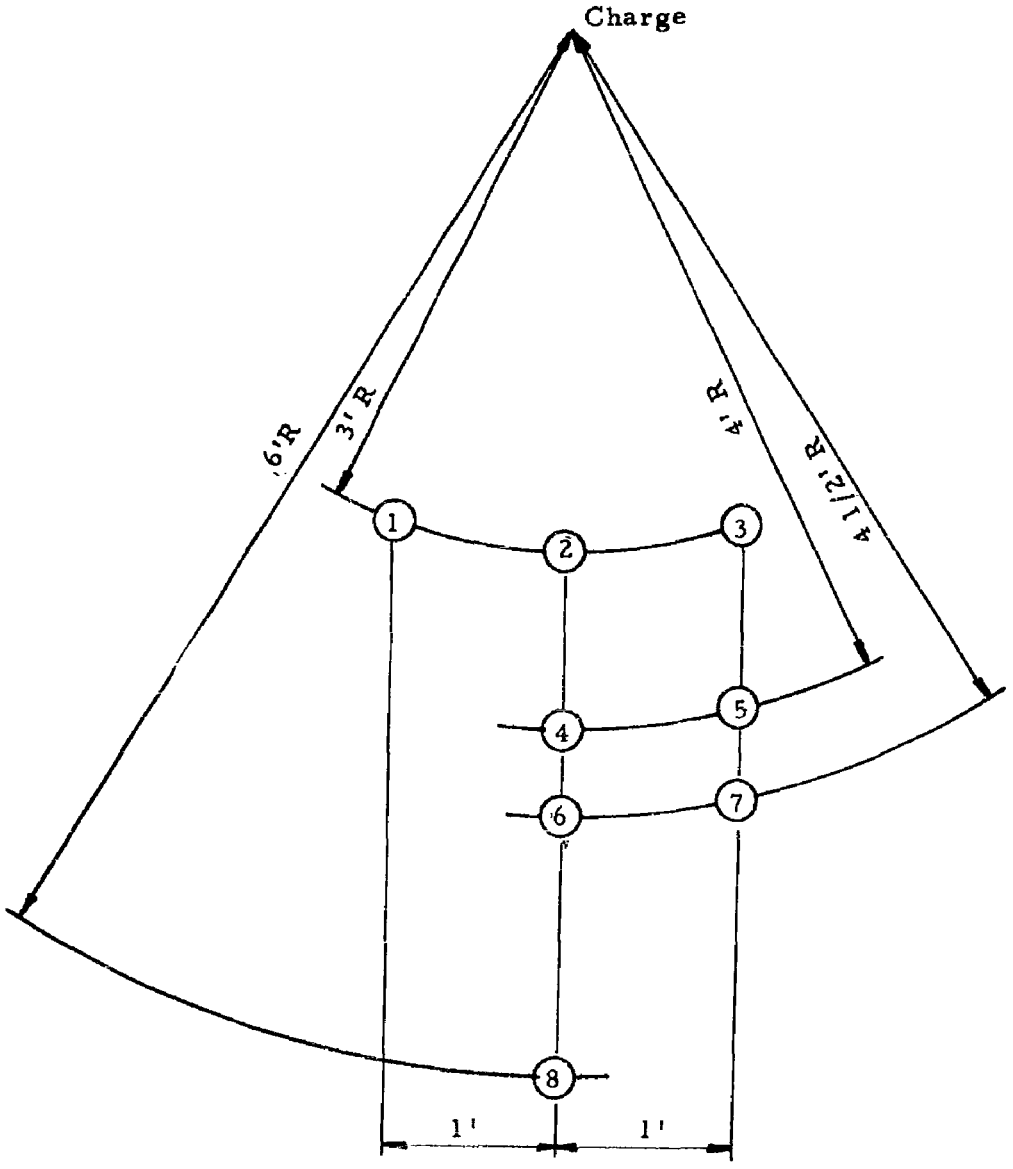

Figure 3.14 Model positions for tests 7 through 19.

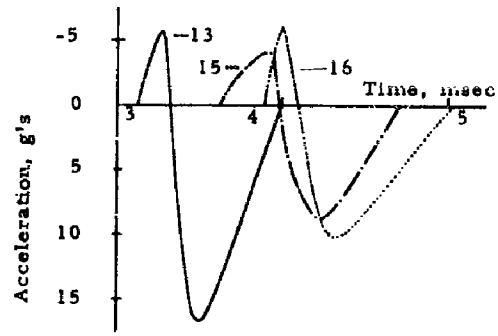

a. Upper horizontal accelerometer.

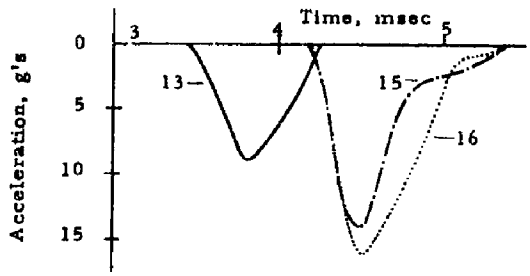

b. Lower horizontal accelerometer.

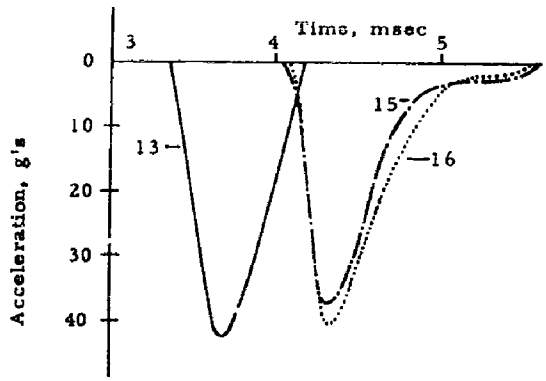

c. Vertical accelerometer.

Figure 3.15 Comparison of tests 13, 15, and 16 at position 1.

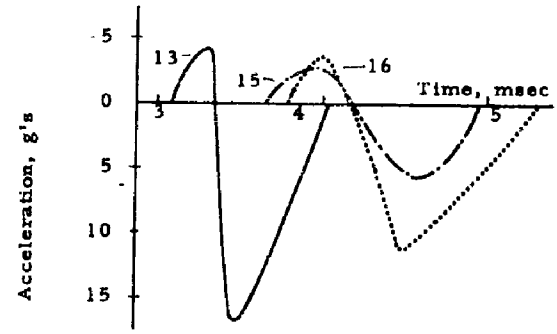

a. Upper horizontal accelerometer.

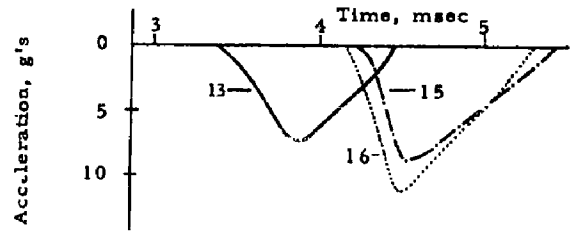

b. Lower horizontal accelerometer.

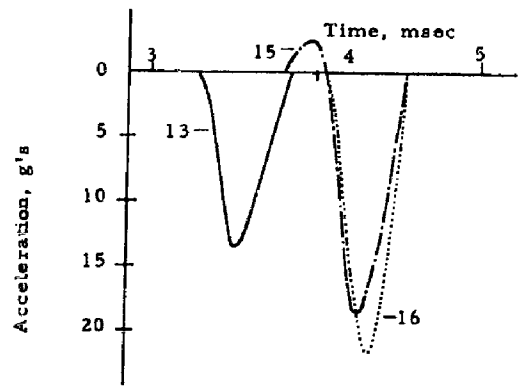

c. Vertical accelerometer.

Figure 3.16 Comparison of tests 13, 15, and 16 at position 2.

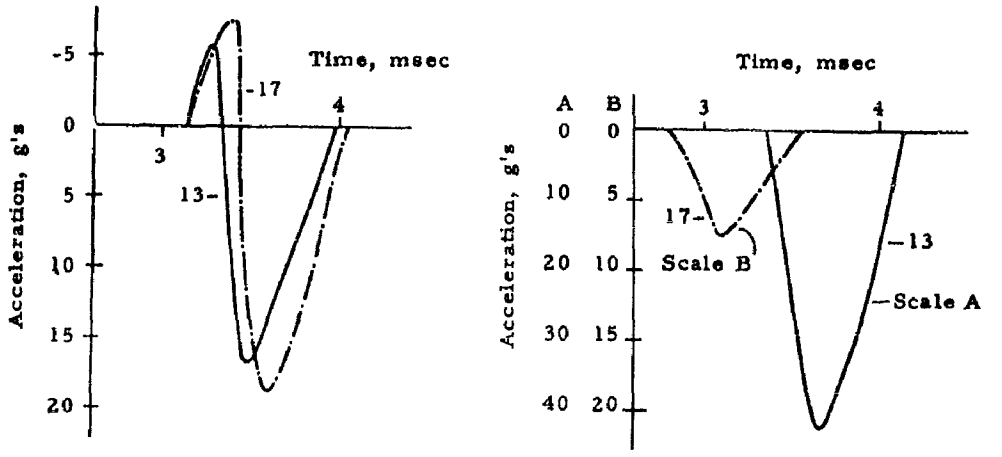

a. Upper horizontal accelerometer b. Vertical accelerometer

Figure 3.17 Comparison of tests 13 and 17 at position 1.

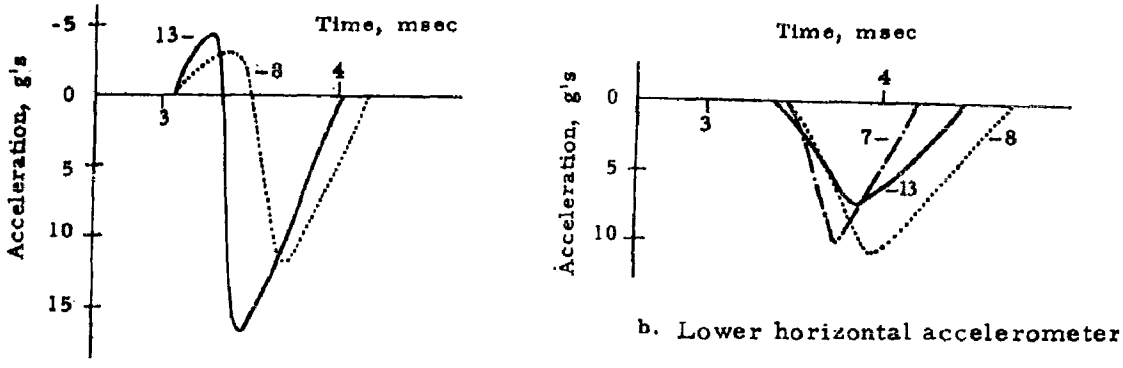

b. Lower horizontal accelerometer

a. Upper horizontal accelerometer

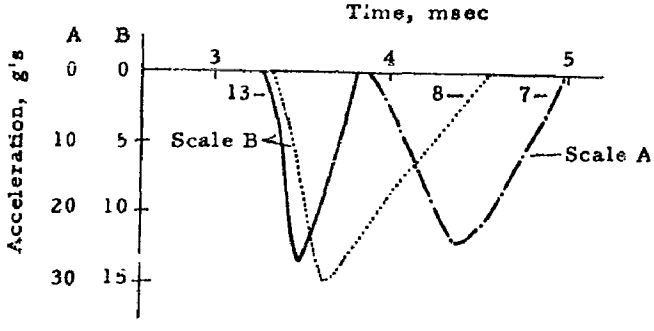

c. Vertical accelerometer

Figure 3.18 Comparison of tests 7, 8, and 13 at position 2.

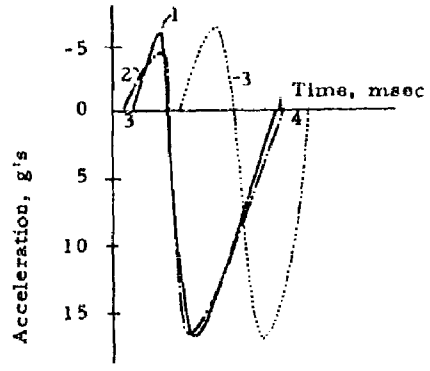

a. Upper horizontal accelerometer.

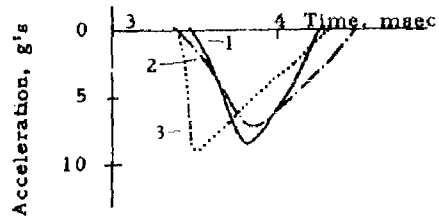

b. Lower horizontal accelerometer.

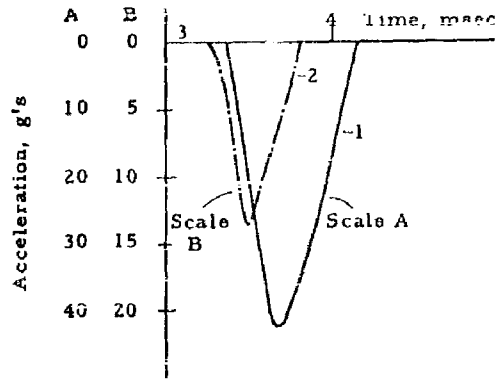

c. Vertical accelerometer.

Figure 3.19 Comparison of positions 1, 2, and 3 in test 13.

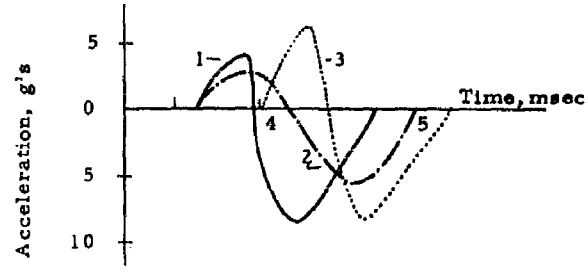

a. Upper horizontal accelerometer.

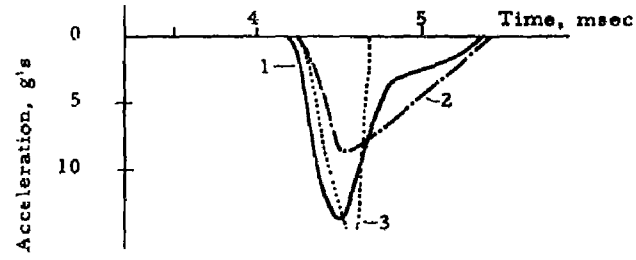

b. Lower horizontal accelerometer.

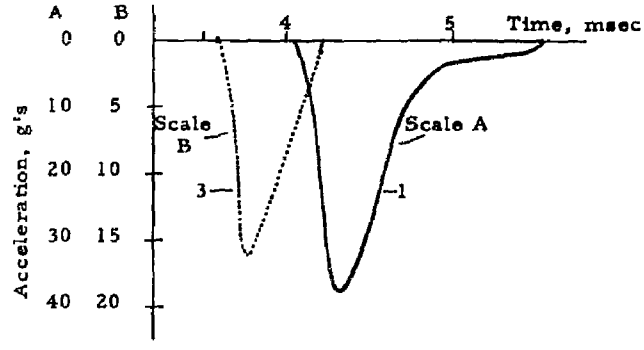

c. Vertical accelerometer.

Figure 3.20 Comparison of positions 1, 2, and 3 in test 15.

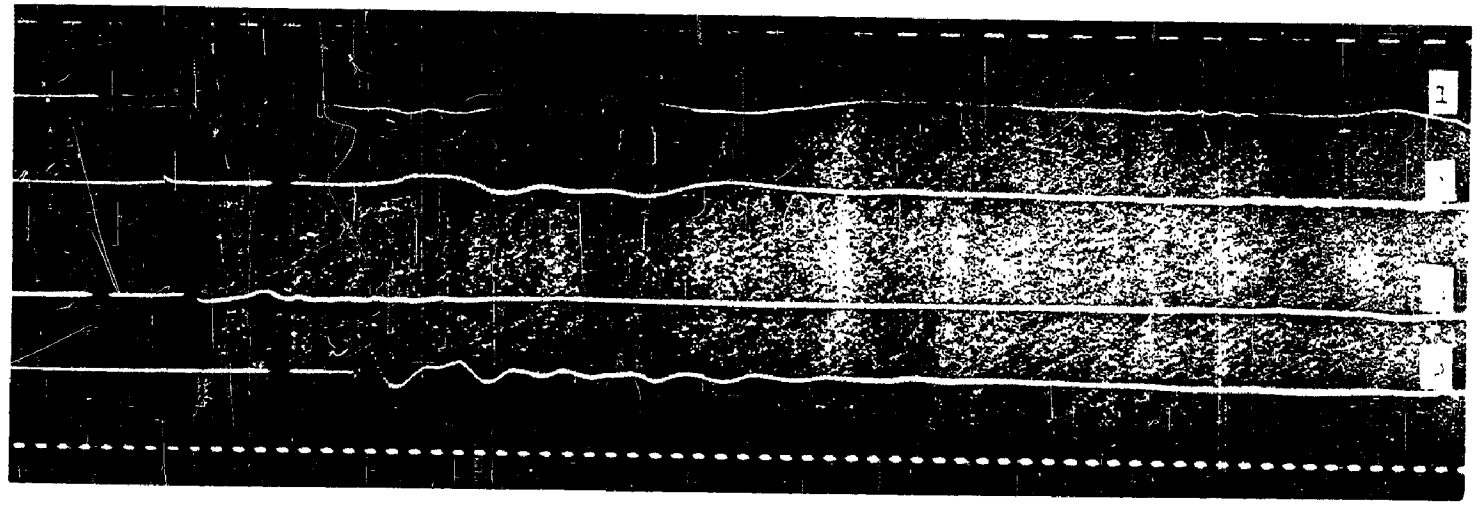

Figure 3.21 Tests 19 accelerometer records. Lower horizontal accelerometer in models 1, 2, 3, and 4.

a. One-half-inch foam isolation (Model No. 1).

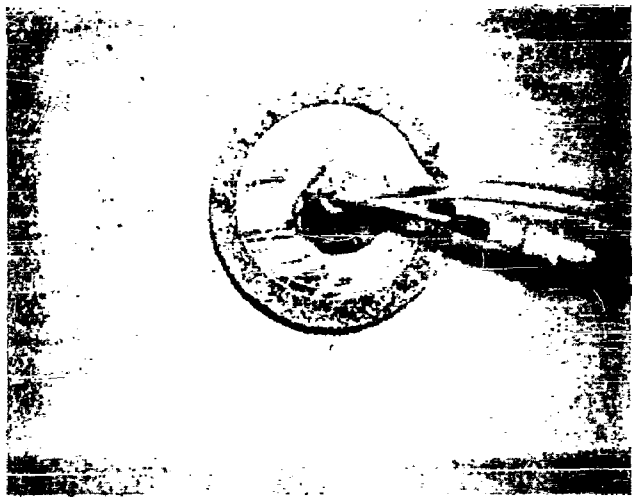

b. One-quarter-inch foam isolation (Model No. 2).

Figure 3.22 Polyurethane foam isolation models in place.

a. Void isolation (Model No. 3, test 17).

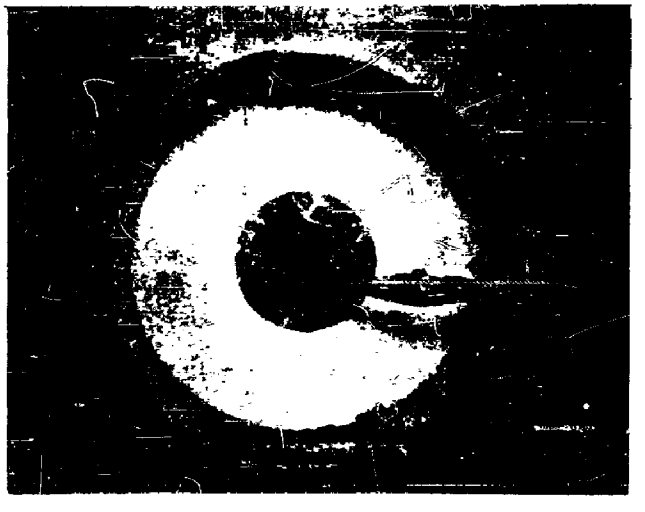

b. Polystyrene beads (Model No. 3, tests 18 and 19).

Figure 3.23 Pile isolation model in place.

Chapter 4

THEORETICAL INVESTIGATIONS

The general problem of shock transmission in soils and soil-structure interaction is of such complexity that theoretical treatment cannot supplant the need for experimentation at this time. However, theoretical considerations of any sort which provide aid in the direction and interpretation of the experiments clearly are desirable. One can list three major problem areas of interest, namely, (1) free-field phenomena, (2) motion of the control model, and (3) motion of the isolation model. The latter two problems refer to the sand-model interaction and the sand-isolation-model interaction, respectively.

4.1 FREE-FIELD THEORY

4.1.1 General Requirements. By free-field theory, one generally refers to a means of predicting particle motion and stress distribution throughout the medium in terms of the energy release of the detonation. The formulation of such a theory is a most formidable undertaking, existing theories being generally inadequate, and one that properly requires independent study. In the present application, however, we are mainly interested in interpreting the response of the model structures for some given free-field input, and in this restricted sense we require a considerably less sophisticated free-field theory. After some deliberation, it was decided to base a free-field theory on the assumption of a linearly elastic sand and, moreover, to treat this as a one-dimensional problem, [1/] in so far as the horizontal component of the disturbance is concerned. A separate treatment for motions in the vertical direction is possible, but was not considered explicitly.

It is well appreciated that experimental data obtained under field conditions tend to discredit the assumption of elastic action, and it would be a bit too much to hope for in any event, living as we are in a predominantly non-linear world. However, as stated above, we are interested primarily in the interaction problem, not in the more general problem of wave transmission, and these objections seem less significant when viewed in this manner.

[1/] An exception to this is the three-dimensional treatment of the Rayleigh surface wave presented in Section 4.2.

One must next consider the efficacy of a one-dimensional treatment. So far as free-field phenomena in the sand bed are concerned, we are faced at best (i.e., if effects of reflection from the sides of the sand container are neglected) with an axisymmetric three-dimensional problem. The sand-moedl interaction is generally three-dimensional and only at the loss of certain effects can it be considered as two-dimensional. To further reduce it to a one-dimensional problem requires some explanation. This is taken up in the following section, but some introductory remarks may be indicated here.

If the free-field phenomena are assumed to be largely one-dimensional within a given horizontal stratum, the interaction problem is two-dimensional. Since we are interested in the response of the model at times prior to the arrival of reflections from the sides of the sand container, our (horizontal) one-dimensional column of sand (containing the model) may be considered as infinite in length. From this point of view, there are three essential differences between the infinite one-dimensional column of sand and the two-dimensional semi-infinite lamina, namely: (1) Under a static force, the column of sand (and hence the model) will undergo an infinite displacement, whereas a localized force acting on a semi-infinite body produces a finite displacement. (2) In two dimensions, the soil-transmitted forces on the model are dependent to some extent on the geometry of the model, whereas in one dimension, geometry plays no role. And (3), in one dimension, particles downstream of the model are disturbed only as a consequence of the motion of the model, whereas in two dimensions, this effect contributes only in part to the downstream particle motion, which in turn influences the net force action on the model.

Of these three effects, it is believed that the first, i.e., the zero stiffness characteristic of the infinitely long, one-dimensional model, is most important. Accordingly, a modification of the one-dimensional formulation that tends to circumvent this objection is described in the following section. The second and third two-dimensional effects are neglected entirely. [2/] This most certainly does not mean, however, that a one-dimensional treatment is employed on the basis of its being wholly adequate; nothing could be less true. Quite simply put, to further complicate the mathematical formulation would practically rule out the possibility of obtaining numerical results with an

expenditure of time and effort compatible with the scope of this contract. For example, it was not possible to obtain a closed-form solution to the control-model response problem when the incident stress pulse was assumed to be of the Rayleigh wave type.

4.1.2 Rayleigh Surface Waves. It was argued in the previous section that a rigorous free-field theory was required only to the extent that it provided a satisfactory basis for formulating the sand-model interaction problem and that, for this purpose, elastic action of the sand seemed admissable. Based on a measured wave-propagation speed of about 800 fps and assuming the duration of the mean acceleration to be approximately equal to the period of the free-field motion, the wave length of the surface wave is indicated to be about ten inches. This suggests that the 2-in.-diameter control model may be largely following the motion of the free field. Accordingly, it was decided to investigate the properties of a Rayleigh surface wave for the conditions of the sand bed. This view was supported by the results presented in Ref 17, to the effect that the Rayleigh wave solution was in good agreement with observed surface strains in a steel block under an impulse surface load.

The existence and propagation of Rayleigh waves are familiar phenomena in the field of elastic wave mechanics, which have been substantiated by experimental studies in stress-wave propagation and by seismic observations during earthquakes and blasting operations. These waves are generated in their most elementary form by the passage of plane shear and dilatational waves parallel to the free surface of a semi-infinite, elastic half-space. The requirements of zero stress on the free surface are satisfied by the existence of a third plane wave, called the Rayleigh surface wave, which attenuates rapidly with depth. Since the analogous three-dimensional solution for a point source of short duration is much more involved, it seems advisable to note here the significant features of the plane case before proceeding to the more general solution.

2/ An approximate treatment of the two-dimensional problem has been developed in Ref 1.

Consider a vertical lamina of a semi-infinite body (the conditions of linear elasticity, homogeniety, and isotropy being assumed throughout) lying in the x-z plane, the z axis being directed normal to the surface with $z = 0$ at the surface. Let u and w be particle displacements associated with the Rayleigh wave in the directions of the x and z axes, respectively. In Ref 14, these displacements are given by

$$u = Ak \left[\exp(-qz) \quad 2qs(s^2 + f^2)^{-1} \exp(-sz)\right] \sin(\omega t - kx) \tag{4.1}$$

$$w = Aq \left[\exp(-qz) - 2f^2(s^2 + f^2)^{-1} \exp(-sz)\right] \cos(\omega t - kx) \ . \tag{4.2}$$

where

A = amplitude of wave

$k = 2\pi/\Lambda$, wave number

Λ = wave length

$q^2 = k^2(1 - \alpha^2 k_1^2)$

$s^2 = k^2(1 - k_1^2)$

$$\alpha_1^2 = \frac{1 - 2\sigma}{2 - 2\sigma}$$

σ = Poisson's ratio

$k_1 = C_R/\beta$

C_R = velocity of Rayleigh wave

β = velocity of distortional wave

ω = circular frequency of wave oscillation

t = time.

The velocity of the Rayleigh wave is found from the solution of the following equation which results from satisfying the condition of zero stress on the surface $z = 0$:

$$k_1^6 - 8k_1^4 + 8(3 - 2\alpha_1^2)k_1^2 + 16(\alpha_1^2 - 1) = 0 \ . \tag{4.3}$$

Equation 4.3, being a cubic in k_1^2, must always have at least one real root. If Poisson's ratio is choosen to be 0.5 for a dense dry sand (corresponding to $\alpha_1 = 0$), Eq 4.3 yields only the one real root

$$k_1^2 = 0.9127 .$$

this in turn, provides

$$k_1 = \frac{C_R}{\beta} = 0.9554 .$$

Thus, in the plane case, the velocity of the Rayleigh wave is but 5% less than that of the distortional wave.

The coefficient of the sine term in Eq 4.1 governs the attentuation of the wave amplitude with depth below the surface, z. Using $\alpha_1 = 0$ and the associated root k_1, this coefficient becomes

$$Ak \left[e^{-kz} - 0.5434\, e^{-0.2955kz} \right] .$$

This expression has a maximum value of 0.4565 Ak at the surface, decreases to zero at a depth of 0.138 wave lengths (i.e., kz = 0.8654), reverses sign and reaches a relative minimum (0.1788 Ak) at 0.413 wave lengths (kz = 2.5959), and then asymptotically approaches zero. It is of interest to note that the particle motion at the free surface is of a retrograde elliptical form.

We consider now the propagation of waves at the free surface of a semi-infinite solid generated by a concentrated force of short duration acting normal to the surface. Following Lamb's procedure, one obtains first the solution for a load distributed over the entire surface and varying as a harmonic function of time. Let r be a radial coordinate and z be normal to the surface with z = 0 taken at the surface. Then the surface forces per unit area,

$$\left[p_{zr}\right]_{z=0} = 0 \text{ and } \left[p_{zz}\right]_{z=0} = Z\, J_o(kr) e^{i\omega t} , \tag{4.4}$$

give rise to horizontal and vertical surface displacements of the form

$$q_o = -\frac{k(2k^2 - k_\beta^2 - 2\nu\nu')}{F(k)} J_1(kr) \frac{Z}{\mu} e^{i\omega t} \tag{4.5}$$

Equation 4.3, being a cubic in k_1^2, must always have at least one real root. If Poisson's ratio is choosen to be 0.5 for a dense dry sand (corresponding to $\alpha_1 = 0$), Eq 4.3 yields only the one real root

$$k_1^2 = 0.9127 .$$

this in turn, provides

$$k_1 = \frac{C_R}{\beta} = 0.9554 .$$

Thus, in the plane case, the velocity of the Rayleigh wave is but 5% less than that of the distortional wave.

The coefficient of the sine term in Eq 4.1 governs the attentuation of the wave amplitude with depth below the surface, z. Using $\alpha_1 = 0$ and the associated root k_1, this coefficient becomes

$$Ak \left[e^{-kz} - 0.5434\, e^{-0.2955kz} \right] .$$

This expression has a maximum value of 0.4565 Ak at the surface, decreases to zero at a depth of 0.138 wave lengths (i.e., kz = 0.8654), reverses sign and reaches a relative minimum (0.1788 Ak) at 0.413 wave lengths (kz = 2.5959), and then asymptotically approaches zero. It is of interest to note that the particle motion at the free surface is of a retrograde elliptical form.

We consider now the propagation of waves at the free surface of a semi-infinite solid generated by a concentrated force of short duration acting normal to the surface. Following Lamb's procedure, one obtains first the solution for a load distributed over the entire surface and varying as a harmonic function of time. Let r be a radial coordinate and z be normal to the surface with z = 0 taken at the surface. Then the surface forces per unit area,

$$\left[p_{zr}\right]_{z=0} = 0 \text{ and } \left[p_{zz}\right]_{z=0} = Z\, J_o(kr) e^{i\omega t} , \tag{4.4}$$

give rise to horizontal and vertical surface displacements of the form

$$q_o = -\frac{k(2k^2 - k_\beta^2 - 2\nu\nu')}{F(k)} J_1(kr) \frac{Z}{\mu} e^{i\omega t} \tag{4.5}$$

$$\omega_o = \frac{k_\beta^2 \vartheta}{F(k)} J_o(kr) \frac{Z}{\mu} e^{i\omega t} \tag{4.6}$$

In the above equations

q_o = horizontal displacement at surface $z = 0$

w_o = vertical displacement at surface $z = 0$

Z = amplitude of normal stress intensity

k = wave number

ω = frequency of force

$k_\beta = \omega/\beta$

$k_\alpha = \omega/\alpha$

β = velocity of distortional waves

α = velocity of compressional waves

$\vartheta^2 = k^2 - k_\alpha^2$

$(\vartheta')^2 = k^2 - k_\beta^2$

μ = Lamé Constant

ρ = density

t = time

J_o, J_1 = Bessel functions of zero and first order, respectively

$F(k) = (2k^2 - k_\beta^2)^2 - 4k^2\vartheta\vartheta'$ = Rayleigh's function.

These results can be superposed to yield the solution for a concentrated force of magnitude L at the origin $z = 0$ by expansion in terms of a Fourier-Bessel integral. That is, one takes

$$\left[p_{zz}\right]_{z=0} = -\frac{L}{2\pi} \int_0^\infty J_o(kr)\, k\,dk\, e^{-i\omega t} \tag{4.7}$$

and sets

$$Z = -\frac{L\,kdk}{2\pi}$$

in Eq 4.5 and 4.6. Upon integrating with respect to k from 0 to ∞, the resulting surface displacements are found to be

$$q_o = \frac{L}{2\pi\mu} \int_o^{\infty} \frac{k^2 (2k^2 - k_\beta^2 - 2\vartheta\vartheta')}{F(k)} J_1(kr)dk\, e^{i\omega t} \tag{4.8}$$

$$\omega_o = -\frac{L}{2\pi\mu} \int_o^{\infty} \frac{k_\beta^2 \vartheta}{F(k)} J_o(kr)dk \tag{4.9}$$

As in Ref 14, the integrals can be evaluated by contour integration in the complex plane. At this point, we introduce a specific time variation for the force and denote it by $S_d(t)$. A reasonable, and particularly convenient, form for this variation is

$$S_d(t) = \frac{pL}{p^2 + t^2} ,$$

where p is a constant.

The resulting surface displacements of the Rayleigh wave are found to be

$$q_o = -\frac{HL}{2\mu(2rC_R)^{1/2}p^{3/2}} \cos^{3/2} v \sin\left(\frac{\pi}{4} - \frac{3}{2}v\right) \tag{4.10}$$

$$\omega_o = \frac{KL}{2\mu(2rC_R)^{1/2}p^{3/2}} \cos^{3/2} v \sin\left(\frac{\pi}{4} - \frac{3}{2}v\right) , \tag{4.11}$$

where

$$v = \arc\cos \frac{p}{\sqrt{p^2 + t_*^2}}$$

$$t_* = t - \frac{r}{C_R}$$

C_R = velocity of Rayleigh wave

H = constant

K = Constant

According to the assumption that the control model is executing the motion of the free field, we are most interested in the radial component of the surface acceleration. This is obtained by implicit differentiation of Eq 4.10 and is

$$\frac{d^2 q_o}{dt^2} \equiv a = \alpha \cos^{7/2} v \sin(\pi/4 - 7v/2), \tag{4.12}$$

where

$$\alpha = \frac{15\ HL}{8\mu(2rC_R)^{1/2} p^{7/2}}$$

The graph of Eq 4.12 is shown in Figure 4.1 where the nondimensional radial acceleration a/ is expressed as a function of the time parameter t_*. Also shown in the figure is the quantity $S_d(t)$, which is the analytical form assumed to represent the detonation input. This expression and the resulting acceleration have been evaluated for $p = 1$ msec. The constant p is a measure of the average pulse width, and the choice of 1 msec is based on the experimental data.[3/] The quantity α governs the radial location. It depends on the elastic properties of the medium and is proportional to the amplitude of the input pulse L. No attempt has been made to evaluate α, since L is unknown and the effective elastic properties of the sand are not well established. However, the results of Fig. 4.1 still provide a means of comparison with the experimental data.

A comparison of the Rayleigh surface accelerations with a typical record from an upper horizontal accelerometer (say, Fig. 3.10) shows definite similarities. It is observed that the first peak in both cases is negative and of considerably smaller magnitude than the second, positive, peak. The ratio of positive to negative peak magnitudes is somewhat

---

3/ Measurements obtained during the preliminary tests indicated that a time delay of about 1 msec occurs between initiation of the firing voltage (the detonator should then ignite within microseconds) and arrival of an air shock immediately above the change.

greater for the theoretical case, but this may possibly be explained by the effect of the sand-model interaction or by the fact that the gage, being slightly below the surface, records an attenuated positive peak. Another similarity is evident in the relative time scales of the experimental and theoretical curves, the peak-to-peak period in both cases being on the order of milliseconds. While this argument is dependent upon the somewhat arbitrary choice of pulse width (i.e., p = 1 msec), it would be discouraging indeed if the time scales differed in a significant manner. Although later peaks occur on both the theoretical and experimental curves, similarities between the two are less evident.

The above comparisons support the view that the control model, at least in its initial motions, executes essentially the motion of the free field. Although other investigators have found that for low stress levels and at large distances from the source (such as under seismic condition), a theory based on a linearly elastic medium conforms well with observed phenomena, the same arguments may not be applicable here. Thus, such mitigating factors as (1) the relative closeness of the point under consideration to the source, (2) apparent density variations within the sand bed, (3) the discounting of the interaction (see Section 4.2), and (4) the uncertainties in the actual time variation of the detonation process and its departure from a concentrated force must all be acknowledged.

4.2 CONTROL MODEL RESPONSE

4.2.1 One-Dimensional Theory. We describe in this section a one-dimensional theory of the control model response based on elastic action of the soil insofar as the sand-model interaction process is concerned. Modification of the theory to include two-dimensional effects and the numerical results obtained are discussed in subsequent sections. It is the purpose of these analyses to investigate whether the experimental data can be better interpreted on the basis of interaction phenomena than on the basis of free-field motions (as considered in the previous section).

Consider a column of sand in which is embedded a rigid mass representing the control model, Fig. 4.2. We image this column to be directed along a radial line in the sand bed, and, since we do not consider reflection effects from the sides of the sand container, the column may be considered infinite

in length. The sand, being assumed a linearly elastic, homogeneous, and isotropic body, satisfies the well-known, one-dimensional wave equation, insofar as its free-field particle motion is concerned. That is,

$$c^2 \frac{\partial^2 u}{\partial x^2} = \frac{\partial^2 u}{\partial t^2} , \tag{4.13}$$

where

x = coordinate defining position of sand particle

u = displacement of sand particle in the direction of the x-axis

$c = \sqrt{E/\rho}$ = speed of elastic wave propagation

t = time

E = compressive modulus of (idealized) sand

ρ = density of sand.

The general solution of Eq 4.13 is known to be of the form[4/]

$$u(x, t) = u_1(x + ct) + u_2(x - ct) \tag{4.14}$$

Let the function u_1 represent the free-field displacement at the point $x = 0$ taken to be just prior to the sand-model interface; $u_1(t)$ thus defines the motion of the wave pulse incident upon the model. Due to the interaction process, a reflected wave, denoted by u_2, is transmitted upstream. The total displacement of the free field at the interface $x = 0$, therefore, is

$$u(t) = u_1(t) + u_x(t) .$$

By continuity at the interface

$$u(t) = y(t) ,$$

where y is the displacement of the control model, Fig. 4.2.

We consider now the computation of the force-per-unit-area on the upstream and downstream faces of the mass. Since we assume intimate contact of the mass with the adjacent sand particles, these stresses are also the stresses in the free field at the respective interfaces. With reference to Fig. 4.2, the time-dependent stress, $\sigma(t)$, on the upstream face may be thought of as the superposition of stresses in the incident and reflected waves, i.e.

4/ See Ref 7 or any textbook on the subject.

$$\sigma(t) = \sigma_1(t) + \sigma_2(t) \quad . \tag{4.16}$$

Since the sand is assumed to obey Hooke's law, the following relation holds between stress and strain:

$$\begin{aligned} \sigma_1(t) &= E \frac{\partial u_1}{\partial x} \\ \sigma_2(t) &= E \frac{\partial u_2}{\partial x} \, . \end{aligned} \tag{4.17}$$

By virtue of the "wave" form of the displacement, Eq 4.14, the strains are proportional to particle velocity. Thus, by Eq 4.14, 4.16, 4.17, and the continuity condition, Eq 4.15,

$$\begin{aligned} \sigma_1(t) &= \rho c \, \dot{u}_1(t) \\ \sigma_2(t) &= -\rho c \, \dot{u}_2(t) = \rho c(\dot{u}_1 - \dot{y}) \\ &= \sigma_1(t) - \rho c \dot{y} \\ \sigma(t) &= 2 \, \sigma_1(t) - \rho c \dot{y} \quad . \end{aligned} \tag{4.18}$$

The quantity ρc is often referred to as the acoustic impedance of the medium. The mass is assumed to be rigid so that the downstream interface moves with velocity y, inducing a stress in the sand of magnitude

$$\sigma_3 = \rho c \dot{y} \quad . \tag{4.19}$$

These being the only forces acting on the mass, the equation of motion of the mass is

$$A \left[\sigma(t) - \sigma_3(t)\right] = M\ddot{y} \, ,$$

or

$$\ddot{y} + \alpha \dot{y} = f(t) \, , \tag{4.20}$$

where

A = area of interface

M = total mass

$\alpha = \frac{2\rho c}{m}$

$m = \frac{M}{A}$

$f(t) = \frac{2\sigma_1(t)}{m}$

For a motion starting from rest, Eq 4.20 is subject to the initial conditions

$$y(0) = \dot{y}(0) = 0 \tag{4.21}$$

4.2.2 Modified One-Dimensional Theory. According to the results of the one-dimensional theory, Eq 4.20, the mass would undergo an infinitely large displacement under the action of a steady force. This is to be expected since the infinitely long column of sand has zero stiffness. However, if a steady force is applied over a finite area to a two- or three-dimensional body of infinite extent, finite displacements result. This is but one manner in which the one-dimensional problem differs from the more general case.

This particular difficulty may be circumvented in a rather simple, if arbitrary, fashion. To provide the necessary restoring force, one has only to imagine a linear spring connected to the mass in parallel with the free field, as indicated schematically in Fig. 4.3. A basis for selecting a suitable linear spring may be argued in the following manner. A well-known solution in the three-dimensional theory of elasticity is that of a semi-infinite body acted on by normal stresses distributed over some area A of the free surface. In Ref 41 it is shown that the average deflection of the loaded surface w_{avg} is given by

$$w_{avg} = \frac{m(1 - \sigma^2) P}{E \sqrt{A}} , \tag{4.22}$$

where

P = total load on the area

σ = Poisson's ratio

E = Young's modulus

m = constant depending on the shape of the loaded area.

The constant m is generally of the order of unity, being equal to 0.96 for a circular area, and 0.95 for a square, and having the value

$$0.94 \geq m \geq 0.71$$

for rectangular areas whose sides are in the ratio of

$$1.5 \leq a/b \leq 10 .$$

This, then, indicates a linear spring of rate

$$k = \frac{P}{w_{avg}} = \frac{E\sqrt{A}}{m(1 - \sigma^2)} \tag{4.23}$$

and suggests the average value,

$k \approx E$ per unit length.

If we consider the spring to connect the mass to the free field, it exerts a restoring force on the mass given by[5] $k(y - u_1)$. The particle displacement of the incident wave at the interface $x = 0$ is related to the incident stress wave as follows:

$$u_1(t) = \frac{1}{\rho c} \int_0^t \sigma_1(\tau)d\tau = \frac{m}{2\rho c} \int_0^t f(\tau)d\tau = \frac{1}{\alpha} 1(t) . \tag{4.24}$$

---

[5] This assumption ensures an oscillation of the mass about an equilibrium position relative to the free field but still permits an absolute permanent displacement since u_1 is not restricted.

The quantity

$$I(t) = \int_0^t f(\tau)d\tau$$

is proportional to the impulse of the incident stress wave and implies that $u_1(0) = 0$.

The equation of motion of the mass now becomes

$$\ddot{y} + \alpha\dot{y} + \omega^2 y = f(t) + \frac{\omega^2}{\alpha} I(t) , \tag{4.25}$$

where

$$\omega^2 = \frac{k}{M} .$$

This equation is subject to the initial conditions of Eq 4.21 and replaces Eq 4.20 for the motion of the mass. It is recognized as the equation of forced motion of a viscously damped, linear oscillator. Equation 4.25 may be put into the convenient nondimensional form:

$$\eta'' + 2\beta\eta' + \eta = g(\tau) , \tag{4.26}$$

where

$$\beta = \frac{\alpha}{2\omega}$$

$$\eta = \frac{k}{2A\sigma_o} y \quad . \; . \; . \quad \text{nondimensional displacement of mass}$$

$$\tau = \omega t \quad . \; . \; . \quad \text{nondimensional time}$$

σ_o = amplitude of incident stress pulse

$$g(\tau) = \frac{1}{a_o \alpha}\left[f(\tau/\omega) + \frac{\omega^2}{\alpha} I(\tau/\omega)\right]$$

$$a_o = \sigma_o/\rho c \quad . \; . \; . \quad \text{particle velocity of incident pulse}$$

and the primes indicate differentiation with respect to τ

Solutions to Eq 4.26 have been obtained for both cosine and triangular forms for the incident stress pulse. The analytical solutions are summarized in Appendix C; the results of a limited variation-of-parameter study conducted on the ARF analog computer are discussed in the following section.

4.2.3 Variation-of-Parameter Study. Equation 4.26 involves two essential quantities, the parameter β which depends on the properties of both the sand and the model, and the function $g(\tau)$ which depends primarily on the incident stress pulse. Inasmuch as neither of these quantities is well defined, it seemed desireable to investigate the nature of the solution over some range of the parameters. To this end, a limited variation-of-parameter study was conducted with the aid of the ARF analog computer.

The value of β is of particular interest, since the steady motion is either of an oscillatory or non-oscillatory type as the value of β is less than or greater than unity. (β may be thought of as representing the percentage of critical damping for the system.) For a value of 800 fps for the wave speed c , 110 lb/ft^3 for the weight of sand, and the measured weight of the model, β is computed to be about 1.8. This indicates an overdamped motion, a result which is intuitively satisfying since the model would not be expected to undergo a vibratory motion when immersed in the sand bed. It was thus decided to limit variations in β , and for the most part computer solutions were obtained with $\beta = 2.0$.

Partly for the sake of simplicity, it was decided to study solutions based on a triangular form for the incident stress pulse. Typical results for a representative range of inputs are shown in Fig. 4.4 through 4.9.[6/] Some difficulties which limited the number of solutions obtained were encountered with the computer. The computer solutions show the acceleration asymptotically approaching zero after the negative peak. Careful numerical evaluation indicates that a small, second, positive peak actually occurs. Also, it was not possible to obtain solutions for extremely short rise times. However, the computer results presented here are correct in their essential details.

[6/] For the parameter values mentioned above, a nondimensional pulse width of 4.5 time units on the computer corresponds to 1 msec real time.

While the predicted acceleration is somewhat reminiscent of the experimental data, there are noticeable dissimilarities, due mostly to the simplified incident stress pulse considered. The shape and relative magnitude of the first positive and negative acceleration peaks depend mostly on the rise and decay rates of the pulse. As expected, amplitude increases as the rise or decay time decreases. A pronounced flattening of the peaks occurs with increasing rise times. It seems clear that reasonably good agreement with the experimental results could be obtained by suitable choice of the incident stress pulse. This choice would have a relatively more rapid decay rate than rise rate and likely would exhibit a small tension phase similar to the Rayleigh surface stress wave. We observe that while neither the free-field nor interaction theories conflict with observed results, it cannot be said that either of these approaches, or their underlying assumptions, is necessarily substantiated. We can only conclude, therefore, that either point of view is probably adequate for predicting the gross behavior of the models under the test conditions, but inadequate for a phenomonological understanding of the problem.

4.3 TWO- AND THREE-DIMENSIONAL EFFECTS

The theory described above is based on a one-dimensional, elastic, mathematical model of the sand-model interaction, modified so as to introduce a two-dimensional effect of possible importance. As mentioned previously, the physical setup is strictly a three-dimensional problem, and we omit treating certain effects by virtue of our simplifications. Thus, we discount (1) surface effects at the free boundary, (2) possible variation in response with depth, and (3) two-dimensional effects at a given depth.

Of these, item 1 is likely to be of greatest significance, in that a one-dimensional approach offers no way in which to account for the actual geometry of the model. Reference 1 attempts to do just this by drawing analogy to the corresponding air-blast loading problem. Inasmuch as this approach has not been substantiated and since our present aims are of necessity rather limited, it was decided not to employ these results.

4.4 ISOLATION MODEL RESPONSE

Two classes of isolation mechanisms were considered, either applicable to the polyurethane foam isolation tested, depending on the stress levels involved: (1) an elastic or non-energy-dissipative mechanism and (2) an energy-dissipative mechanism. The elastic mechanism, which appears to have been realized in the experiments, is discussed in Section 4.1.1. The dissipative mechanism, which apparently does not occur at the low stress levels achieved in the experiments, is discussed in Section 4.4.2.

4.4.1 Elastic Isolation Systems. An elastic isolation system refers to what is in essence a linear spring (or spring-dashpot) mounting of the structure relative to the surrounding medium. To be effective, it seems clear that this should be a "soft" mount, that is, one for which the rigid-body mode of vibration of the structure is of a sufficiently low frequency. One can then visualize a low-frequency, low-amplitude oscillation of the structure (relative to the surrounding medium) resulting from a relatively much more intense input with high-frequency components. Thus, the structure-isolation system simply cannot respond to the local time details of the input soil motion; as a result, its response is primarily dependent upon the total impulse of the input.

From this point of view, the interaction problem occurs at the soil-isolation interface; the motion of the structure is more the ordinary matter of external excitation. Thus, we may visualize some short-duration motion of the soil-isolation interface (which is essentially that of a free soil interface due to the low compliance of the isolation "spring") acting as input to the isolation. The subsequent motion of the structure, then, is essentially a free vibration relative to a "rigid" soil boundary.

To the extent that this view proves admissable, the governing theory is straightforward and simple. For example, if a displacement compatible with the cosine stress pulse considered in Appendix C is imparted to one end of the spring, the maximum acceleration of the structure is found to be inversely proportional to the square of the period of the system, T_m, providing that this period is long compared to the duration of the pulse, T_p. The maximum displacement is proporational to the ratio $(T_p/T_m)^2$.

Thus, the amplitude of the transmitted acceleration pulse, as well as the displacement of the structure relative to its surroundings, can be made as small as desired. Of course, there is a corresponding increase in period of the induced motion.

Reference 28 deals with upper and lower bounds to the response of the linear mass-spring system and is of interest in the present application. Specifically, absolute upper and lower bounds to the maximum displacement have been determined for the class of non-negative forcing functions characterized only by total impulse and duration. Thus, given the impulse and duration of the input to the system, one is able to state in advance both the maximum and minimum possible maximum displacements of the system regardless of the particular time-variation of the input. It appears that these results could be extended to yield bounds for the response as measured by acceleration of the mass.

4.4.2 Energy-Dissipative Isolation Systems

4.4.2.1 Introduction. Existing studies of the ground shock-isolation problem all seem to consider the use of some sort of energy-dissipative device, the "gin bottle" experiment of Ref 29 being the most conspicuous example. Possible alternative approaches were discussed in Section 2.3. In this section, we consider a particular class of energy-dissipative materials, the so-called totally locking material, which appears to be applicable to prototype installations. The results of the analysis suggests, however, that the assumed action of the material, while possible, may not be practically achieved.

It may be imagined that the incident ground shock causes sudden, largely permanent displacements of the soil and that the structure moves through this distance. Potentially destructive forces and accelerations result from the sudden arrestment of the structure. Viewed in this manner the isolation problem is similar to the dynamic cushioning problems of recent interest to the packaging industry. Reference 15, for example, discusses the concept of optimum cushioning and presents static and dynamic test data on the properties of a variety of cushioning materials.

The materials of interest in the packaging problem are generally flexible and of low density (e.g., hair latex, cellular rubber, flexible polyurethane) and in application are characterized by large strains (up to about eighty percent). A typical static stress-strain curve is that for a flexible polyurethane foam material shown in Fig. 4.10 (Ref 15).

Consider a material in an unstrained state suddenly subjected to a stress at its surface. If the stress is of sufficient intensity some portion of the material will be strained to its limiting value, and this portion will move as a rigid body continually acting to compact material ahead of itself. A material behaving in this fashion will be termed a "totally locking material", following Ref 25.[7] We will first develop the properties of such a material and then introduce it into the interaction problem.

4.4.2.2 Totally Locking Material. Figure 4.11 shows a one-dimensional length of the isolation material. The incident stress wave at the interface causes a shock front to be transmitted into the material with velocity U_s and causes the interface itself to move with velocity U_i Denote the density of the uncompacted material (ambient density) ahead of the shock front by ρ_o, and the compacted density behind the shock by ρ. According to the assumption of a totally locking material, ρ is a constant, so that the length of material behind the shock front $(z - x)$, Fig. 4.11, moves as a rigid body with the velocity of the interface U_i. Accordingly, conservation of mass requires

$$\rho_o U_s = \rho (U_s - U_i) = m_1 , \tag{4.27}$$

where the constant m_1 may be thought of as the mass flux through the surface of the shock front. Equation 4.27 yields the following relation between the interface and shock velocities:

$$\frac{U_i}{U_s} = 1 - \rho_o/\rho \equiv e_c , \tag{4.28}$$

where the constant e_c is termed the compaction strain.

---

[7] Reference 25 presents an interesting free-field theory for a non-cohesive sand medium based on this type of behavior.

Applying conservation of momentum across the shock front,

$$\rho \; U_i \, (U_s - U_i) = \sigma_s \tag{4.29}$$

where σ_s is the stress (i.e., pressure) in the compacted material just behind the shock front; the ambient material is taken to be stress free. By Eq 4.27 and 4.28, the stress at the shock front is

$$\sigma_s = \rho_o \, e_c \, U_s^2 \; . \tag{4.30}$$

In order to sustain the shock front, the stress σ_s must be at least as large as the stress associated with the compaction strain, e_c (see Fig. 4.10). That is, we assume

$$\sigma_s \geq \sigma_c \tag{4.31}$$

throughout this discussion.

Apply now conservation of energy across the shock front, and use the well-known form of the energy equation, Ref 43,

$$\frac{1}{2}\left(\frac{1}{\rho_o} - \frac{1}{\rho}\right) \sigma_s = E^* / \rho \quad , \tag{4.32}$$

where E^* is the internal energy per unit volume behind the shock and the energy datum of the ambient material is taken to be zero. Thus, E^* represents the increase in internal energy due to the compaction process. Substituting the above results into Eq 4.32 yields

$$E^* = \frac{1}{2} \rho \; U_i^2 \; . \tag{4.33}$$

Equation 4.32 can be interpreted to mean that the increase in internal energy across the shock front is due to the work done by the mean stress in performing the compression. The result of Eq 4.33 shows that this increase in energy is numerically equal to the kinetic energy per unit volume of the compacted material. This, by the way, demonstrates the fact that the compaction process is indeed an energy-dissipative process. Finally, it is important to note that these results in no way have involved specifying the stress-strain properties of the material or the mechanism of compaction.

It has only been assumed that the particle velocity is independent of position behind the shock (rigid-body motion of the compacted portion) and that the incident stress is of sufficient intensity to maintain the shock front. No attempt will be made here to treat the problem wherein the latter condition is not met, e.g., during unloading.

4.4.2.3 Response of Isolation Model. We will now extend the one-dimensional theory developed in Section 4.2.2 to include a totally locking isolation material interspaced between the rigid mass representing the model structure and the surrounding elastic medium. With reference to Fig. 4.12 consider a free-field stress pulse $\sigma_1(t)$, incident upon the sand-isolation interface a-a. We will assume that the transmitted stress exceeds the compaction stress for the material so that the interface a-a is displaced with velocity $U_i = \dot{x}$. As in the development in Section 4.2.1 the stress on the moving interface a-a is

$$\sigma(t) = 2\,\sigma_1(t) - \rho c \dot{x}$$

where ρc is the acoustic impedance of the sand. The equation of motion of the "rigid" portion of the material bounded between the interface a-a and the shock front is

$$\sigma(t) = \frac{d}{dt}(\rho_o z \dot{x}) ,$$

where $\rho_o z$ is the total enclosed mass and coordinate z measures the portion of the shock front relative to the original position of the interface (see Fig. 4.11).

From the above two relations and Eq 4.28, the equation governing the position of the shock front is found to be

$$\frac{d}{dt}(z\dot{z}) + \frac{\rho c}{\rho_o}\dot{z} = \frac{2}{\rho_o e_c}\sigma_1(t) \tag{4.34}$$

This may be integrated once to yield

$$z\dot{z} + \frac{\rho c}{\rho_o} z = \frac{2}{\rho_o e_c} I(t) , \tag{4.35}$$

where

$$I(t) = \int_0^t \sigma_1(\tau)\, d\tau \tag{4.36}$$

is the impulse of the incident free-field stress pulse, and the initial condition $z(0) = 0$ has been employed. Eq 4.35 is a non-linear equation, and closed form solutions to it may be obtained only in special cases depending on the nature of $I(t)$ In particular, when $I(t)$ is a linear function of time (corresponding to a step pulse for σ_1), the equation is recognized as a linear fractional form for which the solution is straightforward.

Equation 4.35 is valid providing the shock front has not yet reached the isolation-structure interface b-b , i.e., for $z < L$, Fig. 4.12, and provided that the compaction process can be maintained, i.e., that Eq 4.31 holds. We will assume the latter to be true and will proceed to the isolation-structure interaction.

When the shock front reaches the interface b-b, the upstream isolation material impacts the structure as one rigid body upon another. If it is assumed that the impact is plastic (i.e., no rebound), an initial velocity is imparted to the mass. The subsequent motion is that of the combined mass of isolation material and structure, acting as a rigid body and being resisted by the downstream isolation material and sand. From momentum conservation, the initial velocity of the structure, $\dot{y}_o$, is given by

$$\dot{y}_o = \frac{\rho_o L e_c \dot{z}_L}{\rho_o L + m} , \tag{4.37}$$

where $\dot{z}_L$ is the velocity of the shock front at the time $z = L$, and m is the mass of the structure. By Eq 4.35,

$$\dot{z}_L = \frac{2}{\rho_o L e_c} I(t_L) - \frac{\rho c}{\rho_o} ,$$

where

$$z(t_L) = L .$$

In order for a compaction front to propagate into the downstream isolation material, the stress at interface c-c must exceed σ_c . This prescribes a minimum value of $\dot{y}_o$ for which the compaction process will continue. From Eq 4.30, this condition is

$$\dot{y}_o > \sqrt{\frac{e_c \, \sigma_c}{\rho_o}} \; . \tag{4.38}$$

An equation for the position of the shock front z , in the downstream isolation material, analogous to Eq 4.34, can now be written. This, in turn, yields the equation of motion of the structure, since continuity must be maintained at interfaces b-b and c-c . Accordingly, one obtains as the governing equation for y(t) ,

$$\left.\begin{aligned} &\frac{d}{dt}\left[\left(m + \rho_o L + \frac{\rho_o y}{e_c}\right)\dot{y}\right] + \rho c y = 2\,\sigma_1(t) \\ &y(t_L) = 0;\; \dot{y}(t_L) = y_o,\; t \geq t_L \; . \end{aligned}\right\} \tag{4.39}$$

Integrating Eq 4.39 yields

$$\left(m + \rho_o L + \frac{\rho_o y}{e_c}\right)\dot{y} + \rho c y = 2I(t) - \rho c L e_c \; . \tag{4.40}$$

An explicit form for y can only be obtained in very special cases.

Equation 4.40 is now valid for $t_L < t < 2t_L$, or $z < L$, that is until the shock front reaches the isolation-sand interface d-d . The subsequent motion of the structure is easily formulated, but, as discussed below, there appears to be little point in doing so.

In order to investigate the conditions under which this type of isolation material can act as assumed above, we consider as a particular example a step-pulse incident stress wave and isolation properties corresponding to a flexible polyurethane foam material. For $\sigma_1(t) = \sigma_o$, the solution of Eq 4.35 is found to be

$$z(t) = At \; , \tag{4.41}$$

where

$$A = \frac{\rho c}{2\rho_o}\left[\sqrt{\frac{8\,\sigma_o\,\rho_o}{e_c\,\rho^2\,c^2} + 1}\right] - 1$$

The stress at the compaction front is

$$\sigma_s = \rho_o\, e_c\, \dot{z}^2 = \rho_o e_c\, A^2 \tag{4.42}$$

Thus, the stress is constant throughout the compacted portion of the material.

In order for the compaction process to occur, we require $\sigma_s > \sigma_c$ This implies the following minimum value for the incident stress σ_o :

$$\sigma_o > \frac{1}{2}\left[\sigma_c + \rho c\sqrt{\frac{e_c\,\sigma_c}{\rho_o}}\right] \tag{4.43}$$

Consider the following numerical values for an Ottawa sand and an isolation material such as a flexible polyurethane foam, shown in Fig. 4.10:

$$\left.\begin{aligned} \rho &= 3.4 \text{ lb sec}^2/\text{ft } (110 \text{ lb/ft}^3), \\ c &= 800 \text{ fps} \end{aligned}\right] \text{dry Ottawa sand}$$

$$\left.\begin{aligned} \rho_o &= 0.062 \text{ lb sec}^2/\text{ft}^4 \ (2 \text{ lb/ft}^3) \\ e_c &= 0.8 \\ \sigma_c &= 6 \text{ psi} \end{aligned}\right] \text{polyurethane foam}$$

From Eq 4.43,

$$\sigma_o = \frac{1}{2}\left[6 + 2000\right] \cong 1000 \text{ psi}$$

which is the minimum stress for the compaction front to form in the upstream isolation material. For this value of stress, from Eq 4.41 and 4.42,

$$A = \dot{z} = 142 \text{ fps} \ .$$

This result -- that a 1000-psi incident stress pulse is transmitted into the isolation material as a 6-psi pulse -- indicates that the polyurethane foam effectively acts as a void relative to the adjacent sand. Thus, at stress levels of the order attained in the experiments (i.e., about 1 psi), compaction of the foam definitely would not be expected. This being the case, there is no point in continuing further with application of the theory to the present experimental situation.

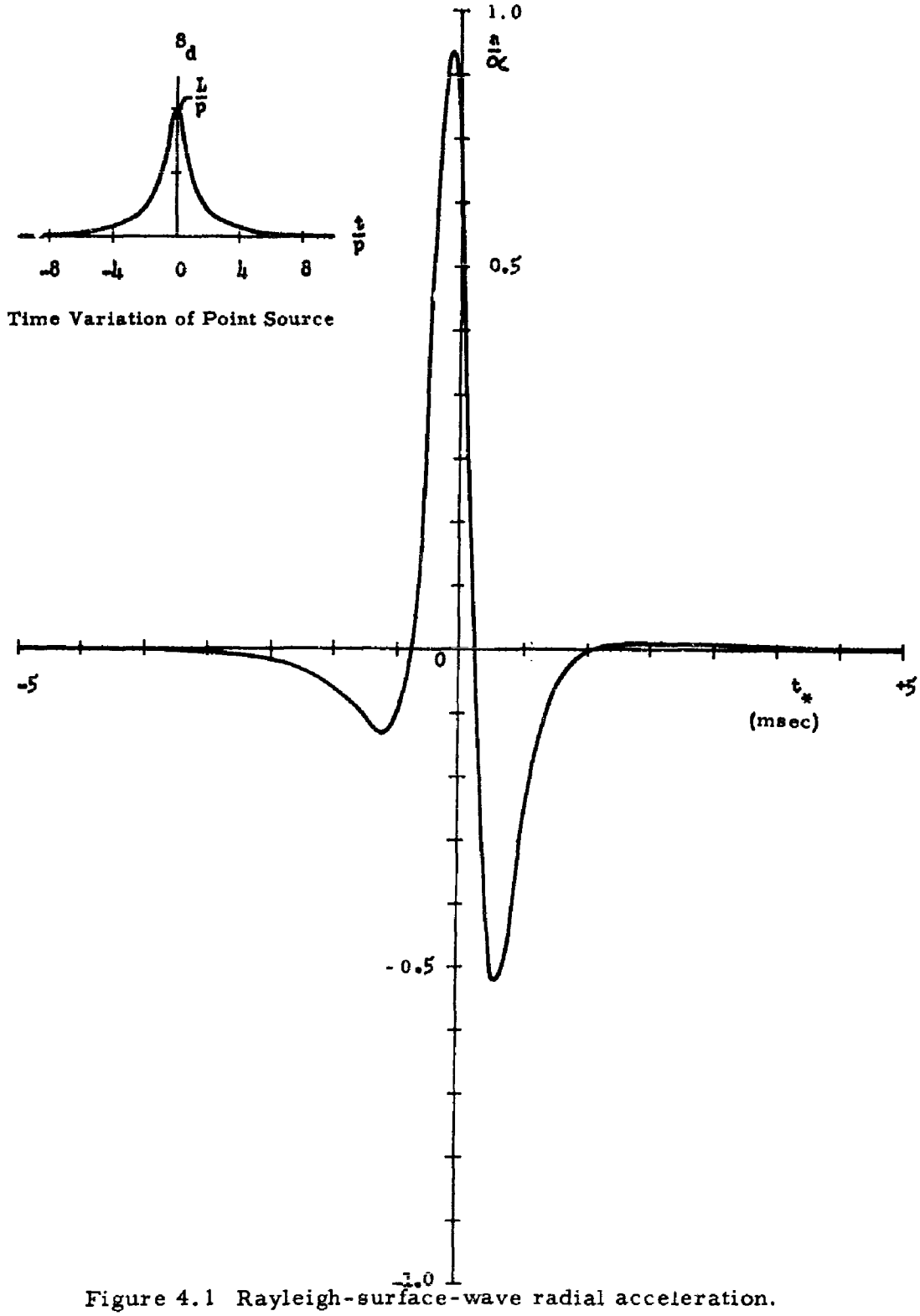

Figure 4.1 Rayleigh-surface-wave radial acceleration.

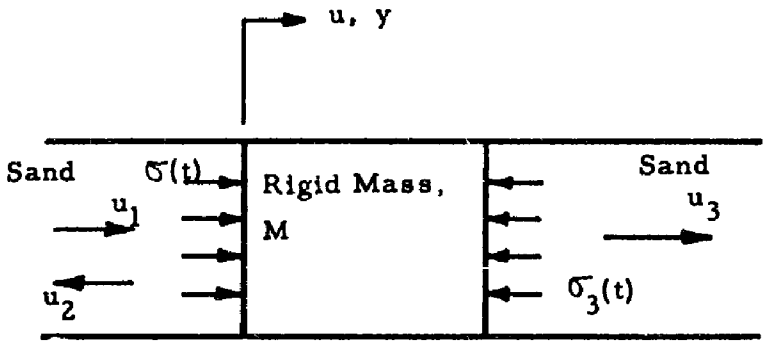

Figure 4.2 One-dimensional sand-model configuration.

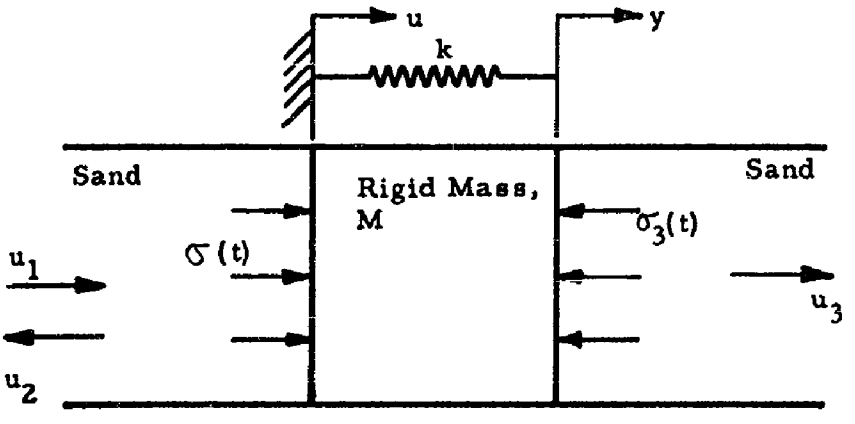

Figure 4.3 Modified one-dimensional sand-model configuration.

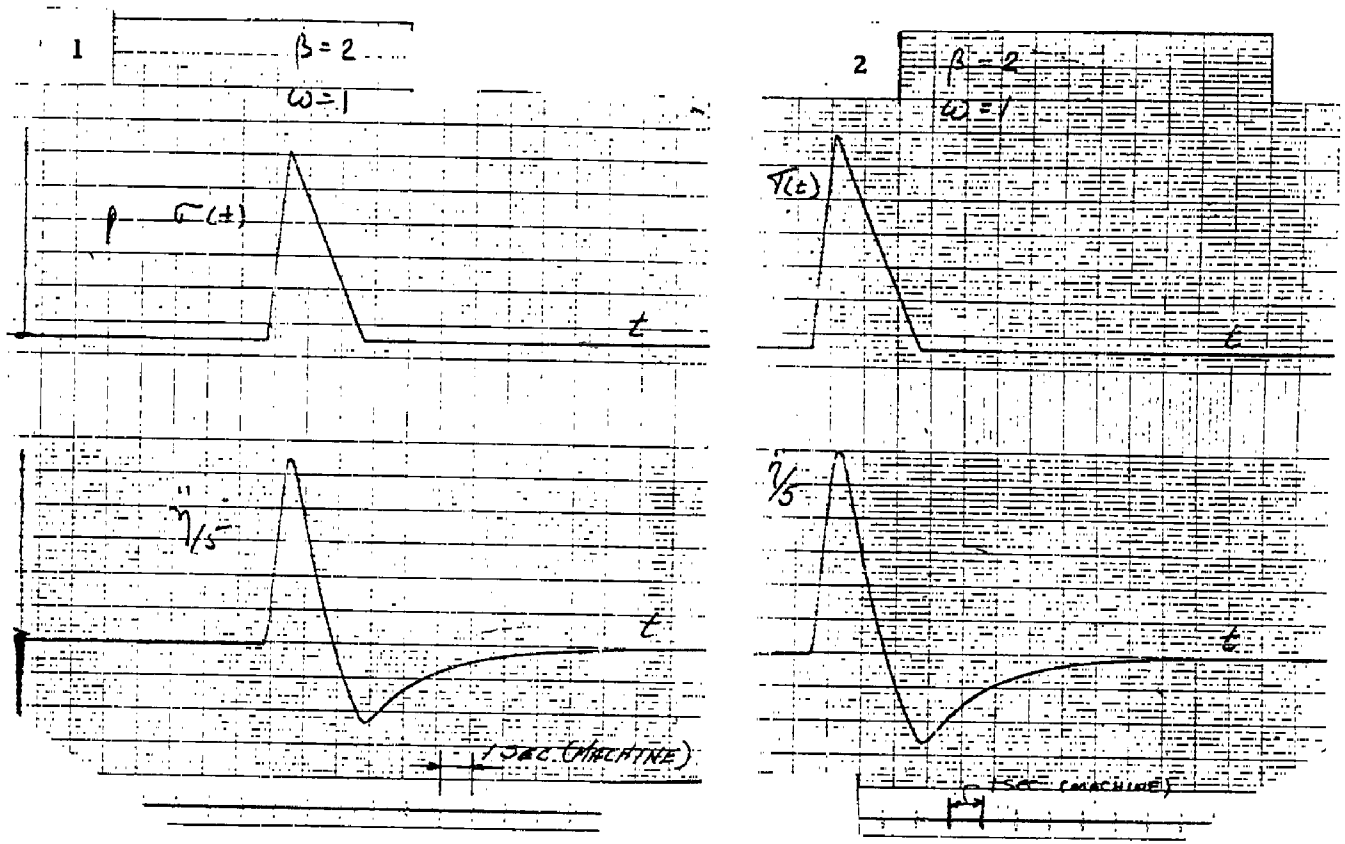

Figure 4.4 Triangular stress pulse and response.
Short rise time, $\beta = 2$.

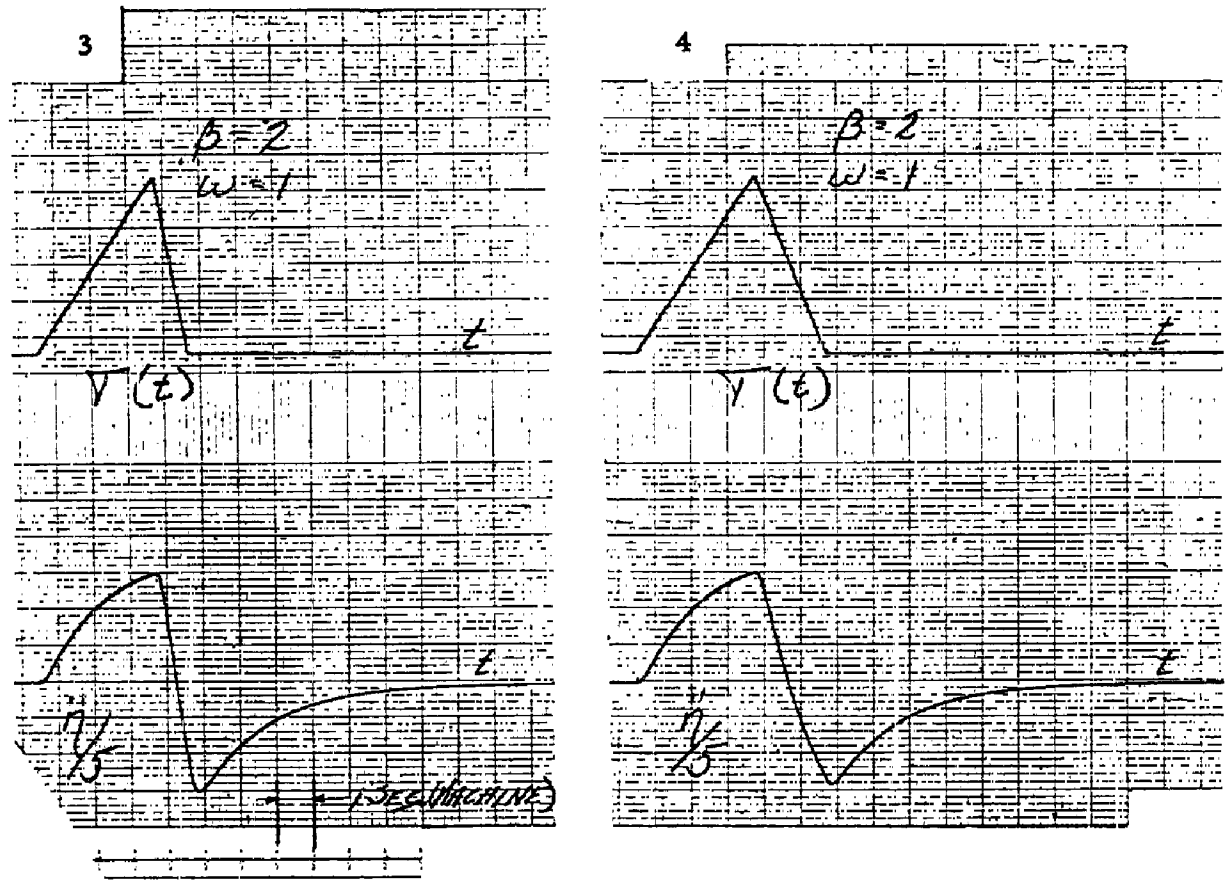

Figure 4.5 Triangular stress pulse and response.
Short decay time, $\beta = 2$.

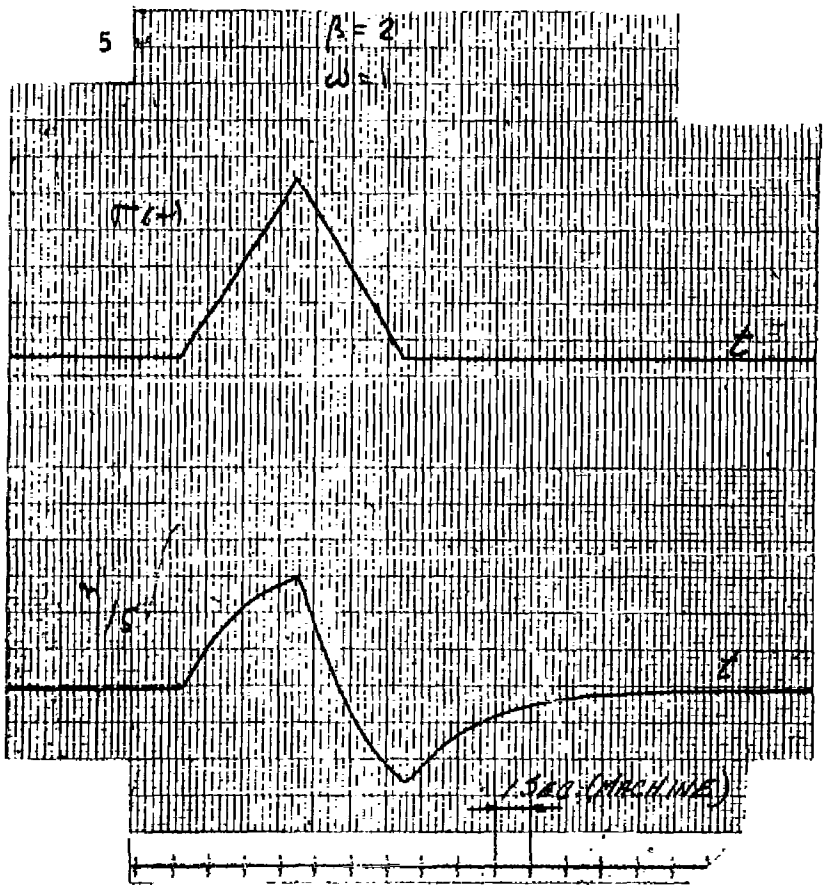

Figure 4.6 Triangular stress pulse and response. Equal rise and decay time, $\beta = 2$.

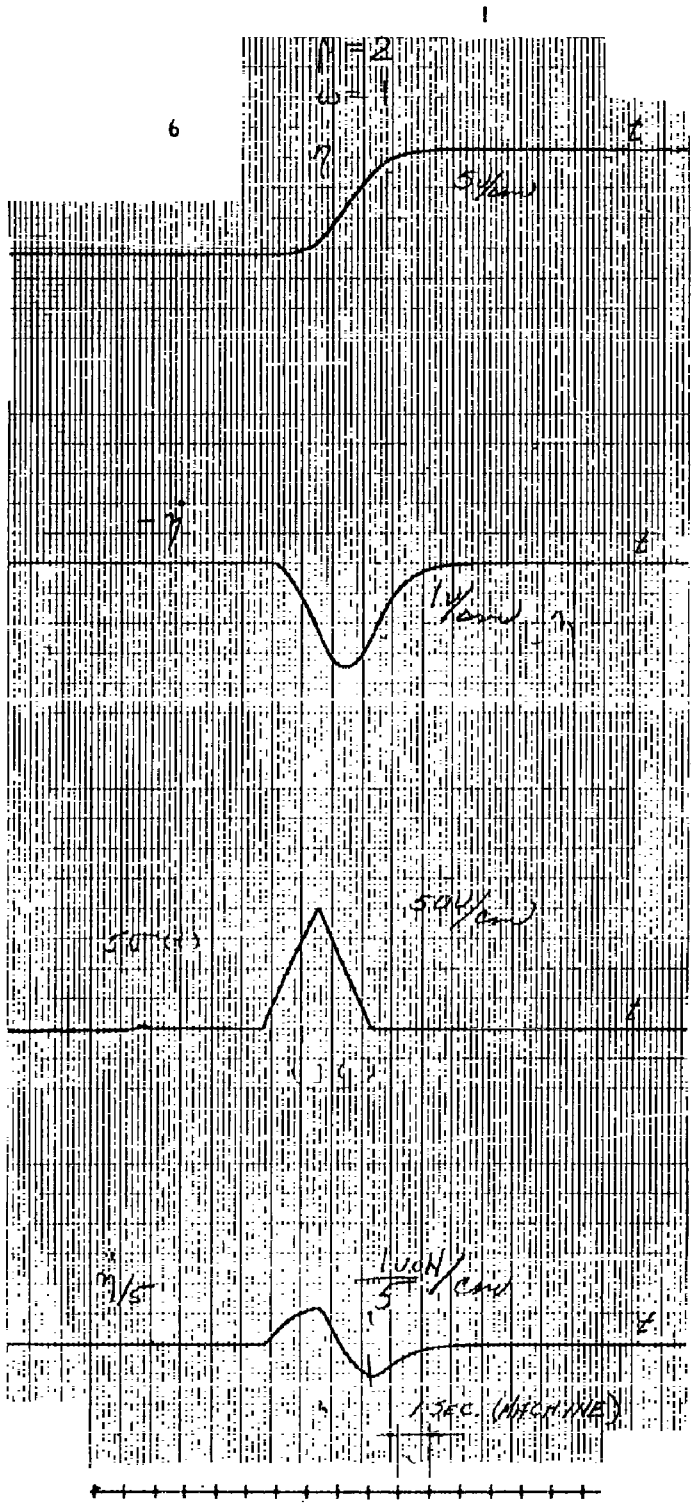

Figure 4.7 Triangular stress pulse and response. Displacement, velocity, acceleration, $\beta = 2$.

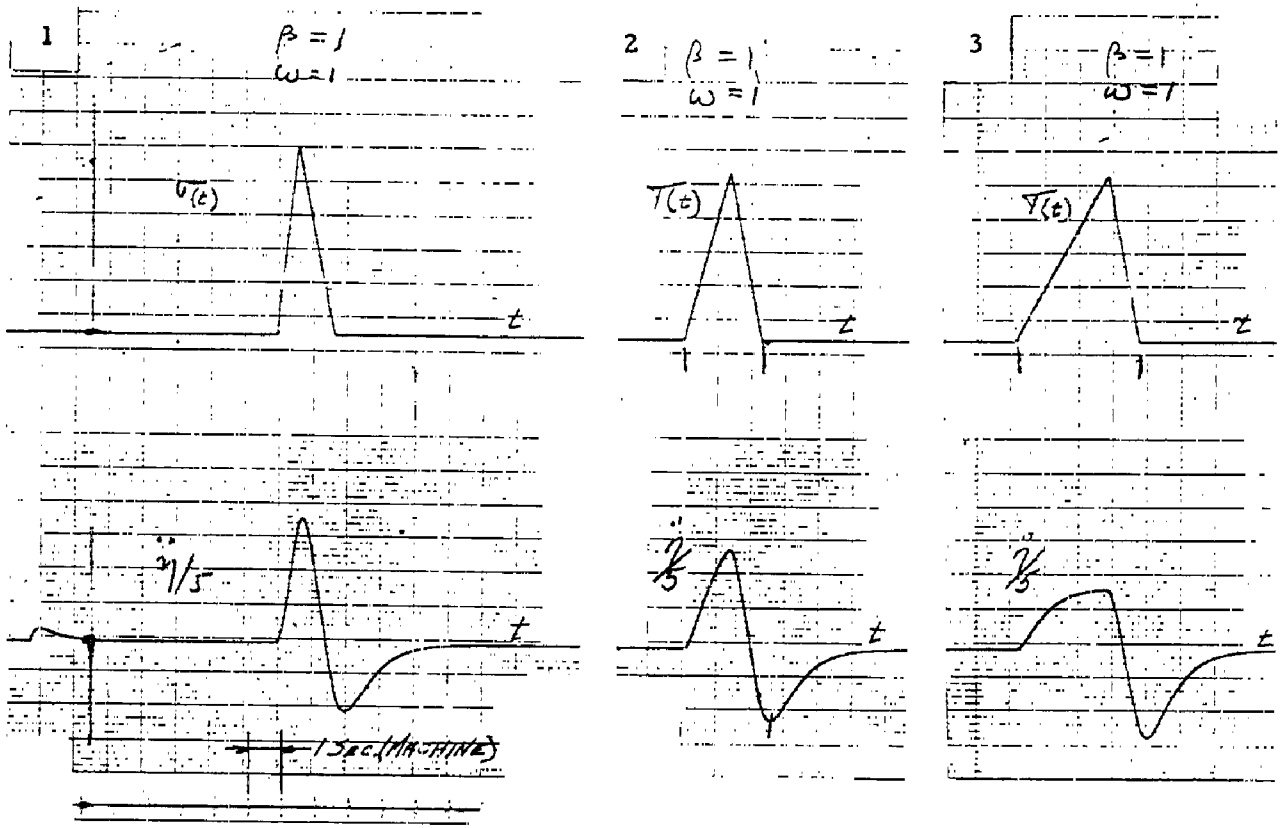

Figure 4.8 Triangular stress pulse and response.
1, 2 - Equal rise and decay time, $\beta = 1$.
3 - Short decay time, $\beta = 1$.

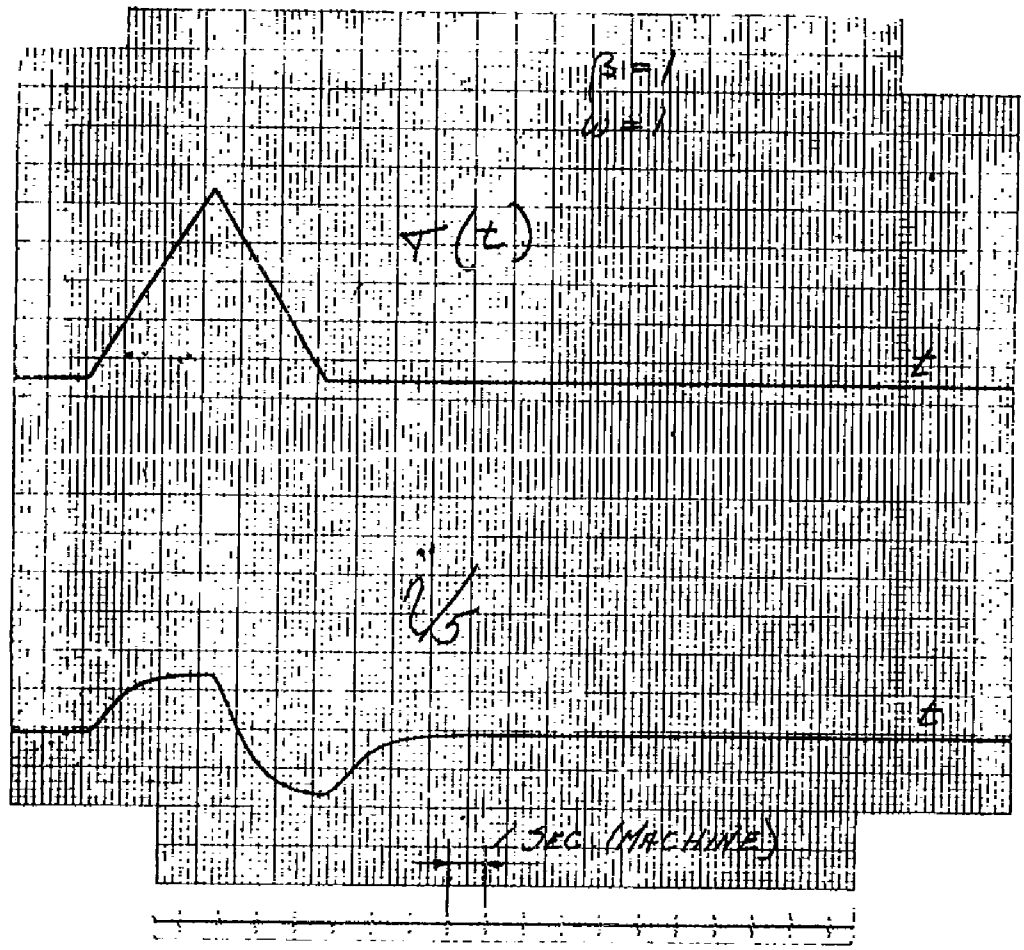

Figure 4.9 Triangular stress pulse and response. Equal rise and decay time, $\beta = 1$.

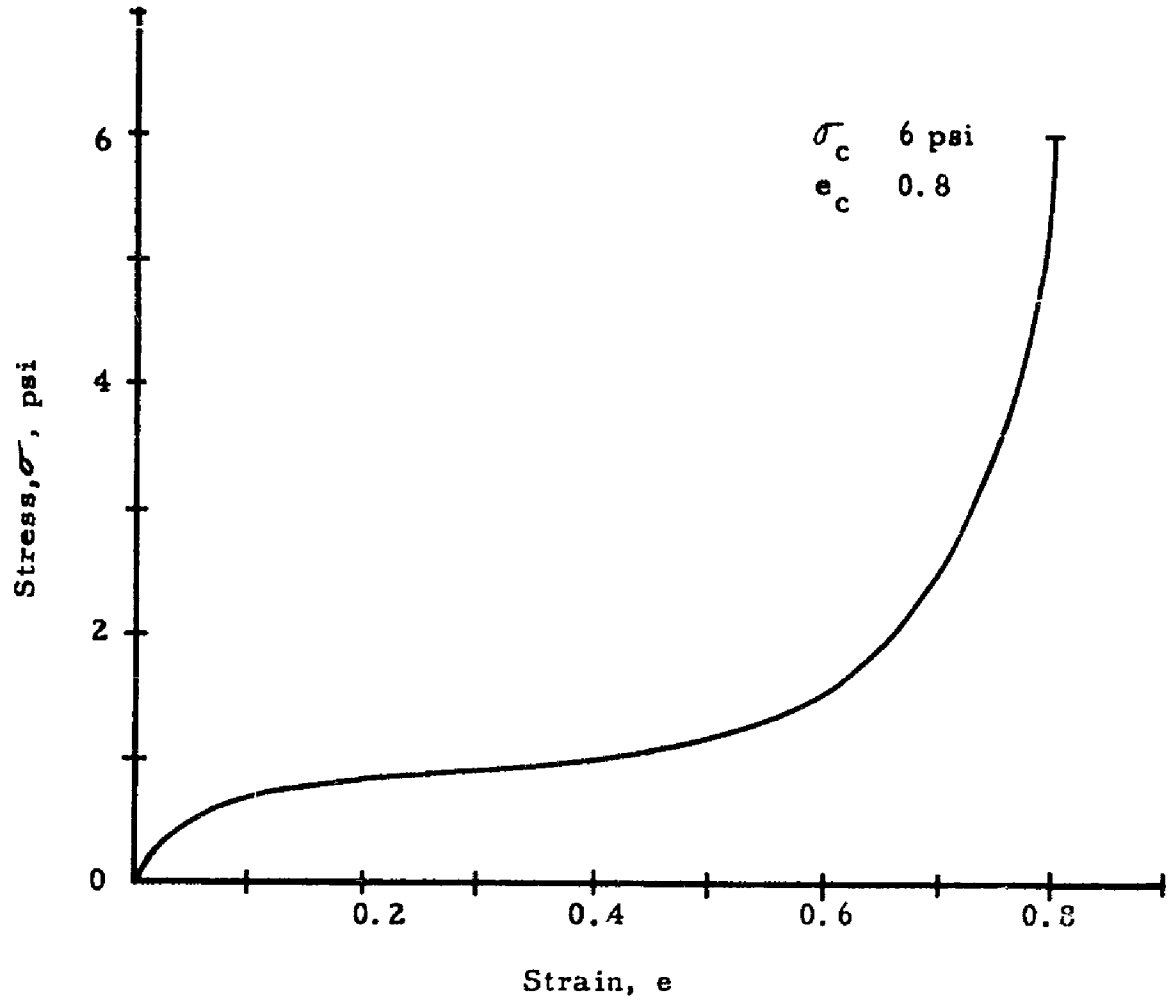

Figure 4.10 Stress-strain curve of flexible polyurethane foam (1/2 lb/ft^3).

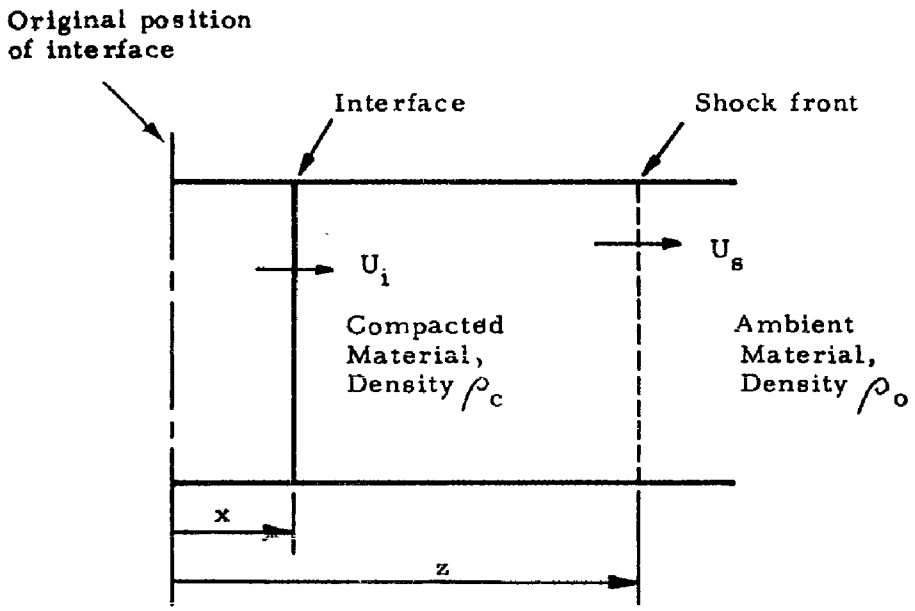

Figure 4.11 One-dimensional length of totally locking element.

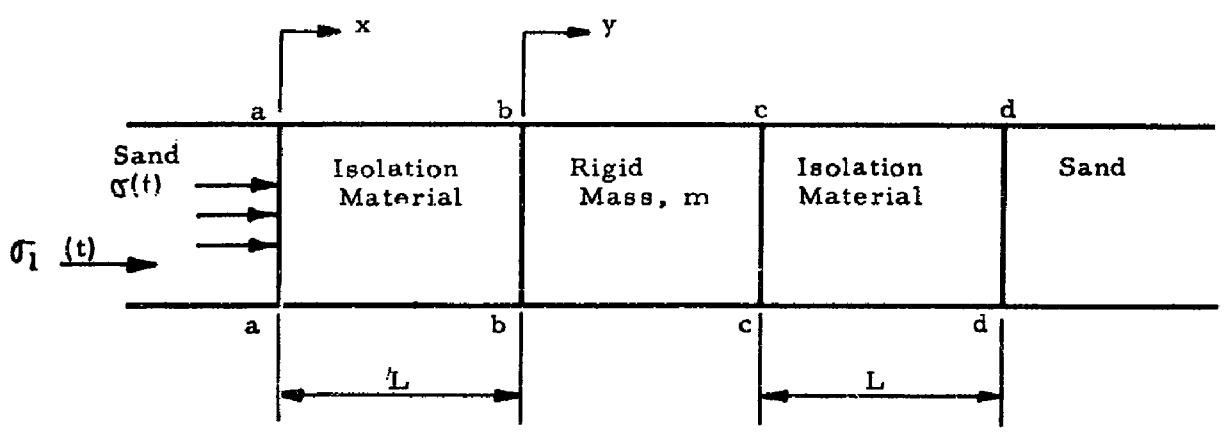

Figure 4.12 One-dimensional sand-isolation-model configuration

Chapter 5

DISCUSSION OF RESULTS

5.1 THE EXPERIMENTAL PROCEDURE

The results obtained are considered to demonstrate the feasibility of the experimental approach, at least insofar as reproducibility of effects is concerned. Success in this direction has proven to be mostly a matter of experimental technique, and the present procedure can doubtless be improved with continuing experimentation. From a quantitative point of view, the shot-to-shot variation in control-model response is practically negligible as compared to the differences in response between the control and isolation models. Thus, one would have confidence in utilizing this experimental approach to establish the effectiveness of a (model) isolation device on either a single- or repeated-shot basis. However, when one demands assurance of a highly reproducible input, as might be the case in rating relative effectiveness of different isolation devices, the matter is by no means as clear-cut.

The data indicate that effects are well reproduced on successive first shots on the bed, i.e., when the bed is completely reconditioned between shots, but that the effects recorded on a first shot are not as well reproduced in the second or later shots on the same bed. However, discounting the first shot, the effects are reasonably well reproduced in subsequent shots on the same bed. This rather curious result could indicate that the first detonation serves to shake the bed into more of an equilibrium state than is attained through vibration and that subsequent detonations then leave the bed relatively undisturbed. The explanation may have mostly to do with the condition of the crater area, however. That is, we may not have been successful in recompacting the crater area to its pre-first-shot condition for the second and later shots. This could be investigated by digging up the crater area after emplacing the models prior to a first shot and then restoring it in the manner of a second shot.

The greatest differences in behavior between shots were observed in the vertical accelerations. A possible explanation for this might be that the vibration process tends to "float" or rotate the model slightly[1/]. It is well appreciated that a uniform and high compaction of the bed is not easily attained. The mechanics of the vibration process are extremely involved: a major effort would be required to establish the proper type of vibrating tool, its operating frequency and amplitude, and the pattern and extent of vibration required to gain maximum compaction of the sand bed.

The responses of the control models were in reasonable agreement at the same radial location for any one shot. The differences attest to the variation in physical properties (mostly, relative density) throughout the bed. This is not believed to be due to asymmetrical behavior of the charge, since the crater was always quite symmetrical and very well reproduced in dimensions from shot-to-shot.

All things considered, the following procedure is recommended for future testing: The bed should be conditioned in the present manner, and three to four tests should be run without otherwise disturbing the models. The models should then be removed, the bed entirely reconditioned, and the same procedure repeated. Depending on the results obtained, it might be desirable to run this cycle of tests again. This unfortunately time consuming procedure seems essential if relatively small differences in model behavior are to be recognized.

5.2 THE EXPERIMENTAL RESULTS

It appears that the control model primarily executes the motion of the free field. This suggests the possibility of using the measured acceleration to estimate incident free-field stress levels. Based on the parameter values given in Section 4.4.2.3, the maximum positive acceleration of the model due to a cosine-type stress wave (see Appendix C) corresponds to a stress amplitude of about 0.1 psi per g. For a 10-g peak

---

1/ The weight of the sand displaced by the model exceeds the weight of the model itself, thus possibly creating a bouyancy effect when the sand particles are in motion.

acceleration, this predicts a peak stress of 1 psi and an associated maximum displacement of 6×10^{-4} in. While these are not claimed to have been the actual test conditions, they seem of reasonable value.

The tests with polyurethane foam indicate this material to be highly effective as an isolation device. The observed low-frequency low-amplitude motion is suggestive of elastic (i.e., non-energy-dissipative) behavior, as if the model were spring-mounted from a rigid surface. This view is also supported by theoretical considerations. The theory of a totally locking isolation material indicates that the dissipative action of the foam should obtain only at extremely high incident stress levels, while the observed relative behavior of the two thicknesses of foam is as expected on the basis of elastic response. Thus, the compliance of the foam springs being proportional to their length, one would expect the thicker material to exhibit the greater period and the lesser acceleration amplitude. This behavior was observed in the tests, although it is not possible to gain a strictly quantitative comparison between the two models.

Little can be said concerning the general significance of the experimental results since, at best, this matter can never be settled within the context of miniature-scale experimentation alone. Moreover, the major effort of the program to date has been in the establishment of an experimental technique, and the gathering of data has only just begun. Necessarily, this discussion will be brief.

The practical problem of achieving a satisfactory level of shock isolation clearly seems dependent upon the scale of the motions of the free field. Thus, the effects of transient ground motions of several inches might be ameliorated in various ways, whereas motions of several feet or more pose problems that are at least different in degree and possibly in kind. In pressure regions of current interest, however, the concensus of opinion (if not of fact) suggests that the gross motions of the soil are of tolerable proportions, and this would tend to support the reasonableness of the present experimental approach, the differences in ground shock and geometric scale notwithstanding. Granted this, the results so far are encouraging. Specifically, it is suggested that simple non-energy-dissipative systems are effective and, moreover, that a material such as the polyurethane foam

used in the tests may be practically applicable to prototype installations. This latter suggestion, in a way, is more than had been anticipated, since our original view discounted the possibility of actually testing prototype systems. However, the properties of this particular class of materials seem to demand further consideration.

Chapter 6

CONCLUSIONS AND RECOMMENDATIONS

6.1 CONCLUSIONS

Within the scope of the work as set forth in this report the following conclusions have been reached.

1. A satisfactory experimental procedure was evolved for producing ground shock disturbances in a non-cohesive (Ottawa) sand medium using small HE charges. Stress levels achieved to date are estimated to be of the order of 1 psi at the test locations.

2. It is possible to achieve reasonably good reproducibility of effects within the bed from shot-to-shot. While strict duplication of free-field conditions for any two shots cannot be guaranteed, these differences are considered insignificant insofar as evaluating the effectiveness of a model isolation device is concerned.

3. A model isolation device consisting of a thickness of a flexible polyurethane foam interspaced between a rigid silo-like model and the sand was shown to be effective in reducing peak accelerations executed by the structure. Peak accelerations are reduced by a factor of eight or more, with a corresponding increase in the period of the motion. While the foam material can act as an energy-dissipating medium at extremely large incident stress levels (1000 psi), the experimental results indicate that its action is elastic and approximates that of a linear spring at the low stress levels of this experiment.

6.2 RECOMMENDATIONS

1. It is believed that a continuation of the experimental work described herein is justified. This would involve primarily an investigation of the isolation effectiveness of various formulations of foam materials (or their equivalents) under the highest practical stress levels.

2. Consideration should be given to the design of a small-scale experimental program, utilizing HE-generated ground shock and models several times the scale of the present tests. These tests would be conducted out-of-doors so as to achieve higher stress levels than are now practical and to more closely simulate the combined effects of both direct and air-induced ground shock. However, such tests could not imply a known means of modeling structural response or of scaling to large HE or nuclear bursts.

3. Consideration should be given to the practical employment of such materials as flexible polyurethane foam in the shock isolation of prototype structures.

BIBLIOGRAPHY

1. Armour Research Foundation, "Concepts and Preliminary Design of Structure Projects for Underground Detonations", Final Report ARF Project No. D163, AFSWC, Cntr. AF 29(610)1169, August 1959. (Secret).

2. Armour Research Foundation, "Investigation of Wave Propagation in Semi-Solids", Final Report, ARF Project No. K115, AFSWC, Cntr. AF(601)-465, Project No. 1080, March 1958.

3. Armour Research Foundation, "Research Study of Stress Waves in Model Earth Media", Final Report, ARF Project No. K148, AFSWC, AF29(601)-1167, August 1959.

4. Baron, H. L., and Bleich, H. H., "Further Studies of the Response of a Cylindrical Shell to a Transverse Shock Wave", Office of Naval Research, Report No. 10, Cntr. 266(08), 1955.

5. Bernhard, R. K., and Finelli, J., "Pilot Studies on Soil Dynamics", Symposium on Dynamic Testing of Soils, ASTM Special Technical Publication No. 156, Fifty-sixth Annual Meeting, July 1953.

6. Berry, D. S., "Stress Propagation in Visco-Elastic Bodies", Journal of Mechanics and Physics of Solids, 1958.

7. Bronwell, A., Advanced Mathematics in Physics and Engineering, McGraw-Hill Book Co., Inc., New York, 1953.

8. Courant, R., and Friedrichs, K. O., Supersonic Flow and Shock Waves, Interscience Publishers, New York, 1948.

9. Crandell, F. J., "Ground Vibration Due to Blastings and Its Effect Upon Structures", Journal of the Boston Society of Civil Engineers, 1949-1950.

10. Crede, C. E., Shock Isolation, J. L. Wiley & Sons, Inc., New York, 1941.

11. Creskoff, J. J., Dynamics of Earthquake Resistant Structures, McGraw-Hill Book Co., Inc., New York, 1934.

12. Duvall, G. E., and Lwolinski, B. J., "Entropic Equations of State and Their Application to Shock-Wave Phenomena in Solids, Journal of Accoustical Society of America, Vol. 27, No. 6, 1955.

13. Engineering Research Associates, Inc., "Underground Explosion Test Program", Final Report, Vol. I, Cntr. DA-04-167-ENG-298, Department of the Army, Corps of Engineers, 1952. (Confidential).

14. Ewing, W. M., Jordetsky, W. S., and Press, F., Elastic Waves in Layered Media, McGraw-Hill Book Co., Inc., New York, 1957.

15. Franklin, P. E., and Hatae, M. T., "Optimum Cushioning Properties of Packaging Cushioning Materials", North American Aviation, Inc., AL-2478, May 1957.

16. Gassmann, F., "Electric Waves through a Packing of Spheres", Geophysics, Vol. 16, 1951.

17. Goodier, J. H., Jahsman, W. E., and Ripperger, E. A., "An Experimental Surface-Wave Method for Recording Force-Time Curves in Elastic Impacts", Journal of Applied Mechanics, Paper No. 58-A-51, 1958.

18. Institute of Research, Lehigh University, "Explosions in Earth Engineering Analysis of Bomb Damage Surveys", Phase 1-B, Terminal Ballistics, Progress Report 4A, Cntr.36-034-ORD-7640, 1958. (Confidential).

19. Kolsky, H., Stress Waves in Solids, Oxford University Press, London, 1953.

20. Lang, H. A., "The Complete Solution for an Elastic Half-Space under a Point Step Load", The Rand Corporation, October 1957.

21. Leet, L. D., "Blasting Vibrations Effects", Explosives Engineer, 1950-51.

22. Macinante, J. A., "Survey on Vibration and Shock Isolation", Australia Commonwealth Scientific and Industrial Research Organization, Technical Paper N7, 1955.

23. Mindlin, R. D., "Mechanics of Granular Material", Columbia University, ONR, Project NR-064-388, Technical Report 14, June 1954.

24. Morris, G., "Vibrations due to Blasting and Their Effect on Building Structures", The Engineer, 1950.

25. Salvadori, M. G., and Weidlinger, P., "Induced Ground Shock in Granular Media", Reports No. 1 and 2, Paul Weidlinger, Consulting Engineer, New York, 1958. (Confidential).

26. Scopek, J., "Sand Density Determination Using Gamma Radiation", Proceedings Fourth International Conference on Soil Mechanics and Foundation Engineering, Vol. 1, Butterworth's Scientific Publications, London, 1957.

27. Serbin, H., "The Intense Stress Field Produced in the Elastic Earth by a Bomb Blast at the Surface", The Rand Corporation, 1957.

28. Sevin, E., "Min-Max Solutions for the Linear Mass-Spring System", Journal of Applied Mechanics, Vol. 24, No. 1, March 1957.

29. Slocum, S. E., "Experimental Research on Vibration Insulators", ASCE Trans., 1931.

30. Sezawa, K., "On the Decay of Waves in Visco-Elastic Solid Bodies", Earthquake Research Institute, Tokyo, 1927.

31. Sezawa, K., "On the Propagation of Rayleigh-Waves on Plane and Spherical Surfaces", Earthquake Research Institute, Tokyo, 1926.

32. Sezawa, K., "Propagation of Elastic Waves from an Elliptic or a Spherical Origin", Earthquake Research Institute, 1926.

33. Sezawa, K., "Scattering of Elastic Waves and Some Allied Problems", Earthquake Research Institute, Tokyo, 1927.

34. Sezawa, K., and Genrokuro, N., "Rayleigh-type Waves Propagated along an Inner Stratum of a Body", Earthquake Research Institute, Tokyo, 1928.

35. Stanford Research Institute, "Ground Motion Produced by Above Ground Nuclear Explosions", Part II, Summary and Correlation of Data, Interim Report No. I. AFSWC, Cntr. AF29(601)-542, Project No. 1080, Task 10801. (Secret).

36. Stanford Research Institute, "Isolation of Structures for Ground Shock", Operation Plumbbob - Project 3.5, AFSWC, IRT 1424, 1957 . (Confidential

37. Stanford Research Institute, "Propagation of Stress Waves in Soil", Part I., AFSWC, Cntr. AF29(601)-540, Proj. 1080, 1958. (Secret).

38. Synge, J. L., "Elastic Waves in an Isotropic Media", Journal of Mathematics and Physics, Vol. 34, 1957.

39. Terada, T. and Tsuboi, C., "Experimental Studies on Elastic Waves", Earthquake Research Institute, Tokyo, 1927.

40. Terzaghi, K., Theoretical Soil Mechanics, J. L. Wiley & Sons, Inc., New York, 1943.

41. Timoshenko, S., Theory of Elasticity, McGraw-Hill Book Co., Inc., New York, 1934.

42. University of California, "Theoretical Studies of Underground Shock Waves", Operation Jangle - Project 1.9, AFSWC, WT-358, 1957. (Secret).

43. White, R. J., "Elastic Wave Scattering at a Cylindrical Discontinuity in a Solid", Journal of Acoustical Society of America, 1958.

44. Whitman, R. V., et. al., "The Behavior of Soils under Dynamic Loadings", Massachusetts Institute of Technology, Final Report on Laboratory Studies, August 1, 1954.

Appendix A

EXPERIMENTAL DATA

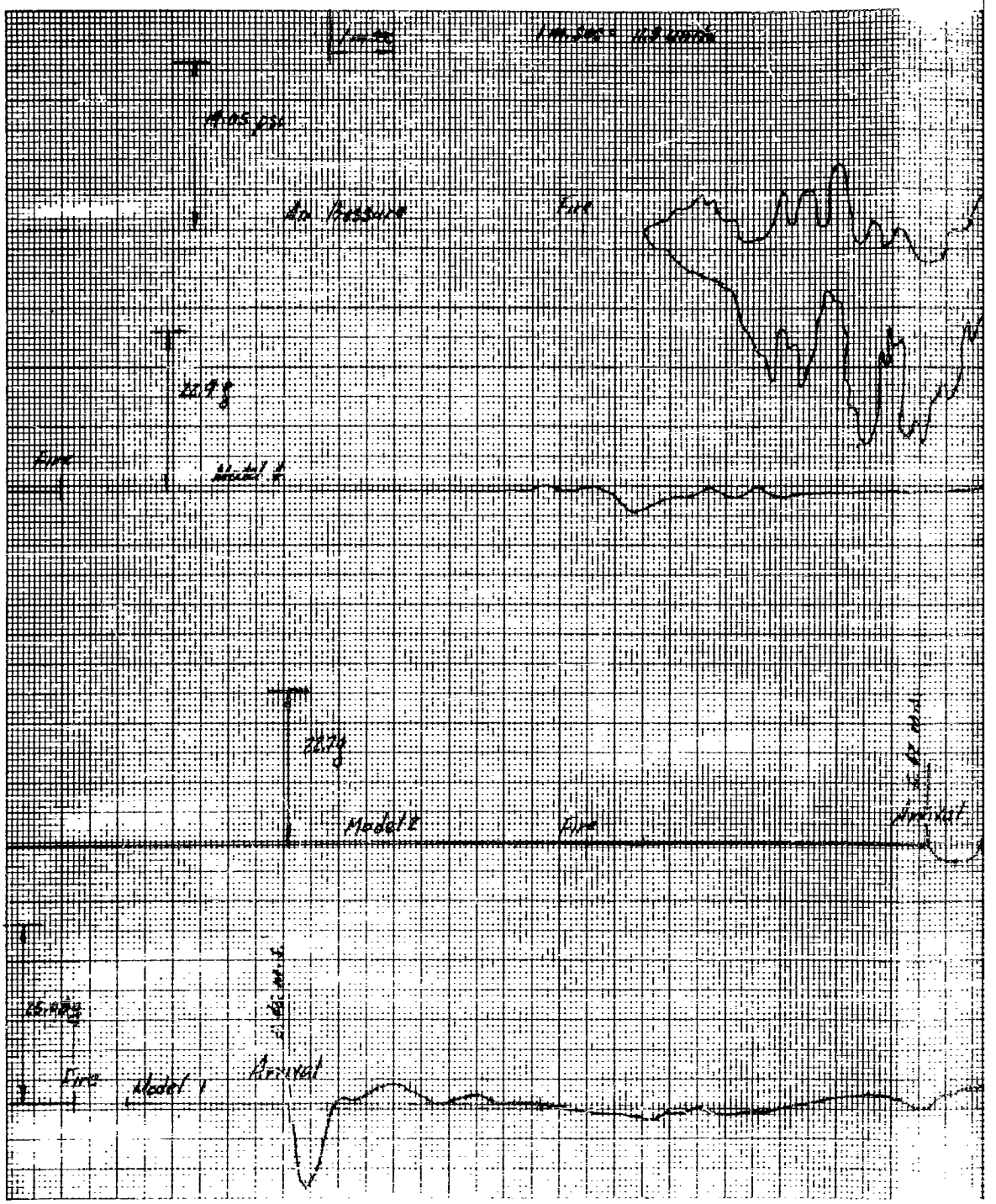

1

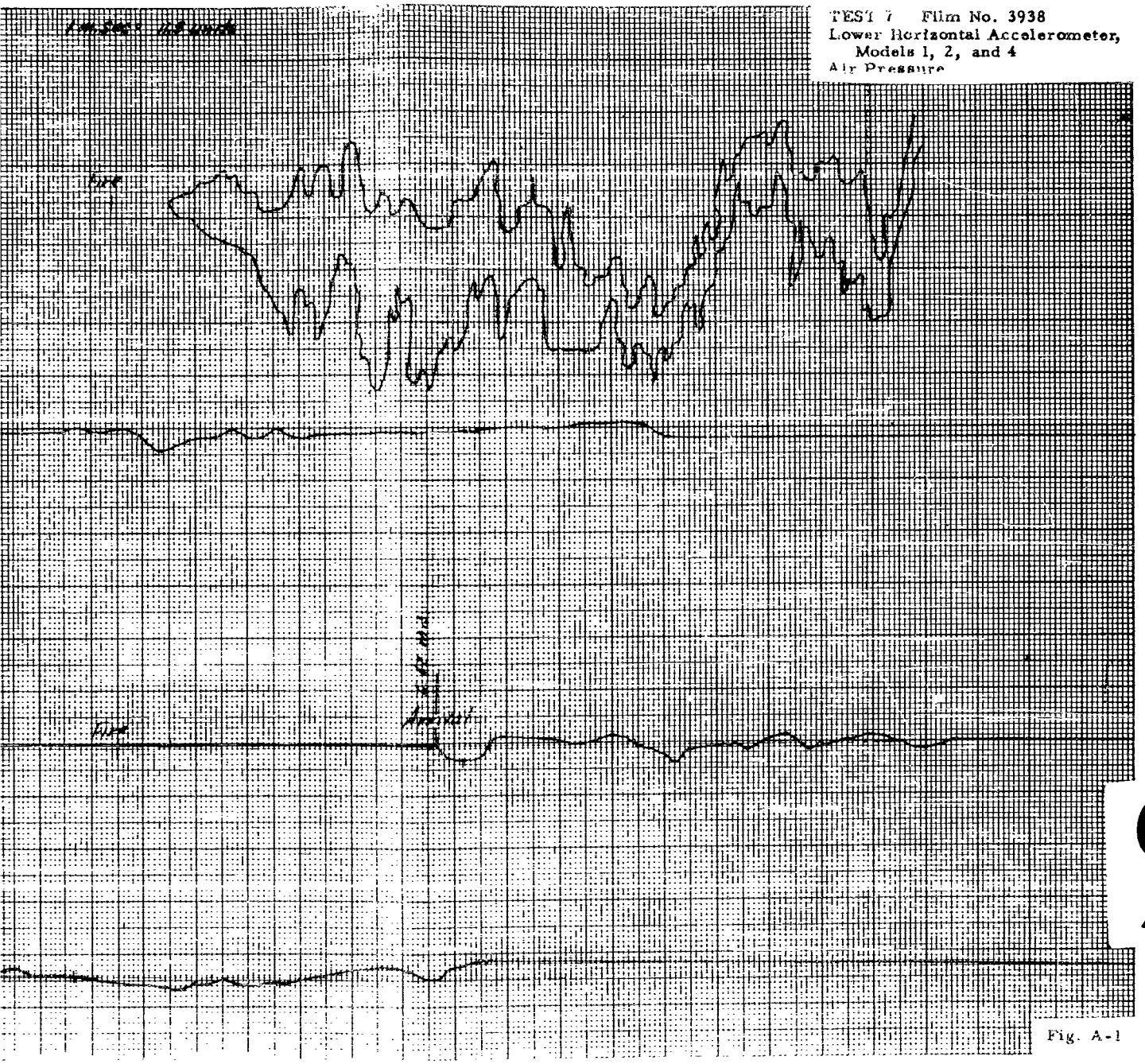

TEST 7 Film No. 3938
Lower Horizontal Accelerometer,
Models 1, 2, and 4
Air Pressure

2

Fig. A-1

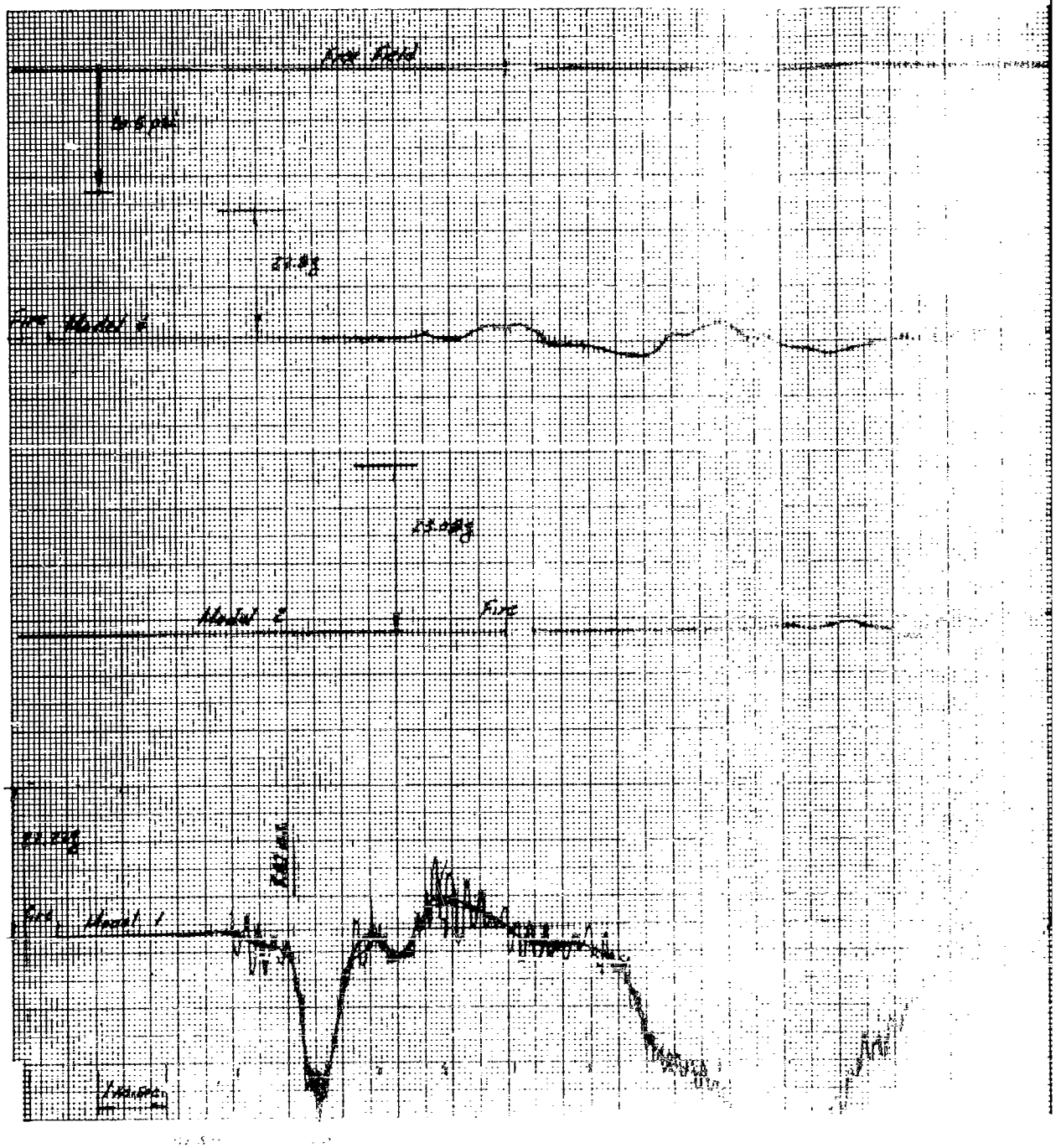

1

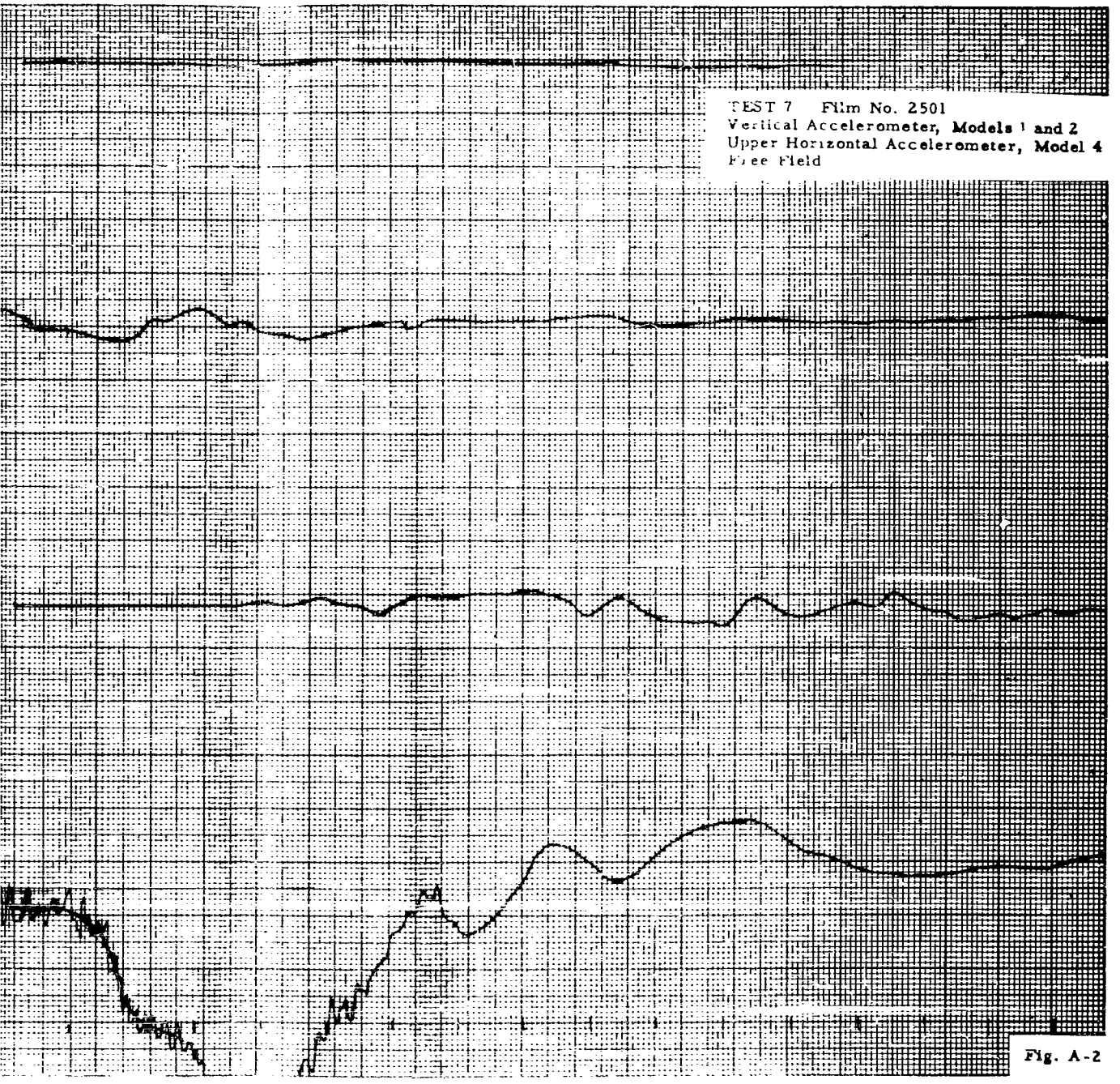
TEST 7 Film No. 2501
Vertical Accelerometer, Models 1 and 2
Upper Horizontal Accelerometer, Model 4
Free Field

Fig. A-2

2

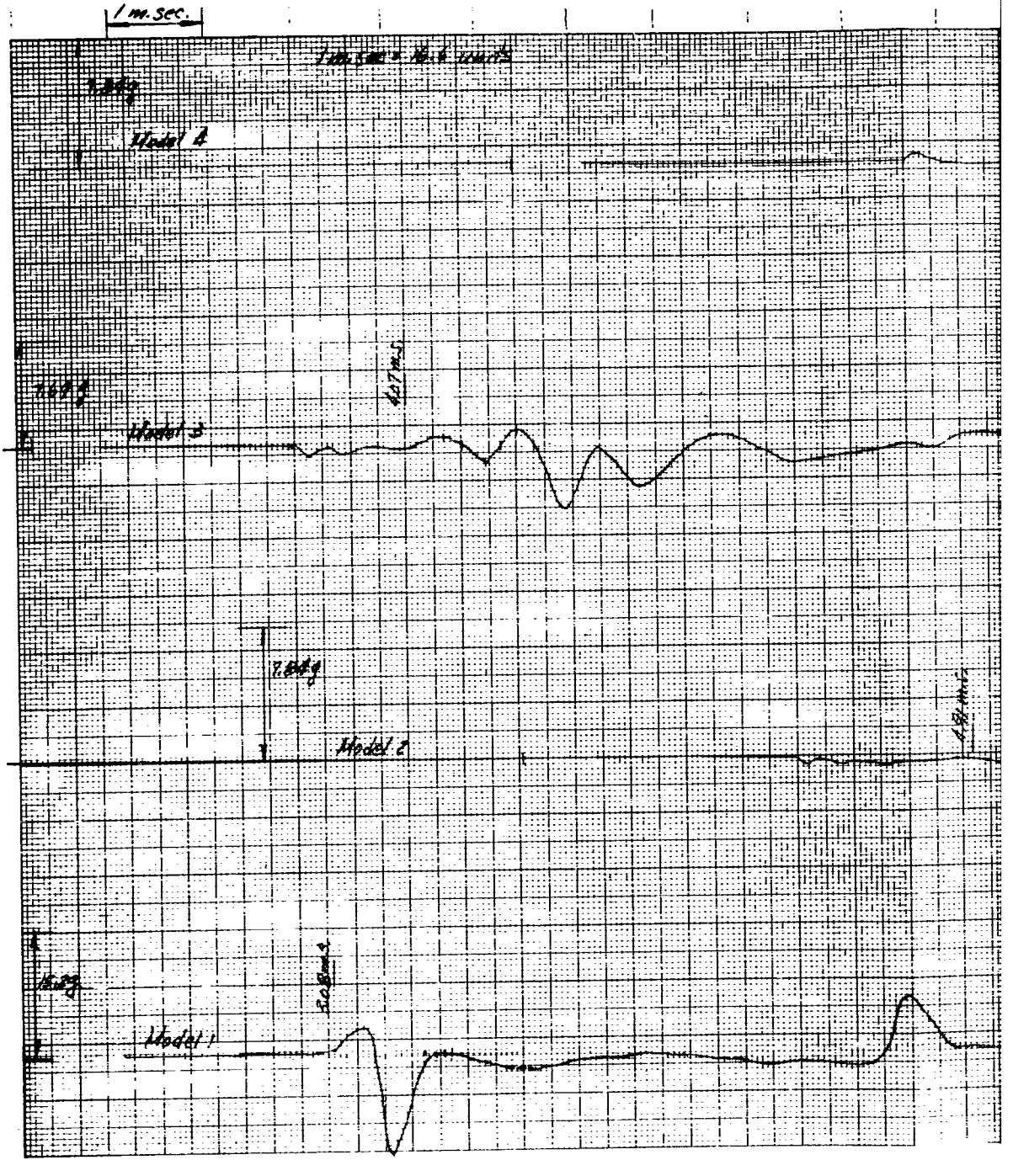

1

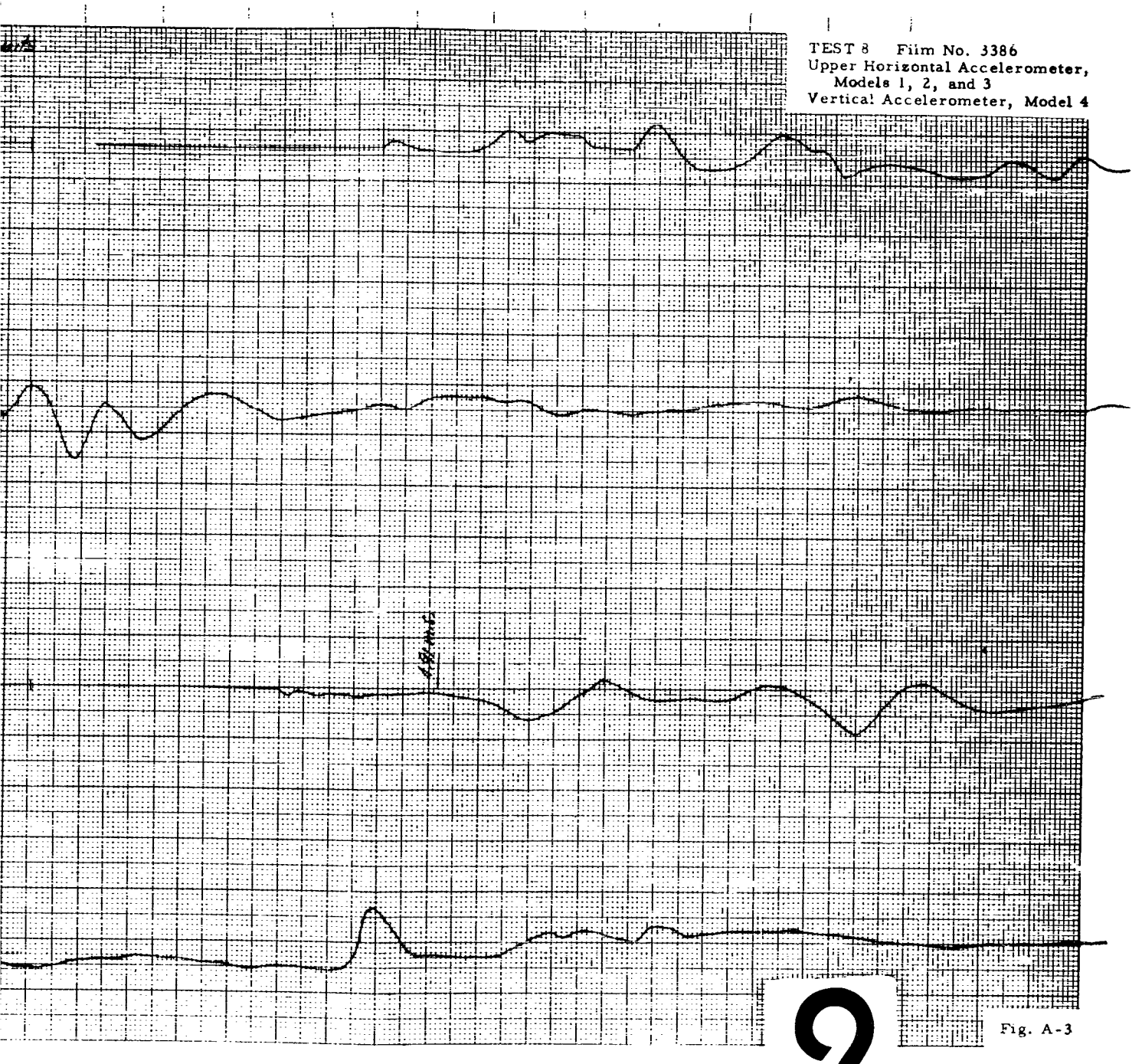
TEST 8 Film No. 3386
Upper Horizontal Accelerometer,
Models 1, 2, and 3
Vertical Accelerometer, Model 4

Fig. A-3

2

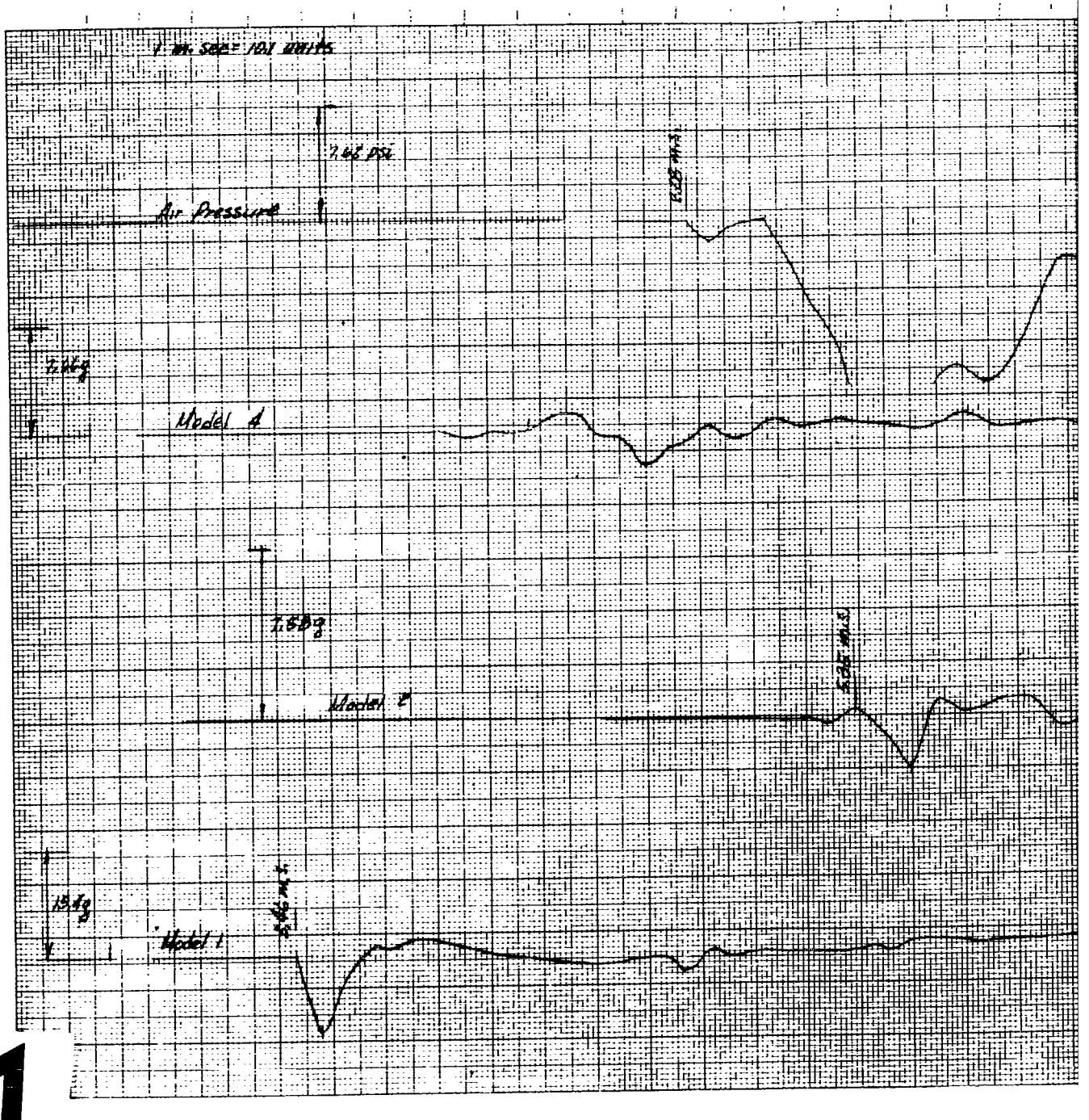
1 in. sec = 101 units
7.46 psi
Air Pressure
7.46g
Model A
7.58g
Model B
15.4g
Model C

1

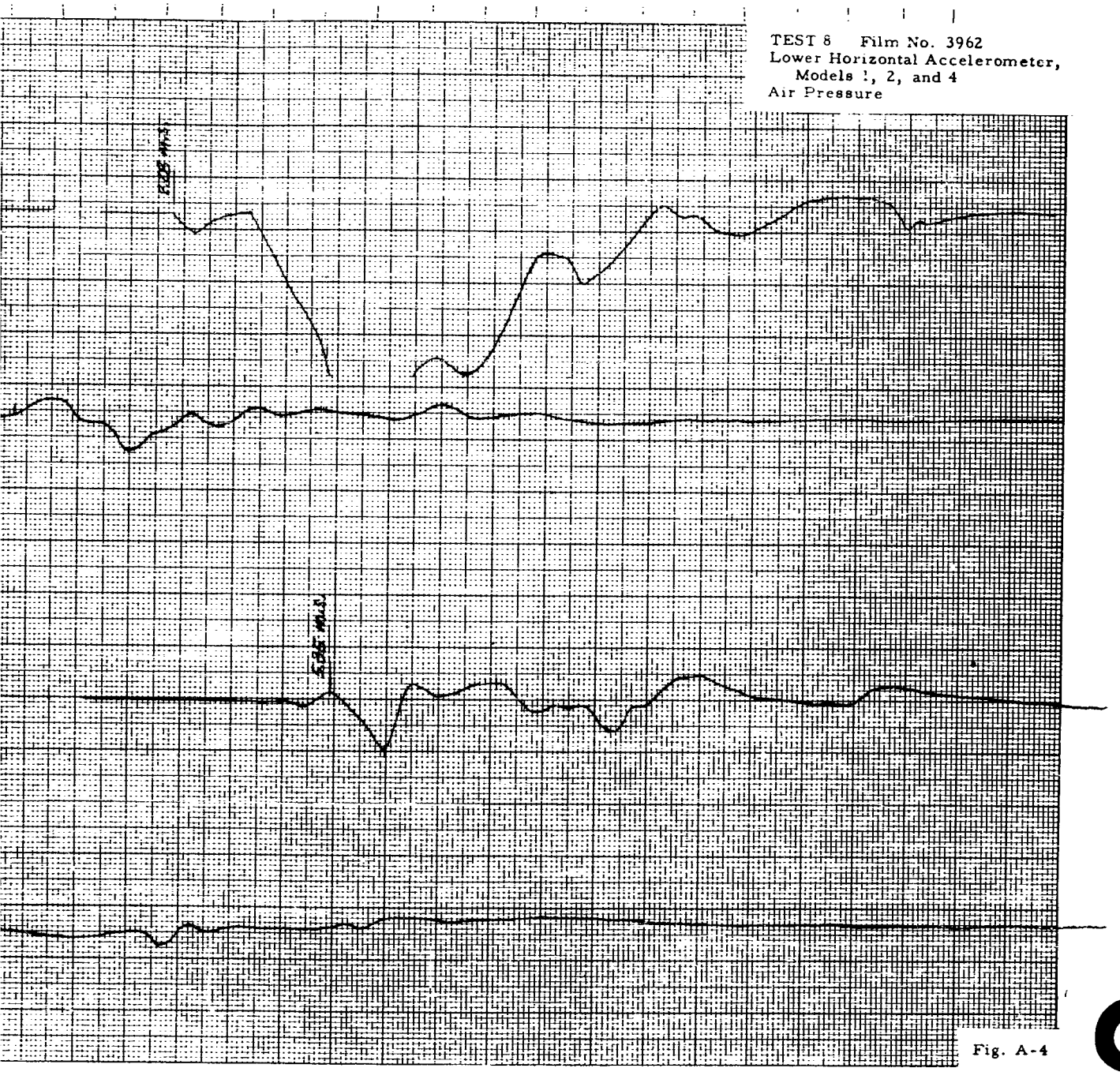

TEST 8 Film No. 3962
Lower Horizontal Accelerometer,
Models 1, 2, and 4
Air Pressure

Fig. A-4

2

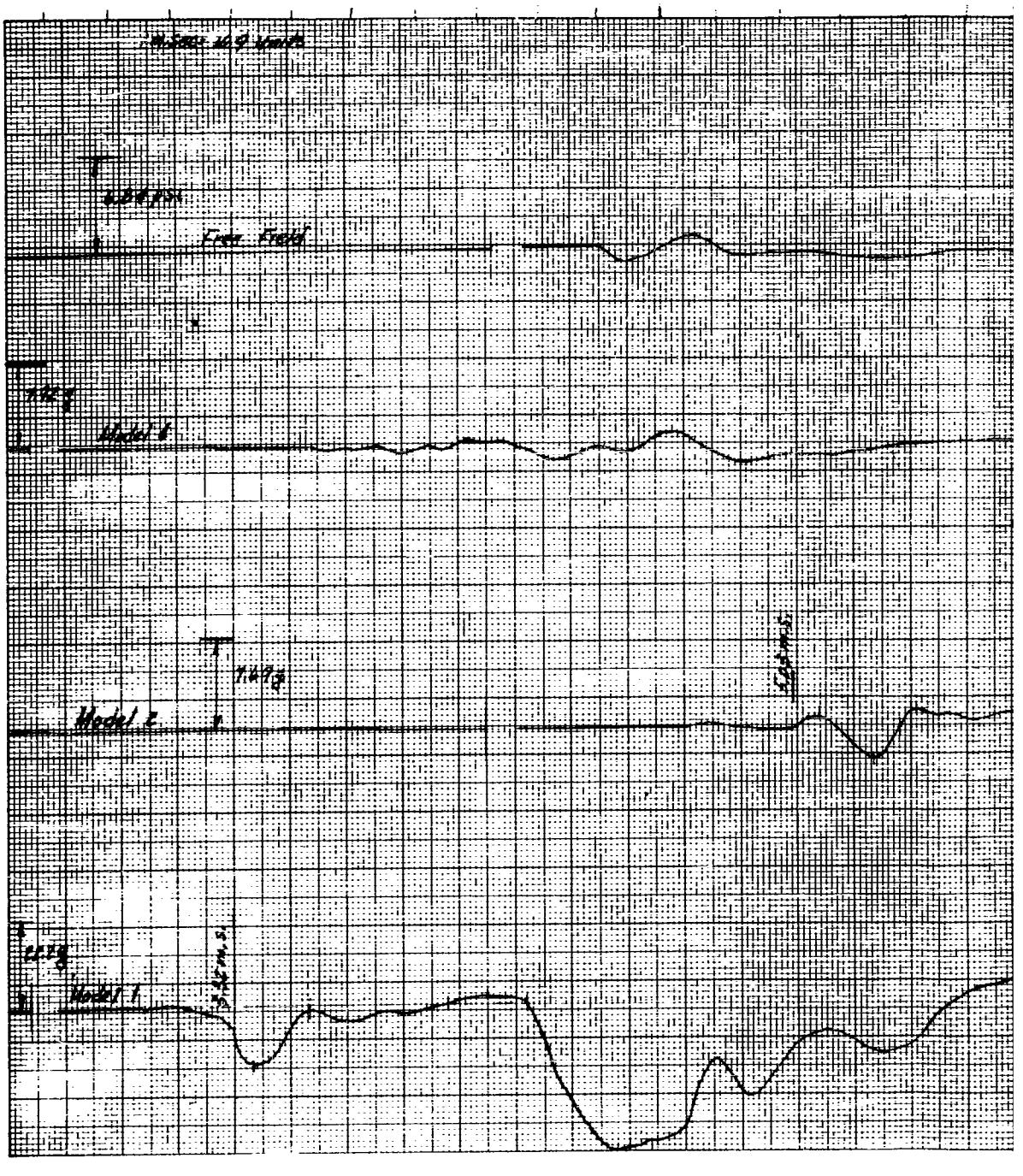

1

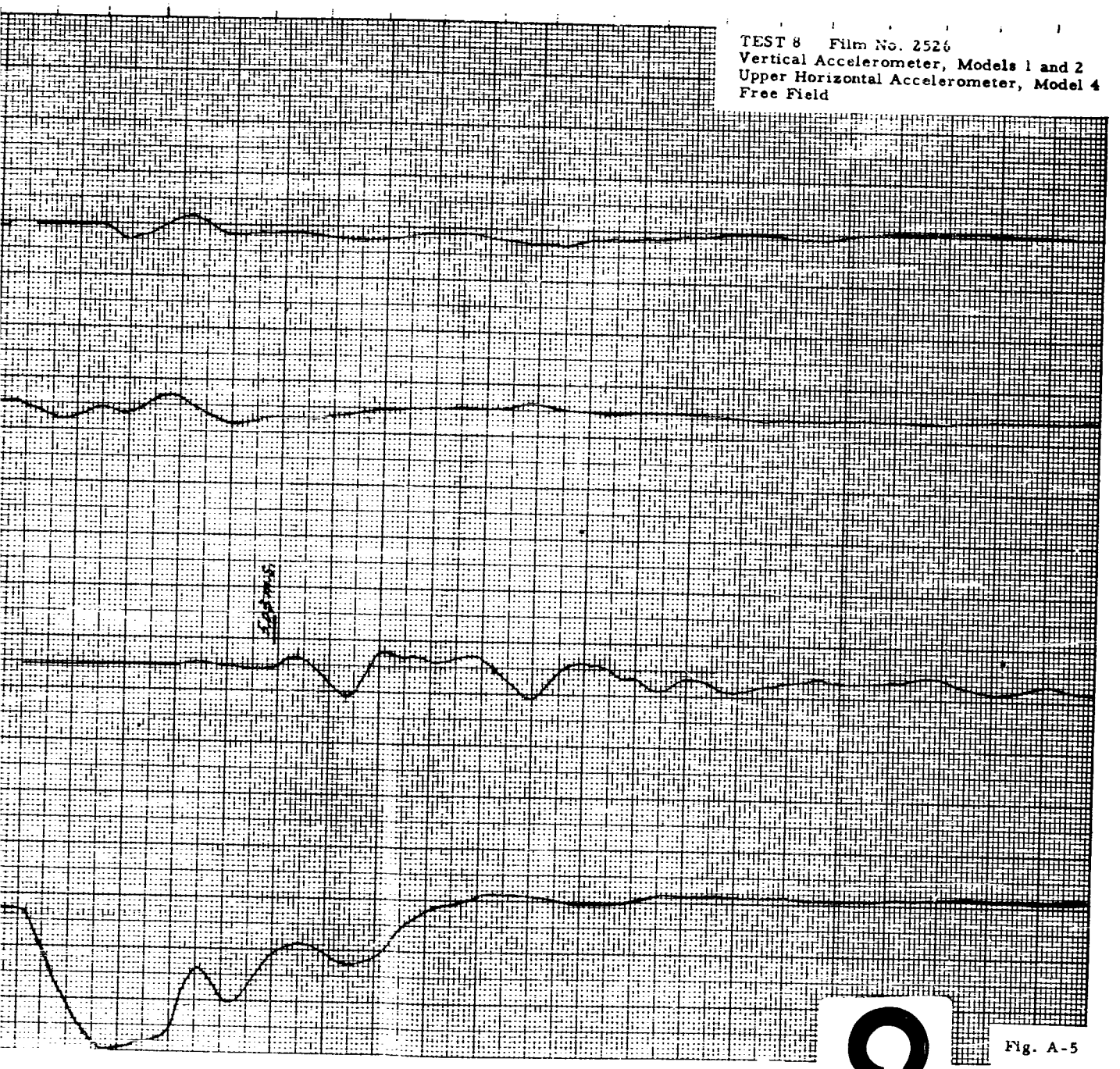
TEST 8 Film No. 2526
Vertical Accelerometer, Models 1 and 2
Upper Horizontal Accelerometer, Model 4
Free Field

2

Fig. A-5

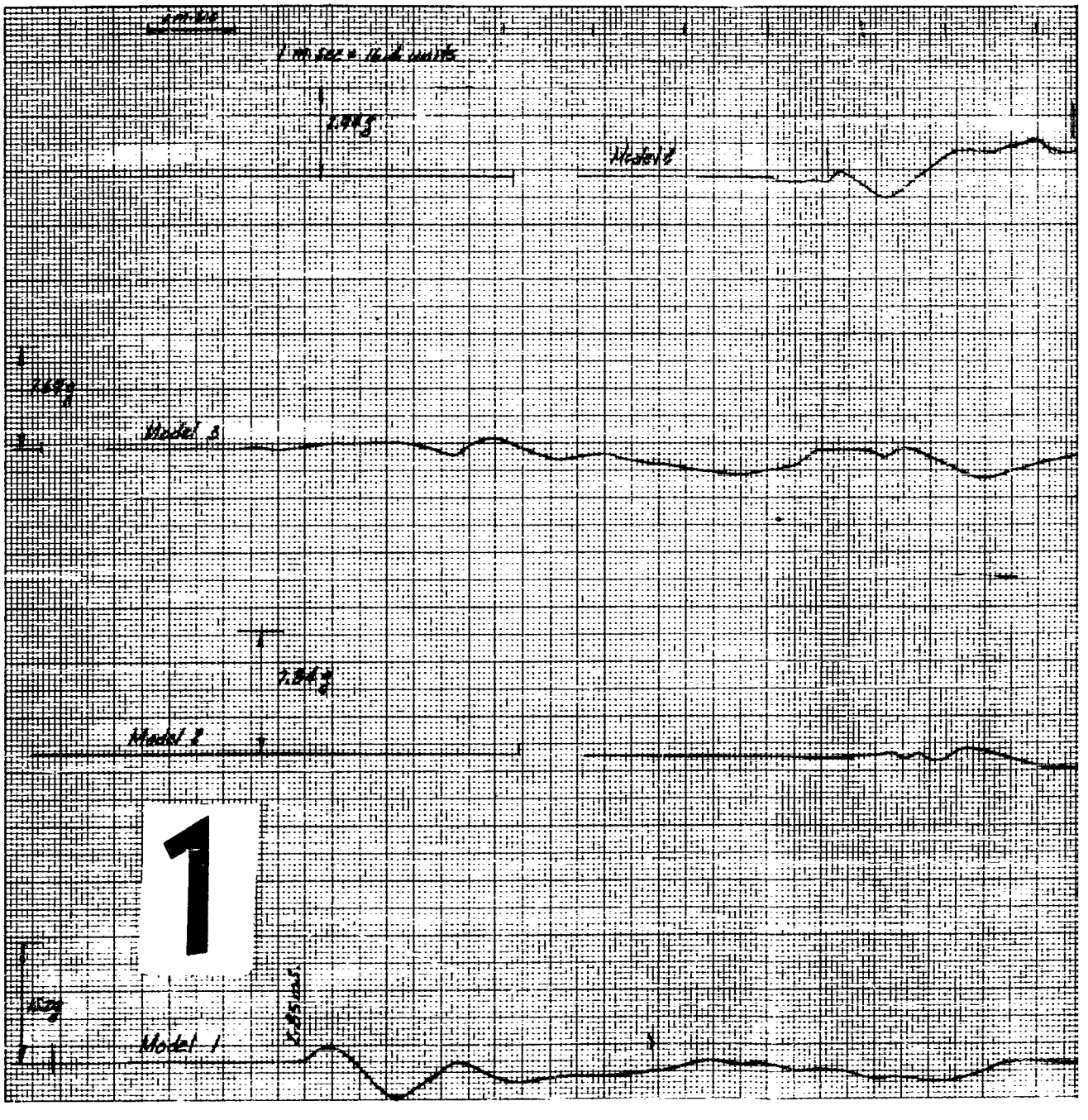

1

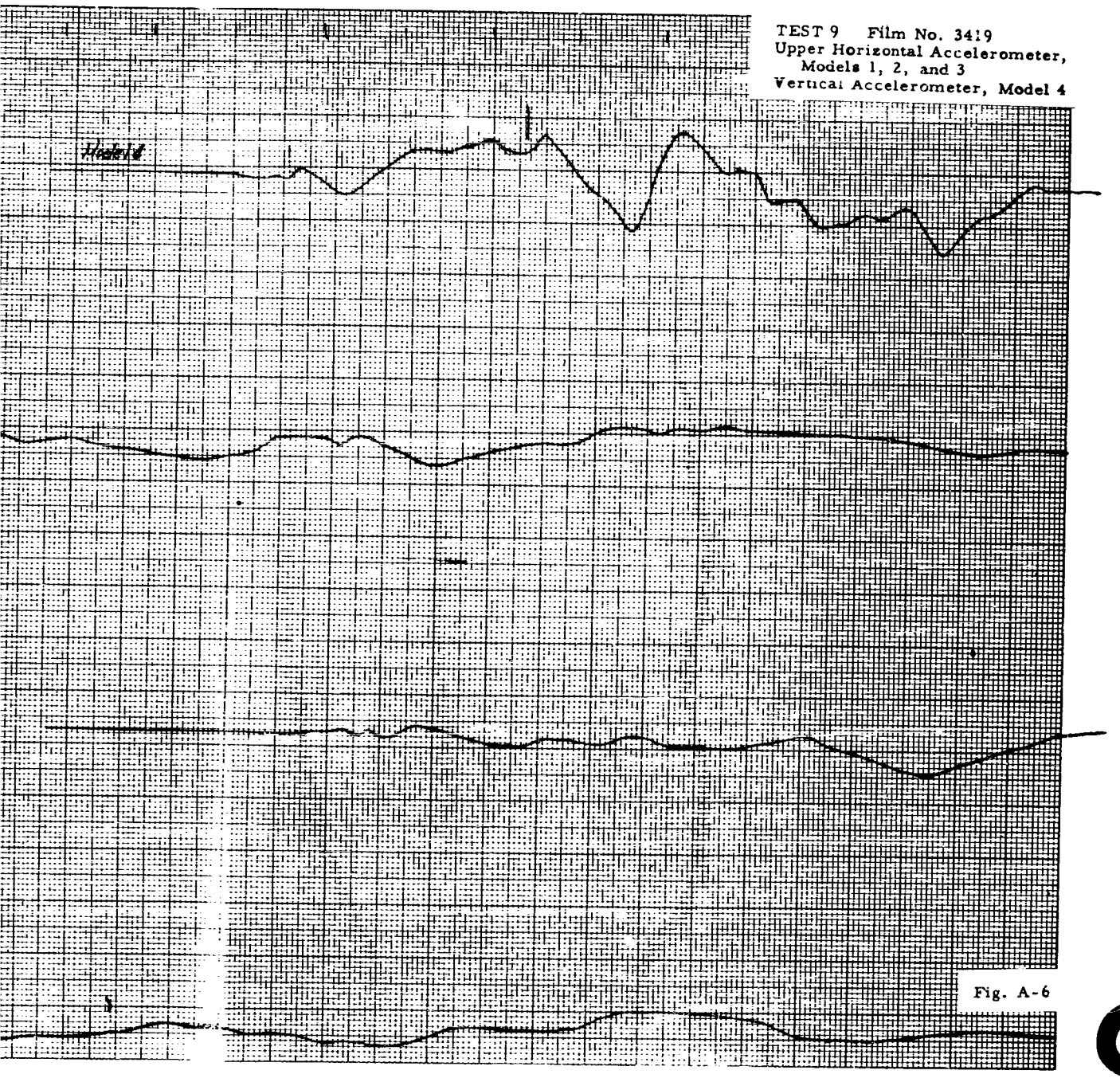
TEST 9 Film No. 3419
Upper Horizontal Accelerometer,
Models 1, 2, and 3
Vertical Accelerometer, Model 4

Fig. A-6

2

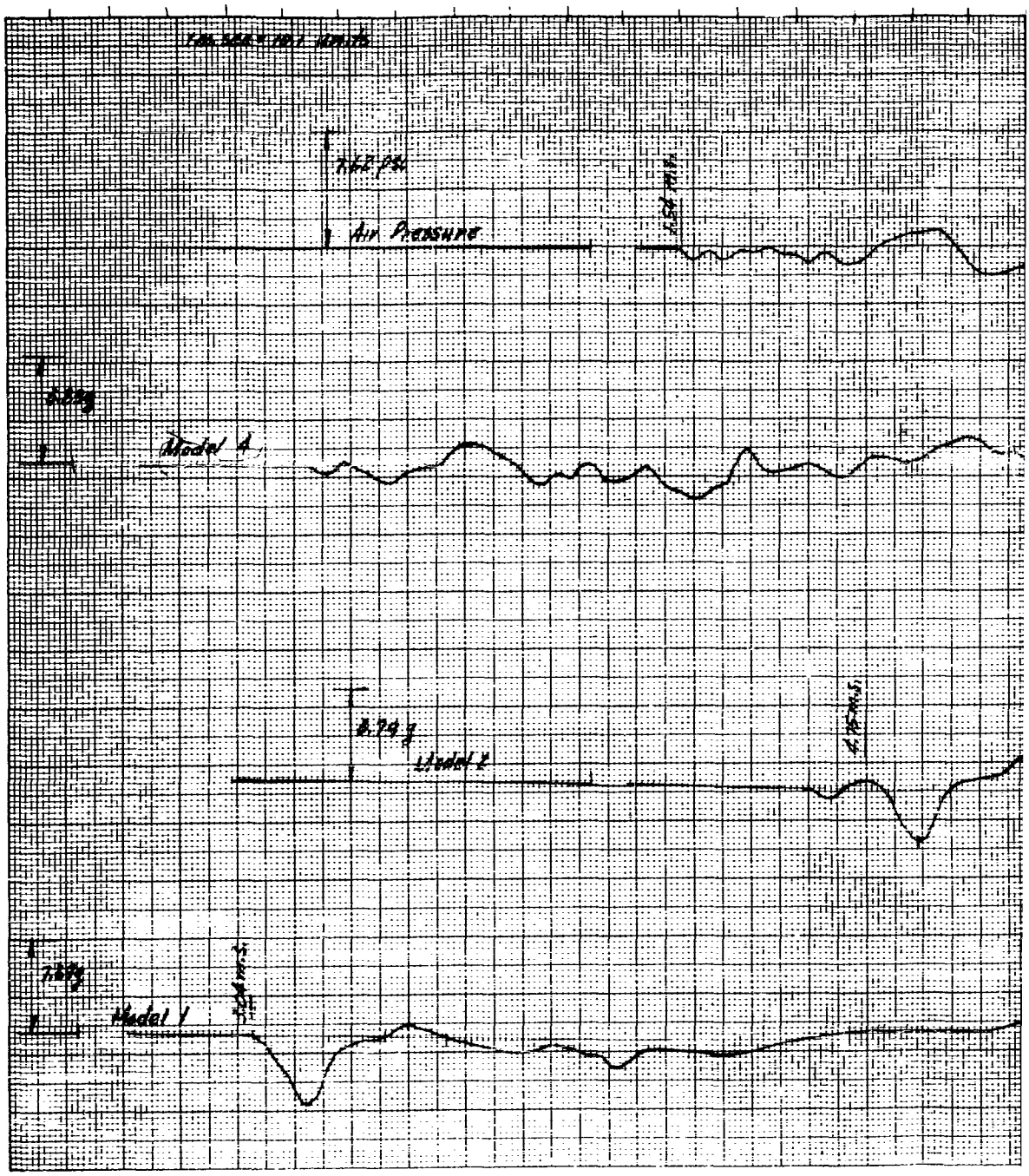

1

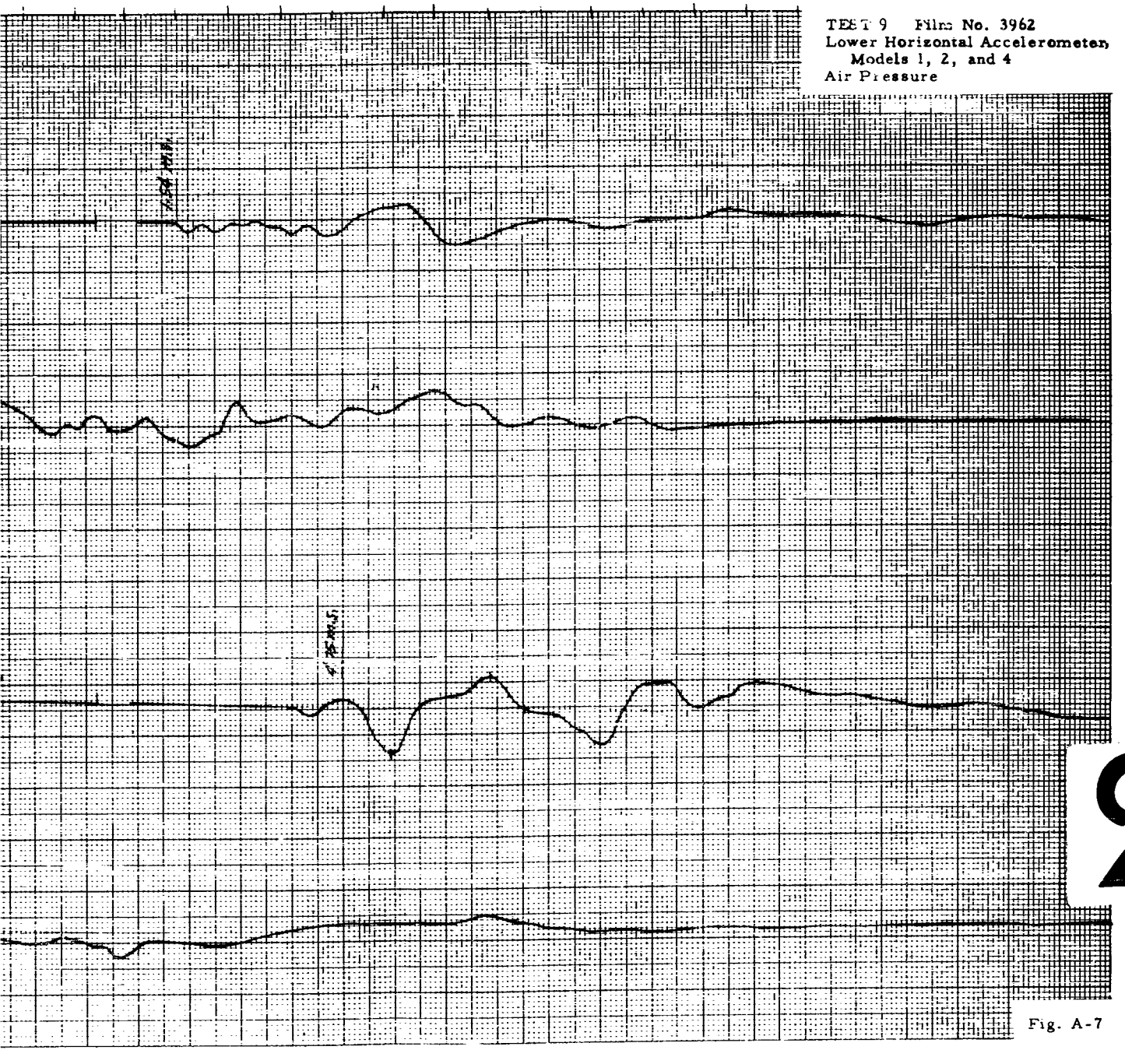

TEST 9 Film No. 3962
Lower Horizontal Accelerometer
Models 1, 2, and 4
Air Pressure

2

Fig. A-7

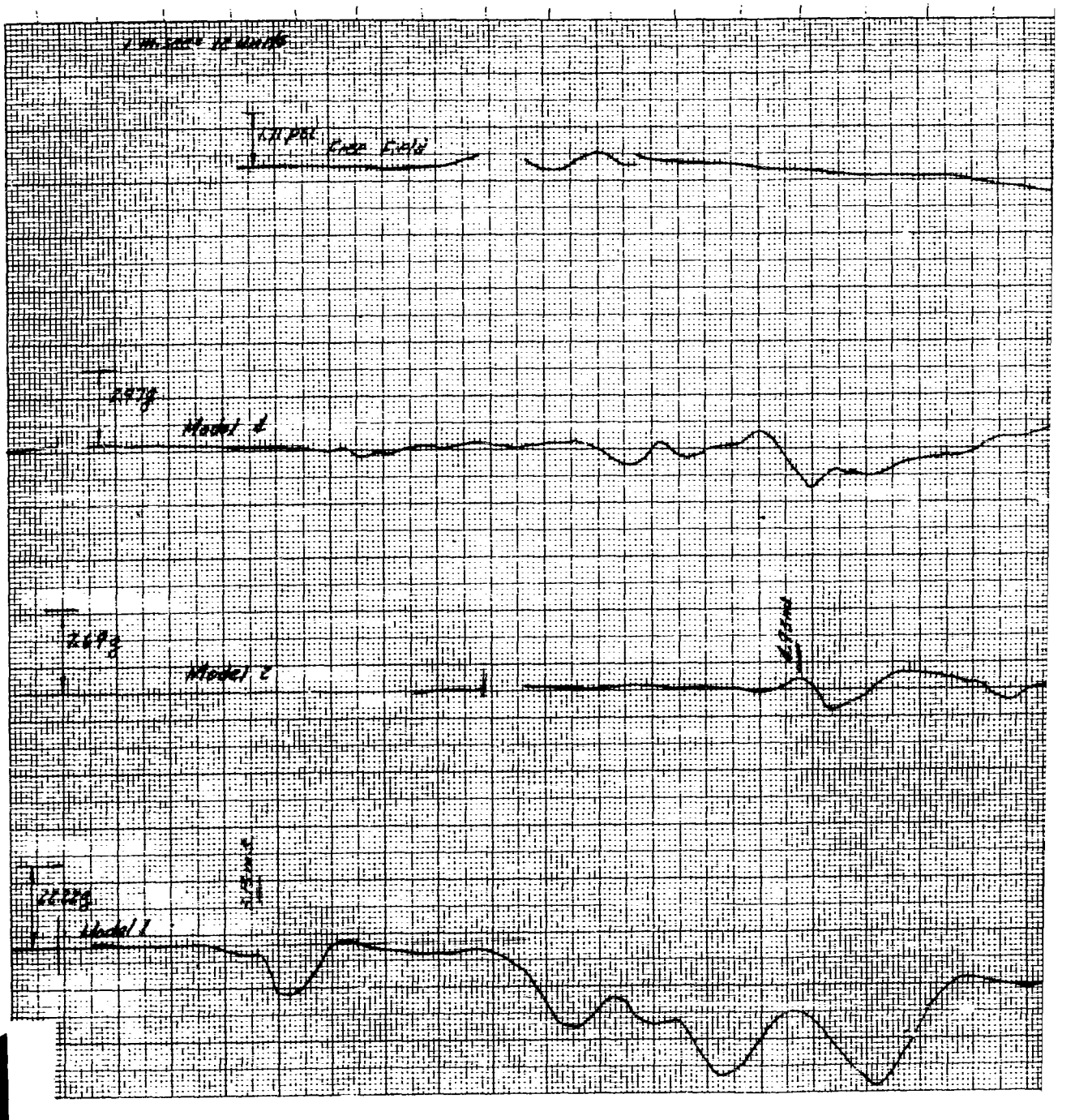

1

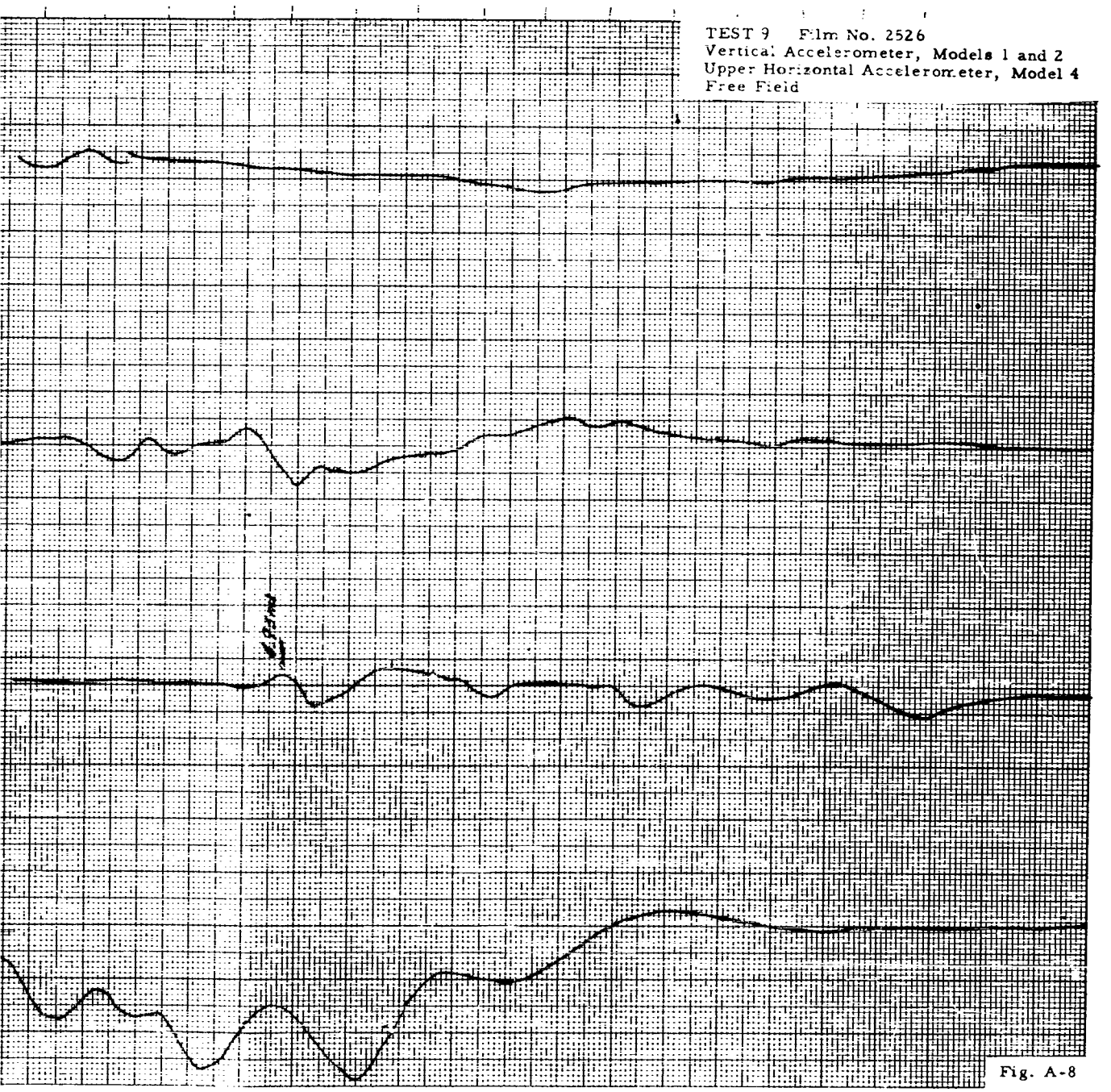
TEST 9 Film No. 2526
Vertical Accelerometer, Models 1 and 2
Upper Horizontal Accelerometer, Model 4
Free Field

Fig. A-8

2

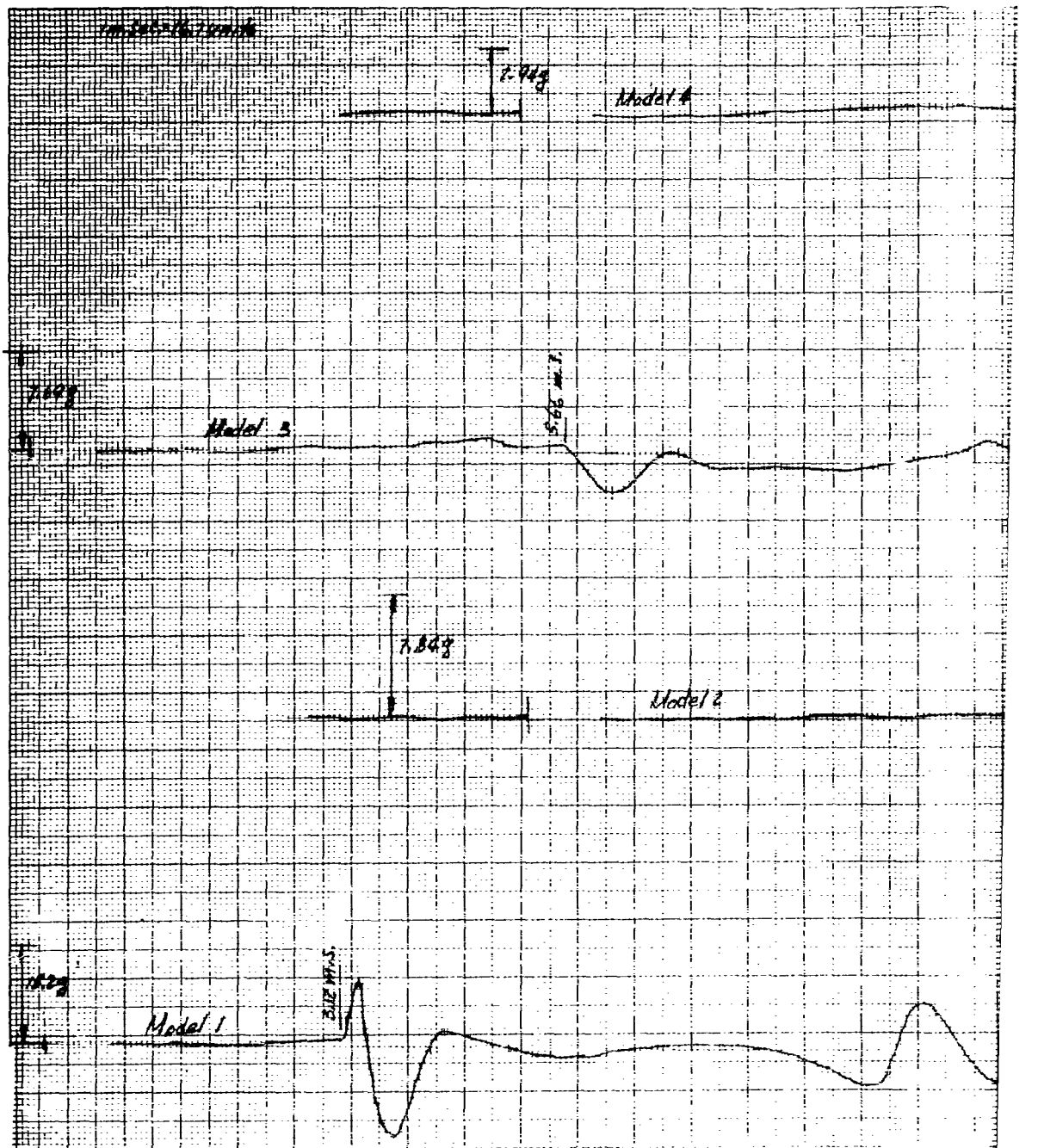

1

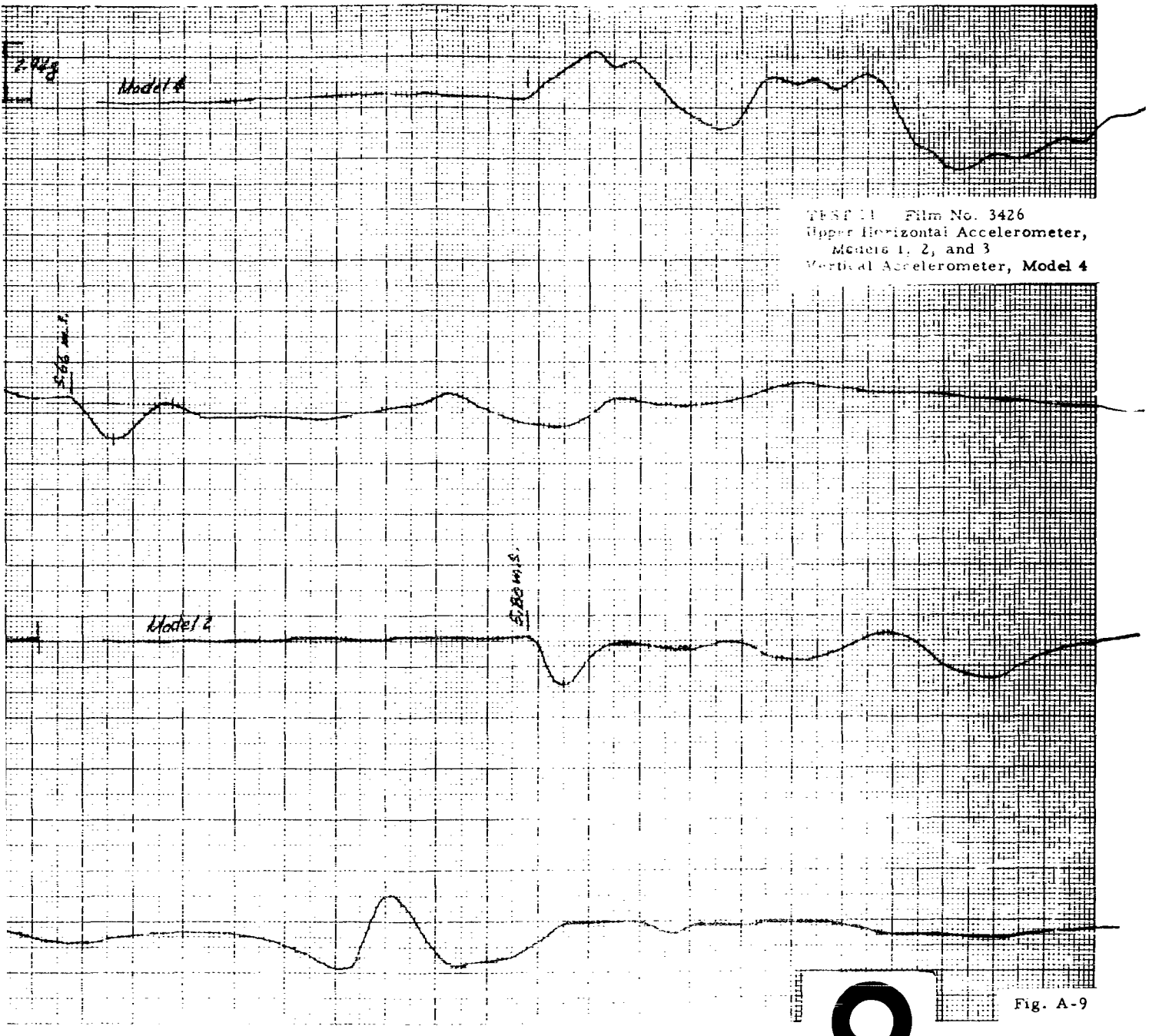

TEST 11 Film No. 3426
Upper Horizontal Accelerometer,
Models 1, 2, and 3
Vertical Accelerometer, **Model 4**

Fig. A-9

2

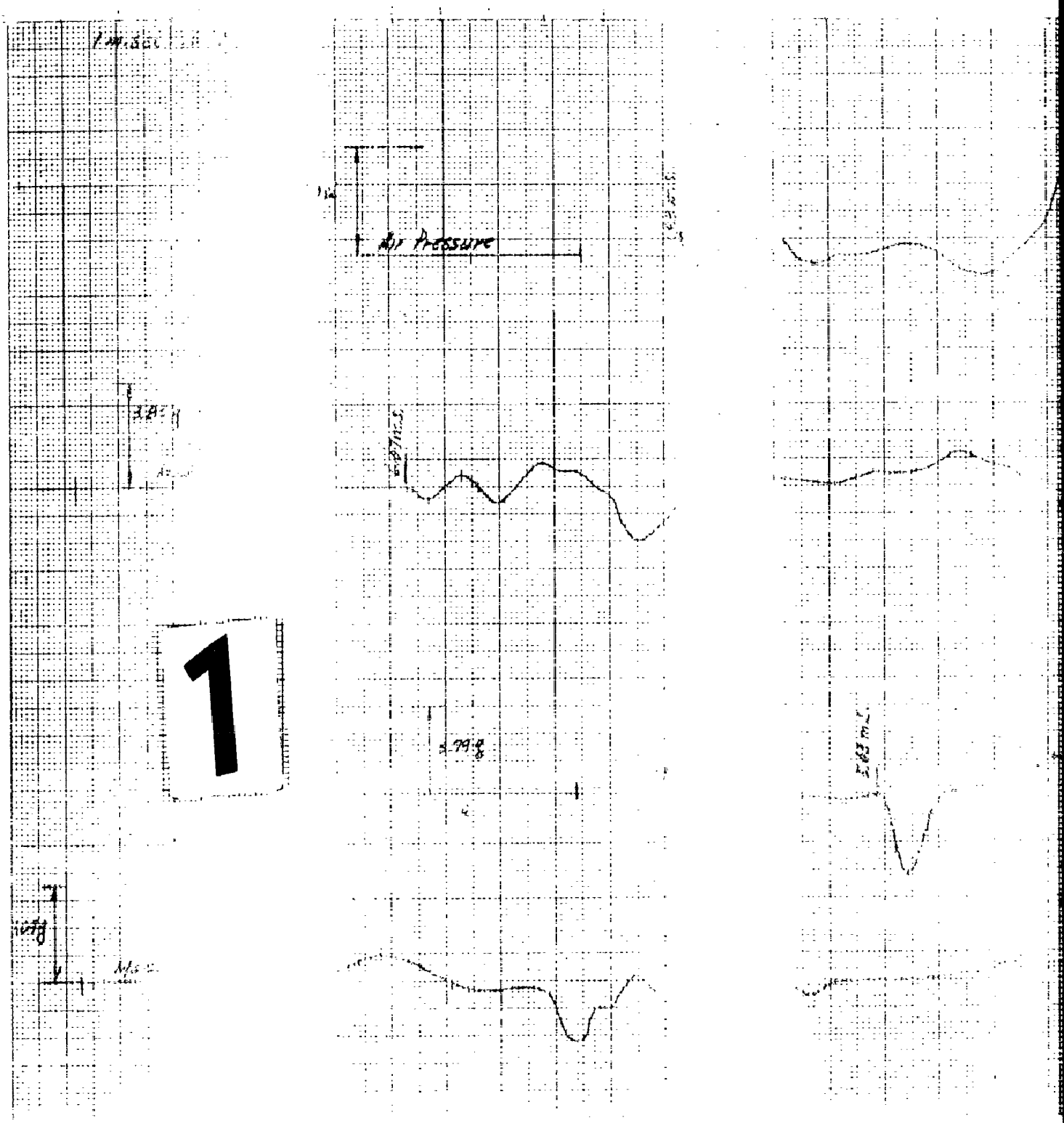
Air Pressure
1

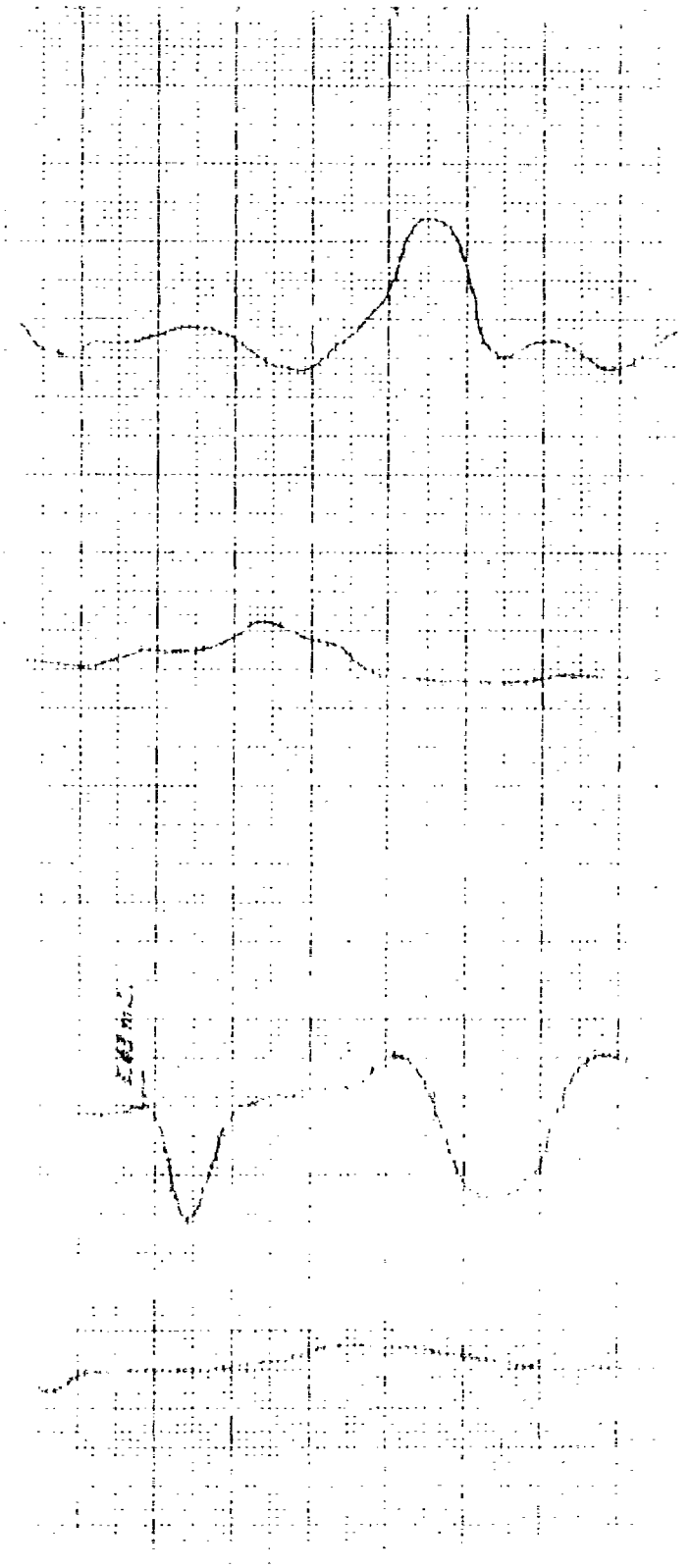

Film No. 3964
Horizontal Accelerometer,
Models 1, 2, and 4
Pressure

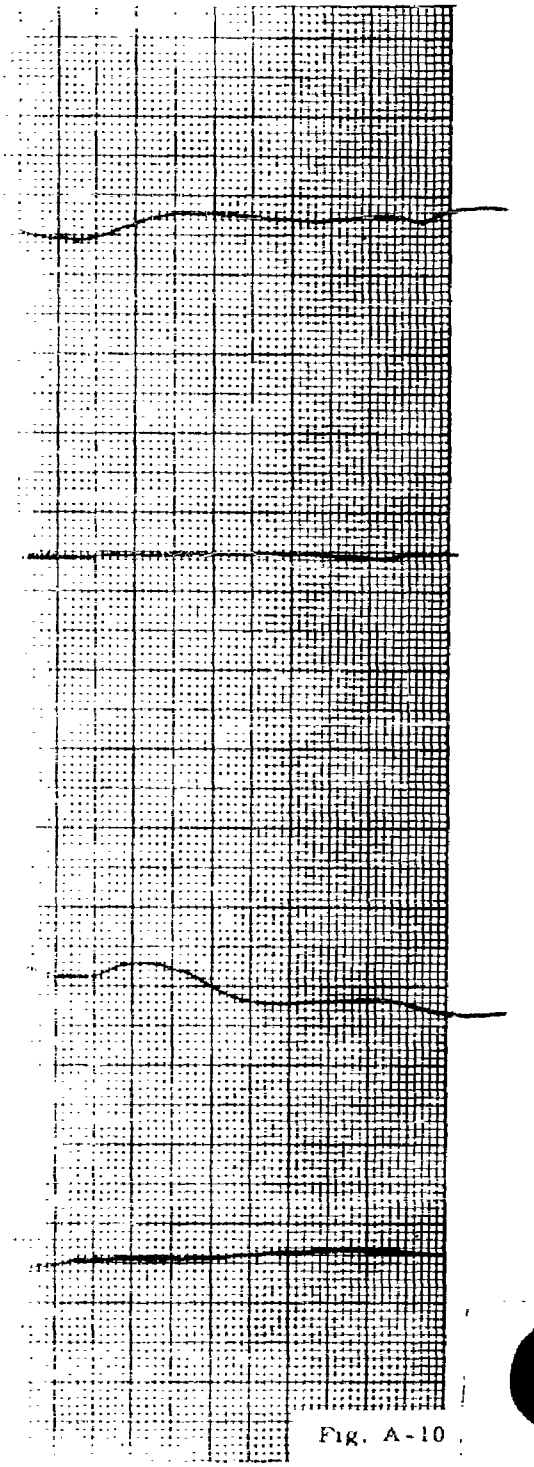

Fig. A-10

2

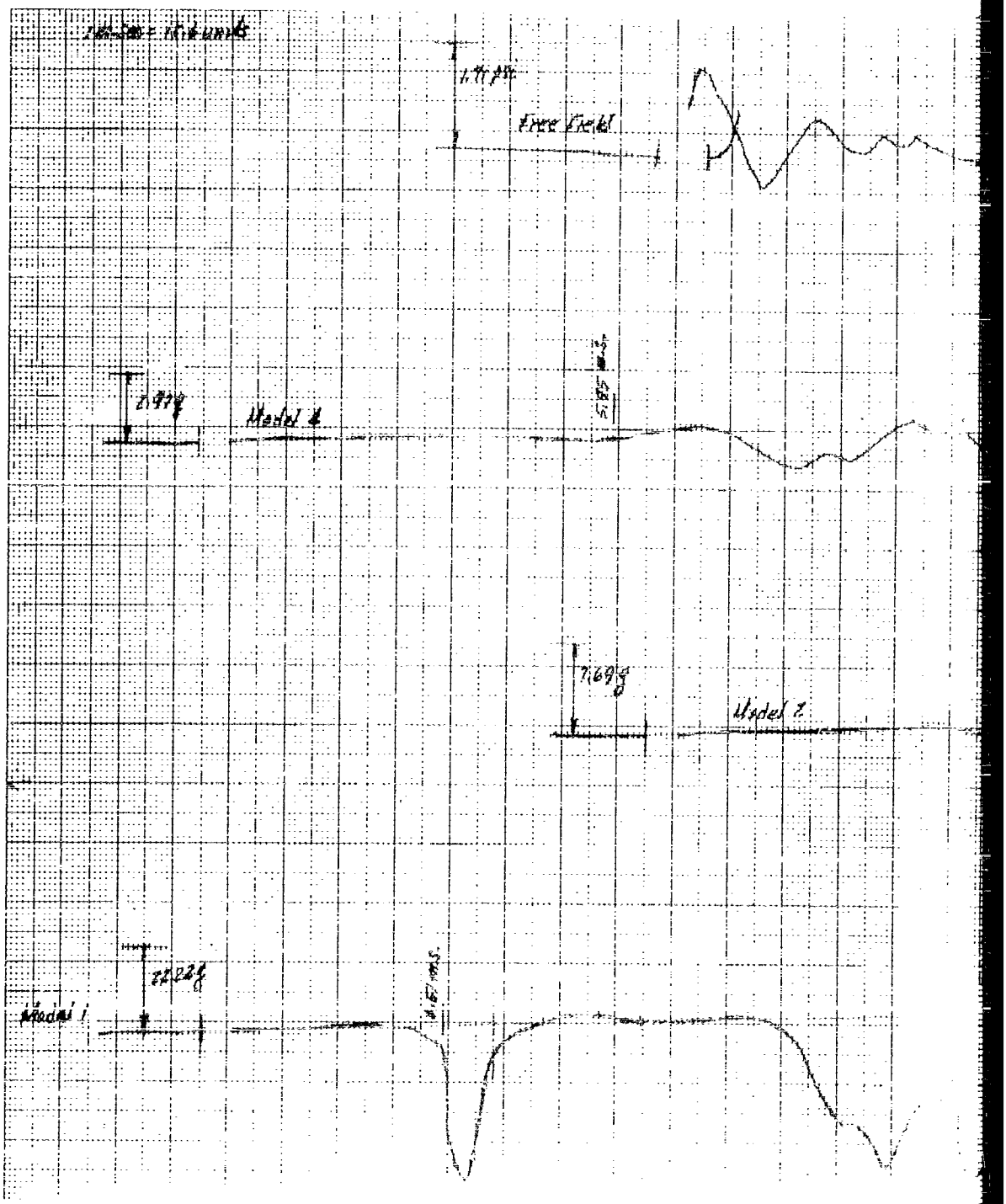
Free Field
Model 4
Model 2
Model 1

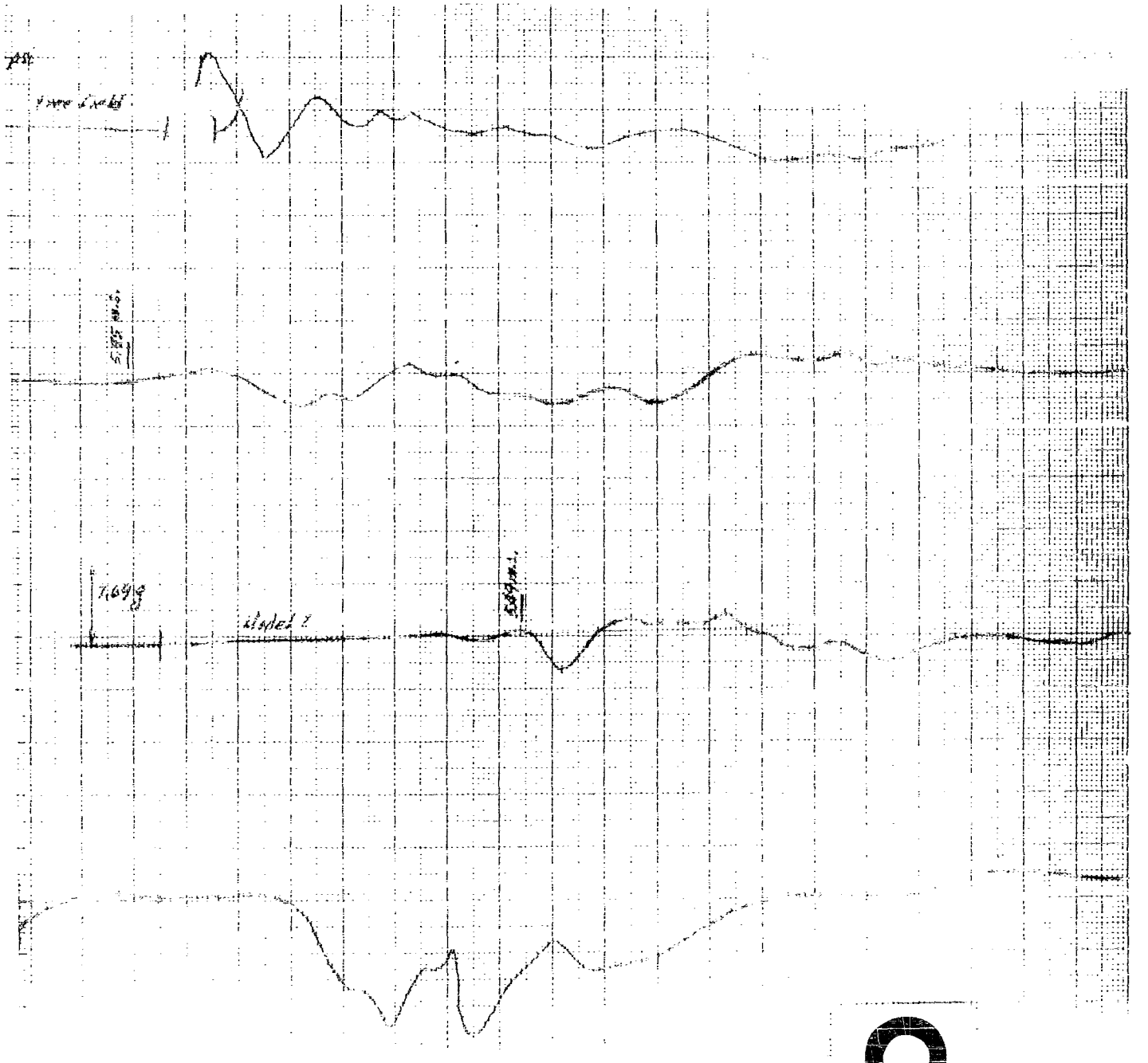

2

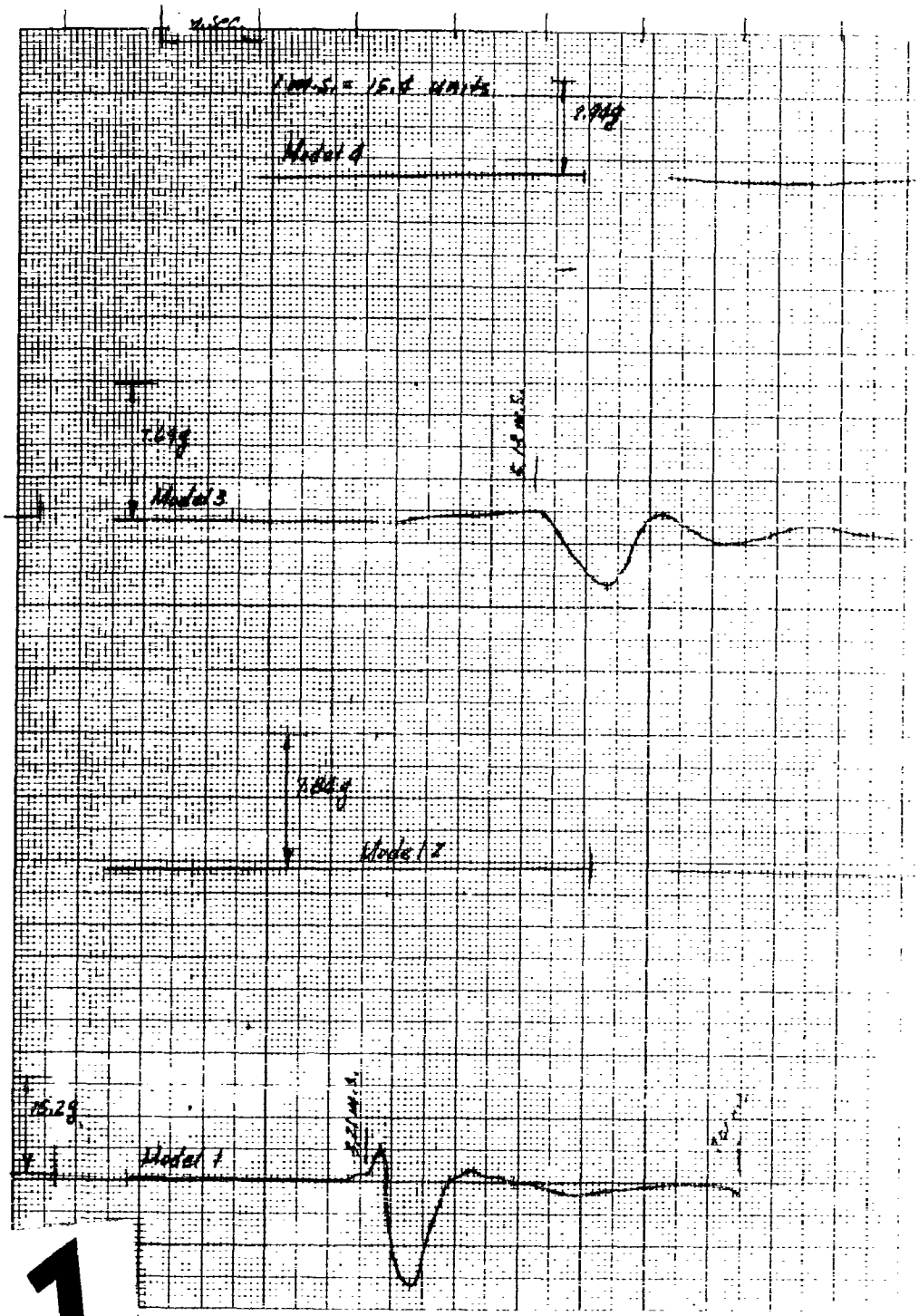

1

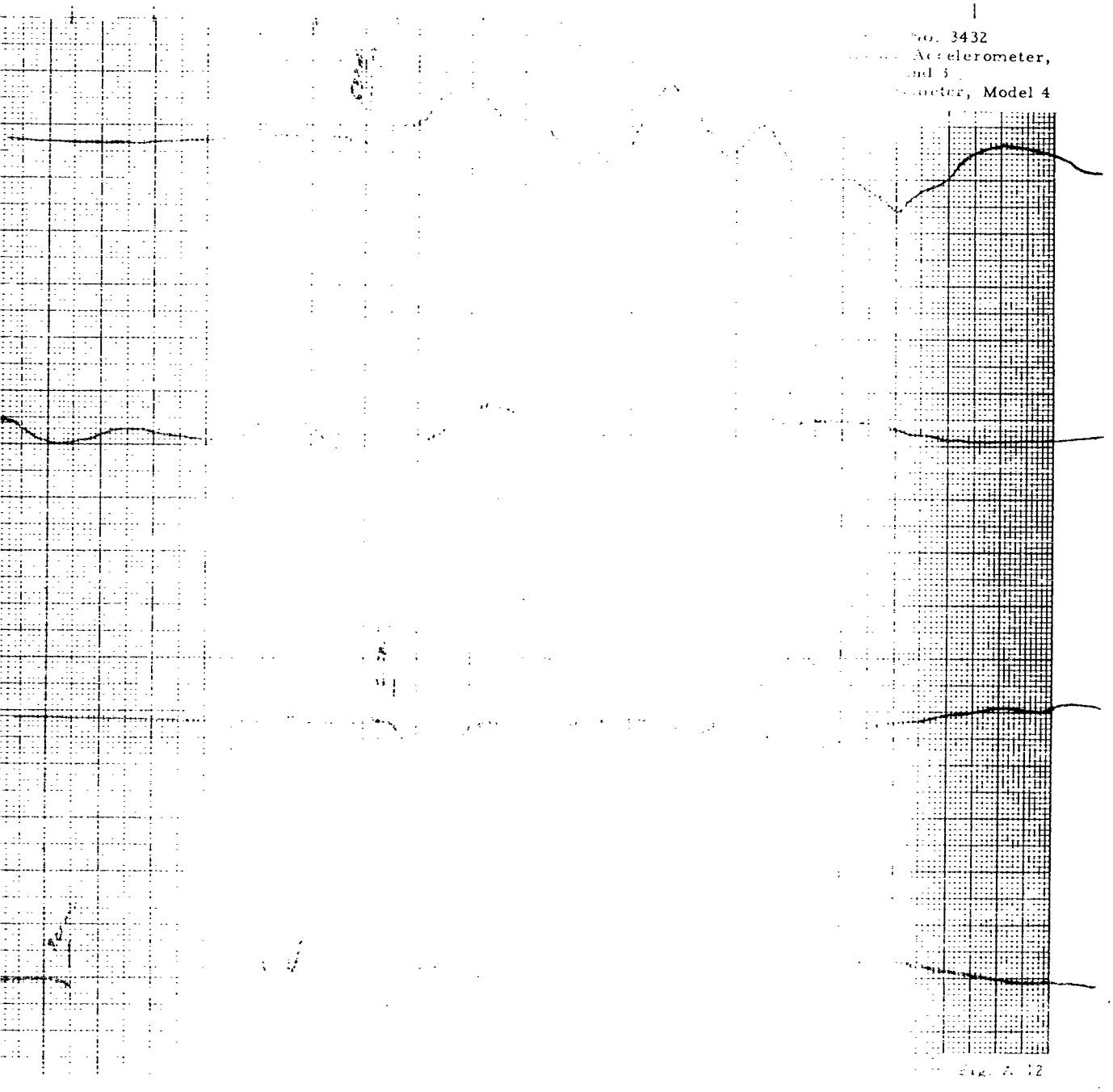

2

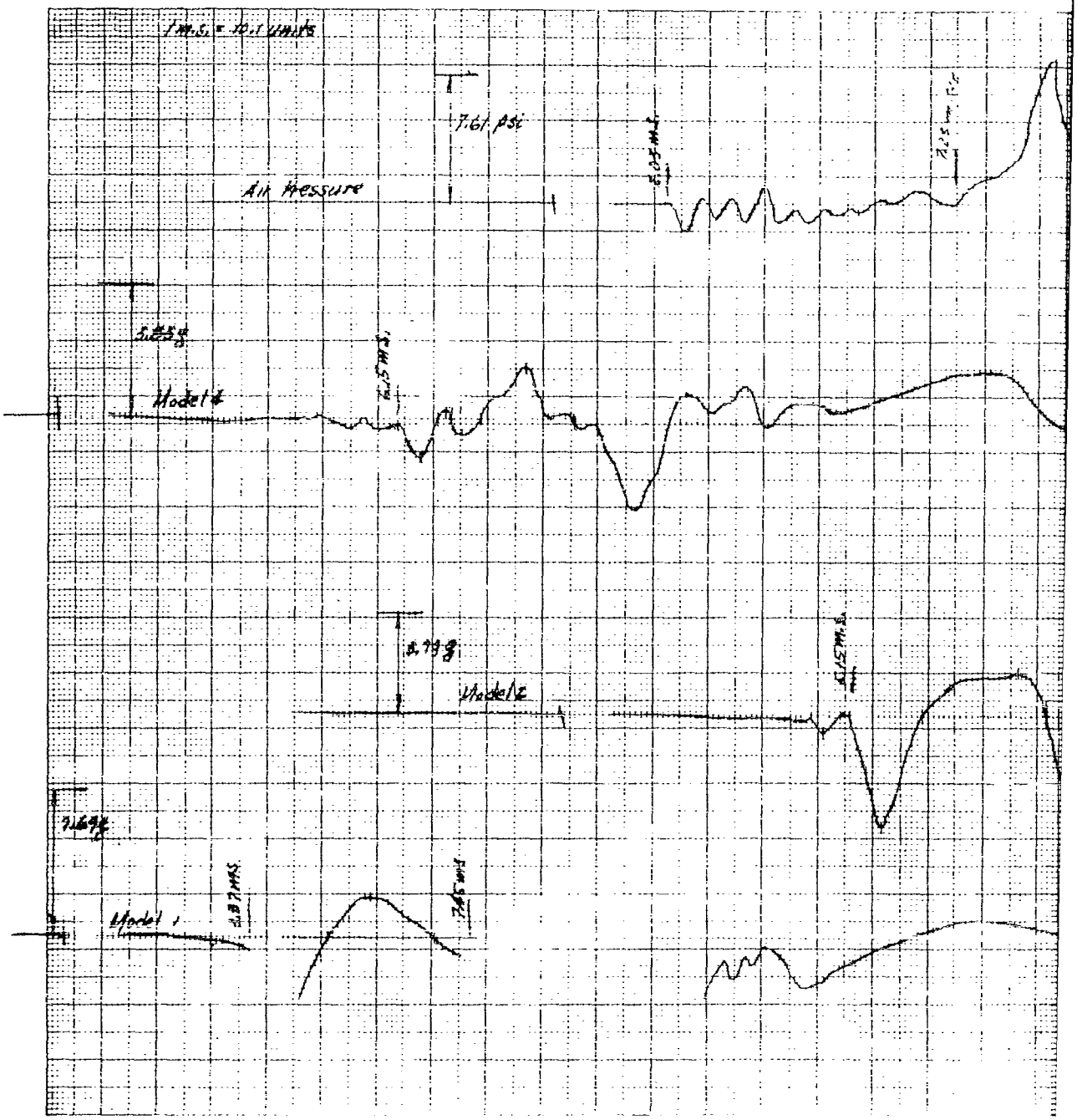

1

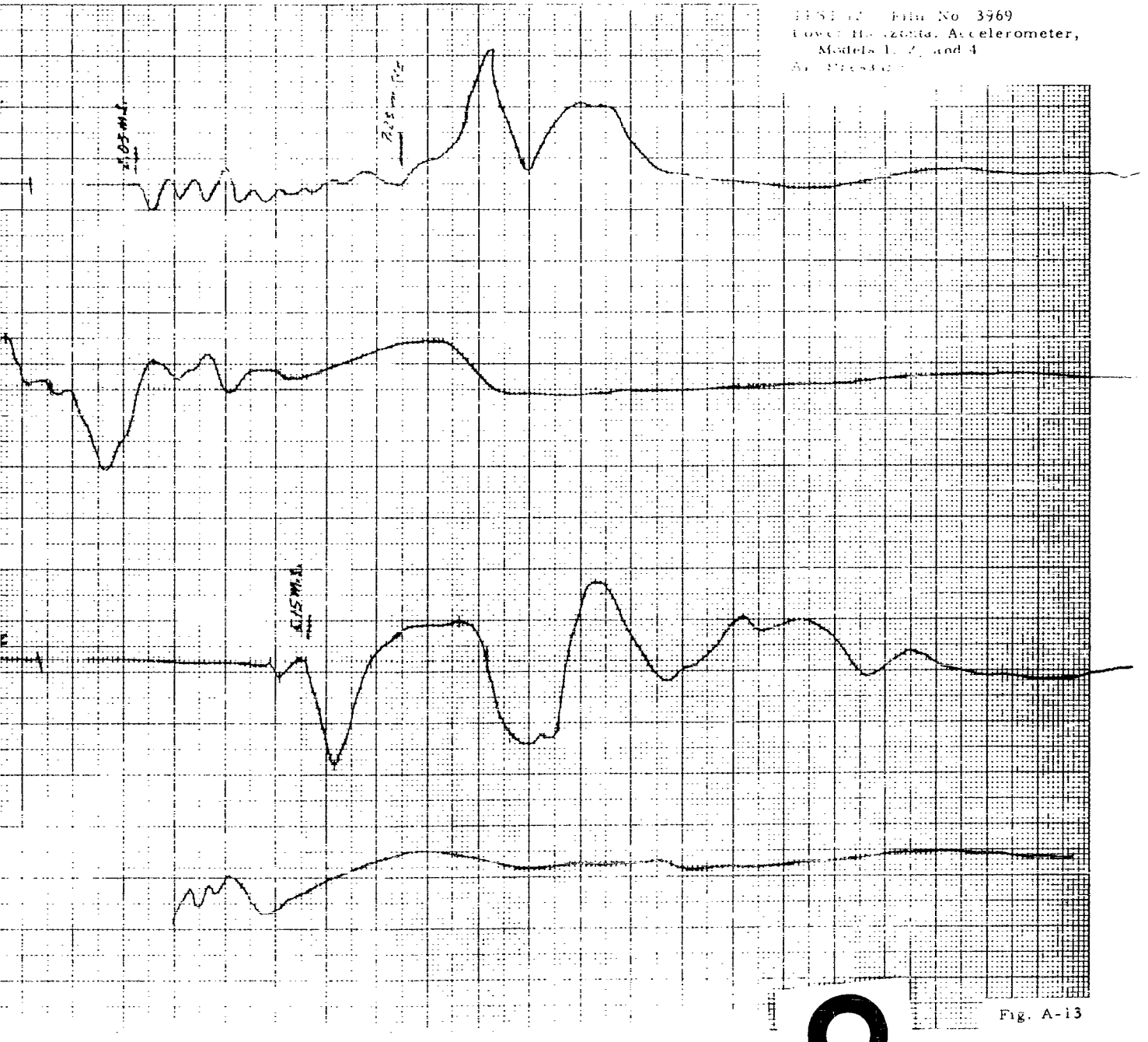

Fig. A-13

2

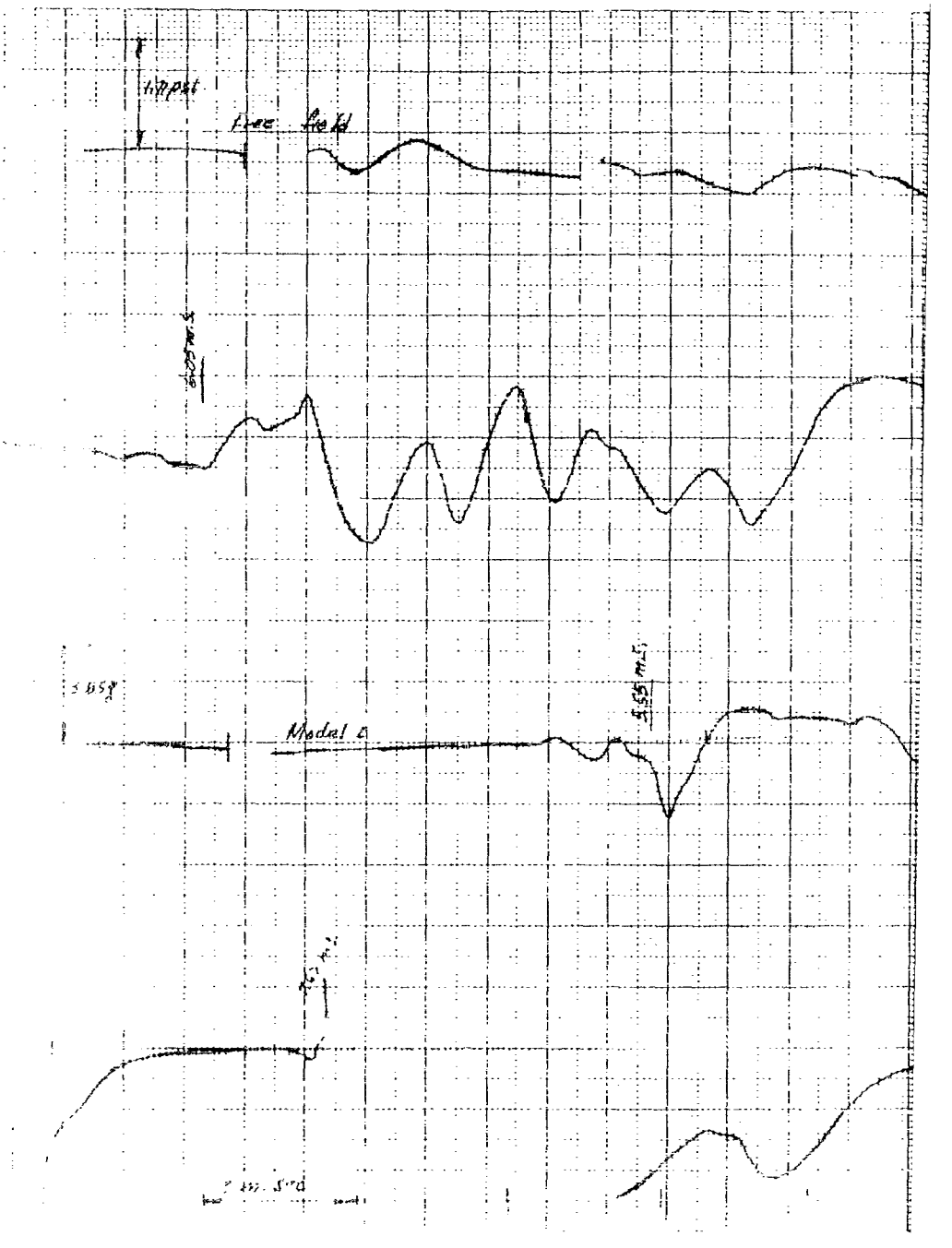

1

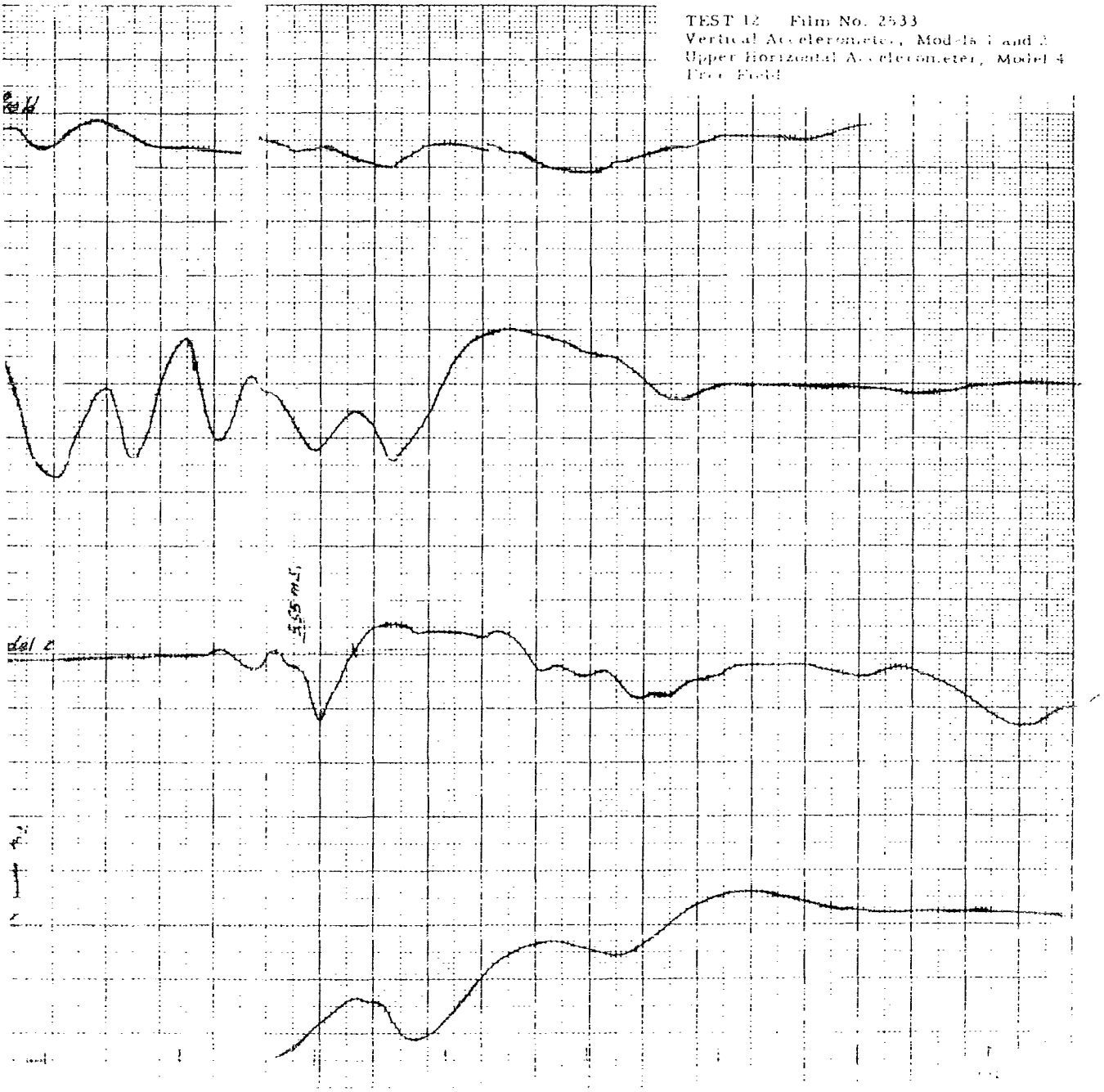
TEST 12 Film No. 2533
Vertical Accelerometer, Models 1 and 2
Upper Horizontal Accelerometer, Model 4
Free Field

2

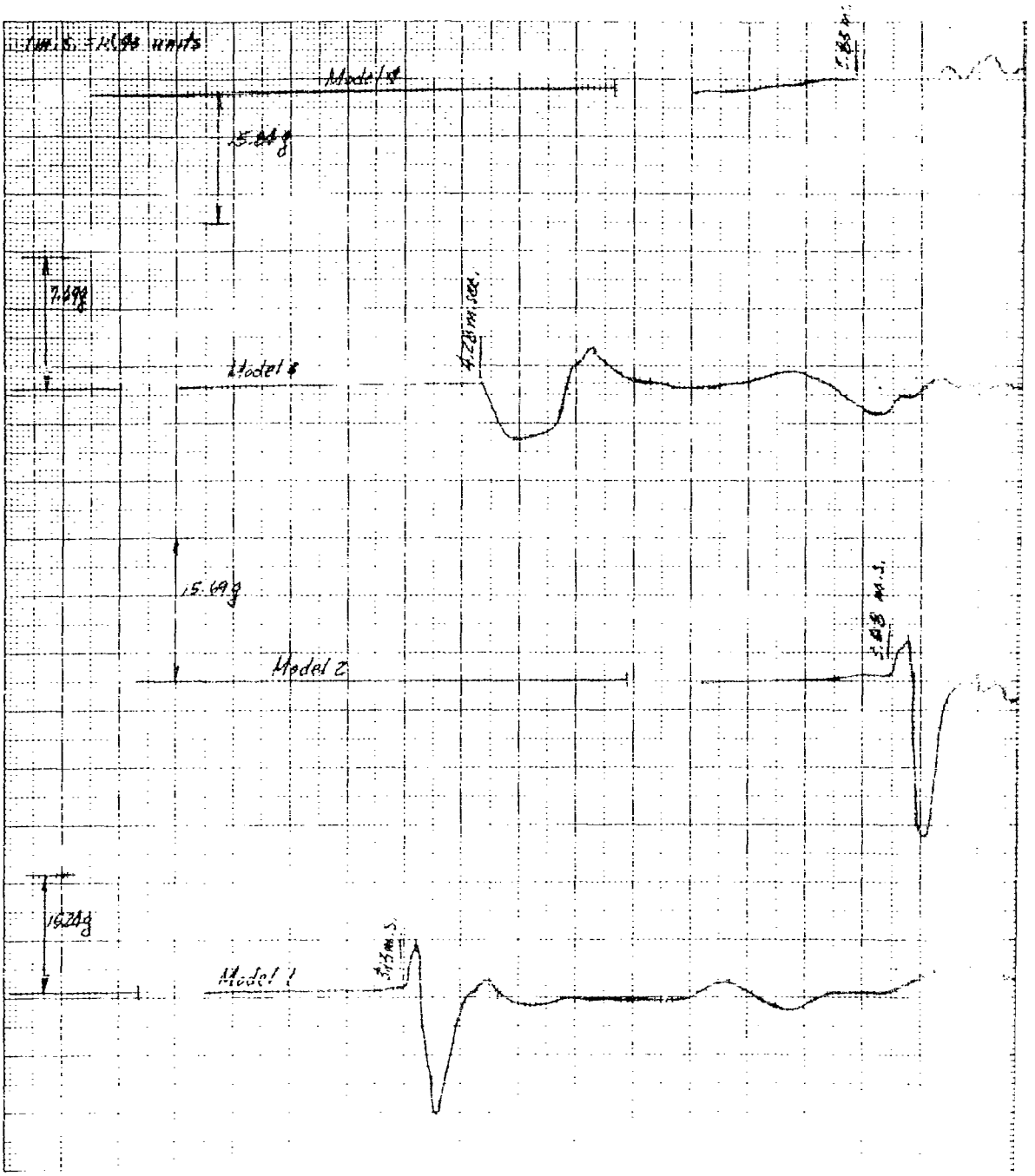

1

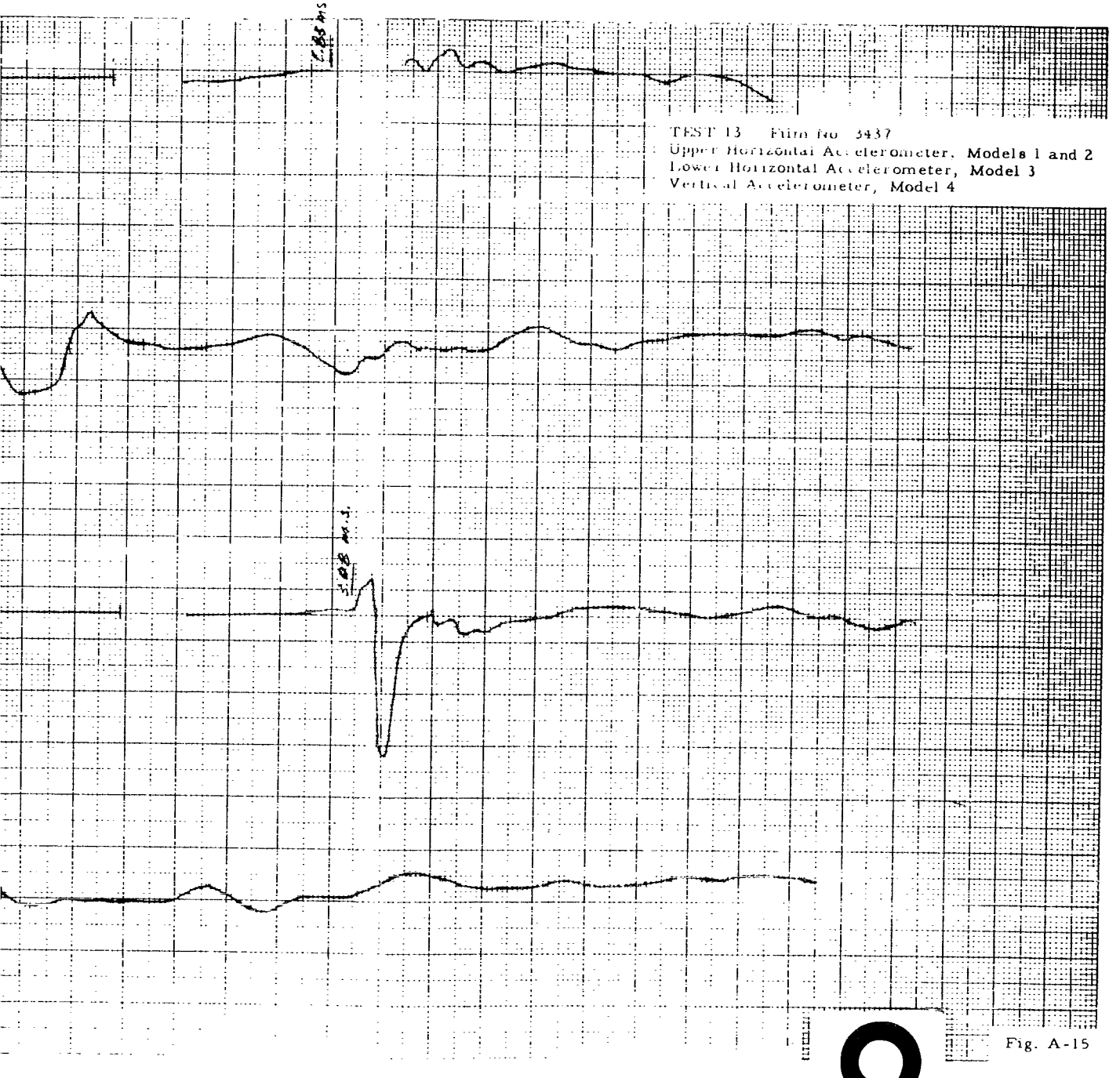
TEST 13 Film No 3437
Upper Horizontal Accelerometer, Models 1 and 2
Lower Horizontal Accelerometer, Model 3
Vertical Accelerometer, Model 4

Fig. A-15

2

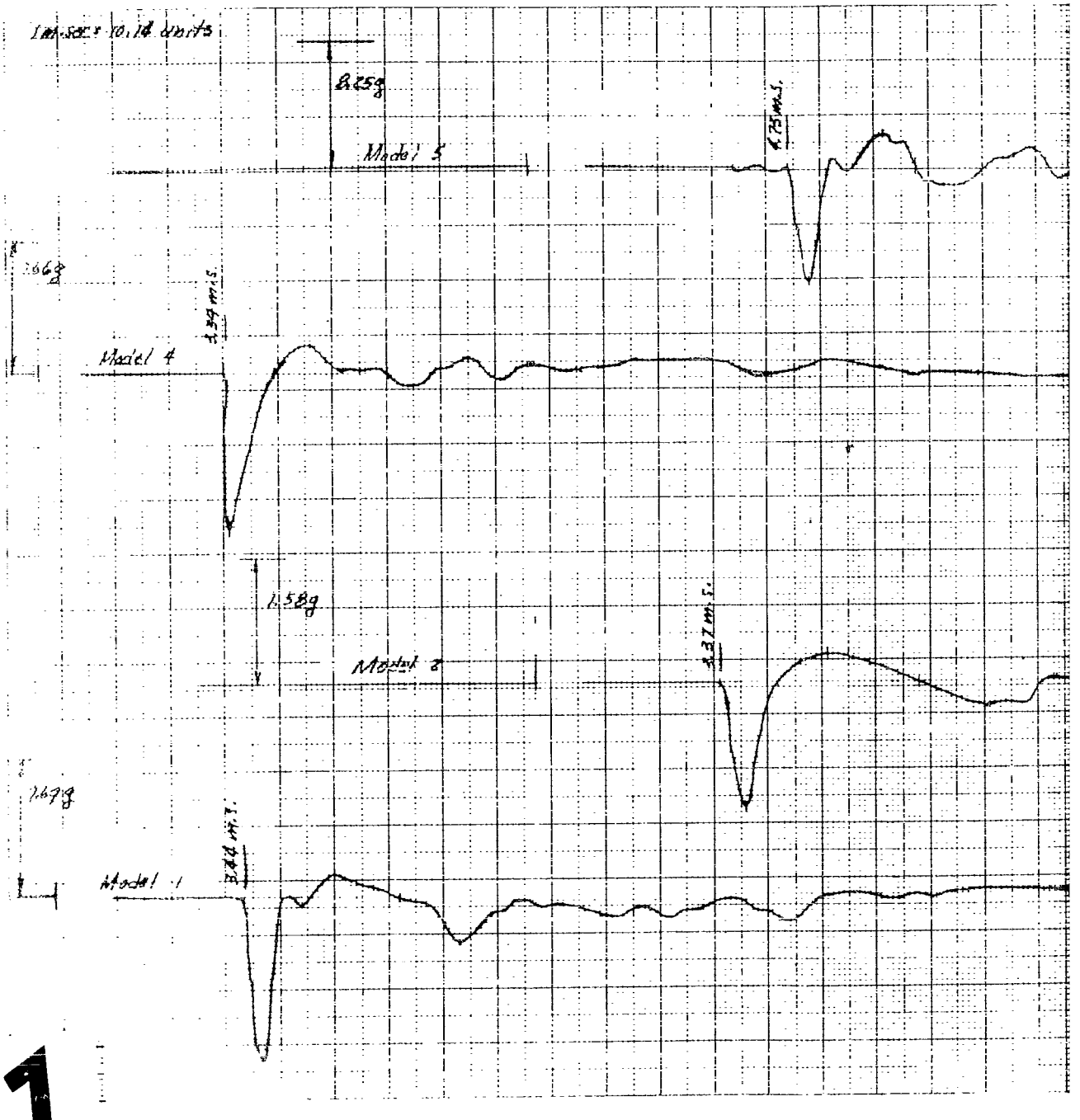
1 m.sec = 10.14 units
0.25g
Model 5
4.75 m.s.
.668g
4.39 m.s.
Model 4
1.58g
3.37 m.s.
Model 3
.669g
3.44 m.s.
Model 1

1

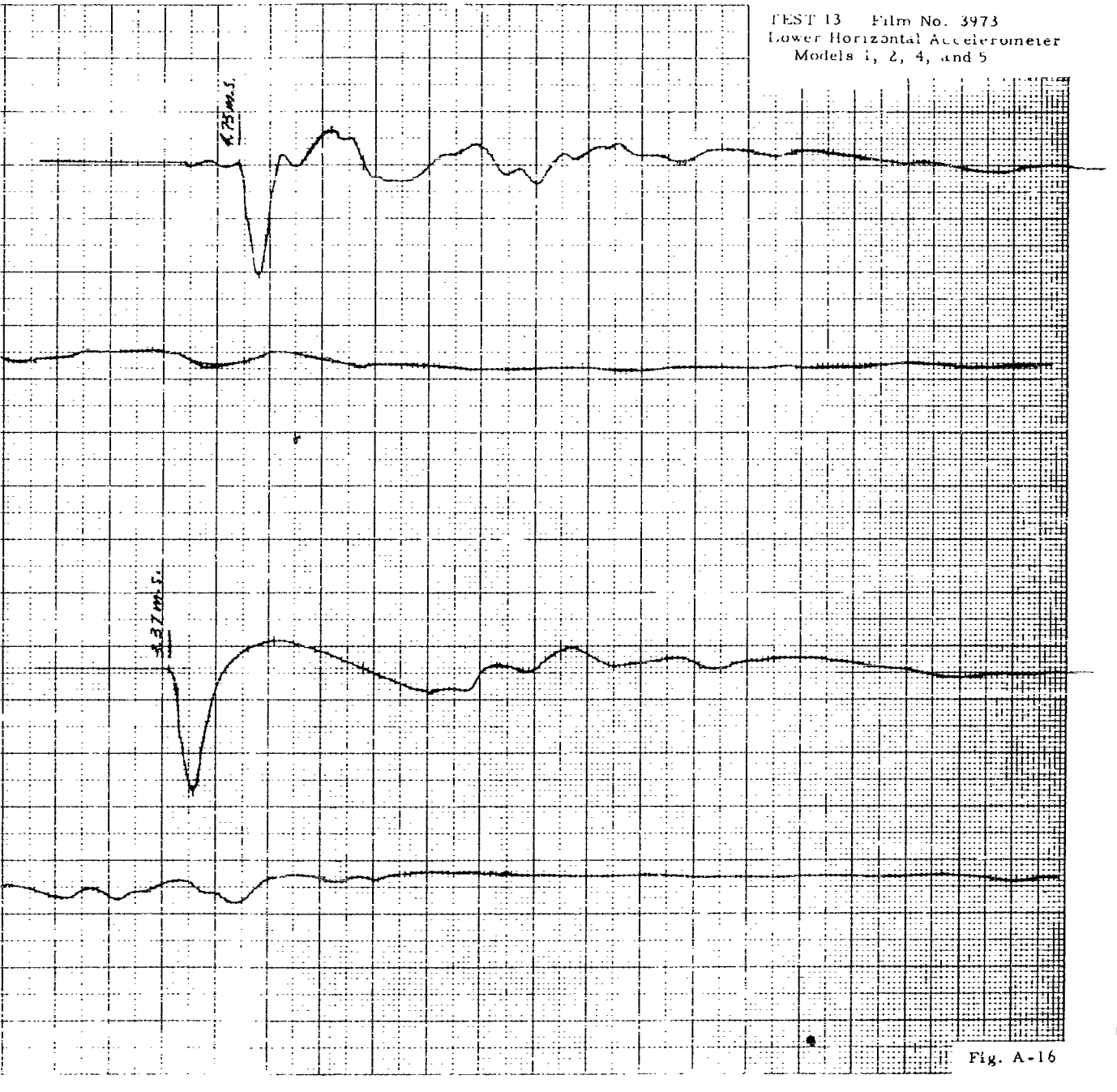
TEST 13 Film No. 3973
Lower Horizontal Accelerometer
Models 1, 2, 4, and 5
4.75 m.s.
3.27 m.s.

Fig. A-16

2

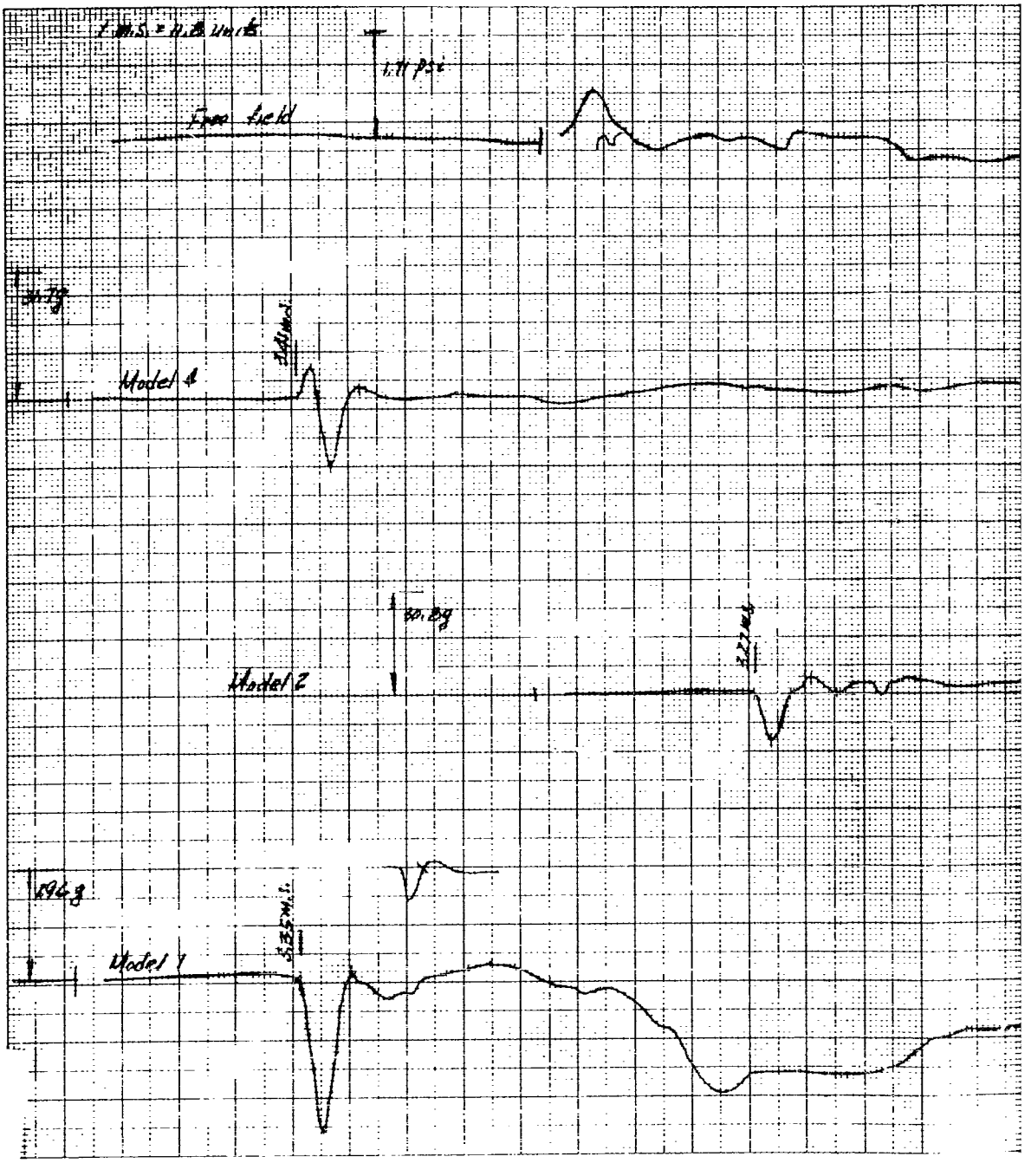

1

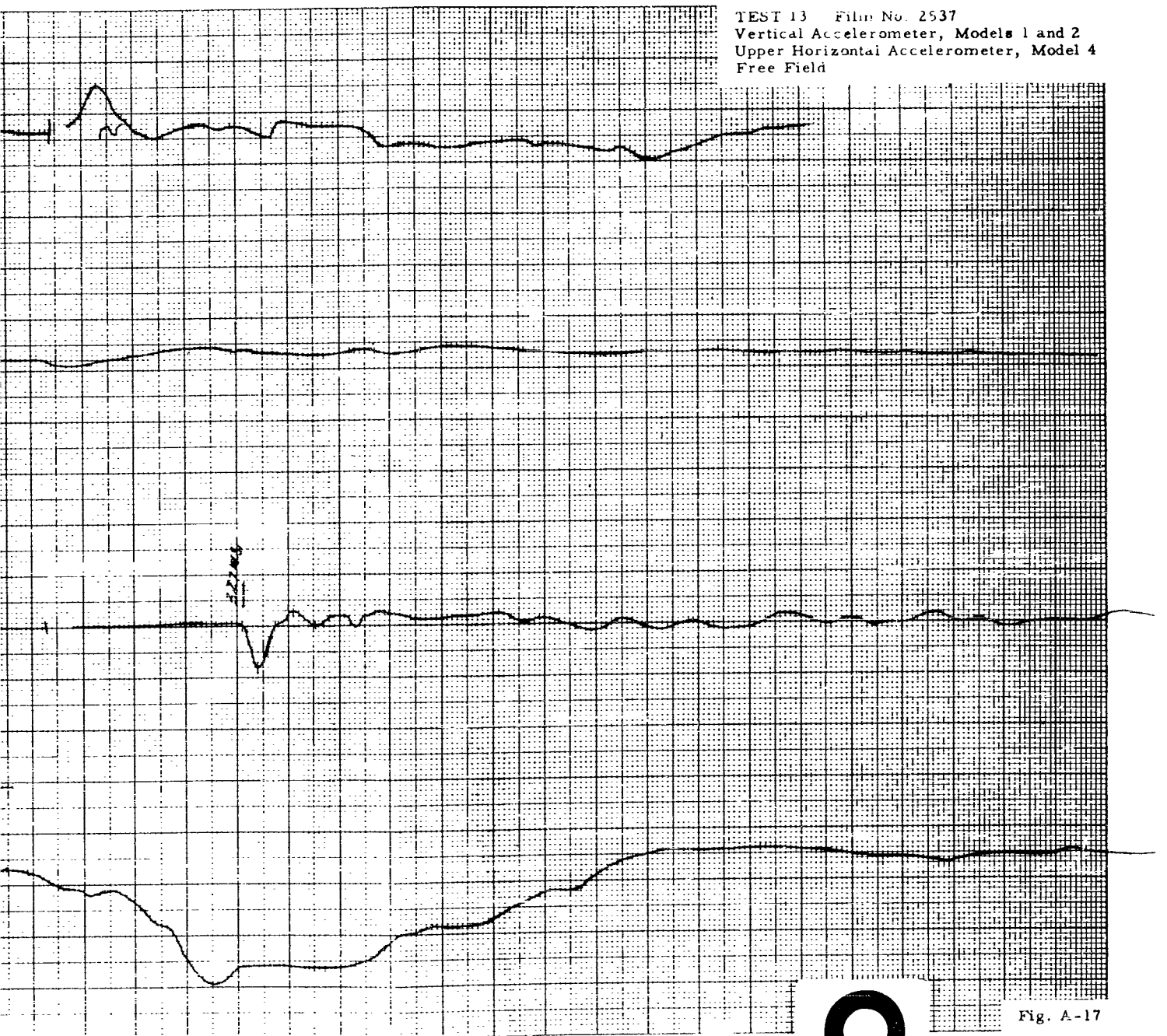
TEST 13 Film No. 2537
Vertical Accelerometer, Models 1 and 2
Upper Horizontal Accelerometer, Model 4
Free Field

Fig. A-17

2

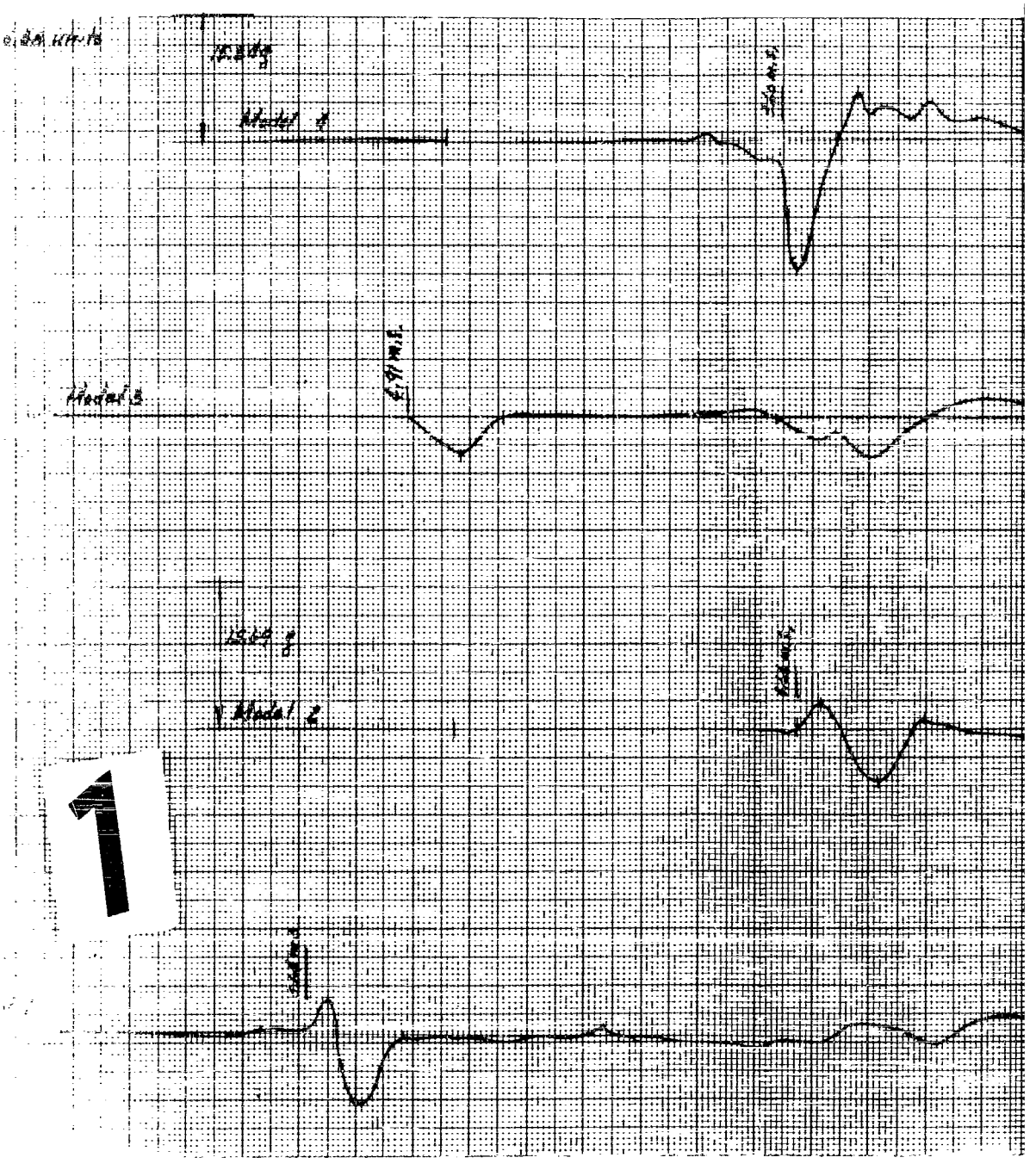
Model 4
Model 3
Model 2
1

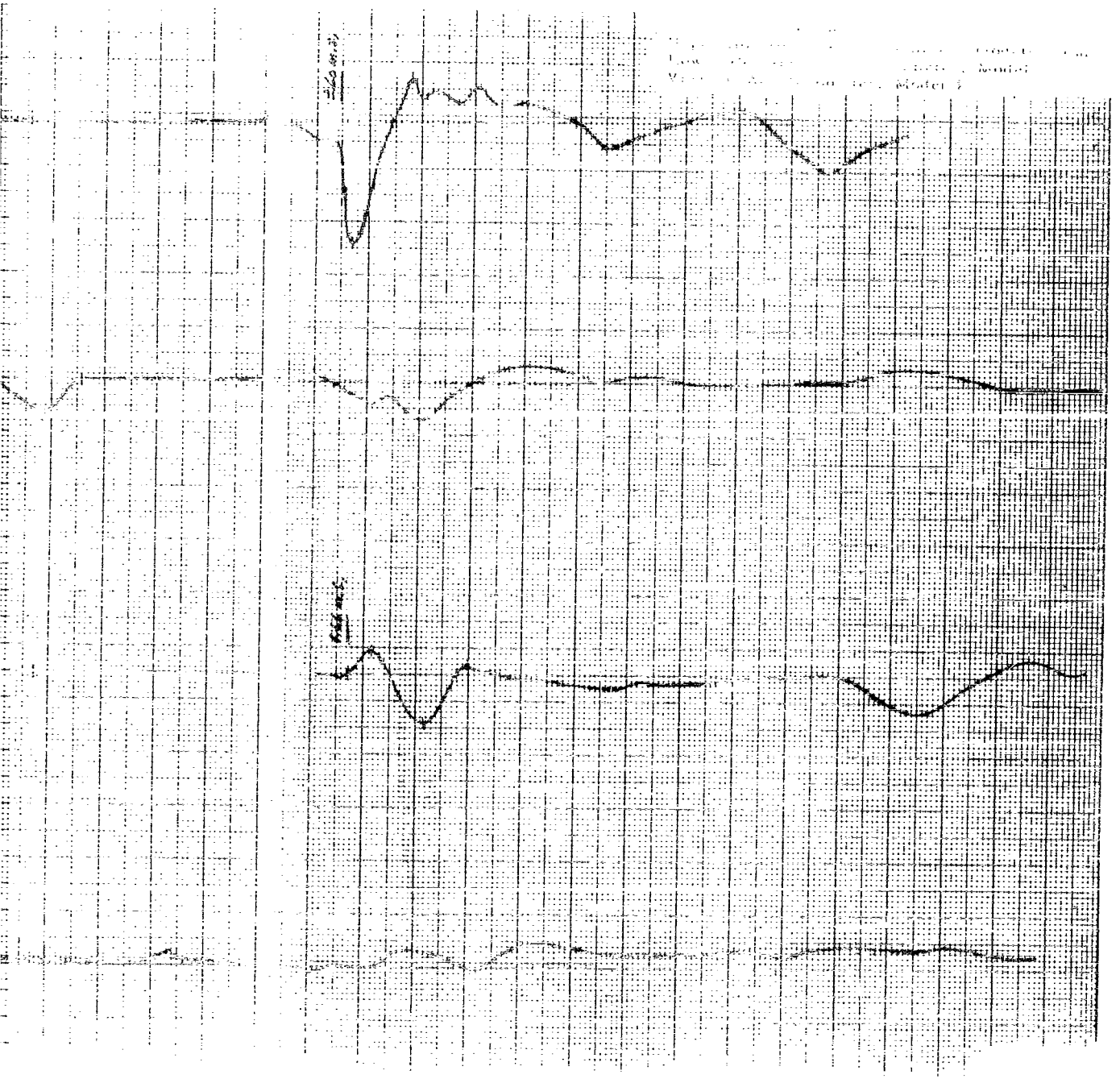

2

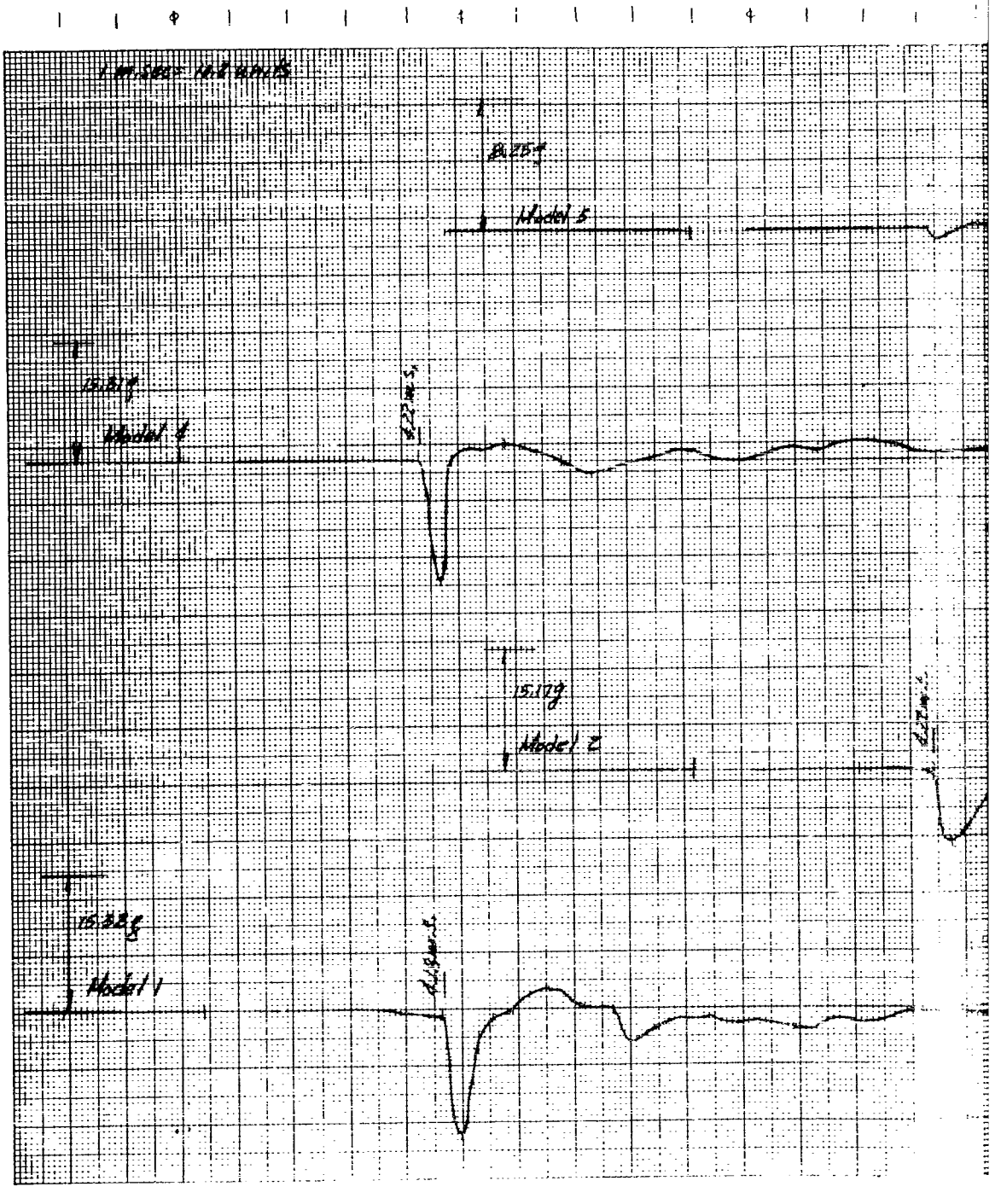

1

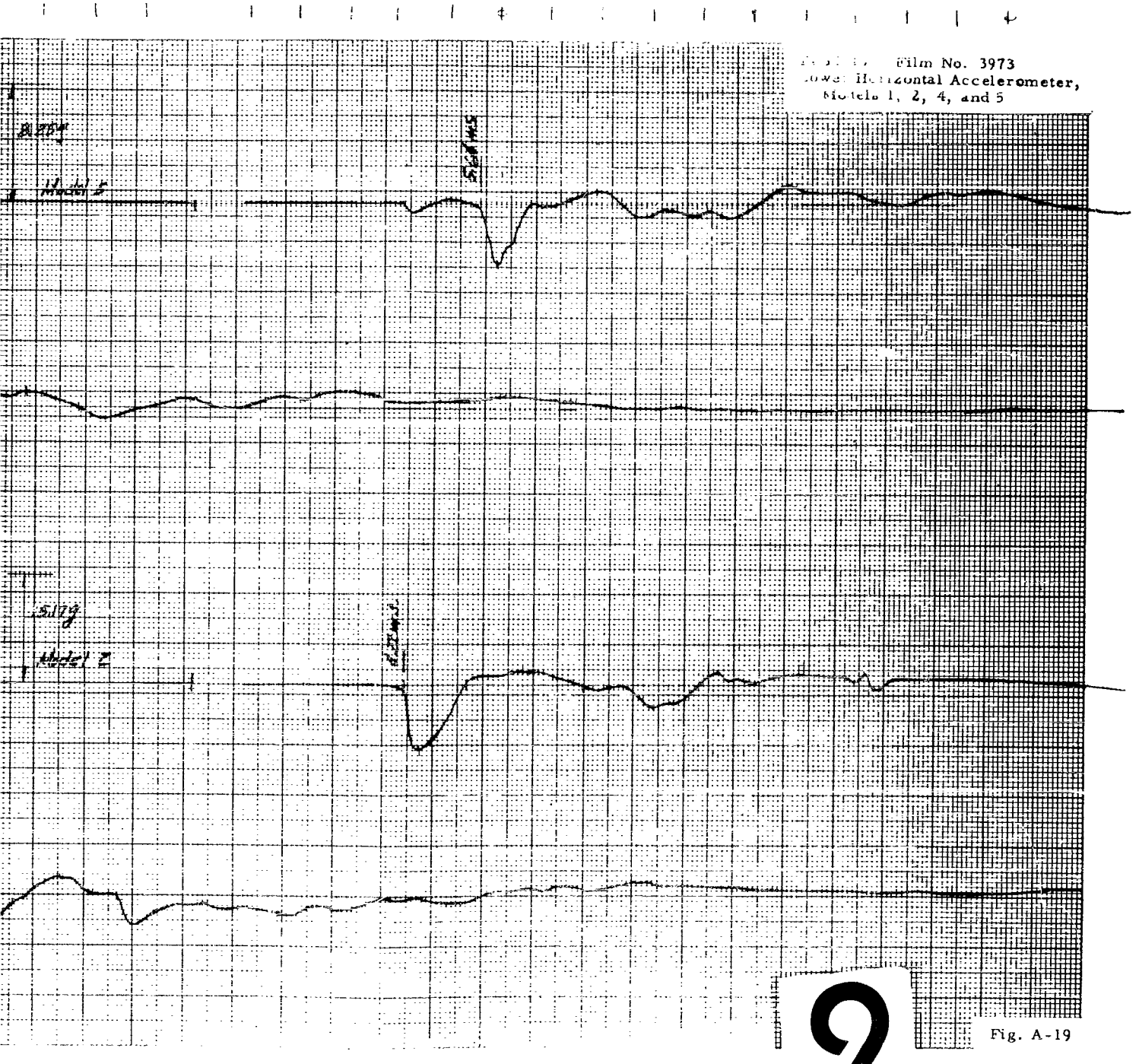
Film No. 3973
Lower Horizontal Accelerometer,
Models 1, 2, 4, and 5

Fig. A-19

2

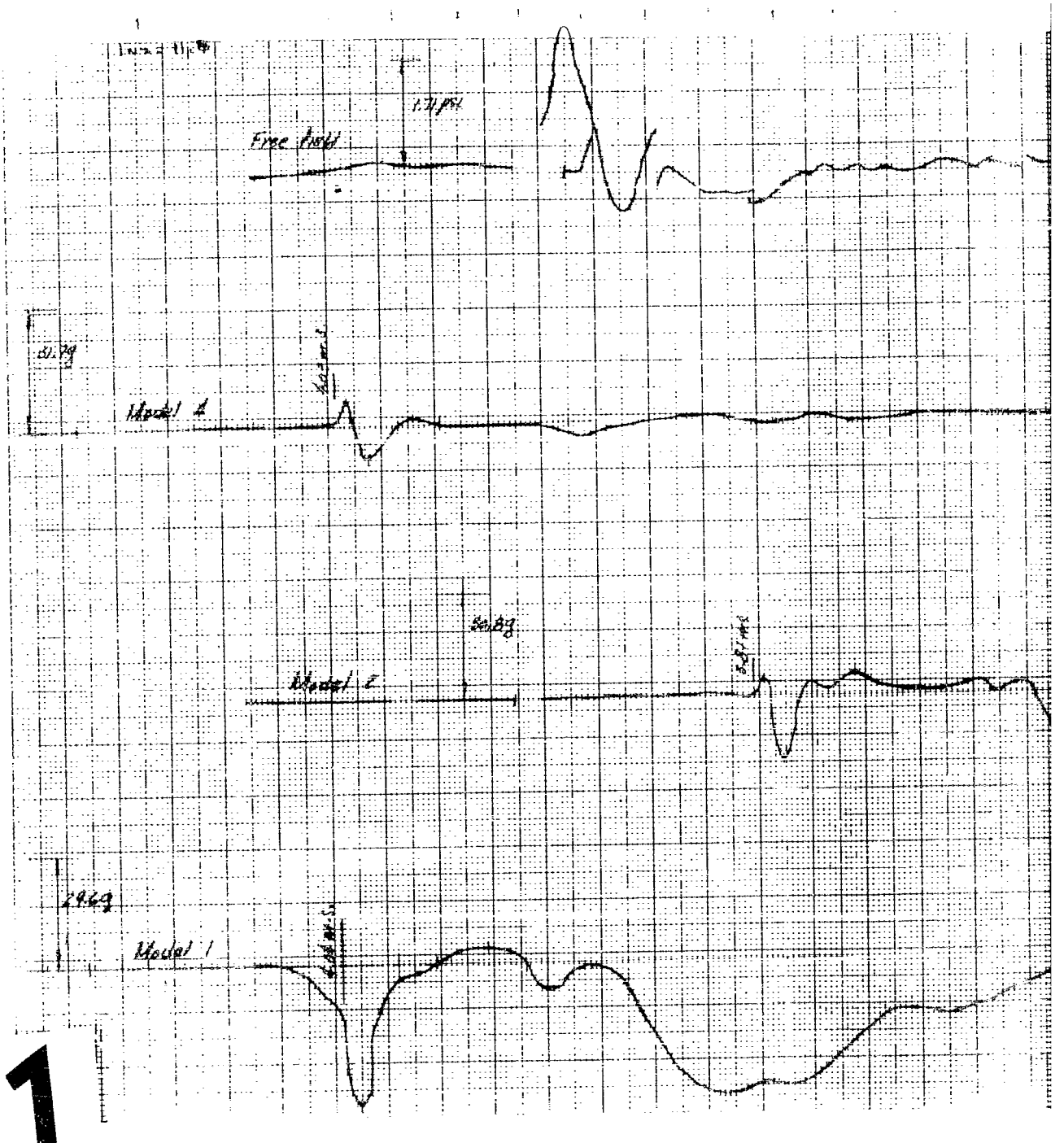

1

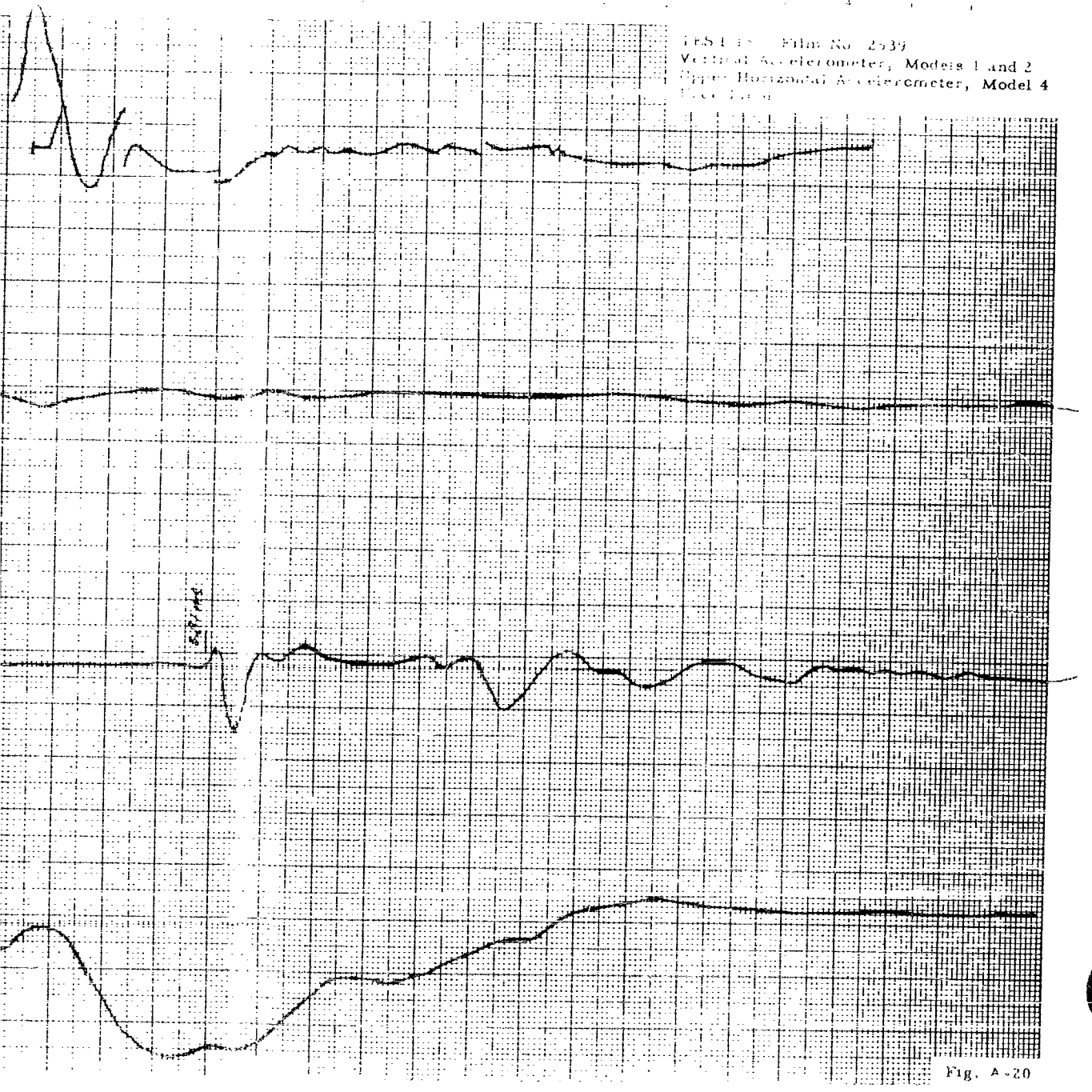
Film No. 2539
Vertical Accelerometer, Models 1 and 2
Upper Horizontal Accelerometer, Model 4

Fig. A-20

2

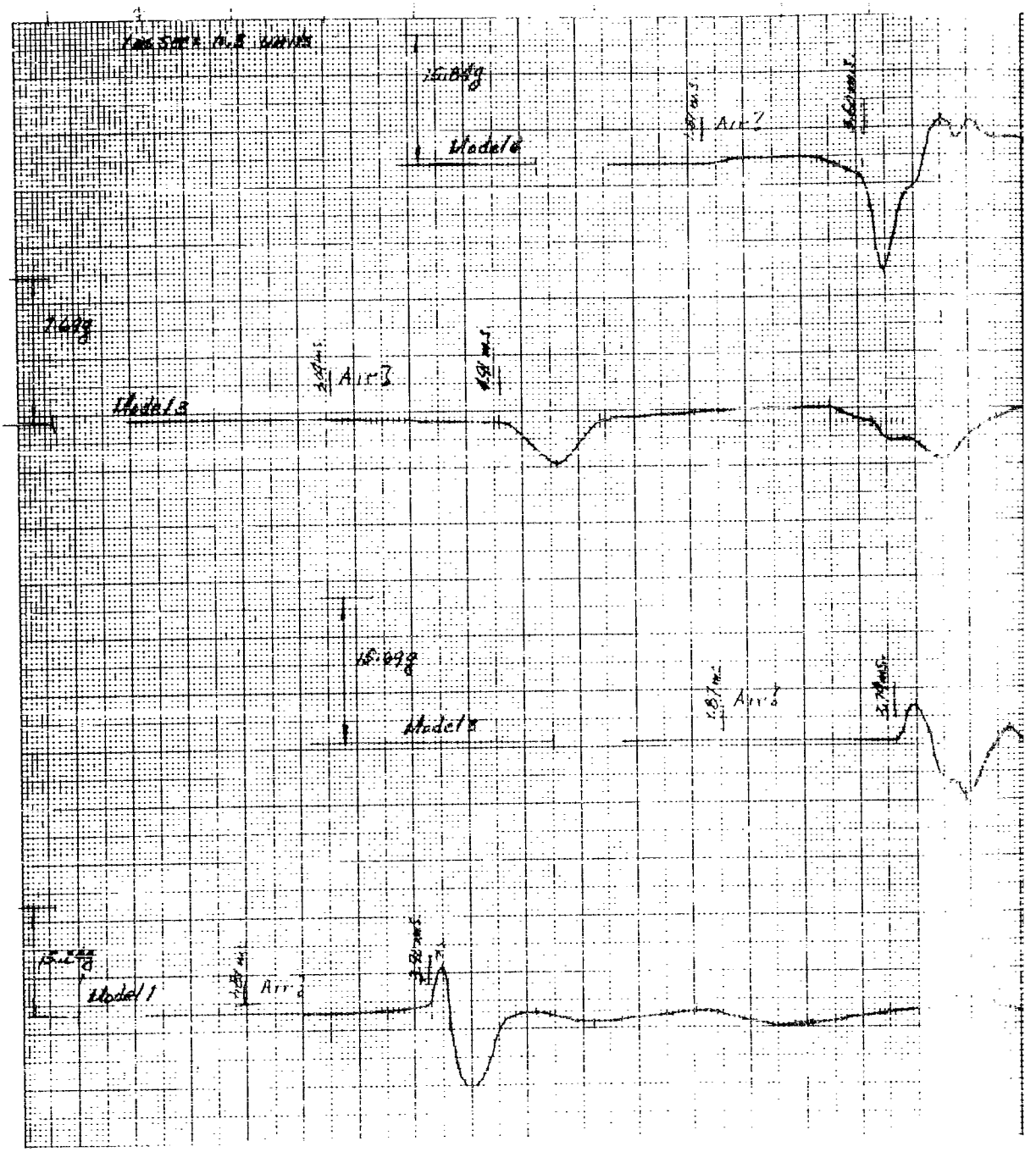
Model 6
Arr 7
Model 3
Arr 3
Model 4
Arr 5
Model 1
Arr 2

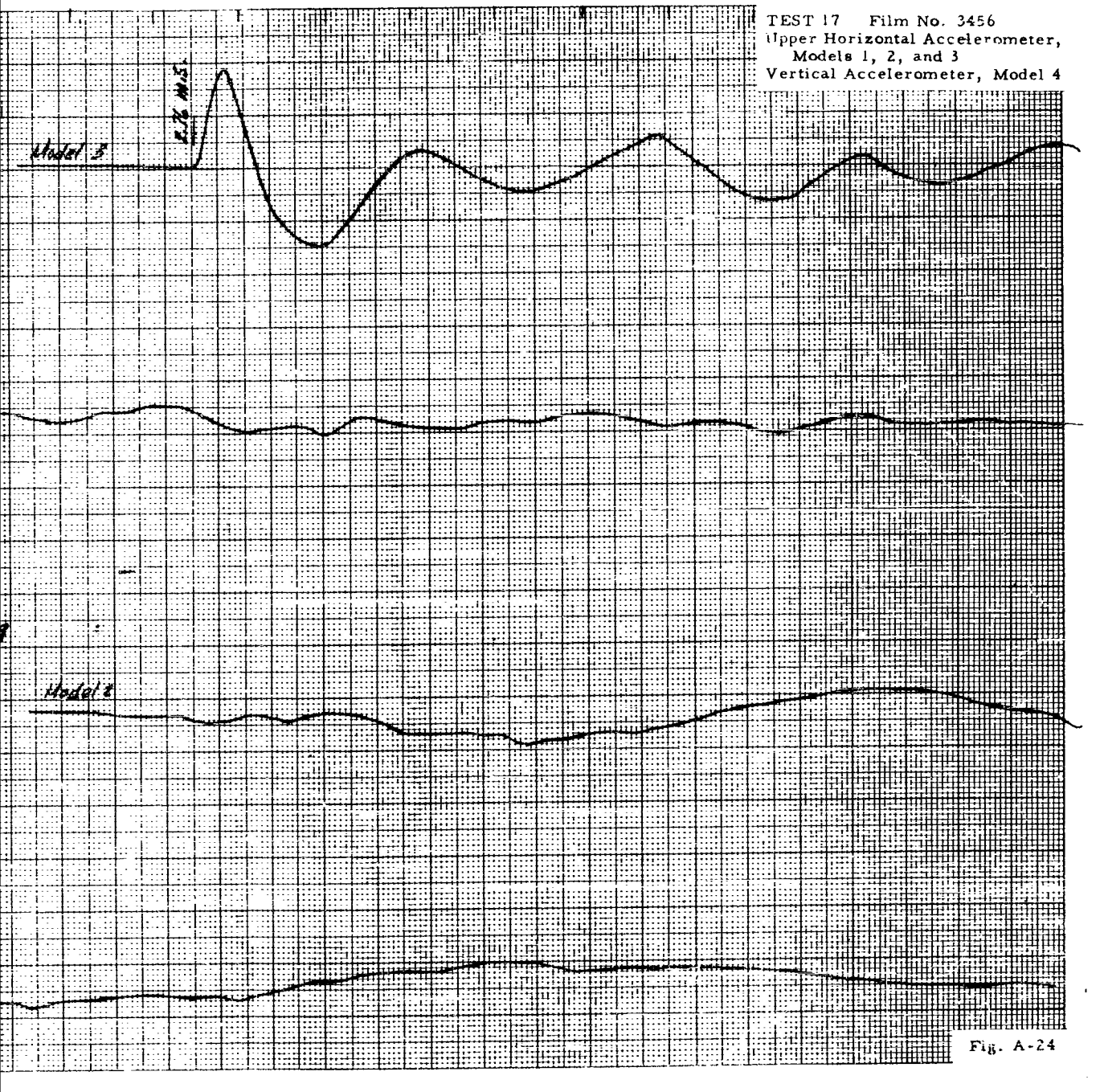

TEST 17 Film No. 3456
Upper Horizontal Accelerometer,
Models 1, 2, and 3
Vertical Accelerometer, Model 4

Fig. A-24

2

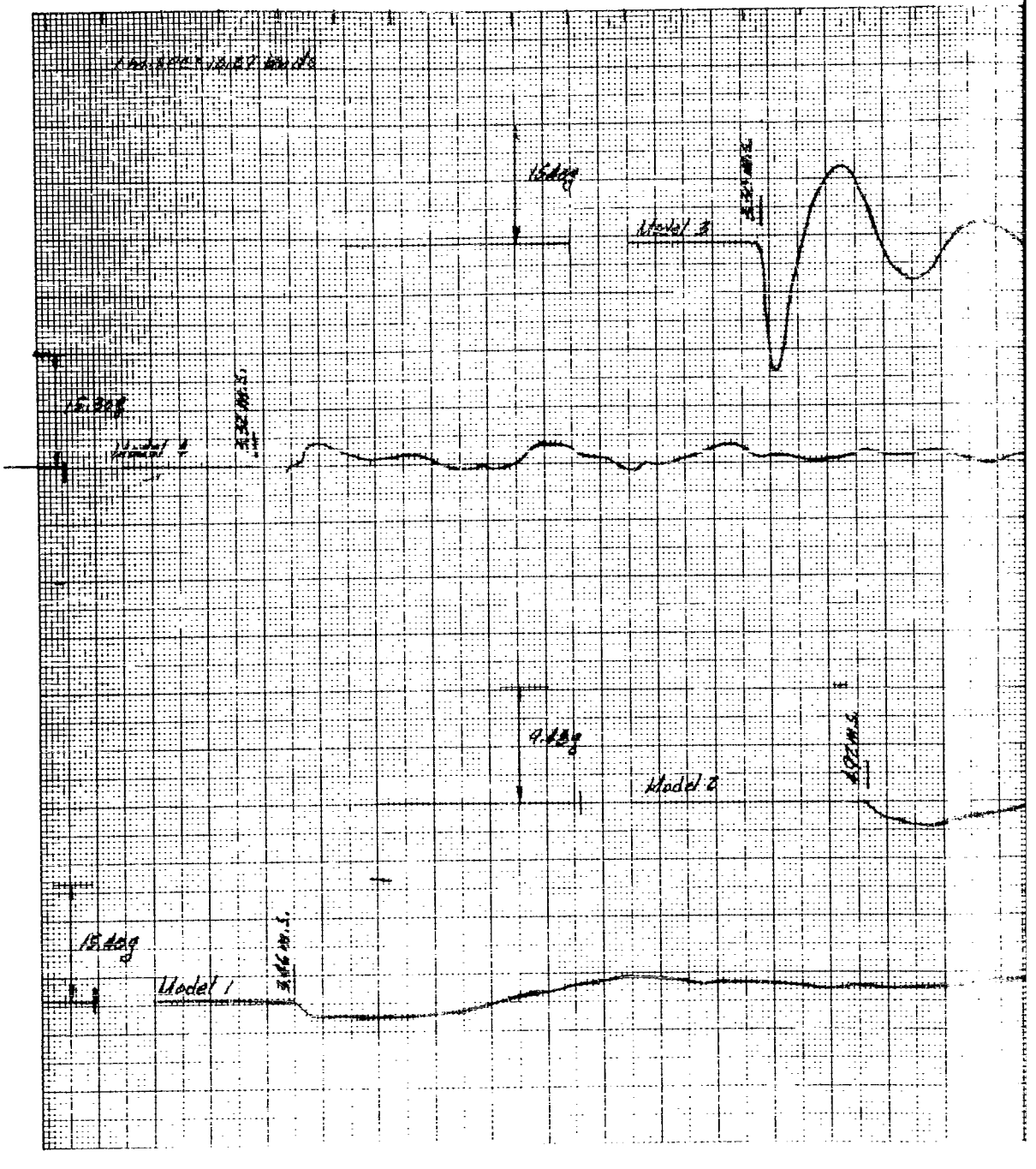

1

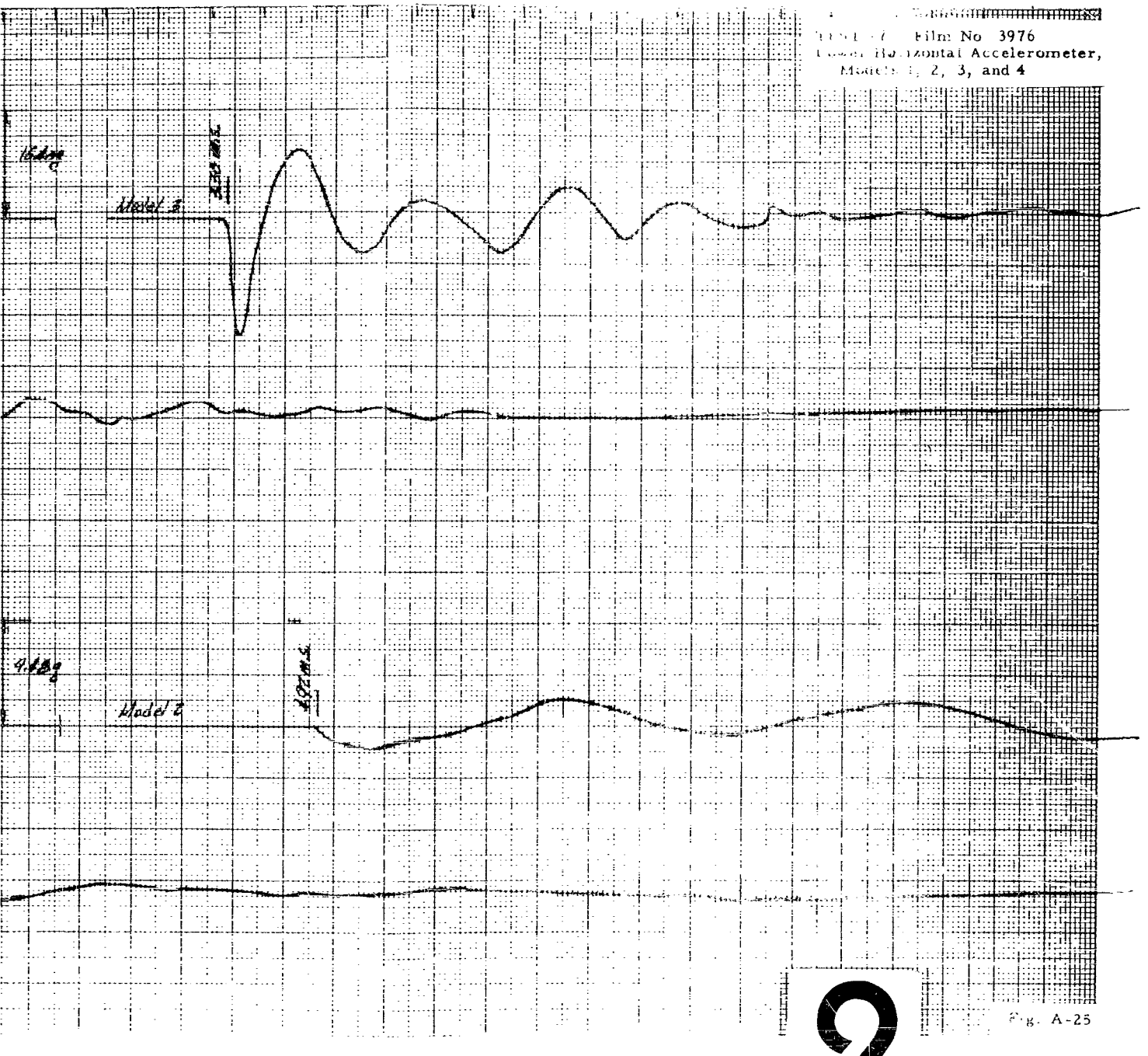

Film No 3976
Horizontal Accelerometer,
Models 1, 2, 3, and 4

Fig. A-25

2

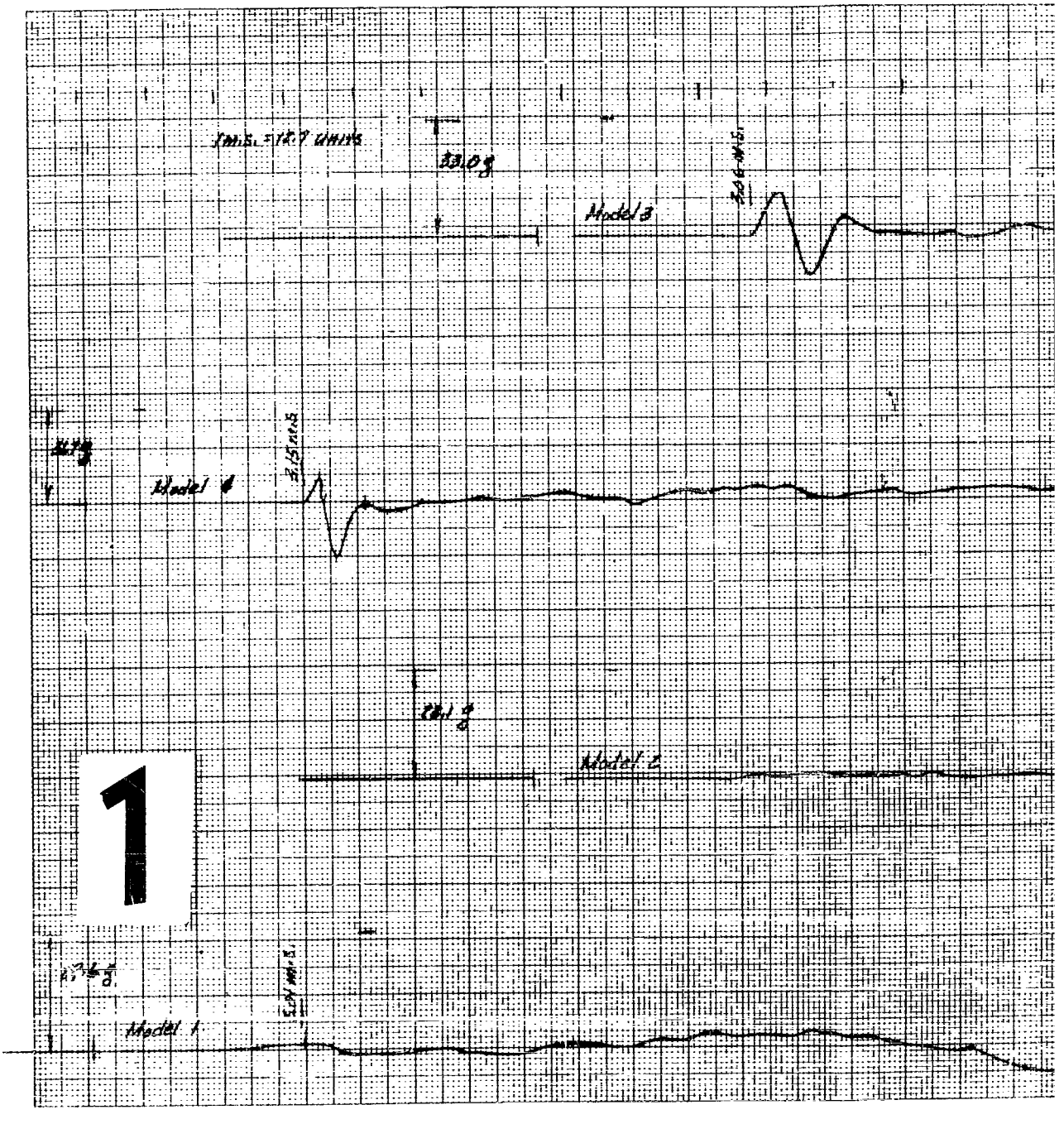

1

TEST 17 Film No. 2541
Vertical Accelerometer, Models 1, 2, and 3
Upper Horizontal Accelerometer, Model 4

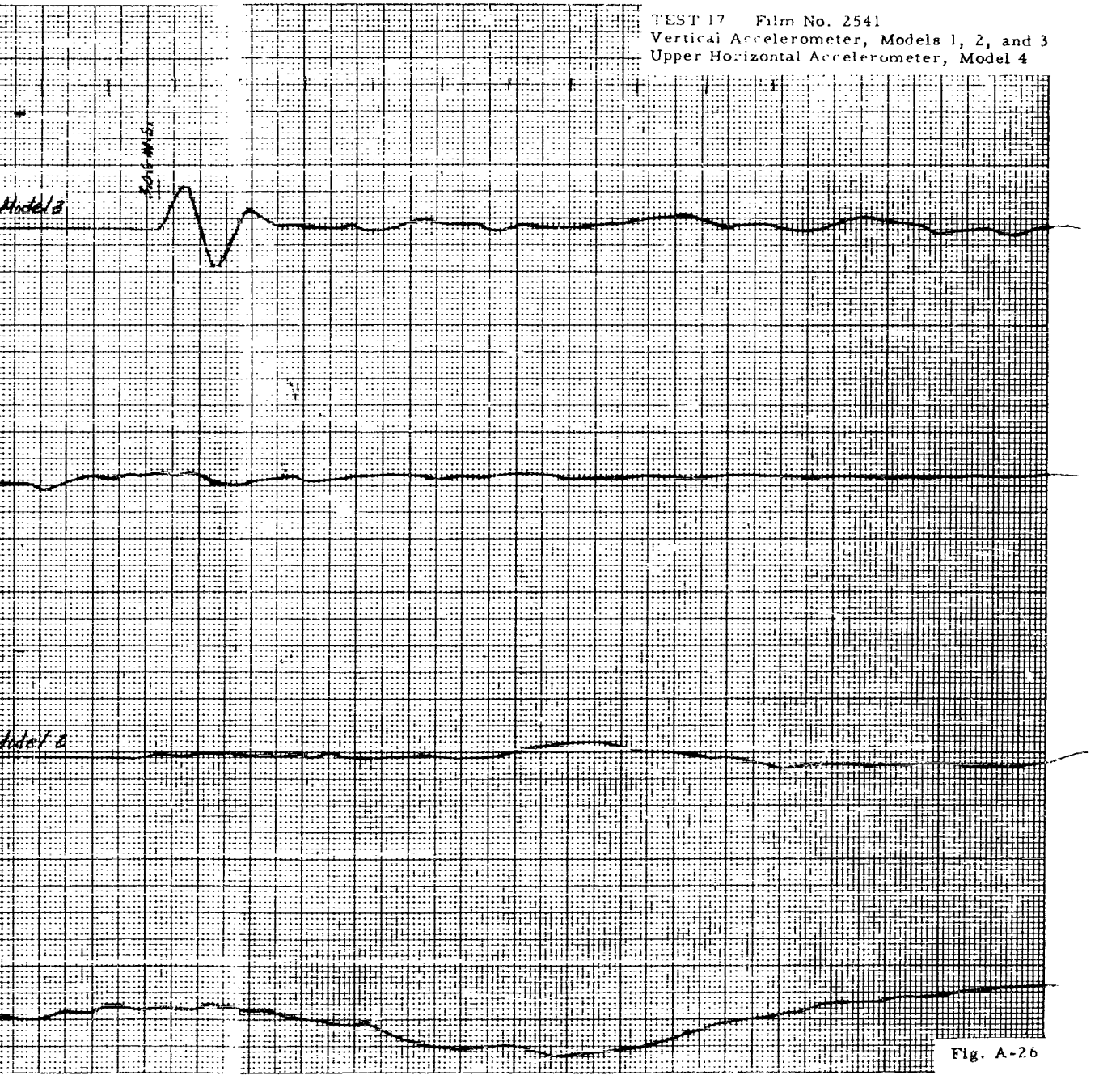

Fig. A-26

2

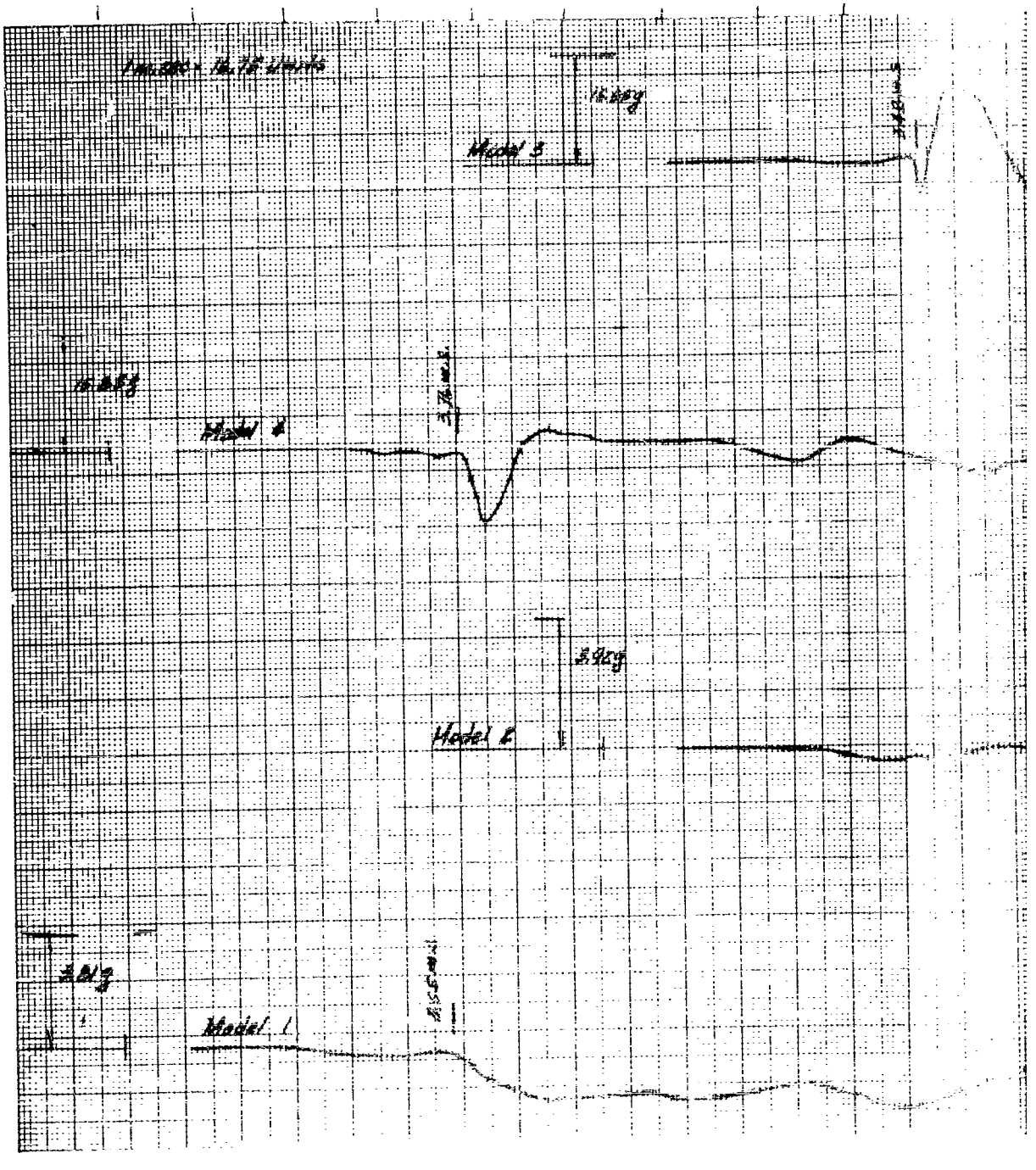

1

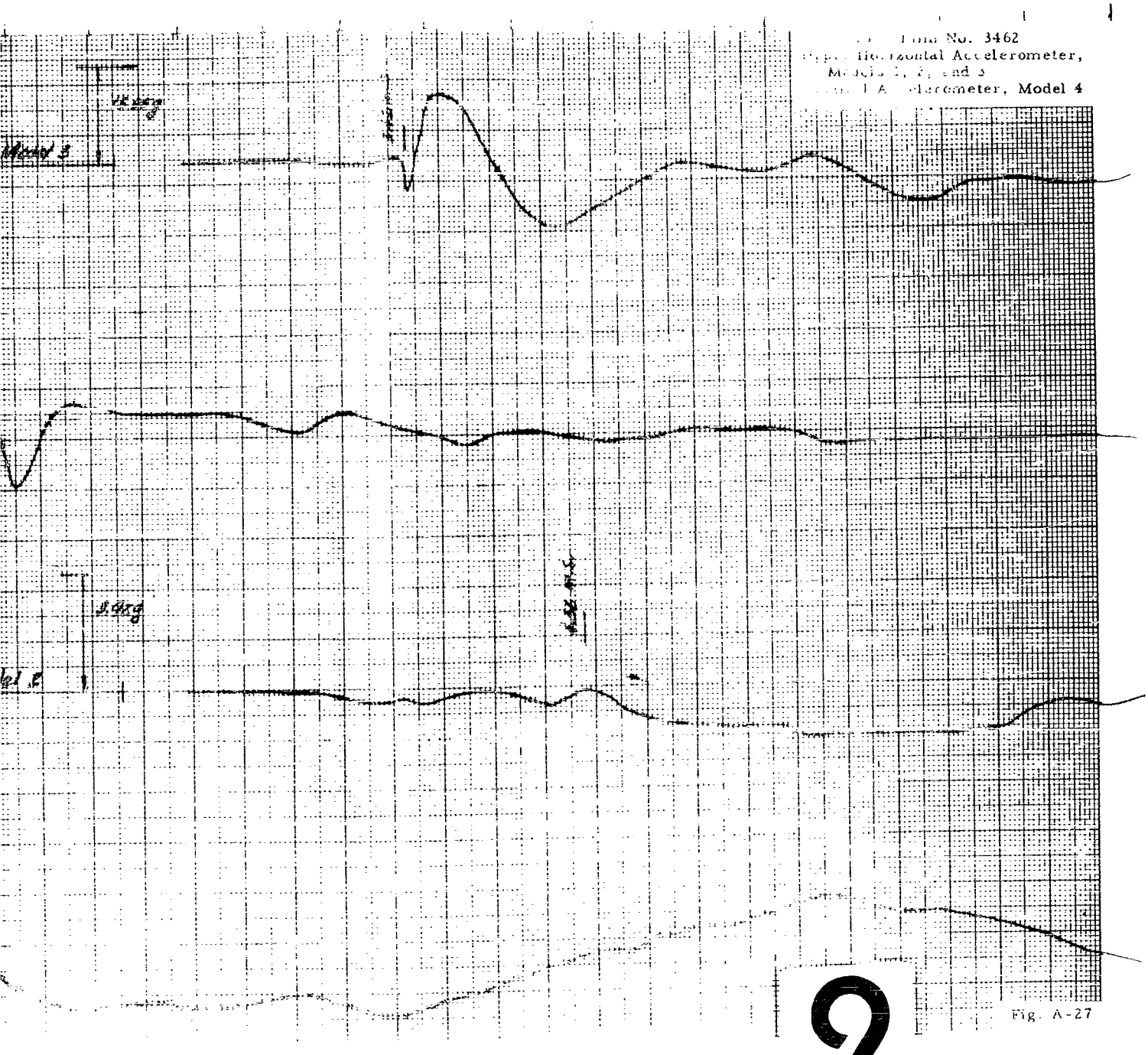

Time No. 3462
Horizontal Accelerometer,
Models 1, 2, and 3
Vertical Accelerometer, Model 4

Fig. A-27

2

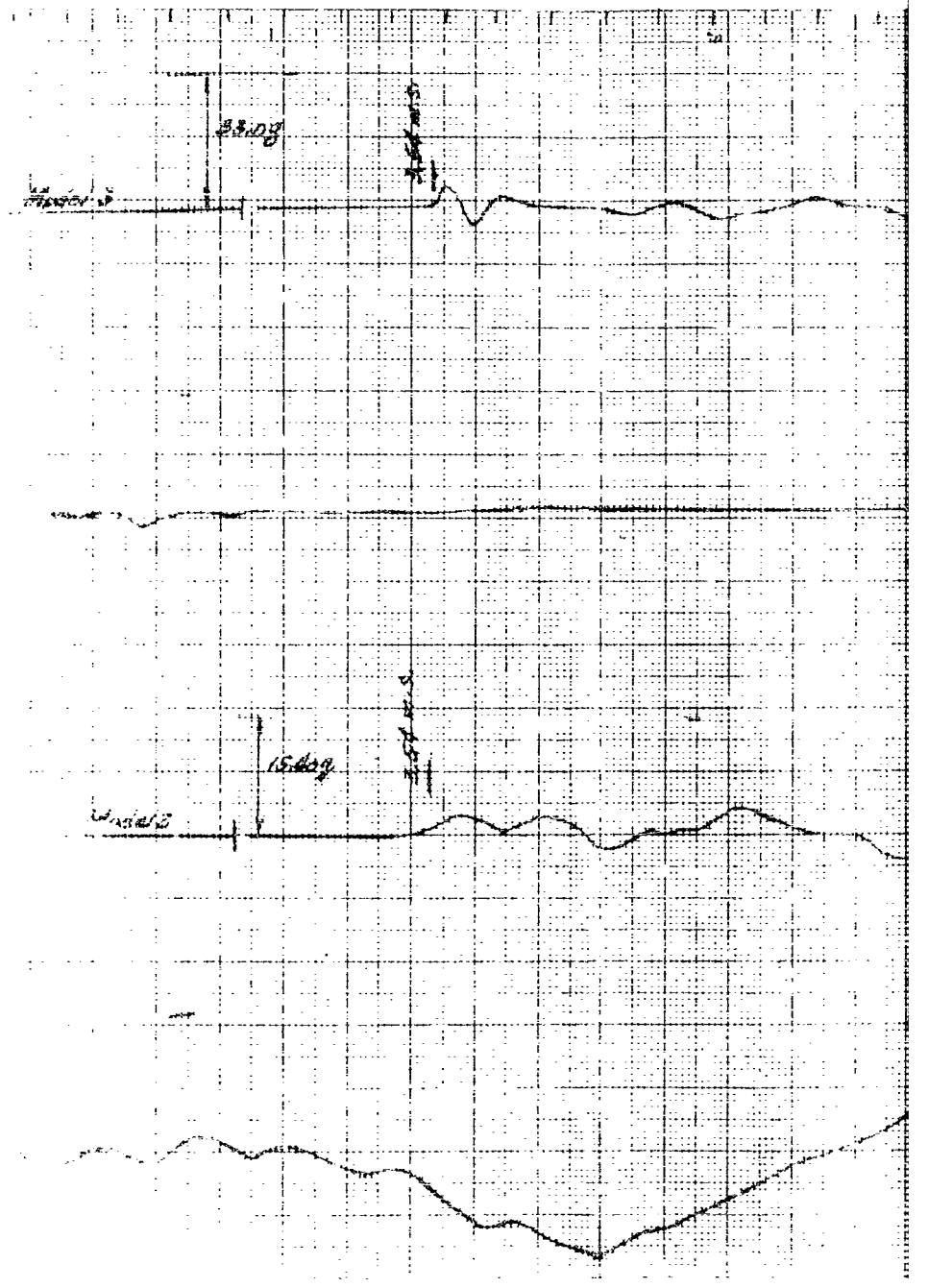

1

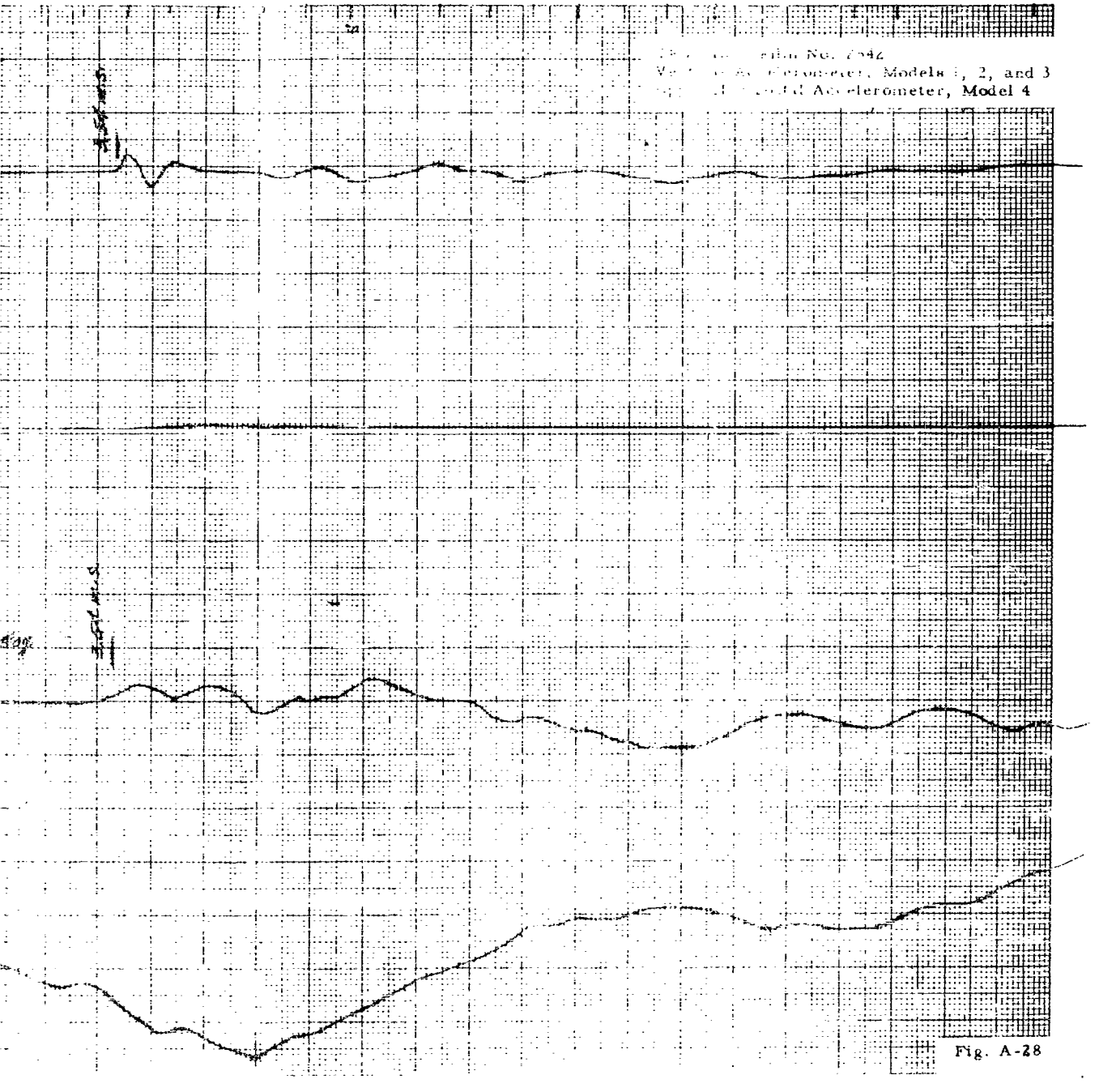

Fig. A-28

2

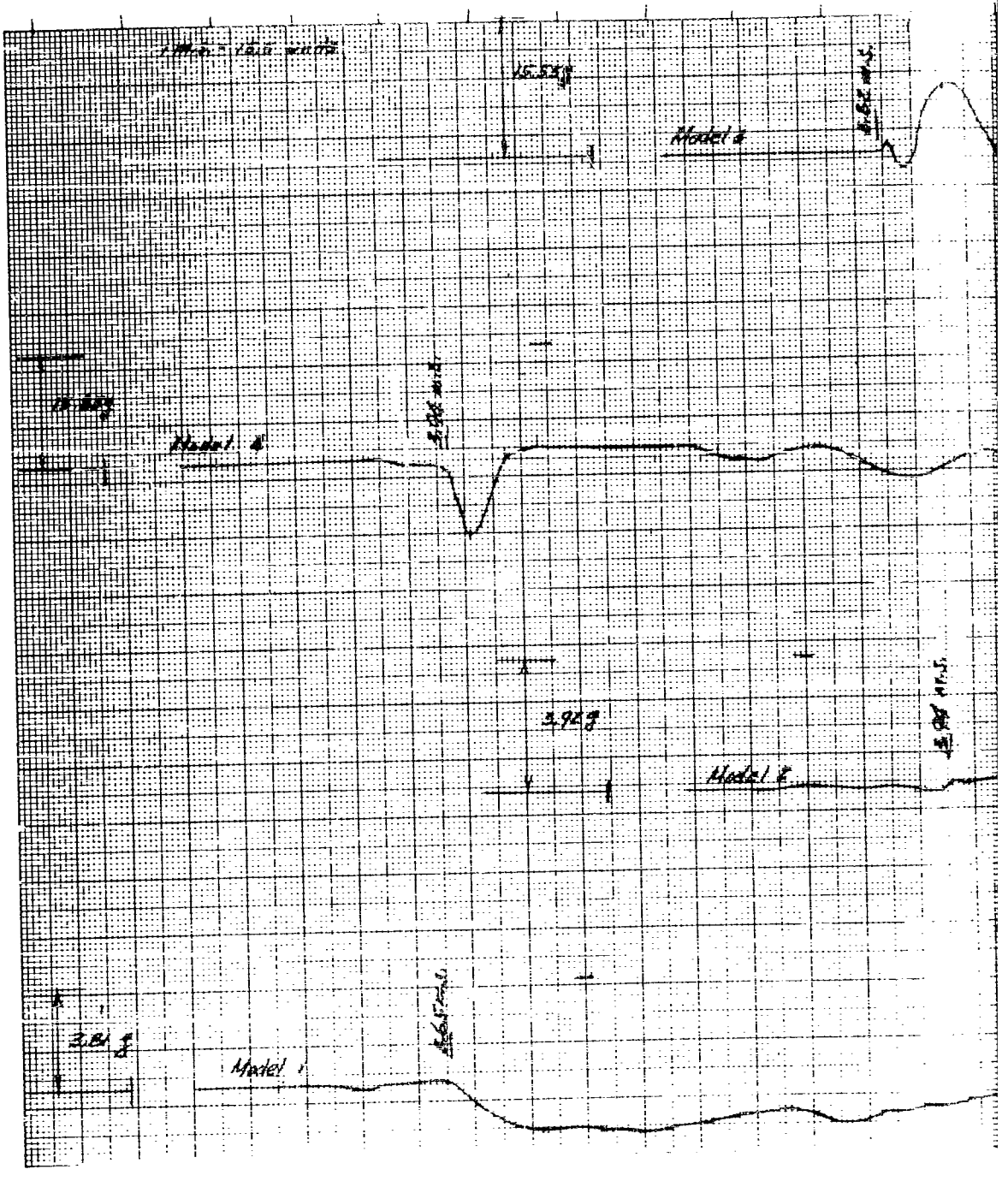

1

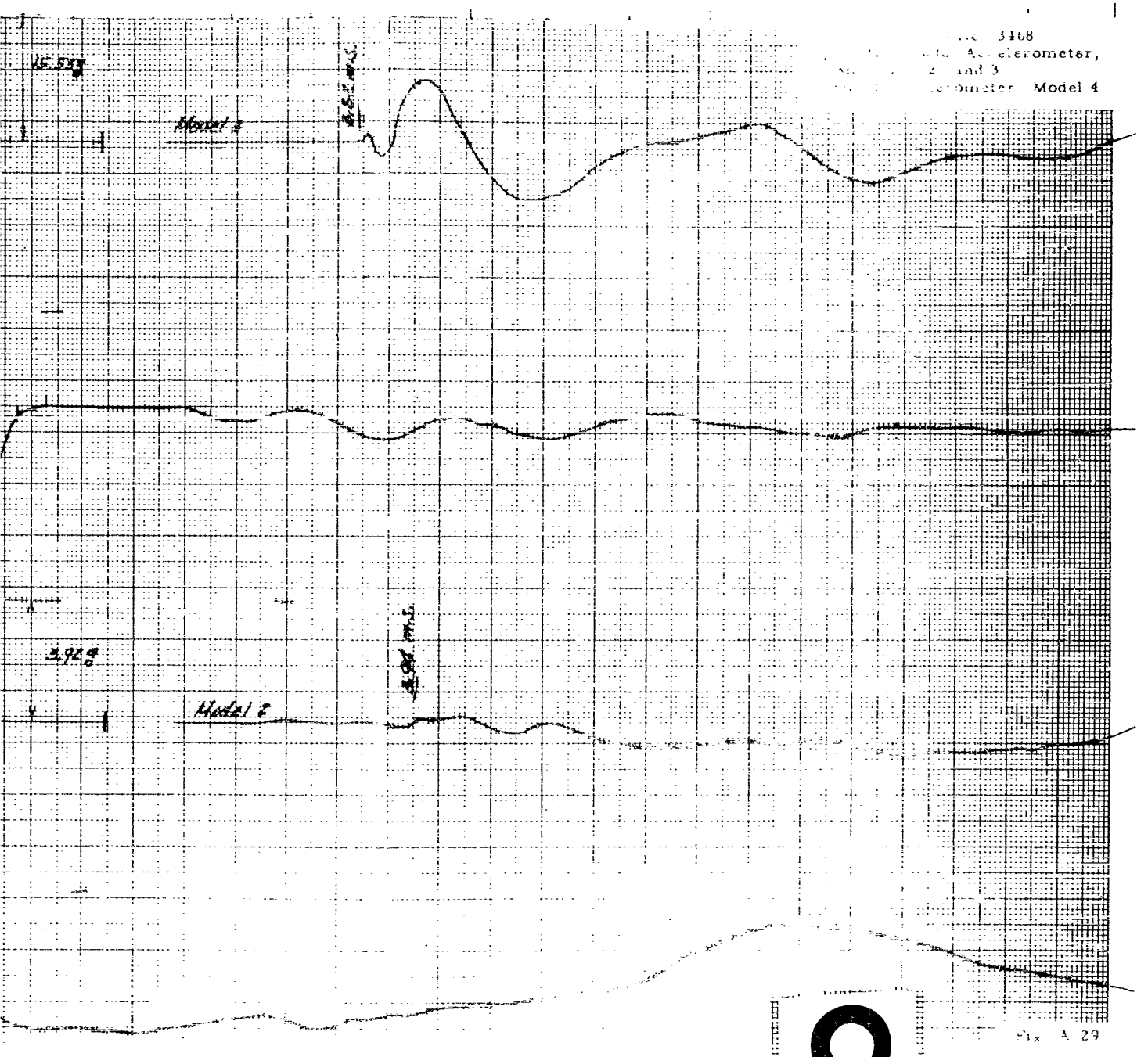

2

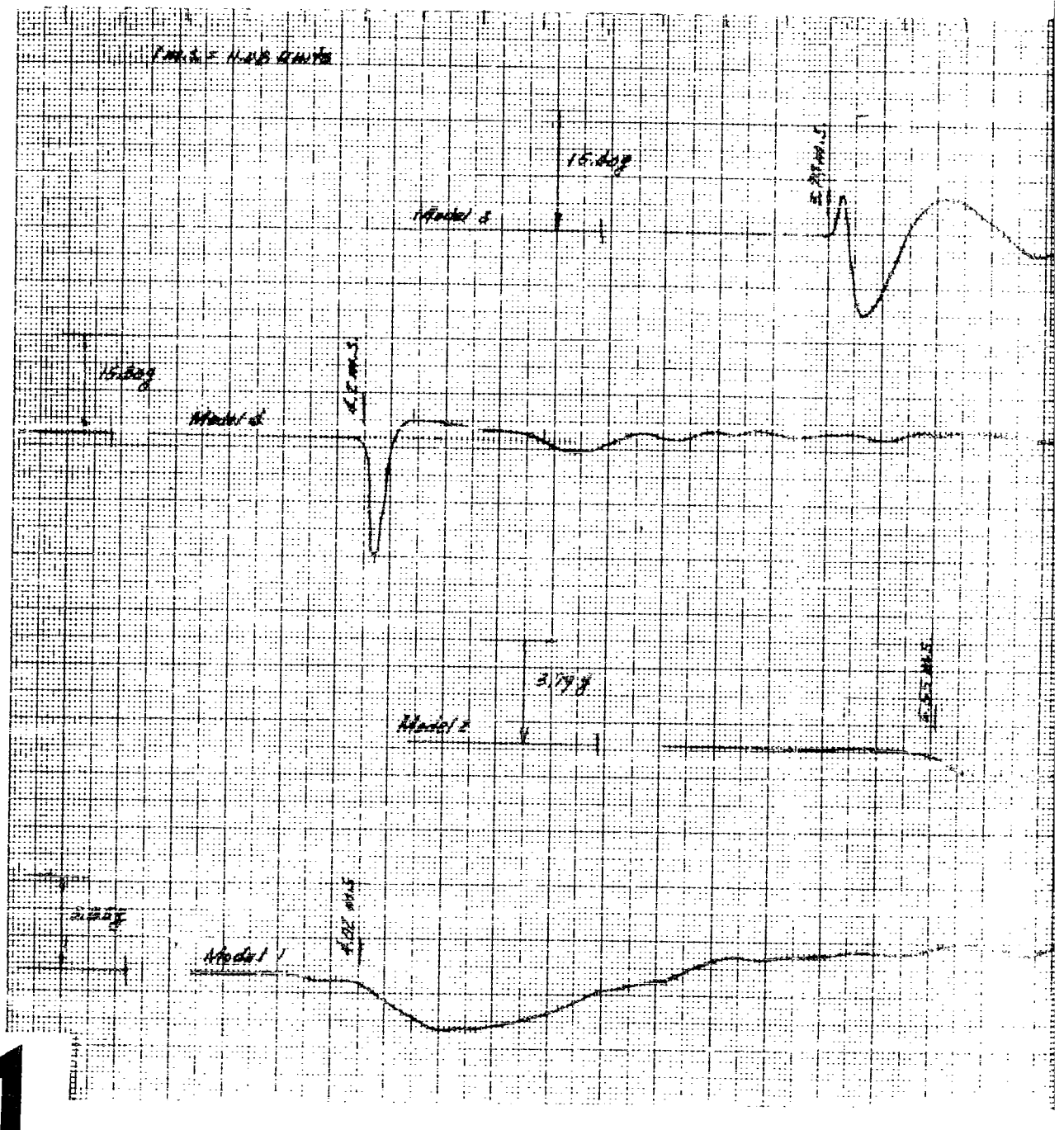

1

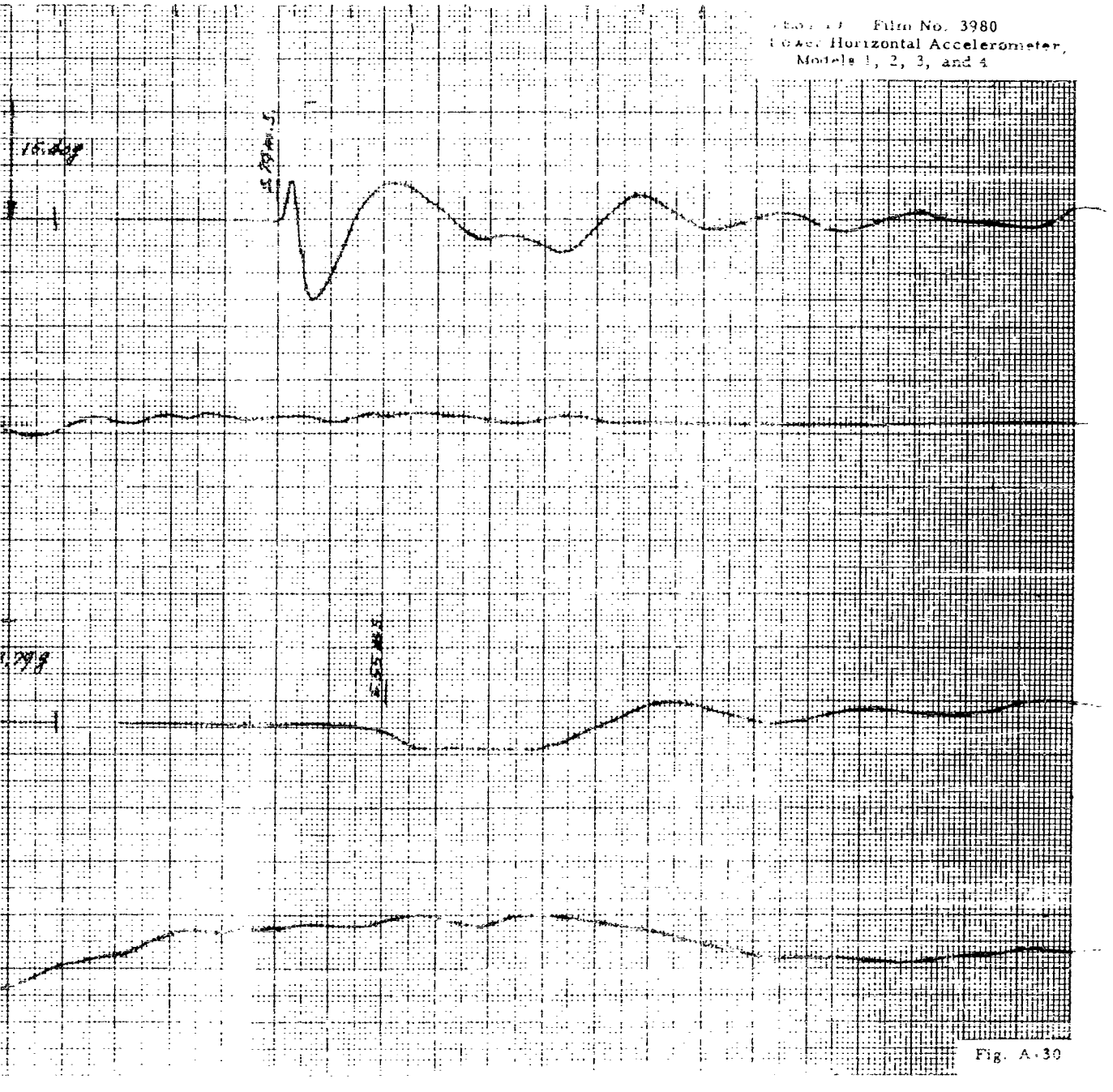

Fig. A-30

2

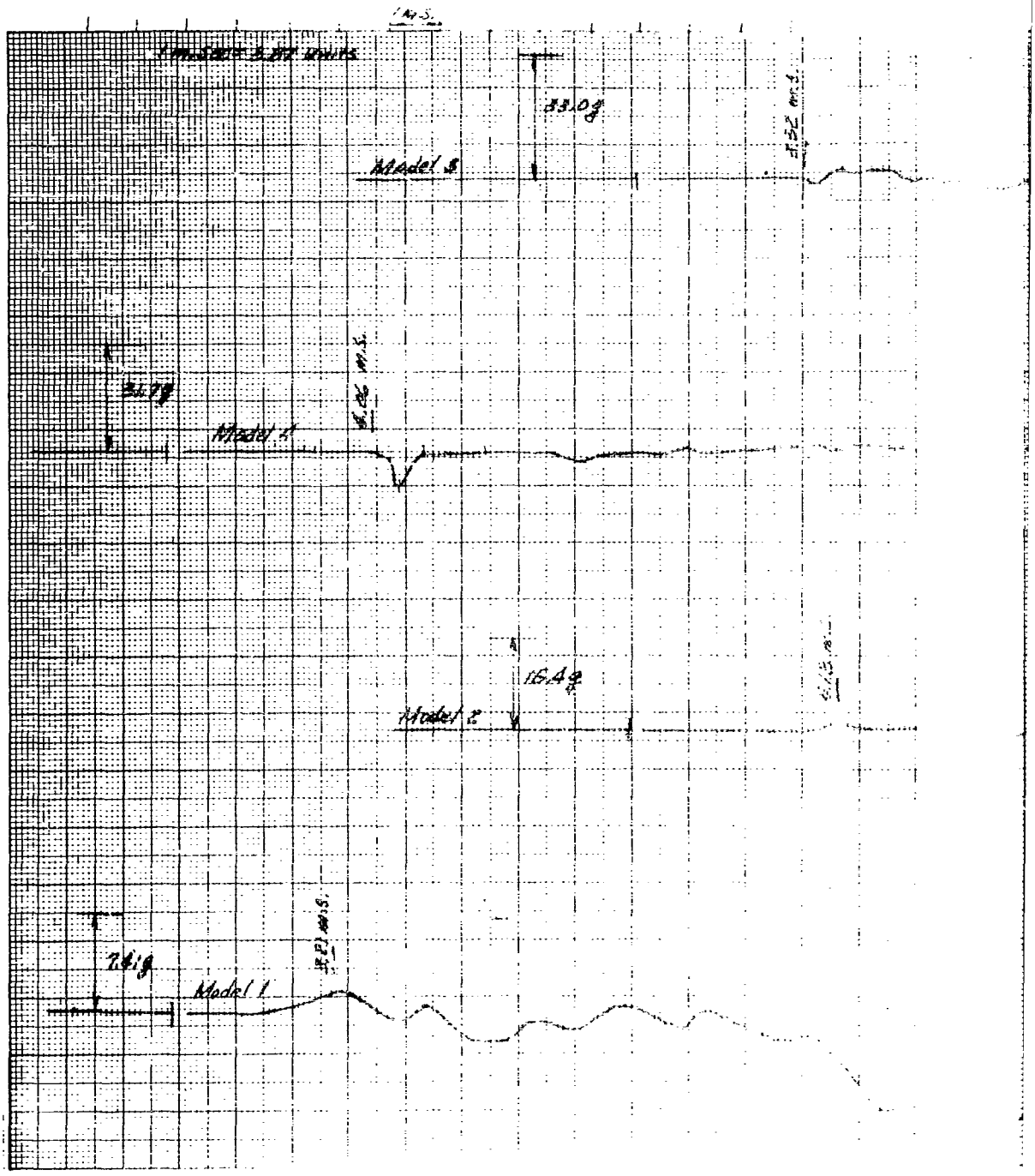

1

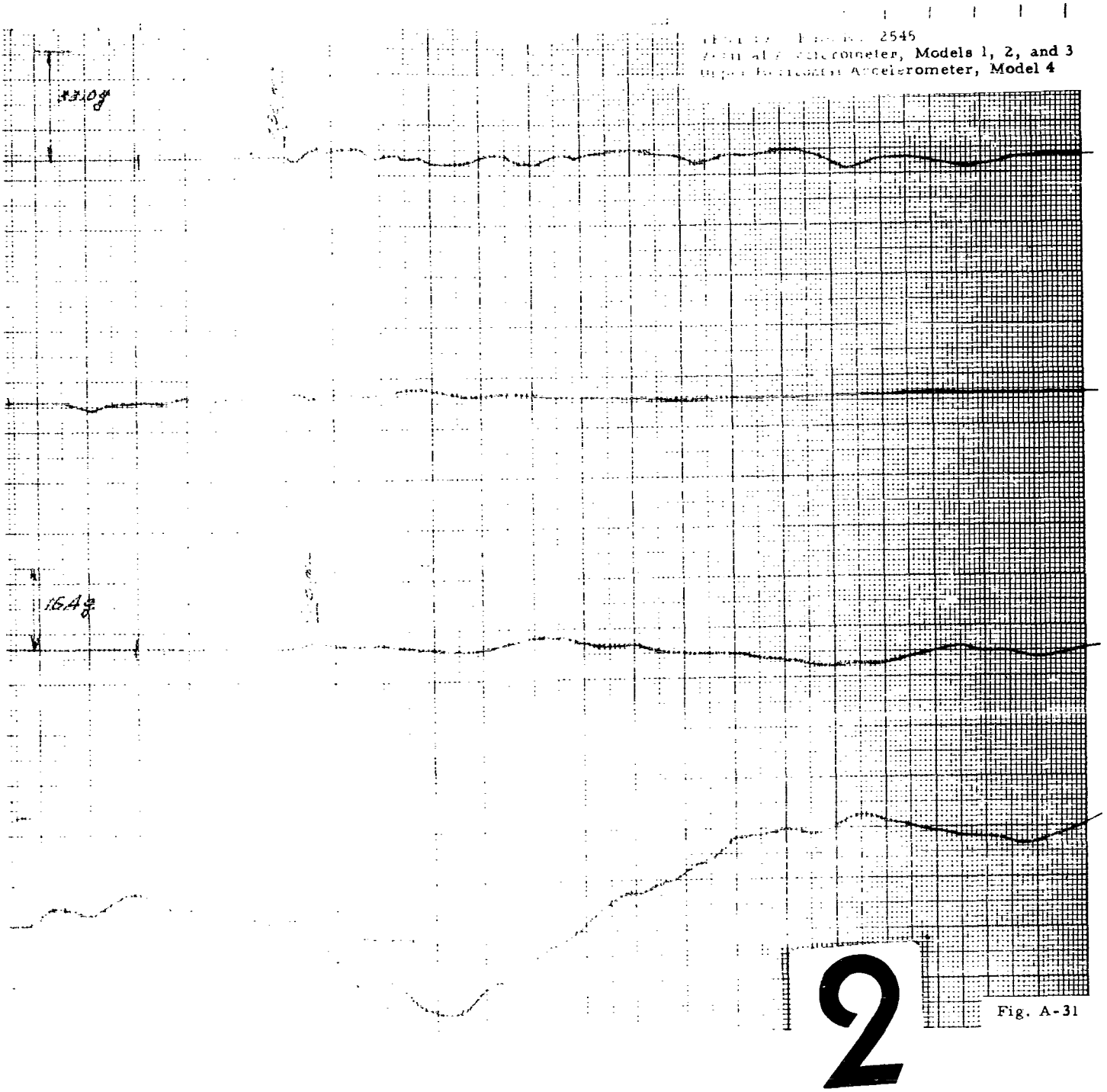

2545
Axial Accelerometer, Models 1, 2, and 3
Lateral Accelerometer, Model 4

Fig. A-31

Appendix B

DESCRIPTION OF SAND

Appendix B

DESCRIPTION OF SAND

B.1 GRAIN-SIZE ANALYSIS

The sand used in the experiments was a uniform Ottawa sand. A grain-size analysis showed that all sand particles pass through the No. 20 sieve and that the smallest particles are retained by the No. 200 sieve. The measured grain-size distribution is shown in Fig. B-1. The grains appear spherical in shape; their specific gravity is 2.64; and the angle of internal friction (ϕ), which depends on the relative density, was determined to be 36° in a triaxial compression test, a reasonable midrange value for Ottawa sand ($32° < \phi < 42°$).

B.2 WATER CONTENT

Water-content tests, which were performed at various times throughout the program, showed a variation of water in the sand from 0 to 0.4%. This indicates that the water content can be attributed to the normal moisture content of the air in the test cell.

B.3 DENSITY MEASUREMENTS

A maximum density of the sand was obtained by vibrating the sand in a container of known volume. After 6 min of vibration a maximum density of 111.4 lb/ft^3 was obtained. For this measurement, the table frequency was 500 cps at an amplitude of 0.0005 in. A minimum density of 95.10 lb/ft^3 was obtained by pouring the sand from a fixed height into a container of known volume.

The sand bed was initially filled with 160 bags of sand, having an estimated average density of 108.8 lb/ft^3. This figure is considered unreliable, however, since inadvertantly only the weight of 10 bags was determined.

In-place density measurements were made at various positions in the bed. This was accomplished by carefully removing a volume of sand from the interior of a stovepipe sunk into the sand bed. The weight of this sand

was determined through weighing, and its in-place volume was found by filling the excavated stovepipe with a calibrated sand. The apparatus used is shown in Fig. B-2. In-place density measurements obtained throughout the bed after the usual vibration and bed preparation (Section 3.4) varied from 107.3 lb/ft^3 to 110.2 lb/ft^3. These correspond, respectively, to relative densities in the range of 77.3% to 93.7%.

Now that the experimental technique has been developed, any future testing should see an increased number of these measurements (both in time and space) in order to obtain a more detailed picture of the density distribution.

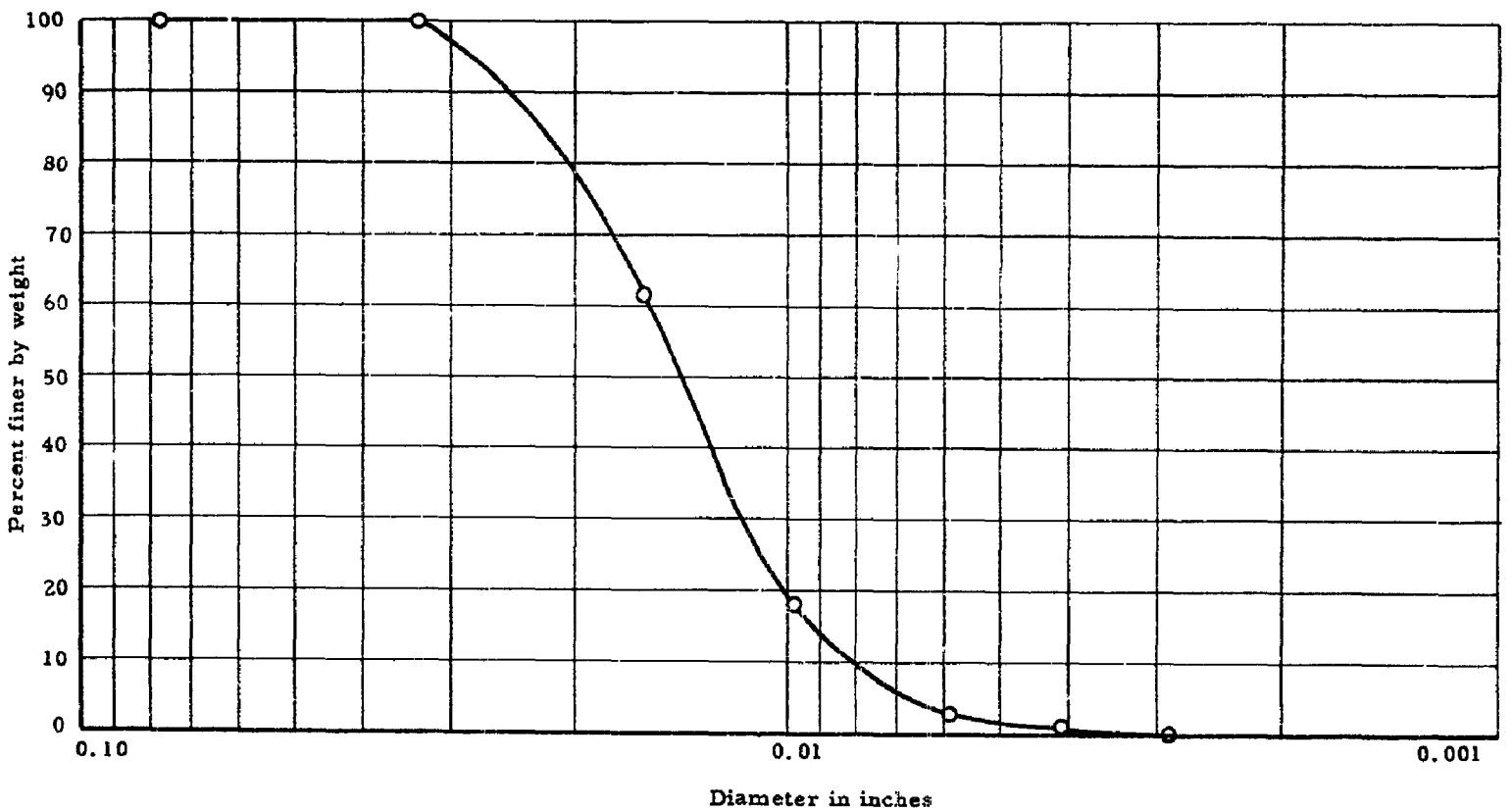

Figure B-1 Grain-size analysis

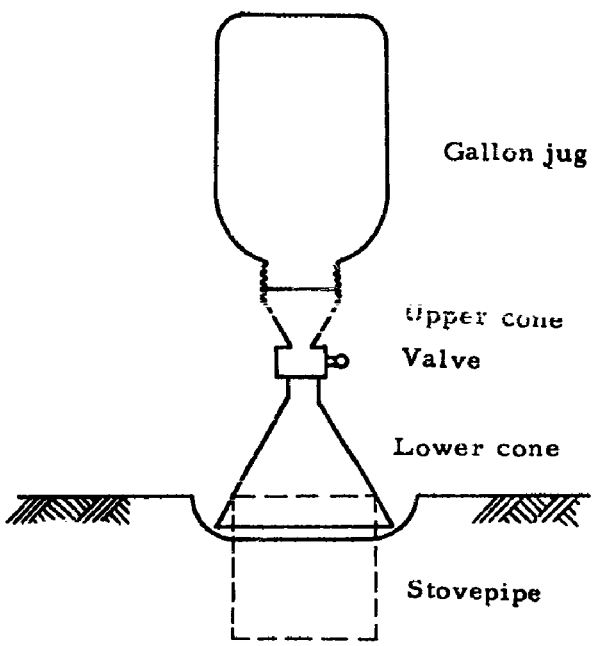

Figure B-2 In-place density apparatus.

Appendix C

SUMMARY OF SOLUTIONS TO CONTROL MODEL EQUATIONS

Appendix C

SUMMARY OF SOLUTIONS TO CONTROL MODEL EQUATIONS

C.1 COSINE STRESS PULSE

Let the incident stress pulse have the form

$$\sigma_1(t) = \begin{cases} \sigma_0(1 - \cos pt) & \ldots\ 0 \le t \le 2\pi/p \\ 0 & \ldots\ t > 2\pi/p \end{cases} \quad . \tag{C-1}$$

Then Eq 4.26 has as its solution,

$$\eta(\tau) = \begin{cases} \eta_1(\tau) & \ldots\ 0 \le \tau \le \tau_1 \equiv \dfrac{2\pi\omega}{p} \\ \eta_2(\tau) & \ldots\ \tau > \tau_1 \end{cases} \quad . \tag{C-2}$$

Two cases are considered, namely,[1/]

Case I $\beta < 1$

Case II $\beta > 1$.

<u>Case 1: $\beta < 1$</u>

$$\eta_1(\tau) = \frac{\tau}{2\beta} + \frac{1}{\mu}\left[\sin(\mu\tau - \phi_1) + \frac{1}{2\beta}\sin(\mu\tau - \phi_2) - k_1 \sin(\mu\tau + \phi_4)\right]\exp(-\beta\tau) - \frac{k_2}{\gamma}\sin(\gamma\tau + \phi_3) \tag{C-3}$$

1/ We do not consider explicitly the critically damped case $\beta = 1$.

$$\eta_2(\tau) = \frac{\pi}{\beta\gamma} + \frac{1}{\mu}\left[\frac{\pi}{\beta\gamma}\sin(\mu\tau - \mu\tau_1 - \phi_1) + \right.$$

$$\left. + \eta_1(\tau_1)\, k_3 \sin(\mu\tau - \mu\tau_1 - \phi_5)\right] \exp\left[-\beta(\tau - \tau_1)\right] \qquad \text{(C-4)}$$

where

$$\mu = \sqrt{1 - \beta^2}$$

$$\gamma = p/\omega$$

$$\phi_1 = \arctan(\mu/-\beta)$$

$$\phi_2 = 2\phi_1$$

$$\phi_3 = \arctan(2\beta\gamma) - \arctan\left[\frac{2\beta\gamma}{1 - \gamma^2}\right]$$

$$\phi_4 = \arctan\left[\frac{2\beta\mu}{1 - 2\beta^2}\right] - \arctan\left[\frac{-2\beta\gamma}{\beta^2 - \mu^2 + \gamma^2}\right]$$

$$\phi_5 = \arctan\left[\frac{\mu}{\beta + \eta_1'(\tau_1)/\eta_1(\tau_1)}\right]$$

$$k_1 = \left[\frac{\gamma^2 + 1/4\beta^2}{(1 - \gamma^2)^2 + 4\beta^2\gamma^2}\right]^{\frac{1}{2}}$$

$$k_2 = \left[\frac{\mu^2 + (\beta^2 - 1/2\beta)^2}{(1 - \gamma^2)^2 + 4\beta^2\gamma^2}\right]^{\frac{1}{2}}$$

$$k_3 = \left\{\left[\beta + \eta_1'(\tau_1)/\eta_1(\tau_1)\right]^2 + \mu^2\right\}^{1/2}$$

<u>Case II: $\beta > 1$</u>

$$\eta_1(\tau) = \frac{\tau}{2\beta} + G_1 \exp(-a\tau) - G_2 \exp(-b\tau) + \qquad \text{(C-5)}$$

$$+ G_3 \cos\gamma\tau - G_4 \sin\gamma\tau$$

$$\eta_2(\tau) = \frac{\pi}{\beta\gamma} + G_5 \exp\left[-a(\tau - \tau_1)\right] - G_6 \exp\left[-b(\tau - \tau_1)\right] \qquad \text{(C-6)}$$

where

$$a = \beta + \sqrt{\beta^2 - 1}$$

$$b = \beta - \sqrt{\beta^2 - 1}$$

$$G_1 = \left[\frac{1}{2\beta}(4\beta^2 - 2a\beta - 1) - b(G_3 + 1) + \gamma G_4\right]/(b-a)$$

$$G_2 = \left[\frac{1}{2\beta}(4\beta^2 - 2b\beta - 1) - a(G_3 + 1) + \gamma G_4\right]/(b-a)$$

$$G_3 = \frac{\gamma^2}{(\gamma^2 - 1)^2 + 4\beta^2\gamma^2}$$

$$G_4 = \frac{2\beta\gamma - (\gamma^2 - 1)/2\beta\gamma}{(\gamma^2 - 1)^2 + 4\beta^2\gamma^2}$$

$$G_5 = \left[\eta_1'(\tau_1) + b\eta_1(\tau_1) - \pi b/\beta\gamma\right]/(b-a)$$

$$G_6 = \left[\eta_1'(\tau_1) + a\eta_1(\tau_1) - \pi a/\beta\gamma\right]/(b-a)$$

C.2 TRIANGULAR STRESS PULSE

Let the incident stress pulse have the form

$$\sigma_1(t) = \begin{cases} 2\sigma_o\, t/t_1 & \ldots\ 0 \le t \le t_1 \\ 2\sigma_o(2 - t/t_1) & \ldots\ t_1 < t \le 2t_1 \\ 0 & \ldots\ t > 2t_1 \end{cases} \qquad \text{(C-7)}$$

Then Eq 4.26 has as its solution,

$$\eta(\tau) = \begin{cases} \eta_1(\tau) & \ldots\ 0 \le \tau \le \tau_1 \\ \eta_2(\tau) & \ldots\ \tau_1 < \tau \le 2\tau_1 \\ \eta_3(\tau) & \ldots\ \tau > 2\tau_1 \end{cases}, \qquad \text{(C-8)}$$

where[2/] for $\beta > 1$

$$\eta_1(\tau) = \frac{1}{2\beta\tau_1}\left[\left(\frac{a}{a-b}\right)\exp(b\tau) - \left(\frac{b}{a-b}\right)\exp(a\tau) + \tau^2/2 - 1\right] \qquad \text{(C-9a)}$$

[2/] We do not consider explicitly the cases $\beta \le 1$.

$$\eta_2(\tau)_{\underline{e}}(\tau) = K_1 \exp(a\tau) + K_2 \exp(b\tau) - K_3\tau^2 + \tau/\beta + K_4 \tag{C-9b}$$

$$\eta_3(\tau)_8(\tau) = K_5 \exp(a\tau) + K_6 \exp(b\tau) + \tau_1/2\beta \tag{C-9c}$$

and where

$$a = -\beta + \sqrt{\beta^2 - 1}$$

$$b = -\beta - \sqrt{\beta^2 - 1}$$

$$K_1 = \frac{1}{a}\left[\eta_1'(\tau_1) - K2b\exp(b\tau_1) + 2K_3\tau_1 - 1/\beta\right]\exp(-a\tau_1)$$

$$K_2 = \frac{\beta}{1-a\beta}\left[\eta_1'(\tau_1) - a\eta_1(\tau_1) + (2K_3 + a/\beta)\tau_1 - \right.$$

$$\left. -a\,K_3\tau_1^{\,2} + aK_4 - 1/\beta\right]\exp(-b\tau_1)$$

$$K_3 = 1/4\beta\tau_1$$

$$K_4 = \left(\frac{1}{\tau_1} - \tau_1\right)/2\beta$$

$$K_5 = \left[b\eta_2(2\tau_1) - \eta_2'(2\tau_1) - b\tau_1/2\beta\right]\exp(-2a\tau_1)/(b-a)$$

$$K_6 = \left[-a\eta_2(2\tau_1) + \eta_2'(2\tau_1) + a\tau_1/\beta\right]\exp(-2b\tau_1)/(b-a) \quad .$$

DISTRIBUTION

Copy No.

HEADQUARTERS USAF

1 Hq USAF (AFDRD), Wash 25, DC

1 USAF Dept IG for Insp (AFCDI-B-3), Norton AFB, Calif

MAJOR AIR COMMANDS

1 ARDC (RDR), Andrews AFB, Wash 25, DC

1 AFBMD (WDIE - Dr. George Young), AF Unit Post Office, Los Angeles 45, Calif

1 AUL, Maxwell AFB, Ala

ARDC CENTERS

1 AFCRC (CRRA), L. G. Hanscom Fld, Bedford, Mass

1 WADD (WCOSI), Wright-Patterson AFB, Ohio

KIRTLAND AFB

AFSWC, Kirtland AFB, NMex

1 (SWNH)

5 (SWOI)

1 (SWRS)

ARMY ACTIVITIES

1 Director, US Army Waterways Experiment Station, ATTN: WESRL, P.O. Box 60, Vicksburg, Miss

OTHER DOD ACTIVITIES

1 Chief, Defense Atomic Support Agency, ATTN: Blast and Shock Division (Mr. J. E. Lewis), Wash 25, DC

1 Commander, Field Command, Defense Atomic Support Agency, ATTN: Lt Col John Kodis, Sandia Base, NMex

OTHER

1 Sandia Corporation, ATTN: Mr. William R. Perret, Sandia Base, NMex

1 University of Illinois, ATTN: Dr. N. M. Newmark, 111 Talbot Laboratory, Urbana, Ill Contract AF 29(601)-1171

DISTRIBUTION (Cont'd)

Copy No.	
1	American Machine and Foundry Company, Mechanics Research Department, ATTN: Mr. T. G. Morrison, 1104 S. Wabash Ave., Chicago 5, Ill Contract AF 29(601)-1190
1	Armour Research Foundation of Illinois, Institute of Technology, ATTN: Mr. Ray Sauer, 10 West 35th Street, Chicago 16, Ill Contract AF 29(601)-1134
1	E. H. Plesset Associates, Inc., ATTN: Mr. Marc Peter, 6399 Wilshire Blvd., Los Angeles 48, Calif Contract AF 04(647)-342 AF BMD Contractor
1	Massachusetts Institute of Technology, Department of Civil and Sanitary Engineering, ATTN: Dr. Robert V. Whitman, Cambridge 39, Mass Contract AF 29(601)-1947
1	St. Louis University, ATTN: Dr. Carl Kisslinger, 3621 Olive Street, St. Louis 8, Mo (FY '60 Consultant)
1	Holmes and Narver, AEC Facilities Division, ATTN: Mr. Sherwood B. Smith, 849 South Broadway, Los Angeles 14, Calif (AEC Contractor)

B Series

10	ASTIA (TIPDR), Arlington Hall Sta, Arlington 12, Va
20	AFSWC (SWOI), Kirtland AFB, N. M.

AD-

Armour Research Foundation of Illinois Institute of Technology, Chicago 16, Illinois
GROUND SHOCK ISOLATION OF BURIED STRUCTURES (UNCLASSIFIED TITLE), by Eugene Sevin. February 1960. 135 p. incl. illus. tables, 44 refs. (Project 1080; Task 10801) (AFSWC TR 59-47) (Contract AF 29(601)-1134)

This report deals with the problem of alleviating the damaging effects of blast-induced ground shock on underground structures of the type presently contemplated for hardened missile sites. The technique of an experimental program utilizing small cylinders and three types of shock-isolation devices with ground disturbance created by means of a small HE charge was developed to the point where a sat-

(over)

isfactory level of shot-to-shot reproducibility of effects was attained. Polyurethane foam material proved most effective of the devices tested, reducing peak accelerations (relative to the unisolated model) by a factor of from 5 to 10. Various theoretical considerations relating to both the unisolated and isolated cylinders are discussed.

Ottawa sand was utilized as a soil (stress level estimated to be on the order of 1 psi); isolation devices consisted of (1) a wrapping of a low-density (2 lb/cu ft) flexible polyurethane foam, (2) a simulated pile foundation with an air void between the cylinder and the sand, and (3) a simulated pile foundation with pre-expanded polystyrene beads between the cylinder and the sand; HE charges weighed 0.02 lb; acceleration measurements were obtained at three points within the cylinders.

AD-

Armour Research Foundation of Illinois Institute of Technology, Chicago 16, Illinois
GROUND SHOCK ISOLATION OF BURIED STRUCTURES (UNCLASSIFIED TITLE), by Eugene Sevin. February 1960. 135 p. incl. illus. tables, 44 refs. (Project 1080; Task 10801) (AFSWC TR 59-47) (Contract AF 29(601)-1134)

This report deals with the problem of alleviating the damaging effects of blast-induced ground shock on underground structures of the type presently contemplated for hardened missile sites. The technique of an experimental program utilizing small cylinders and three types of shock-isolation devices with ground disturbance created by means of a small HE charge was developed to the point where a sat-

(over)

isfactory level of shot-to-shot reproducibility of effects was attained. Polyurethane foam material proved most effective of the devices tested, reducing peak accelerations (relative to the unisolated model) by a factor of from 5 to 10. Various theoretical considerations relating to both the unisolated and isolated cylinders are discussed.

Ottawa sand was utilized as a soil (stress level estimated to be on the order of 1 psi); isolation devices consisted of (1) a wrapping of a low-density (2 lb/cu ft) flexible polyurethane foam, (2) a simulated pile foundation with an air void between the cylinder and the sand, and (3) a simulated pile foundation with pre-expanded polystyrene beads between the cylinder and the sand; HE charges weighed 0.02 lb; acceleration measurements were obtained at three points within the cylinders.

infactory level of shot-to-shot reproducibility of effects was attained. Polyurethane foam material proved most effective of the devices tested, reducing peak accelerations (relative to the unisolated model) by a factor of from 5 to 10. Various theoretical considerations relating to both the unisolated and isolated cylinders are discussed.

Ottawa sand was utilized as a soil (stress level estimated to be on the order of 1 psi); isolation devices consisted of (1) a wrapping of a low-density (2 lb/cu ft) flexible polyurethane foam, (2) a simulated pile foundation with an air void between the cylinder and the sand, and (3) a simulated pile foundation with pre-expanded polystyrene beads between the cylinder and the sand; HE charges weighed 0.02 lb; acceleration measurements were obtained at three points within the cylinders.

AD-

Armour Research Foundation of Illinois Institute of Technology, Chicago 16, Illinois
GROUND SHOCK ISOLATION OF BURIED STRUCTURES (UNCLASSIFIED TITLE), by Eugene Sevin. February 1960. 135 p. incl. illus. tables, 44 refs. (Project 1080; Task 10801) (AFSWC TR 59-47 (Contract AF 29(601)-1134)

This report deals with the problem of alleviating the damaging effects of blast-induced ground shock on underground structures of the type presently contemplated for hardened missile sites. The technique of an experimental program utilizing small cylinders and three types of shock-isolation devices with ground disturbance created by means of a small HE charge was developed to the point where a sat-

(over)

isfactory level of shot-to-shot reproducibility of effects was attained. Polyurethane foam material proved most effective of the devices tested, reducing peak accelerations (relative to the unisolated model) by a factor of from 5 to 10. Various theoretical considerations relating to both the unisolated and isolated cylinders are discussed.

Ottawa sand was utilized as a soil (stress level estimated to be on the order of 1 psi); isolation devices consisted of (1) a wrapping of a low-density (2 lb/cu ft) flexible polyurethane foam, (2) a simulated pile foundation with an air void between the cylinder and the sand, and (3) a simulated pile foundation with pre-expanded polystyrene beads between the cylinder and the sand; HE charges weighed 0.02 lb; acceleration measurements were obtained at three points within the cylinders.

AD-

Armour Research Foundation of Illinois Institute of Technology, Chicago 16, Illinois
GROUND SHOCK ISOLATION OF BURIED STRUCTURES (UNCLASSIFIED TITLE), by Eugene Sevin. February 1960. 135 p. incl. illus. tables, 44 refs. (Project 1080; Task 10801) (AFSWC TR 59-47 (Contract AF 29(601)-1134)

This report deals with the problem of alleviating the damaging effects of blast-induced ground shock on underground structures of the type presently contemplated for hardened missile sites. The technique of an experimental program utilizing small cylinders and three types of shock-isolation devices with ground disturbance created by means of a small HE charge was developed to the point where a sat-

(over)

AD-

Armour Research Foundation of Illinois Institute of Technology, Chicago 16, Illinois
GROUND SHOCK ISOLATION OF BURIED STRUCTURES (UNCLASSIFIED TITLE), by Eugene Sevin. February 1960. 135 p. incl. illus. tables, 44 refs. (Project 1080; Task 10801) (AFSWC TR 59-47) (Contract AF 29(601)-1134)

This report deals with the problem of alleviating the damaging effects of blast-induced ground shock on underground structures of the type presently contemplated for hardened missile sites. The technique of an experimental program utilizing small cylinders and three types of shock-isolation devices with ground disturbance created by means of a small HE charge was developed to the point where a satisfactory level of shot-to-shot reproducibility of effects was attained. Polyurethane foam material proved most effective of the devices tested, reducing peak accelerations (relative to the unisolated model) by a factor of from 5 to 10. Various theoretical considerations relating to both the unisolated and isolated cylinders are discussed.

Ottawa sand was utilized as a soil (stress level estimated to be on the order of 1 psi); isolation devices consisted of (1) a wrapping of a low-density (2 lb/cu ft) flexible polyurethane foam, (2) a simulated pile foundation with an air void between the cylinder and the sand, and (3) a simulated pile foundation with pre-expanded polystyrene beads between the cylinder and the sand; HE charges weighed 0.02 lb; acceleration measurements were obtained at three points within the cylinders.

(over)

AD-

Armour Research Foundation of Illinois Institute of Technology, Chicago 16, Illinois
GROUND SHOCK ISOLATION OF BURIED STRUCTURES (UNCLASSIFIED TITLE), by Eugene Sevin. February 1960. 135 p. incl. illus. tables, 44 refs. (Project 1080; Task 10801) (AFSWC TR 59-47) (Contract AF 29(601)-1134)

This report deals with the problem of alleviating the damaging effects of blast-induced ground shock on underground structures of the type presently contemplated for hardened missile sites. The technique of an experimental program utilizing small cylinders and three types of shock-isolation devices with ground disturbance created by means of a small HE charge was developed to the point where a satisfactory level of shot-to-shot reproducibility of effects was attained. Polyurethane foam material proved most effective of the devices tested, reducing peak accelerations (relative to the unisolated model) by a factor of from 5 to 10. Various theoretical considerations relating to both the unisolated and isolated cylinders are discussed.

Ottawa sand was utilized as a soil (stress level estimated to be on the order of 1 psi); isolation devices consisted of (1) a wrapping of a low-density (2 lb/cu ft) flexible polyurethane foam, (2) a simulated pile foundation with an air void between the cylinder and the sand, and (3) a simulated pile foundation with pre-expanded polystyrene beads between the cylinder and the sand; HE charges weighed 0.02 lb; acceleration measurements were obtained at three points within the cylinders.

(over)

isfactory level of shot-to-shot reproducibility of effects was attained. Polyurethane foam material proved most effective of the devices tested, reducing peak accelerations (relative to the unisolated model) by a factor of from 5 to 10. Various theoretical considerations relating to both the unisolated and isolated cylinders are discussed.

Ottawa sand was utilized as a soil (stress level estimated to be on the order of 1 psi); isolation devices consisted of (1) a wrapping of a low-density (2 lb/cu ft) flexible polyurethane foam, (2) a simulated pile foundation with an air void between the cylinder and the sand, and (3) a simulated pile foundation with pre-expanded polystyrene beads between the cylinder and the sand; HE charges weighed [illegible] lb; acceleration measurements were obtained at three points within the cylinders.

isfactory level of shot-to-shot reproducibility of effects was attained. Polyurethane foam material proved most effective of the devices tested, reducing peak accelerations (relative to the unisolated model) by a factor of from 5 to 10. Various theoretical considerations relating to both the unisolated and isolated cylinders are discussed.

Ottawa sand was utilized as a soil (stress level estimated to be on the order of 1 psi); isolation devices consisted of (1) a wrapping of a low-density (2 lb/cu ft) flexible polyurethane foam, (2) a simulated pile foundation with an air void between the cylinder and the sand, and (3) a simulated pile foundation with pre-expanded polystyrene beads between the cylinder and the sand; HE charges weighed [illegible] lb; acceleration measurements were obtained at three points within the cylinders.

AD-

Armour Research Foundation of Illinois Institute of Technology, Chicago 16, Illinois
GROUND SHOCK ISOLATION OF BURIED STRUCTURES (UNCLASSIFIED TITLE), by Eugene Sevin. February 1960. 135 p. incl. illus. tables, [illegible] refs. (Project 1080; Task 1.8011; [illegible]) (Contract AF 29(601)-1131)

This report deals with the problem of alleviating the damaging effects of blast-induced ground shock on underground structures of the type presently contemplated for hardened missile sites. The technique of an experimental program utilizing small cylinders and three types of shock-isolation devices with ground disturbance created by means of a small HE charge was developed to the point where a sat-

over

AD-

Armour Research Foundation of Illinois Institute of Technology, Chicago 16, Illinois
GROUND SHOCK ISOLATION OF BURIED STRUCTURES (UNCLASSIFIED TITLE), by Eugene Sevin. February 1960. 135 p. incl. illus. tables, [illegible] refs. (Project 1080; Task 1.8011; [illegible]) (Contract AF 29(601)-1131)

This report deals with the problem of alleviating the damaging effects of blast-induced ground shock on underground structures of the type presently contemplated for hardened missile sites. The technique of an experimental program utilizing small cylinders and three types of shock-isolation devices with ground disturbance created by means of a small HE charge was developed to the point where a sat-

over